Secreted hepatitis B virus (HBV)-RNA associates with extracellular vesicles in the supernatant of infected hepatocytes

Delphine Bousquet

N°d'ordre NNT :
2021LYSE1234

THESE de DOCTORAT DE L'UNIVERSITE DE LYON

Opérée au sein de

L'Université Claude Bernard Lyon 1

Ecole Doctorale N° 340

Biologie Moléculaire Intégrative et Cellulaire (BMIC)

Spécialité de doctorat : Virologie et Biologie Moléculaire

Discipline : Infectiologie

Soutenue publiquement le 26/11/2021, par :

Delphine Bousquet

Secreted hepatitis B virus (HBV)-RNA associates with extracellular vesicles in the supernatant of infected hepatocytes

Devant le jury composé de :

Mr. **Massimo Levrero**, PU-PH, CRCL/HCL, Lyon	Président
Mme **Reinhild Prange**, PU, Université Johannes Gutenberg, Mayence	Rapporteur
Mr. **Eloi Verrier**, CR Inserm, U1110-HepSYS, Strasbourg	Rapporteur
Mme **Lorena Martin-Jaular**, PhD, Inserm UMR_S932	Examinateur
Mme **Marintha Heil**, PhD, Roche Molecular Systems, Pleasanton (USA)	Examinateur
Mr. **Philippe Roingeard**, PU-PH, Université de Tours/U 1259 – MAVIVH	Examinateur
Mme **Barbara Testoni**, CR INSERM, CRCL, Lyon	Co-directeur de thèse
Mr. **Fabien Zoulim**, PU-PH, CRCL/HCL, Lyon	Directeur de thèse

« Un matin comme tous les autres
Un nouveau Paris
Rechercher un peu de magie
Dans cette inertie morose

Clopin-clopan sous la pluie
Jouer le rôle de sa vie
Puis un soir le rideau tombe
C'est pareil pour tout l'monde

Rester debout mais à quel prix
Sacrifier son instinct et ses envies
Les plus essentielles

Mais tout peut changer aujourd'hui
Et le premier jour du reste de ta vie
Plus confidentiel

Pourquoi vouloir toujours plus beau
Plus loin plus haut
Et vouloir décrocher la lune
Quand on a les étoiles

Quand les certitudes s'effondrent
En quelques secondes
Sache que du berceau à la tombe
C'est dur pour tout l'monde

Rester debout mais à quel prix
Sacrifier son instinct et ses envies
Les plus confidentielles

Mais tout peut changer aujourd'hui
Et le premier jour du reste de ta vie
C'est providentiel

Debout peu importe le prix
Suivre son instinct et ses envies
Les plus essentielles

Tu peux exploser aujourd'hui
Et le premier jour du reste de ta vie
Non accidentel»

Le Premier Jour du Reste de ta Vie.

UNIVERSITE CLAUDE BERNARD - LYON 1

Président de l'Université	**M. le Professeur Frédéric FLEURY**
Président du Conseil Académique	M. le Professeur Hamda BEN HADID
Vice-président du Conseil d'Administration	M. le Professeur Didier REVEL
Vice-président du Conseil Formation et Vie Universitaire	M. le Professeur Philippe CHEVALIER
Vice-président de la Commission Recherche	M. Petru MIRONESCU
Directeur Général des Services	M. Pierre ROLLAND

COMPOSANTES SANTÉ

Faculté de Médecine Lyon Est – Claude Bernard	Doyen : M. le Professeur Gilles RODE
Faculté de Médecine et de Maïeutique Lyon Sud – Charles Mérieux	Doyenne : Mme. Carole BURILLON
Faculté d'Odontologie	Doyenne : Mme Dominique SEUX
Institut des Sciences Pharmaceutiques et Biologiques	Directeur : Mme. Christine VINCIGUERRA
Institut des Sciences et Techniques de la Réadaptation	Directeur : M. Xavier PERROT
Département de formation et Centre de Recherche en Biologie Humaine	Directeur : Mme. Anne-Marie SCHOTT

COMPOSANTES ET DEPARTEMENTS DE SCIENCES ET TECHNOLOGIE

UFR Biosciences	Directrice : Mme Kathrin GIESELER
Département Génie Electrique et des Procédés	Administratrice provisoire : Mme Rosaria FERRIGNO
Département Informatique	Administrateur provisoire : M. Behzad SHARIAT
Département Mécanique	Administrateur Provisoire : M. Marc BUFFAT
UFR – Faculté des Sciences	Administrateur provisoire : M. Bruno ANDRIOLETTI
UFR STAPS	Directeur : M. Yannick VANPOULLE
Observatoire de Lyon	Directrice : Mme Isabelle DANIEL
Ecole Polytechnique Universitaire Lyon 1	Directeur : M. Emmanuel PERRIN
Ecole Supérieure de Chimie, Physique, Electronique (CPE Lyon)	Directeur : M. Gérard PIGNAULT
Institut Universitaire de Technologie de Lyon 1	Directeur : M. Christophe VITON
Institut de Science Financière et d'Assurances	Directeur : M. Nicolas LEBOISNE
Ecole Supérieure du Professorat et de l'Education (ESPE)	Administrateur provisoire : M. Pierre CHAREYRON

Résumé

LES ARNS SÉCRÉTÉS PAR LE VIRUS DE L'HÉPATITE B SONT TRANSPORTÉS PAR LES VESICULES EXTRACELLULAIRES DANS LE SURNAGEANT DES HEPATOCYTES INFECTÉS

L'infection chronique par le virus de l'hépatite B (VHB) demeure un problème de santé publique puisque les stratégies antivirales actuelles ne permettent pas d'obtenir une guérison complète. Le développement de biomarqueurs non invasifs est nécessaire pour améliorer la prise en charge des patients et l'évaluation de nouvelles thérapies.

Les milieux de culture d'hépatocytes infectés par le VHB et traités ou non avec de la lamivudine (3TC) ont été collectés et concentrés. Les vésicules extracellulaires (VEs) ont été séparés par un gradient de densité. La distribution des protéines (virales ou marqueurs d'exosomes) et la distribution des ARN-VHB a été étudiée. L'analyse de suivi des nanoparticules (NTA), la microscopie électronique (MET) et l'analyse protéomique basée sur la spectrométrie de masse (MS) ont été utilisés pour caractériser les exosomes.

L'expression de marqueur des exosomes a été détectée dans les fractions légères, dépourvues de protéine de capside. De plus, 15% des ARN-VHB ont été détectés dans ces fractions enrichies en exosomes, comme le confirment les analyses NTA et MET. L'analyse spécifique des ARN-VHB a suggéré que l'ARN de 3,5 Kb n'est pas l'unique espèce d'ARNs secrétée par les hépatocytes infectés. Le traitement avec le 3TC augmente la sécrétion d'ARN-VHB, principalement dans les fractions associées aux exosomes. Enfin, l'analyse MS a montré que le VHB impacte la sécrétion des protéines extracellulaires.

Nos résultats montrent que les exosomes transportent des ARN-VHB. Ces connaissances aideront au développement et à l'interprétation des ARN sériques du VHB en tant que nouveau biomarqueur de l'infection chronique par le VHB.

Mots Clés : Virus de l'hépatite B, Vésicules Extracellulaires, Exosomes, ARNs Viraux, Biomarqueur

Abstract

SECRETED HEPATITIS B VIRUS (HBV)-RNA ASSOCIATES WITH EXTRACELLULAR VESICLES IN THE SUPERNATANT OF INFECTED HEPATOCYTES

Chronic Hepatitis B virus (HBV) infection remains a global health burden since current antiviral strategies are unable to achieve a complete cure. Non-invasive biomarkers are necessary to improve patients' management and evaluation of new therapies.

Supernatants from HBV-infected hepatocytes treated or not with lamivudine were processed through density gradient to allow physical separation of extracellular vesicles (EVs) and viral particles according to their buoyant density. Viral and EVs-associated proteins were analyzed, while HBV-RNAs were quantified by specific droplet digital (dd)PCR. Nanoparticle tracking analysis (NTA) and Transmission Electron Microscopy (TEM) were used to characterize the viral and non-viral components.

CD9 expression, marker of exosomes/EVs, was detected only in lower density fractions, which were deprived of HBc. Interestingly, 15% of HBV-RNAs were detected in lighter fractions enriched for exosomes, as confirmed by NTA and TEM analysis. ddPCR analysis using assays spanning the 5' region of 3.5Kb RNA or the HBx region suggested that 3.5 Kb RNA is the predominant but not the only viral RNA specie in cell supernatants. Treatment with 3TC increased the secretion of HBV-RNA, mainly in the fractions associated with exosomes. Finally, MS study revealed an impact of HBV on extracellular proteins secretion.

Our results show evidence for EVs carrying HBV RNAs and will help understanding the molecular biology of serum HBV RNA secretion. This knowledge will aid the development and interpretation of serum HBV RNAs as a novel biomarker for chronic HBV infection.

Key Words: Hepatitis B Virus, Extracellular Vesicles, Exosomes, Viral RNAs, Biomarker.

Résumé Substantiel

LES ARNS SÉCRÉTÉS PAR LE VIRUS DE L'HÉPATITE B SONT TRANSPORTÉS PAR LES VESICULES EXTRACELLULAIRES DANS LE SURNAGEANT DES HEPATOCYTES INFECTÉS.

Travaux de thèse réalisés par Delphine Bousquet, sous la direction du Pr. Fabien Zoulim et du Dr. Barbara Testoni, au sein du Centre de Recherche en Cancérologie de Lyon (CRCL), UMR INSERM U1052, CNRS 5286, Centre Léon Bérard, dirigé par Dr. Patrick Mehlen

Contexte Scientifique

Malgré le développement croissant de stratégies antivirales, l'infection chronique par le virus de l'hépatite B (VHB) reste un problème majeur de santé mondiale puisque les traitements actuellement disponibles ne permettent pas d'achever une guérison complète. La molécule en cause de la persistance du virus est un épisome viral maintenu dans le noyau des hépatocytes infectés appelé ADNccc pour ADN circulaire clos de manière covalente qui sert de matrice pour la transcription des ARN du VHB. Actuellement, le traitement de l'infection chronique par le VHB repose sur deux schémas thérapeutiques : l'interferon pégylé (PEG-IFN) et les analogues de nucléot(s)ides (ANs). Le PEG-IFN réduit la transcription virale, mais il est responsable d'effets secondaires graves limitant sa tolérance par les patients. Compte tenu de leur meilleure tolérance, la thérapie par ANs est souvent préférée, permettant un traitement à long terme. Toutefois, en inhibant la transcription inverse, les ANs empêchent la formation de nouveaux virions mais n'éliminent pas l'ADNccc intrahépatique, qui est le déterminant clé de la chronicité de l'infection par le VHB dans les hépatocytes. Une surveillance précise des niveaux et de l'activité de l'ADNccc intrahépatique est donc essentielle pour stratifier et surveiller les patients. Cependant, sa quantification est entravée par la nécessité de procédures de biopsie hépatique invasive. Par conséquent, il nécessaire d'identifier et de caractériser de nouveaux marqueurs non invasifs pour l'évaluation du pool d'ADNccc intrahépatique. À cet égard, les ARN du VHB, qui ont été identifiés dans le sérum des patients, pourraient être utiles dans l'évaluation de nouvelles thérapies antivirales visant à une guérison fonctionnelle de l'infection par le VHB. Malgré la littérature croissante sur le sujet, les ARN-VHB circulants restent encore insuffisamment caractérisés. Les méthodes d'isolement, de détection et de quantification diffèrent d'une étude à l'autre, empêchant une connaissance cohérente et solide des différentes espèces d'ARN et de leur association avec les particules circulantes.

Objectifs de l'étude et Stratégie Expérimentale

Dans cette étude, nous avons profité de modèles *in vitro* pertinents d'infection par le VHB pour établir une stratégie expérimentale solide afin caractériser les espèces d'ARN du VHB et les particules extracellulaires associées dans le surnageant des hépatocytes infectés. Pour ce faire, le projet de recherche a été divisé en trois axes principaux :

1. Caractérisation des entités physiques transportant les ARN-VHB secrétés dans le surnageant d'hépatocytes infectés.

Les hépatocytes infectés par le VHB libèrent des particules virales et des vésicules extracellulaires (VE) non virales lors de l'infection. Cependant, les mécanismes sous-jacents à la sécrétion d'ARN-VHB et les entités physiques dans lesquelles ils sont transportés sont encore mal caractérisés. Des rapports récents suggèrent que l'ARN du VHB est présent dans des particules de type virion et des capsides nues dans le surnageant cellulaire et le sérum du patient. Ainsi, comme le VHB utilise la machinerie de sécrétion de l'hôte pour sa propre sécrétion, nous avons émis l'hypothèse que les vésicules extracellulaires non virales telles que les exosomes pourraient également être impliquées dans la sécrétion des ARN du VHB. Pour explorer cette hypothèse, nous avons déterminé la distribution des ARN-VHB dans les différentes entités physiques présentes dans le surnageant cellulaire après une stratégie de séparation en gradient de densité spécifiquement adaptée. ELISA, Western Blot, suivi des nano-vésicules en suspension (NTA) et la microscopie électronique à transmission (MET) ont été utilisés pour définir la répartition des VEs et des particules virales, tandis que la PCR numérique à gouttelettes (ddPCR) a été utilisée pour détecter et quantifier les ARN du VHB sécrétés.

2. Identification de la nature des ARN-VHB sécrétés et de l'impact du traitement par les NA sur la composition de ces ARN.

Il a été proposé que les ARN-HBV extracellulaires étaient principalement constitués de l'ARN pré génomique (ARNpg). Cependant, des variantes d'épissage d'ARNs du VHB et l'ARNm HBx ont également été détectés dans le surnageant de culture de cellules dans lequel est intégré le génome du VHB ainsi que dans les sérums de patients atteints d'hépatite B chronique. Dans cette étude, nous avons utilisé une double approche pour clarifier la nature d'ARN-VHB extracellulaires dans les diverses populations d'EVs (particules virales ou exosomes) et évaluer si le traitement par les ANs pouvait affecter la nature des ARNs viraux sécrétés. En particulier, les extrémités 5' ont été caractérisées en couplant la technologie de 5' RACE (amplification rapide d'extrémités d'ADN complémentaire par réaction en chaîne par polymérase) et le séquençage « à longue lecture » à l'aide de la technologie Oxford Nanopore (ONT) MinION. En parallèle, des couples

d'amorces et de sondes spécifiques ont été conçus pour détecter et quantifier les troncatures à l'extrémité 3' des transcrits du VHB en ddPCR.

3. Profilage des protéines associées aux exosomes sécrétés par les hépatocytes : effet de l'infection par le VHB et du traitement des ANs.

Comme la biogenèse des exosomes a un chevauchement considérable avec l'assemblage et la sortie des particules virales, il est suggéré que certains virus puissent détourner la voie exosomale pour se propager de cellule à cellule ou éviter la surveillance immunitaire. Il est donc raisonnable de supposer que les protéines associées aux exosomes puissent être modulées par un état pathologique tel que l'infection par le VHB. Le profil des protéines qui sont contenues dans les exosomes peuvent donner une signature protéomique qui pourrait être informative lors de l'infection. À ce jour, seules quelques publications ont documenté l'implication des exosomes dans l'infection par le VHB et l'effet de l'infection par le VHB sur la signature protéomique des exosomes. Pour obtenir une analyse de compréhension de ces deux aspects, nous avons réalisé une étude de spectrométrie de masse en collaboration avec l'équipe de l'EDyP de Grenoble (France). L'objectif principal de notre étude était de mieux comprendre la modulation de la sécrétion de protéines associées aux exosomes lors de l'infection (avec ou sans traitement par les ANs) et d'identifier les facteurs clés qui pourraient être impliqués dans le transport d'ARN du VHB dans les exosomes.

Résultats et Perspectives

Les tests ELISA ainsi que le Western Blot permettant de détecter les protéines virales de surface (HBs) et de capside (HBc), ainsi que la quantification de l'ADN-VHB au sein des différentes fractions du gradient de densité ont montré que les virions étaient trouvés dans des fractions correspondant à une densité de 1,17-1,20 g/ml. L'expression concomitante de CD9 et la flotillin-1, deux marqueurs de exosomes, n'a été détectée que dans les fractions de plus faible densité, dépourvues de HBc. Fait intéressant, bien que la majorité des ARNs viraux ait été détectée dans les fractions associées aux virions et aux capsides nues, environ 15% ARN du VHB ont été détectés dans des fractions plus légères enrichies en exosomes, comme le confirment les analyses NTA et MET. De façon surprenante, nous avons également observé une augmentation de la quantité d'ARNs VHB sécrétés dans le surnageant de cellules traitées avec les ANs, plus particulièrement dans les fractions associées aux exosomes. L'analyse ddPCR utilisant des tests spécifiques pour les régions 5' de l'ARN de 3,5 Kb ou HBx a suggéré que l'ARN de 3,5 Kb est l'espèce d'ARN viral prédominante mais pas l'unique dans les surnageants cellulaires. De plus, des variants d'épissages et des transcrits d'HBx de longueurs variables ont été identifiés par

5’RACE. La distribution des ARN du VHB dans les fractions de gradient n'a montré aucune différence significative entre les échantillons traités ou non avec les ANs. Enfin, les analyses de MS ont montré un impact de l’infection par le VHB sur la sécrétion de protéines extracellulaires dans les fractions légères associées aux exosomes.

En conclusion, notre étude a été la première à caractériser en profondeur l'association entre les ARN-VHB extracellulaires et les exosomes. En concordance avec la littérature, il semble que les exosomes jouent un rôle important dans l'infection virale, même si la recherche sur les rôles des exosomes dans la réplication du VHB et l'infection par l'hépatite B est encore à un stade précoce. Une compréhension plus étendue et plus approfondie de l'interaction des exosomes et du VHB est nécessaire pour obtenir plus d'informations sur leur signification clinique à utiliser comme biomarqueur potentiel pour l’infection chronique par les VHB.

TABLE DES MATIERES

Table des matières 1
Illustration Table 5
Abbreviations 7
Introduction 13
I. Overview 13
II. Hepatitis B Virus (HBV) 15
1. Background 15
i. History 15
ii. Viral Classification 15
iii. Genotypes 17
iv. Common routes of transmission 17
2. HBV Biology 19
i. Viral Structure 19
ii. Genome Structure and Organization 21
iii. RNA Transcripts 25
iv. Viral Proteins 28
1. Viral Cycle 37
i. Viral Entry: Attachment to the hepatocyte surface 39
ii. HBV Particles Intracellular Trafficking 40
iii. Uncoating and Nuclear Import 40
iv. cccDNA Formation and Regulation 43
v. pgRNA transcription, encapsidation and retro-transcription 45
vi. Fate of mature nucleocapsids: Envelopment & Secretion 49
vii. Release of Subviral Particles: Spheres and Filaments 52
2. Models for the study of human HBV infection 55
i. *In vitro* models 55
ii. *In vivo* models 56
3. Chronic Hepatitis B (CHB) 57

i. Classification of patients with HBV infection 57
ii. Treatments 61
iii. Biomarkers in CHB 63
III. Extracellular Vesicles (EVs) and viruses 75
1. Generalities about EVs 77
i. What are EVs? 77
ii. Exosome Biogenesis 77
iii. Biological function of exosomes 78
2. Molecular Characteristics 81
i. Exosome heterogeneity 81
ii. EV-specific proteins? 81
iii. RNAs contained within exosomes 82
3. Isolation Techniques 82
IV. Exosomes and viruses 83
1. Viral impact on EV content 83
2. Evading Immune Responses 84
3. Invasion and Replication within the Host Cell 85
4. Exosomes Contribute to Host Immunity against Viral Infection 85
V. Exosomes and HBV 87
1. Exosomes Participate in HBV Replication 87
2. Exosomes Modulate Immune Responses during HBV Infection 88
3. Exosomes as Markers for HBV Diagnosis or monitoring? 89
Research Project 91
I. Scientific Background 91
II. Context of the project 93
Results: Part 1 99
I. Quantification of intrahepatic viral markers after NAs treatment using a qPCR method 99
II. Quantification of secreted viral markers in supernatant of infected hepatocytes 102
III. HBV-RNA are associated with viral and non-viral particles in the supernatant of infected hepatocytes 104
IV. Circulating RNAs are contained within EVs in the supernatant of infected hepatocytes 118
V. Modulation of exosome secretion 120
Results: Part 2 126
I. Various HBV-RNAs species are secreted in the supernatant of infected hepatocytes 126
Results: Part 3 134

I. General Experimental Design 134
II. Exosomes enrichment and characterization 136
III. Differential profiling of HBV infected HepG2-NTCP derived exosomes 140
Discussion & Perspectives 146
I. Objectives of the research project 146
II. Experimental Models 146
III. Which particles carry HBV-RNAs in cell supernatant? 148
IV. How are HBV-RNAs shuttled into exosomes? 150
V. What could be the role of exosomes derived from HBV-infected hepatocytes? 152
1. Dual role in the regulation of immune responses 152
2. Are exosome derived from HBV-infected hepatocyte able to generate de novo infection on naïve hepatocytes? 154
3. Role of exosomes derived from HBV-infected cells in the pathogenesis of liver disease 156
VI. Heterogeneity of extracellular HBV-RNA species and effect of NA treatment 157
VII. HBV-RNAs in exosomes as non-invasive biomarker for HBV infection 157
VIII. Perspectives 161
Material & Methods 164
Supplementary Figures 174
References 184
Acknowledgements 186
Appendices 192
I. Circulating Hepatitis B Virus (HBV)-RNAs associates with extracellular vesicles (EVs) in cell supernatant and patient's serum (Article in preparation) 192
II. Huh7-3D29 Clonal cell line secretes HBV RNA in excess and low quantities of HBV DNA: the generation of an HBV RNA standard (Article in preparation) 192
III. Communications 192
1. Oral Presentations 192
2. Poster Presentations 192

2

ILLUSTRATION TABLE

Figure 1. Distribution of HBV Genotypes across the world. 16
Figure 2. HBV Routes of Transmission. 16
Figure 3. Schematic Diagram of HBV Particles 18
Figure 4. HBV rcDNA. 21
Figure 5. cccDNA AND ORFs. 22
Figure 6. Viral transcripts and regulatory elements. 24
Figure 7. Summary of HBV splice variants described in the literature. 26
Figure 8. Structure and proposed transmembrane topology of HBV envelope proteins. 29
Figure 9. Capsid proteins sequences and structural domains 30
Figure 10.HBc and HBeAg processing. HBcAg, 32
Figure 11. Viral polymerase. 32
Figure 12. Schematic representation of HBX. 34
Figure 13. Schematic representation of singly spliced HBV-RNA and HBSP translation product. 34
Figure 14. Schematic overview of the HBV cycle. 36
Figure 15. Viral entry. 38
Figure 16. cccDNA formation. 42
Figure 17. pgRNA secondary structure. 45
Figure 18. From pgRNA TO rcDNA: retrotranscription. 46
Figure 19. Model for HBV viral and subviral particle morphogenesis. 50
Figure 20. Human cell culture systems for the study of HBV infection. 54
Figure 21. Different stages of hbv chronic infection 57
Figure 22. HBV Cure 59
Figure 23. Timeline showing the year of US FDA approval for individual HBV treatment agents. 60
Figure 24. Schematic representation of the HBV cycle and the targets of direct-acting antivirals. 60
Figure 25. What is a good biomarker?. 63
Figure 26. HBV biomarkers. 64
Figure 27. Physical characteristics of different EVs subtypes. 76
Figure 28. Sorting machineries involved at different steps of exosome biogenesis. 76
Figure 29: Identity and the heterogeneity of exosomes. 80
Figure 30 : Evaluation of Lamivudine treatment (3TC) effect on intracellular viral parameters. 98
Figure 31 : Evaluation of Lamivudine treatment (3TC) effect on extracellular viral parameters. 100
Figure 32: Scheme of Iodixanol / Sucrose density gradient. 103
Figure 33. Analysis of viral and non-viral proteins across density gradient separation of exosomes, subviral particles, and virions in HepG2-NTCP. 105

Figure 34. Analysis of viral and non-viral proteins across density gradient separation of exosomes, subviral particles, and virions in HepG2-NTCP. 107
Figure 35. HBV-DNA and RNAs repartition across fraction in each individual replicate in HepG2-NTCP. 108
Figure 36. HBV-DNA and RNAs repartition across fraction in each individual replicate in PHH. 109
Figure 37. EVs collected from HepG2-NTCP cells supernatant treated or not with 3TC were fractionated by density gradient separation using iodixanol 111
Figure 38: (A) Concentration and (B) Size measurement of EVs in each fraction after density gradient. 113
Figure 39 : F4 is mainly composed of exosomes and SVPs. 115
Figure 40 : MNase protection assay. 117
Figure 41. EVs and HBV-RNAs schematic repartiton across density gradient 117
Figure 42 : Different doses of EtOH were added to HepG2-NTCP cells and particles were quantified by NTA. 119
Figure 43 : Manumycin A and GW4869 inhibit exosomes secretion by blocking two independent pathways. 119
Figure 44 : Manumycin A and GW4869 dose response. 121
Figure 45: Exosomes associated proteins and HBs detected by western blot. 121
Figure 46: NTA quantification and size distribution of the particles treated or not with 10µM of GW4869. 122
Figure 47: 5'RACE analysis of RNA secreted by infected hepatocytes. 125
Figure 48. Alignment of sequenced amplicons with respect to HBV genotype D (reference sequence GenBank U95551.1). 127
Figure 49. Heatmap of the RNAs species found in each fractions of the gradients in (A) HepG2-NTCP and (B) PHH. 128
Figure 50. Characterization of HBV-RNA species contained in extracellular compartments of infected HepG2-NTCP cells and PHH. 129
Figure 51. Venn diagram of proteins identified in HegG2-NTCP exosomes by mass spectrometry. 137
Figure 52. Gene enrichment according to cellular components.. 137
Figure 53. PCA of sEVs and sEVS + SVPs samples. 139
Figure 54. Heatmap visualization of protein secretion profiles in each sample preparation. 139
Figure 55. Gene ontology analysis in term of biological process was done on the differentially secreted host proteins. 141
Figure 56. Proposed model for the increase of HBV-RNAs secretion under NAs therapy. 149
Figure 57. Exosome have a dual effect on the modulation of antiviral response. 153
Figure 58. Proposed model for pgRNA 3'truncation. 159

ABBREVIATIONS

3TC: Lamivudine

AASLD: American Association for the Study of Liver Diseases

ADV: Adefovir dipivoxil

Alix: Apotosis-linked gene 2[ALG-2]-interacting protein

ALT: Alanine Aminotransferase

ANR: National Research Agency

AP2: Adaptator Protein 2

APCs: Antigen-Presenting Cells

APOBEC3A: Apolipoprotein B MRNA Editing Enzyme Catalytic Subunit 3A

ASO: Antisense Oligonucleotide

Atg5: Autophagy related 5

NES: Nuclear Export Signal

bp: base pair

CAGE: Cap analysis gene expression

cccDNA: Covalently Closed Circular DNA

CCL2: C-C motif chemokine ligand 2

CHB: Chronic Hepatitis B

ChIP: Chromatin ImmunoPrecipitation

CHMP: Charged Multivesicular Bodies Protein

CLEIA: Chemiluminescent Enzyme Immunoassay

CoxIV: Cytochrome C Oxidase Subunit 4

CPB: CREB Binding Protein

CpG: Cytosine and Guanine separated by one phosphate

CsCl: Cesium Chloride

CTD: Carboxyl Terminal Domain

CUL4: Cullin4

DAAs: Direct-Acting Antivirals

DDB1: DNA Damage Binding Domain 1

DHBV: Duck Hepatitis B Virus

DMSO: Dimethyl sulfoxide

DNA: Deoxyribonucleic Acid

DR: Direct Repeat

ddPCR: droplet digital PCR

dsL-DNA: double-stranded linear DNA

DYNLL1: Dynein Light-Chain LL1

EASL: European Association for the Study of the Liver

EBV: Epstein Barr virus

ECs: epithelial cells

EE: Early Endosome

EEA1: Early Endosome Antigen

EGFR: Epidermal Growth Factor Receptor

ELISA: Enzyme-Linked Immunosorbent Assay

Enh: Enhancer

Eps15: Epidermal Growth Factor Receptor Pathway Substrate 15)

ER: Endoplasmic Reticulum

ESCRT: Endosomal Sorting Complexes Required for Transport

EtOH: Ethanol

EV: Extracellular Vesicle

FACS: Fluorescence-Activated Cell Sorting

FDA: Food and Drug administration

FEN1: Flap Endonuclease 1

flRNA: full length RNA

GCN5: General Control Nonderepressible 5

GM130: Cis-Golgi Matrix Protein

Grp94: Heat Shock Protein 90kDa Beta

GSHV: Ground Squirrel Hepatitis Virus

HAV: hepatitis A virus

HBc: Hepatitis B Capsid protein

HBcAb: Hepatitis B core antibody

HBDSP: Hepatitis B Doubly Spliced Protein

HBeAg: Hepatitis "e" antigen

HBs: Hepatitis B Surface protein

HBSP: Hepatitis B Spliced Protein

HBV: Hepatitis B Virus

HBx: HBV X Protein

HCC: Hepato Cellular Carcinoma

HCMV: human cytomegalovirus

HCV: Hepatitis C virus

HDAC1: Histone Deacetylase 1

HGS: Hepatocyte Growth factor

HIV: Human Immunodeficiency Virus

HNFs: Hepatocyte Nuclear Factors

hnRNP: Heterogeneous Nuclear Ribonucleoprotein

Hsp: Heat shock proteins

HSPGs: Heparan Sulfate Proteoglycans

HSV: Herpes Simplex Virus

HTAs: Host-Targeting Agents

IgG : Immunoglobulin G

IL : Interleukin

ILVs: Intra-Luminal Vesicles

ISGs: Interferon-Stimulated Genes

IU: International unit

Kb: kilo bases

KD: Knockdown

kDa: kilo Dalton

LAMP2: Lysosome-Associated Membrane Protein 2

LE: Late Endosome

L-HBS: Large HBV Surface Protein

LIG1 : DNA ligases 1

LIG3 : DNA ligases 3

LMP1: Latent Membrane Protein 1

LNA: Antisense Locked Nucleic Acid

LNPCs: Liver Nonparenchymal Cells

LOD: Limit Of Detection

MAVS: Mitochondrial Antiviral Signaling Protein

M-HBS: Medium HBV Surface Protein

MHC: Major Histocompatibility Complex

miRNAs: micro RNA

ml: milliliter

MNase: Micrococcal nuclease

MVB: Multi Vesicular Bodies

MyD88: Myeloid differentiation factor 88

NAs: Nucleo(s)tides Analogues

NCs: Naked Capsids

NFκB: Nuclear Factor Kappa B

NK: Natural Killer

NKG2D: Natural Killer (NK) Group 2D

NLS: Nuclear Localization Signal

nm: Nanometer

NPC: Nuclear Pore Complex

nt: Nucleotide

NTA: Nanoparticle Tracking Analysis

NTCP: Sodium Taurocholate Cotransporting Polypeptide

NTD: Arginine terminal domain

ONT: Oxford Nanopore Technology

ORF: Open Reading Frame

p22cr: 22 kDa PreCore Protein

p300: Histone acetyltransferase p300

PAS: Poly Adenylation Signal

PCAF: P300/CBP-associated factor

PCR: Polymerase chain reaction

pcRNA: precore RNA

PD1: Programmed cell Death protein 1

PDL1: Programmed death-ligand 1

pegIFN-α: Pegylated interferon-alpha

pgRNA: pregenomic RNA

PHH: Primary Human Hepatocytes

PKC: Protein kinase C

Pol: Polymerase

POLα: DNA polymerase alpha

POLκ: DNA polymerase kappa

PRE: post-transcriptional regulatory element

P-S FP: Polymerase-Surface Fusion Protein

PTA : Phosphotungstic acid

PUF60: poly(U) binding splicing factor 60

qHBsAg: Quantitative Hbs Antigen

RACE: Rapid amplification of cDNA ends

rcDNA: Relaxed circular DNA

RNA: Ribonucleic Acid

ROC: Receiver Operating Characteristic

RT: Reverse Transcription

RT-qPCR: Quantitative Reverse Transcription PCR

SBP: Surface Antigen Binding Protein

SEM: Scanning Electron Microscopy

sEVs: Small Extracellular Vesicles

S-HBs: Small HBV Surface Protein

shRNA: Short Hairpin RNA

siRNAs: Small interfering RNA

Sirt1: Sirtuin 1

Smc5/6: Structural Maintenance of Chromosomes

SP: Splicing Product

ss: splicing site

SVPs : Sub Viral Particles

TAR : Transactivation Response Element

TARDBP: TAR DNA Binding Protein

TDP2: tyrosyl-DNA-phosphodiesterase 2

TEM: Transmission Electron Microscopy

TFV: Tenofovir

TICAM-1: Toll Like Receptor Adaptor Molecule 1

TLR: Toll Like Receptor

TM: TransMembrane

TNF-α: Tumor Necrosis Factor Alpha

trRNAs: Truncated RNAs

TSG101: Tumor susceptibility gene 101

TSS: Transcription Start Site

Vps4: Vesicle-fusing ATPase

WHV: Woodchuck Hepatitis Virus

INTRODUCTION

Overview

Hepatitis B Virus

Extracellular Vesicles (EVs) & Viruses

Exosomes & HBV

INTRODUCTION

I. Overview

Despite the availability of a prophylactic vaccine and antiviral treatments, Hepatitis B Virus (HBV) remains the main causative agent of chronic hepatitis, since it affects more than 250 million people worldwide. Chronic carriers have a high risk of developing severe liver complications, such as fibrosis, cirrhosis and hepatocellular carcinoma (HCC) (Trépo et al., 2014). As a consequence, chronic hepatitis B (CHB) remains a major health burden, with more than 800 000 deaths attributed to its associated disease. Current treatments such as nucleo(s)tide analogs (NAs) do not enable to achieve a complete cure because of the key viral molecule implicated in HBV persistence, the so-called covalently closed circular DNA (cccDNA). This episomal form of the viral genome stably resides in the nucleus of infected hepatocytes. cccDNA carries the complete viral genomic information and is the only template for viral replication (Nassal, 2015). By inhibiting the viral polymerase and the subsequent release of new infectious particles, current treatments, mainly NAs, maintain viral load under control to undetectable levels. However, these treatments neither affect intrahepatic pool nor transcriptional activity since they act downstream of cccDNA formation and viral RNA synthesis from cccDNA. For these reasons, new strategies toward a curative therapy for HBV involving direct targeting of cccDNA, either by degradation, or by transcriptional shutdown are highly needed (Roca Suarez et al., 2021). Equally important is the development of non-invasive biomarkers for monitoring intrahepatic cccDNA levels and activity, as they could facilitate the evaluation of emerging therapeutic drugs. In this respect, the quantification of circulating HBV-RNAs has recently raised much interest. Several studies have provided evidence that HBV-RNAs could be used as a surrogate marker of cccDNA transcription in the liver. However, many unresolved questions about their nature, the extracellular compartments involved in their transport and their biological and clinical prognostic relevance still remain (Charre et al., 2019). Although several methodologies have been put forward as means to study circulating HBV-RNA and determine its clinical relevance, the implementation of a general standardized technique is still needed to get insights into this new biomarker, mainly in response to NAs therapy.

II. Hepatitis B Virus (HBV)

1. Background

i. History

HBV is an enveloped, hepatotropic and non-cytolytic DNA virus belonging to the *Hepadnaviridae* family. Written 3000 years BC, it was in the "First Medical Treatise" that Hippocrates documented outbreaks of jaundice for the first time. Later, Lurman made the first description of an epidemic of “serum hepatitis” in 1885. He documented an hepatitis syndrome touching almost 200 German workers after a vaccination campaign using human lymph, which inadvertently contained an infectious agent (Block et al., 2016). Afterwards, many cases have been reported; however, it was not until 1964 that Blumberg et al. reported a novel antigen in sera of Australian aboriginal population. Firstly named “Australia Antigen”, it took three more years to link this antigen with post-transfusion hepatitis and to declare it a prototype seromarker of active hepatitis B (Blumberg et al., 1967). The antigen was studied under an electron microscope which suggested that it was likely to be a virus capsid which was later confirmed by Dane and colleagues (Dane et al., 1970). In 1976, Blumberg was awarded the Nobel Prize in medicine for the discovery of HBV.

ii. Viral Classification

HBV is a partially double-stranded DNA virus replicating through an RNA intermediate retro-transcribed into DNA by the viral polymerase. Based on its tropism, genetic organization, morphology and replication mechanisms, HBV belongs to the Baltimore class VII of pararetroviruses, which is composed of *Hepadnaviridae* and *Caulimaviridae*. This viral family can be further divided into two genuses: i) the orthohepadnaviruses that infect mammals, such as HBV, Woodchuck Hepatitis Virus (WHV), ground squirrel hepatitis virus (GSHV) and ii) the avihepadnaviruses that infect birds, such as Duck Hepatitis B Virus (DHBV). Each of these viruses is indigenous to its host (Schaefer, 2007).

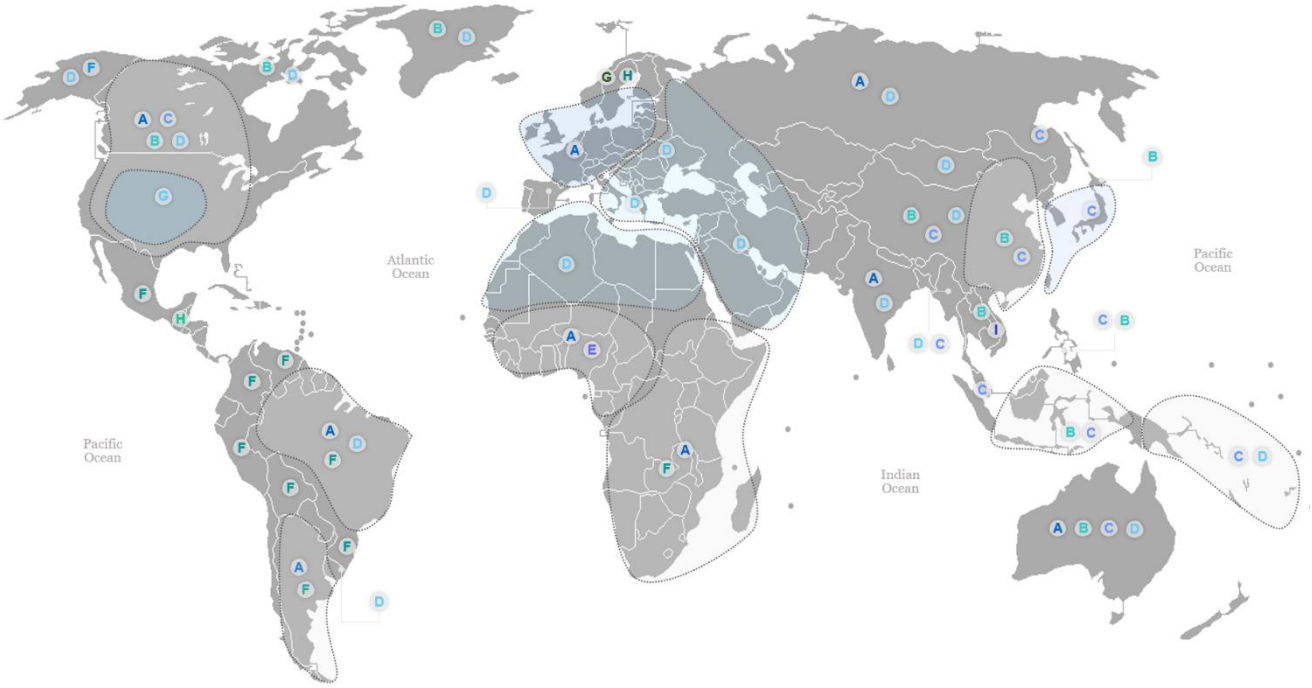

Figure 1. Distribution of HBV Genotypes across the world. HBV is classified into 10 genotypes: A to J. Genotypes are defined by a strain difference higher than 8% in the entire nucleotide sequence. Adapted from Locarnini SA et al. (Front Microbiol. 2020).

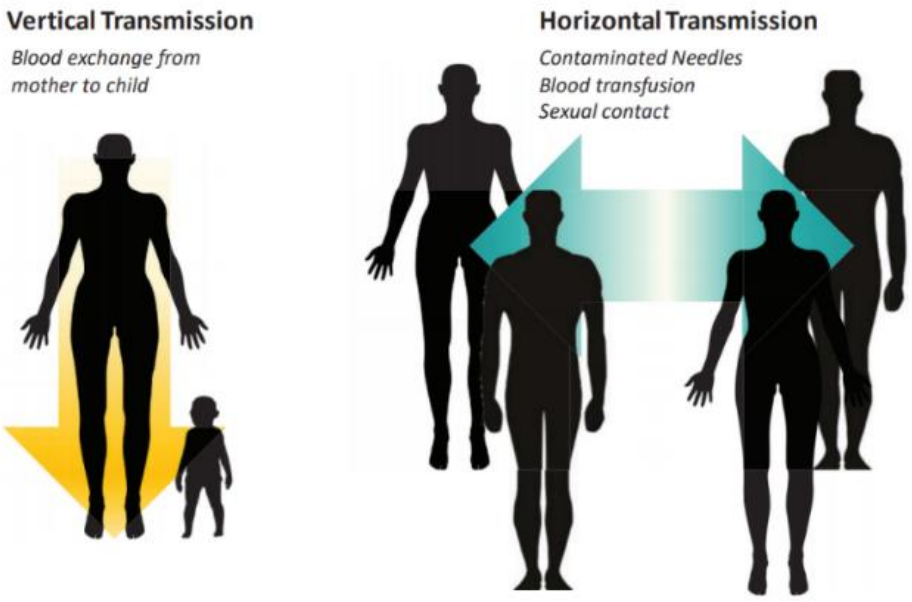

Figure 2. HBV Routes of Transmission. HBV can either be transmitted vertically, which is the main route of transmission in endemic areas, or horizontally, mostly represented in low endemic countries (Chapus F. Thesis illustration).

iii. Genotypes

Over centuries, spontaneous error of viral reverse transcriptase causing punctual mutations in HBV genome led to the emergence of several genotypes, subtypes, mutants, recombinants, and even quasispecies. HBV genotypes have distinct geographical distributions (Fig. 1), which is thought to be directly linked with endemicity, transmission modes, as well as clinical outcomes.

Owing to the genetic divergence of the entire HBV genome, at least 10 HBV genotypes (A to J) and several subtypes have been identified so far. In addition, more than 30 subtypes have been described. One of the consequences of HBV genotypic variability is the appearance of mixed genotypes infection and intergenotypic recombination that could be of great biological and clinical interest (Kramvis, 2014).

iv. Common routes of transmission

HBV can be detected in serum, urine, saliva, nasopharyngeal secretions, urine, tears, vaginal secretions, menstrual blood, and semen (Lavanchy, 2004). For this reason, the main routes of HBV infection involve exposure to blood or blood-derived products, such as during childbirth from an HBV-positive mother, blood transfusion, or other potential sources of percutaneous exposure, including sexual intercourse. Two different types of transmission route exist: horizontal or vertical (Fig. 2).

Vertical transmission is defined by perinatal contact of newborns with an infected mother and varies depending on the geographical regions. Perinatal infection is the most common way of transmission in endemic areas (W. M. Lee, 1997). **Horizontal** transmission can occur by contact with infected blood, mainly transmitted by contaminated needles, blood perfusion or sexual exposure.

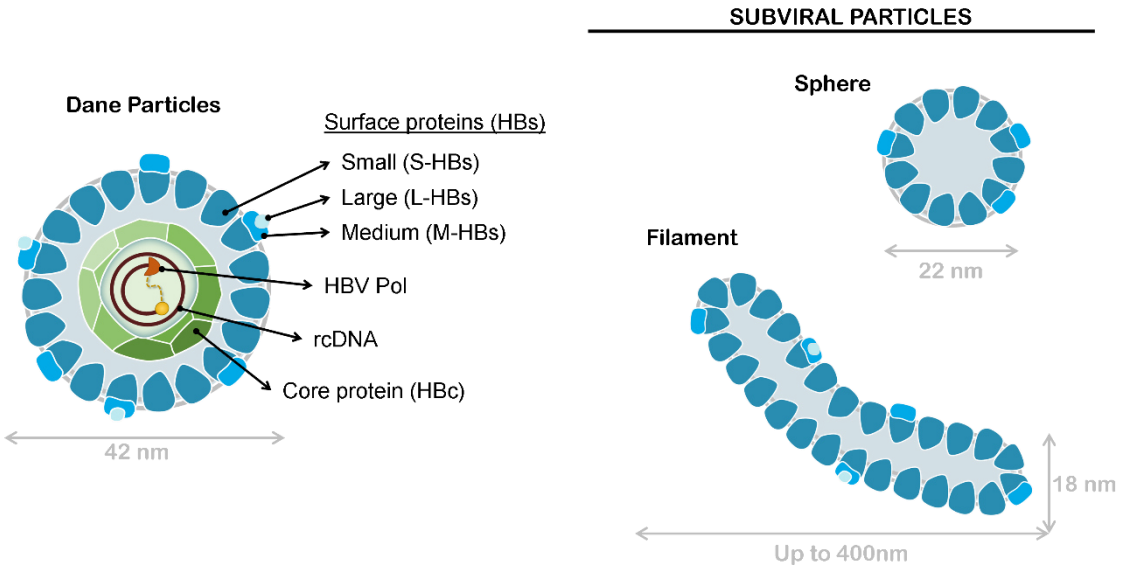

Figure 3. Schematic Diagram of HBV Particles.

2. HBV Biology

i. Viral Structure

Two types of virions are secreted: i) a minor population of complete virions containing a mature nucleocapsid with the partially double-stranded, relaxed circular DNA (rcDNA) genome and ii) a major population containing an empty capsid without viral genome (empty virions). Secretion of both types of virions requires interaction between the HBV core protein (HBc) and HBV Surface protein (HBs).

Virions (Dane Particles)

HBV infectious particle, the Dane particle, named by the researcher who first described it, has a diameter of 42 nm (Fig.3). Dane particles contain rcDNA, which is linked to the viral polymerase and packaged in an inner icosahedral nucleocapsid enveloped by viral HBs. The nucleocapsid is assembled by 120 copies of HBc and the envelope is made of three types of HBs: Small (S-HBs), Medium (M-HBs) and Large (L-HBs), in a ratio of approximately 5:3:2.

Empty "genome-free" virions

The second category of virions released into the blood is the more recently discovered and characterized empty virion (genome-free virion) that contains the capsid and envelope but no viral RNA or DNA (Ning et al., 2011a). Genome-free or empty virions are produced in large excess relative to the number of DNA-containing virions in cell culture and patient's serum (Luckenbaugh et al., 2015; Ning et al., 2011b). Empty virions lacking any DNA genome require the presence of empty nucleocapsids. It is assumed that, in contrast to "regular" immature nucleocapsids, these empty capsids lack signals that prevent envelopment and thus can be enveloped by the surface proteins (J. Hu & Liu, 2017). A more recent study suggested that the light virion particles might actually contain, instead of the normal capsid protein, an aberrantly processed PreCore protein related to the aforementioned HBeAg (Kimura et al., 2005). This protein lacking the arginine-rich C-terminal domain (CTD) can still assemble into capsid particles but fails to bind nucleic acids (Gallina et al., 1989; Kimura et al., 2005). However, other reports claim that the core protein found in empty virions contains the entire CTD (Ning et al., 2017). The clinical significance of empty HBV virions and their role in chronic viral infection remain to be elucidated.

RNA virions

Surprisingly, it appears that HBV can also secrete RNA-containing particles. Recently, several reports identified HBV-RNA in cell culture supernatant and in the serum of patients (Jansen et al., 2016a; Rokuhara et al., 2006; van Bömmel et al., 2015; J. Wang et al., 2016a). These studies suggest that HBV-RNAs represent 0.1 to 1% of HBV DNA levels in the absence of treatment. The nature of the viral RNAs as well as the compartments in which they are transported in the bloodstream remains to be better characterized and will be extensively described later in this manuscript.

Subviral Particles

A major characteristic during HBV infection is the secretion of a large excess of subviral particles (SVPs) in the serum of infected patients (Fig. 3). In contrast to virions, SVPs are devoid of HBV genome and nucleocapsid. The SVPs exist as spheres with a diameter of 22 nm and filaments of 18 nm width and a variable length between 80 and 400 nm. HBs proteins can assemble into secretion-competent SVPs that are composed solely of envelope proteins, lipids, and glycans. SVPs are found in the blood of infected individuals at up to 100,000-fold in excess over the complete virions (at 10^{14}/mL) (Ganem & Prince, 2004).The proportion of the three HBs proteins differ between viral particle types. It is estimated that filaments are composed by S, M and L-HBs at a ratio of approximately 1:1:4 whereas spheres contain less M-HBs compared to filaments with trace amounts of L-HBs (Short et al., 2009). SVPs are compact particles with a reported density of 1.21 g/mL in cesium chloride (CsCl), as compared to the density of infectious virions that ranges between 1.24 and 1.26 g/mL (Dreesman et al., 1972).

Naked Capsids

Besides virions, nucleocapsids can be secreted as naked capsids (NCs). Albeit it has been reported that NCs are poorly detected in the bloodstream of infected patients or chimpanzees (Possehl et al., 1992), they are found in the supernatant of HBV-replicating cell lines (D. Sun & Nassal, 2006). Moreover, it is noteworthy that most patients who have been exposed to HBV can elicit high titers of anti-HBc antibodies, suggesting a direct exposition to HBc even if the capsid might rapidly be cleaned for unknown reasons. Indeed, NCs carrying HBV-specific DNA and RNA species were recently detected in the blood of HBV patients as capsid-antibody-complexes (Bai et al., 2018). Since NCs are able to bind to cell surface-exposed heparan sulfate proteoglycans (HSPGs) and are competent for clathrin-

mediated endocytosis, their uptake may enhance transmission of HBV genomes (Cooper & Shaul, 2006).

ii. Genome Structure and Organization

rcDNA

With a genome size of only 3.2 kb, HBV is the smallest DNA virus described so far. As previously mentioned, the HBV genome is in the conformation of rcDNA (Fig. 4).

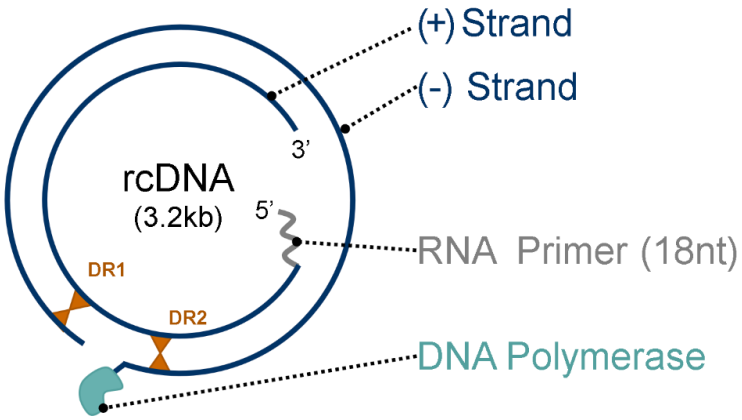

Figure 4. HBV rcDNA. rcDNA is a partially double-stranded relaxed circular DNA of 3.2 kb in length. The negative strand (-) is covalently attached to the viral polymerase via the terminal redundancy sequence. The incomplete positive strand (+) is bound to an RNA primer in its 5' end.

Its incomplete double-stranded structure relies on a complete negative strand (-) and a positive strand (+) having a gap of about 1500 nt. The complete (-) strand is the template for viral transcription and is covalently linked in its 5' end to the viral polymerase (Pol) (Summers et al., 1975). The 5' end of the incomplete (+) strand is associated with a capped RNA oligomer of ≈ 18 nt, derived from the pregenomic RNA (pgRNA), and serving as a primer for the synthesis of the DNA (+) strand during the reverse transcription (RT). The two strands are linked by an overlapping region of around 200 bp, thus maintaining the circular shape of the rcDNA (W. Gao & Hu, 2007). This cohesive overlapping region contains the 11 bp direct repeat sequences DR1 and DR2 (5'-TTCACCTCTGC-3'), involved in rcDNA synthesis. During RT, the RNA primer linked to the 5' end of the (-) strand has to be translocated onto the 3' end of the (+) strand and annealed to the complementary DR2 sequence. Together with hairpin formation at DR1 and sequence identity between DR1 and DR2, these phenomena are mandatory for an efficient retrotranscription of pgRNA (Habig & Loeb, 2006) *(See below "pgRNA transcription, encapsidation and retro-transcription").*

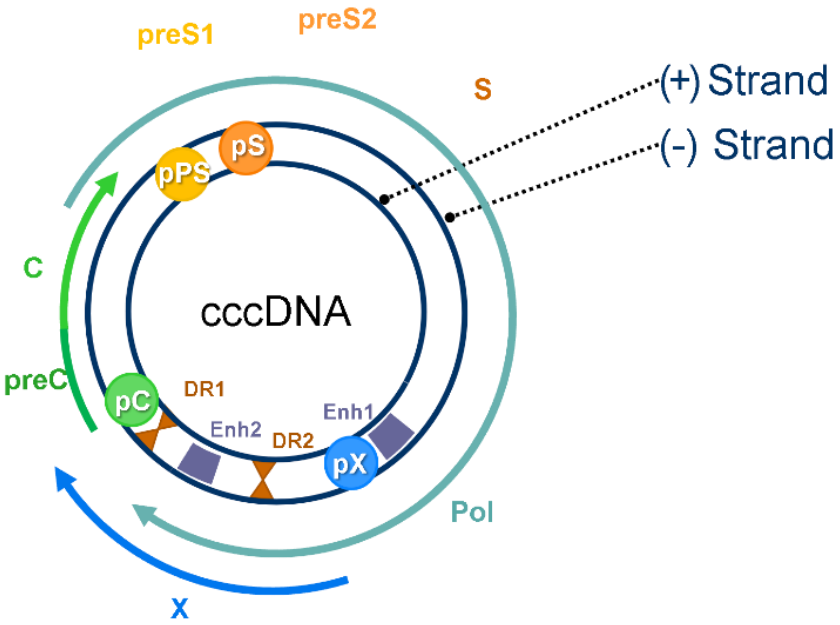

Figure 5. cccDNA AND ORFs. cccDNA contains four overlapping open reading frames (ORF), namely preCore/Core ORF, for the synthesis of HBeAg and HBc; S ORF, for L-, M-, and S-HBsAg; Pol ORF, for the viral polymerase/retro-transcriptase, and X ORF, for HBx.

cccDNA

Once in the nucleus of infected hepatocytes, rcDNA is converted into a covalently closed circular DNA, also called cccDNA. This cccDNA is an episomal form of the HBV genome, which is responsible for viral persistence in HBV-infected hepatocytes. cccDNA is the unique template for transcription of all viral RNAs, including the pgRNA, which is the RNA intermediate during viral replication. Viral transcription is regulated by four promoters, two enhancers, and a common polyadenylation signal. The HBV genome contains four overlapping open reading frames (ORFs) all oriented in the same direction (Nassal, 2015):

- Pol ORF, the longest one, encodes for the viral polymerase.
- Pre-core/Core ORF encodes for HBc and the soluble protein HBeAg, which is essential for establishing chronic infection.
- The surface protein ORF (S-ORF) encodes the three different envelop proteins (S-, M-and L-HBsAg).
- HBx ORF encodes the viral transactivator HBx.

Linear double-stranded DNA (dsL-DNA)

During rcDNA synthesis, RNA primer translocation can be altered, resulting in an *in situ* priming, from DR1 (Habig & Loeb, 2006). This process occurs within 10% of mature nucleocapsids and leads to the formation of a linear double-stranded DNA (dsL-DNA). dsL-DNA can then i) form defective cccDNA, unable to support rcDNA synthesis due to insertion(s) or deletion(s) appearing during the ligation of dsL-DNA extremities; or ii) be integrated into the host cell genome. Integrated HBV sequences can support HBsAg and HBx synthesis, but not the other viral protein production or pgRNA transcription, hence not representing a source of viral replication. However, dsL-DNA integration has been shown to have an impact for tumor initiation and progression in the context of hepatocellular carcinoma (HCC). It is important to note that the mechanisms of HBV-induced HCC carcinogenesis are still poorly understood as they involve many other factors besides viral integration (Levrero & Zucman-Rossi, 2016).

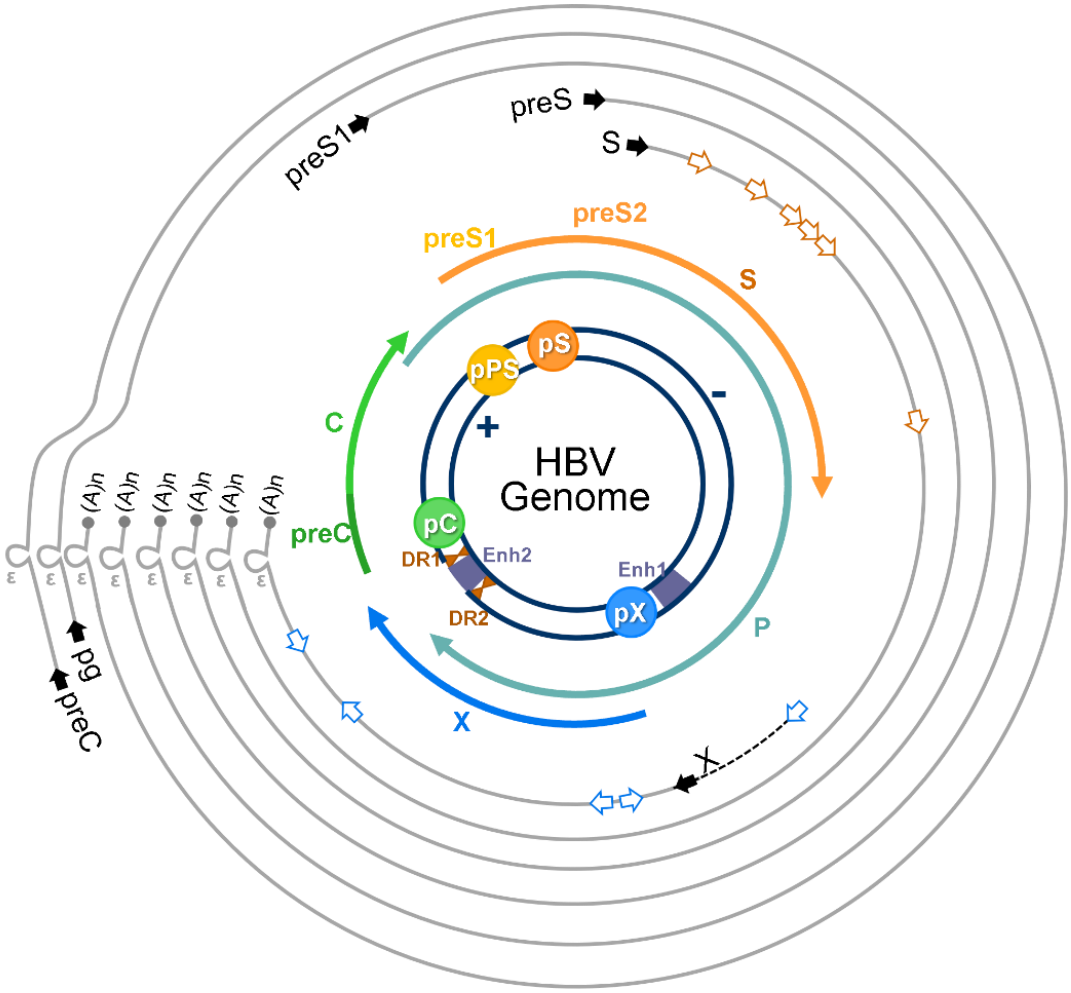

Figure 6. Viral transcripts and regulatory elements. The HBV genome encodes six viral mRNAs: the two longer-than-genome length 3.5 kb precore and pregenomic RNAs, the 2.4 kb preS1 RNA, the 2.1 kb preS2 RNA, the 2.1 kb S RNA and the 0.7 kb X RNA. Major viral transcripts start at distinct TSS (black arrow) and end at a common polyA site (dark grey dot – (A)n). Weaker TSS identified by Altinel et al. (2016), are represented in orange arrow for S transcripts and light blue arrow for X. Viral transcription is regulated by four promoters: promoter C (pC), promoter preS (pPS), promoter S (pS) and promoter X (pX); and by two enhancers: Enh-I and Enh-II.

iii. RNA Transcripts

As mentioned above, cccDNA is the template for the transcription of viral RNAs all having their own Transcription Start Sites (TSS), but sharing a common polyadenylation signal (PAS) (Fig. 6). They are transcribed by the host RNA-Polymerase II machinery, capped in their 5' extremity and they present a polyA tail similar to cellular mRNAs (Rall et al., 1983). Below are the transcribed RNAs that have been reported:

- **The pgRNA** encodes an over length transcript (1.1-fold longer than the genome) including a terminal redundancy of 120 nt containing essential elements for viral replication. pgRNA has the dual function of i) being the template for reverse transcription and ii) encoding HBc and the viral polymerase (Beck & Nassal, 2007). The pol ORF is less efficient than the Pre-core/Core ORF in an 1:240 ratio (Kann & Gerlich, 1994).

- **The Pre-core mRNA** (preC mRNA) encodes the secreted HBeAg. pgRNA and pre-Core mRNA are only 30 bp different in length, pre-core mRNA being longer, and come from two distinct promoters, while generally assumed as the "Pre-core/Core" promoter (Yu & Mertz, 1996).

The 2.4 kb RNA:

- **The PreS1** mRNA is transcribed from the PreS1 promoter and encodes the Large HBsAg.

The 2.1 kb RNAs:

- **The PreS2** mRNA is 2.1 kb long and is synthesized from the PreS2/S promoter. It encodes the Medium HBsAg.
- **The S mRNA** is also 2.1 kb long and is also regulated by the PreS2/S promoter. It encodes the Small HBsAg. PreS2 TSS, starting at position 3182 in D genotype, is only 26 bp upstream S TSS, starting at position 25 in the same genotype, thus giving rise to two independent mRNAs (Altinel et al., 2016; Stadelmayer et al., 2020).

The 0.7 kb RNA:

- **The X mRNA** is the smallest HBV RNA with a 0.7 kb length. It encodes the HBx protein (Moolla et al., 2002).

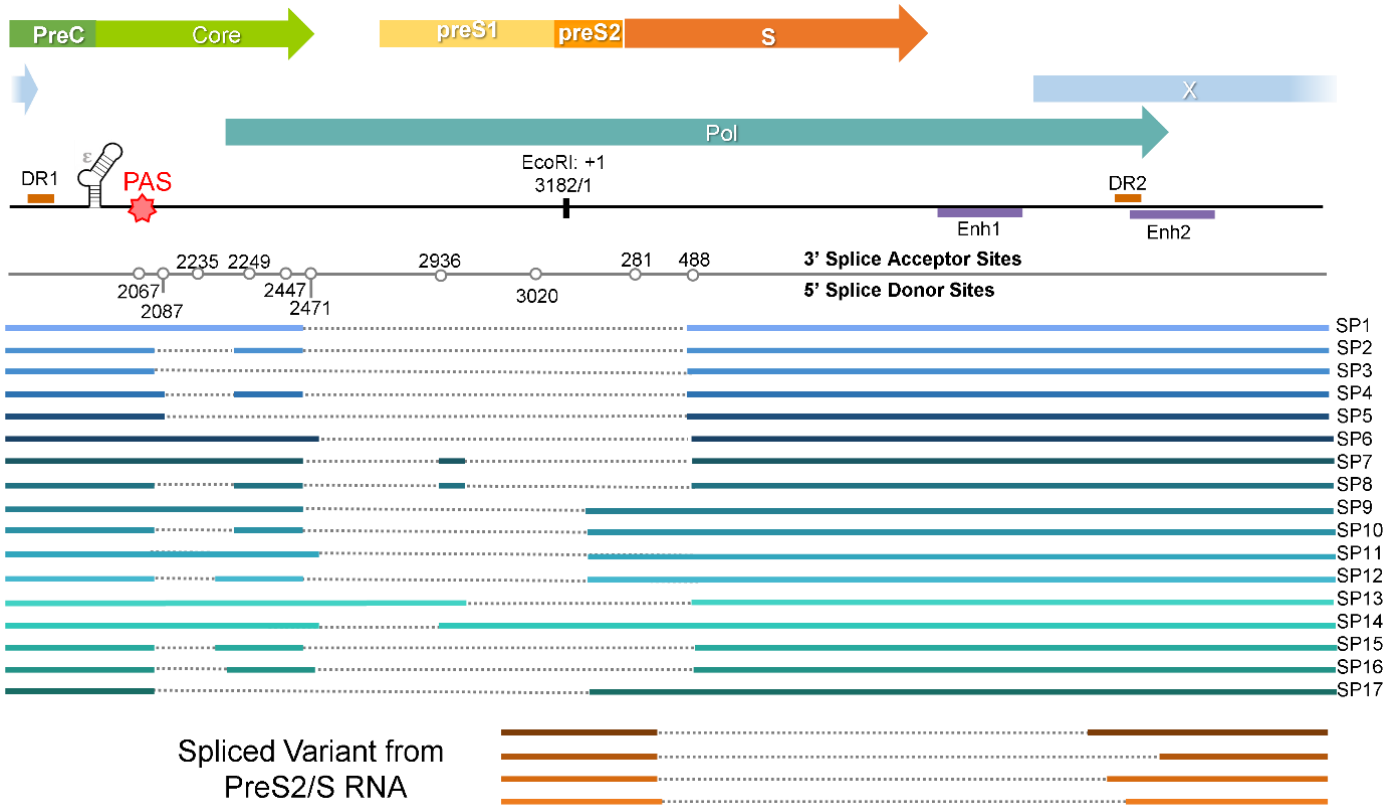

Figure 7. Summary of HBV splice variants described in the literature. pgRNA can be spliced in 17 isoforms according to the use of major donor (upper numeration) and acceptor (bottom numeration) splicing sites (Chen et al., 2015). Viral ORFs are annotated on top of the scheme (preC/C, Pol, S and X ORFs). pgRNA-derived splice variants are named from SP1 to SP17. Four splice variants of the preS2/S mRNA have been identified in transfected cell lines (Candotti & Allain, 2016).

In addition to classical HBx transcripts, shorter and longer transcripts have also been identified within cells, viral particles secreted by cultured hepatocytes and in plasma of patients (Stadelmayer et al., 2020). Indeed, using the Cap analysis gene expression (CAGE) technique, Altinel et al. identified an alternative TSS in the HBx sequence that could give rise to a shorter HBx protein that can function as transactivator in a similar manner to full-length HBx, however their clinical relevance remains unknown (Altinel et al., 2016; Kwee et al., 1992; Zheng et al., 1994). In this study, Altinel et al. also mapped 17 major TSS in HBV transcriptome, in addition to the six already well-described major TSS that initiate the six major HBV transcripts. They discovered 11 weaker TSS, notably in the Pre-core/Core promoter and in the X transcript, which might represent noncoding RNAs implicated in the regulation of HBV transcription.

Spliced variants

Constitutive splicing is an essential biological process regulating eukaryotic gene expression by generating mature mRNAs. In contrast, alternative splicing enriches transcriptome diversity. Splicing is coordinated by the spliceosome and occurs onto specific RNA domains with the help of cis- and trans-acting regulatory elements.

Upon infection, HBV hijacks the host splicing machinery to develop regulatory mechanisms for alternative splicing of the viral transcripts. Its ability to produce spliced variants has been described *in vitro* and in the liver of patients with CHB (T. Suzuki et al., 1989; H. L. Wu et al., 1991). So far, 16 variants derived from pgRNA and four derived from the preS2/S mRNA have been identified (Candotti & Allain, 2016) (Fig. 7). A seventeenth variant (SP17) has been recently identified in patients (Chen et al., 2015). However, the biological significance of HBV RNA splicing, especially in terms of viral replication as well as the detailed regulatory mechanisms underlying post-transcriptional processing events in the HBV cycle are still largely unclear. In addition, Ito et al. have recently suggested that HBV alternative splicing could be cell type-dependent and cannot only be explained by RNA transcription levels (Ito et al., 2019).

In terms of splicing regulatory elements, Heise et al. identified the HBV post-transcriptional regulatory element (PRE), a highly structured cis-acting sequence of approximately 0.5 kb, within the viral transcripts. It is located close to the 3′ end and is involved in the regulation of the 3.5 kb RNA splicing (Heise et al., 2006). These spliced variants result from the activation or repression of splicing sites altogether by cis-acting cellular and/or viral factors. All these variants share the splicing hallmarks generally found

in the cellular RNAs, with a donor 5' splicing site (5'ss) and an acceptor 3' splicing site (3'ss) (Y. Lee & Rio, 2015). So far, only single- and double-spliced isoforms have been identified.

The most reported pgRNA-derived spliced isoform is the so called Singly spliced Product 1, or SP1, which is 2.2 kb long, and spliced between nucleotides 2447 and 489, according to ayw genome (genotype D) nomenclature (T. S. Su et al., 1989). This spliced variant represents almost 30% of pgRNA transcripts in transfected cell culture, and up to 60% in patient samples. pgRNA-derived spliced isoforms can be encapsidated and retro-transcribed onto defective HBV DNA particles. Indeed, such abnormal particles circulate in the sera of infected patients, and are correlated with liver diseases (Soussan et al., 2008). Moreover, the amount of HBV spliced isoforms increases in patient sera prior HCC development (Bayliss et al., 2013). SP1, together with two other spliced variants, namely SP7 and SP14, have been demonstrated to encode spliced proteins, called HBSP, HBDSP and P-S FP respectively (W.-N. Chen et al., 2010; H. L. Huang et al., 2000).

iv. Viral Proteins

Surface proteins (HBsAg): small, medium, and large

The viral envelope is made of host-derived lipids and three surface proteins termed S-HBs, M-HBs and L-HBs. The three surface proteins share the S domain of 226 amino acids (aa), which forms S-HBs. M-HBs contains an additional PreS2 domain with 55 aa, while L-HBs encompasses the PreS2 domain and the PreS1 domain with a length of 108, 118 or 119 aa depending on the genotype. The HBV surface proteins are integral membrane proteins anchored by the S-domain in the membrane. S-HBs is inserted by various transmembrane (TM) regions in the endoplasmic reticulum (ER) membrane where they acquire N-linked glycans. Despite their similarities, the envelope proteins differ in functions. S-HBs is the major component of the viral envelope and builds up its scaffold. By contrast, the function of the M-HBs remains unknown. Although highly conserved through all *Orthohepadnaviruses*, it is not necessary for virion secretion, SVP formation or HBV infectivity (Glebe & Urban, 2007), whereas the co-expression of the S-HBs and L-HBs has been shown to be strictly required for the production of mature viral particles (Bruss & Ganem, 1991).

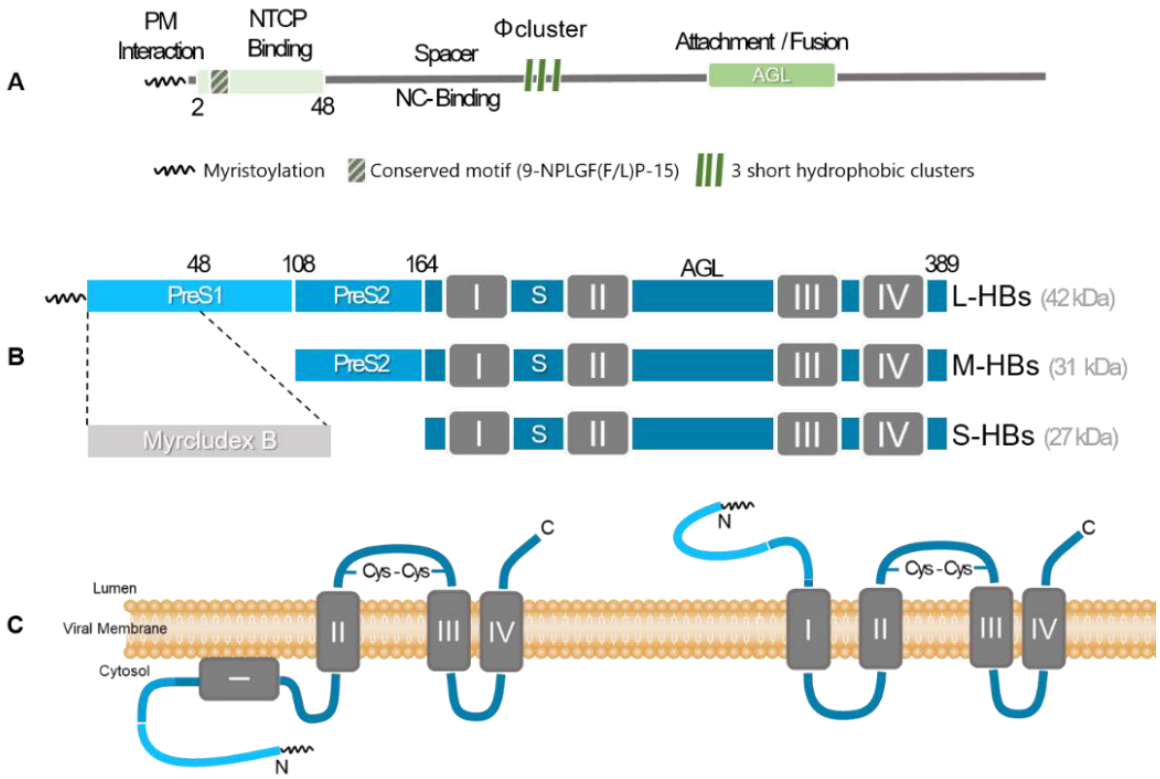

Figure 8. Structure and proposed transmembrane topology of HBV envelope proteins. (A-B) L, M and S envelope proteins are translated from three separate in-phase start codons in the HBV envelope ORF located at aa positions 1, 109, and 164, respectively. The four hydrophobic segments in the S domain are indicated by grey squares, designated I-IV. (C) L-HBs displays an unconventional split mixed topology. Upon cotranslational membrane integration, the pre-S1 and pre-S2 domains of L are initially located on the cytosolic side of the endoplasmic reticulum (ER) membrane (left side) with TM1 not being inserted into the membrane. During maturation, ~50 % of L molecules post-translationally translocate their pre-S region to the luminal space (right side).

Intriguingly, upon maturation, L-HBs forms a dual TM topology by orientating its hydrophilic N-terminal preS1+preS2 domain either at a cytosolic (i.e., corresponding to the virion inside, i-preS) or luminal (i.e., corresponding to the virion outside, e-preS) location (Fig.8). Both topologies of L play crucial roles in the viral cycle, as the i-preS form recruits the mature nucleocapsids to virion-budding sites, while e-preS mediates sodium taurocholate cotransporting polypeptide (NTCP) receptor binding during virus entry (Bruss, 1997; Lambert & Prange, 2001; Yan et al., 2012).

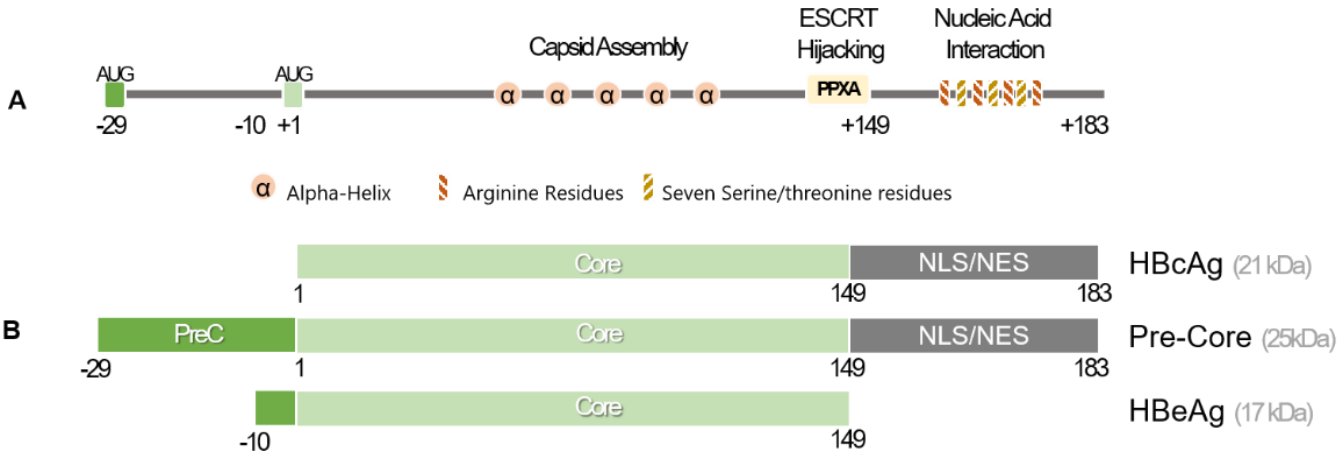

Figure 9. Capsid proteins sequences and structural domains. HBc sequence starts at position +1. The upstream 29 aa sequence corresponds to a peptide signal that drives the translocation of the 25 kDa precore protein into the ER lumen, leading to the synthesis of a secreted form of the core protein, HBeAg. The N-terminal domain (NTD) corresponds to residues 1–140. Circles represent the five alpha helices found in NTD that are essential for HBc to assembly into capsids. The next ten residues contain the PPXA sequence that hijacks the ESCRT machinery for virions secretion. The C-terminal domain (CTD) contains arginine residues (dash orange rectangles) required for the interaction of HBc with nucleic acids (NAs), an activity that is regulated by the phosphorylation of the seven serine/threonine residues (dash brown rectangles), even though S 155, 162 and 170 are considered as the three major phosphorylation sites (de Rocquigny et al., 2020).

Capsid protein (HBcAg)

The HBV HBc is composed of 183-185 aa (according to genotypes variability). HBc is composed of a C-terminal domain (CTD) and N-terminal domain (NTD) connected by a linker region (Fig.9). The NTD consists of the first N-terminal 149 aa, which are sufficient for the self-assembly of viral capsids supported by the presence of five α-helixes (Wynne et al., 1999). NTD was reported to be essential for *in vitro* capsid assembly while CTD was not necessary (Nassal, 1992). The last ten residues of the NTD contains the PPXA sequence that hijacks the Endosomal Sorting Complexes Required for Transport (ESCRT) machinery for virion secretion (Rost et al., 2006). In contrast, CTD contains arginine residues that are essential for nucleic acid packaging and reverse transcription (Lewellyn & Loeb, 2011). This interaction is regulated by the phosphorylation of serine/threonine residues. In addition, nuclear localization signals (NLS) and nuclear export signals (NES) have been described in the CTD, which enables the nucleus/cytoplasmic shuttling of HBc (H.-C. Li et al., 2010). HBc dimer formation is mandatory for capsid assembly (Zhou & Standring, 1992). In general, two different capsids characterized by the triangulation numbers T=3 and T=4 can be assembled into HBc dimers. The capsid in T=3 symmetry consists of 90 HBc dimers while the T=4 symmetry particle is composed of 120 HBc dimers (Crowther et al., 1994) and is preferentially incorporated into virions (Dryden et al., 2006).

Besides its role in the cytoplasm, the HBc protein is present in the nucleus where it is believed to play important regulatory functions by associating with cccDNA. HBc binds preferentially to double-stranded HBV DNA and reduces the nucleosome spacing of the nucleoprotein complexes. This leads to epigenetic modification of cccDNA minichromosome by a series of nucleosome rearrangements in the HBV regulatory elements that positively regulate viral replication (Bock et al., 2001). In addition, HBc acts as a transcriptional activator of the regulatory elements of HBV by enhancing the binding activity of the nuclear factor kappa B (NFκB) to promote viral replication and transcription (Kwon & Rho, 2002). The role of HBc in the regulation of HBV transcription is further supported by a study demonstrating that HBc preferentially binds to the CpG islands in cccDNA (Guo et al., 2011). Recently, Lucifora et al. have suggested that HBc derived from incoming HBV capsids could associate with cccDNA without the need for viral transcription and *de novo* protein synthesis. Whether this association occurs immediately with rcDNA, as soon as it is released into the nucleoplasm or after its conversion into cccDNA is currently unknown (Lucifora et al., 2021).

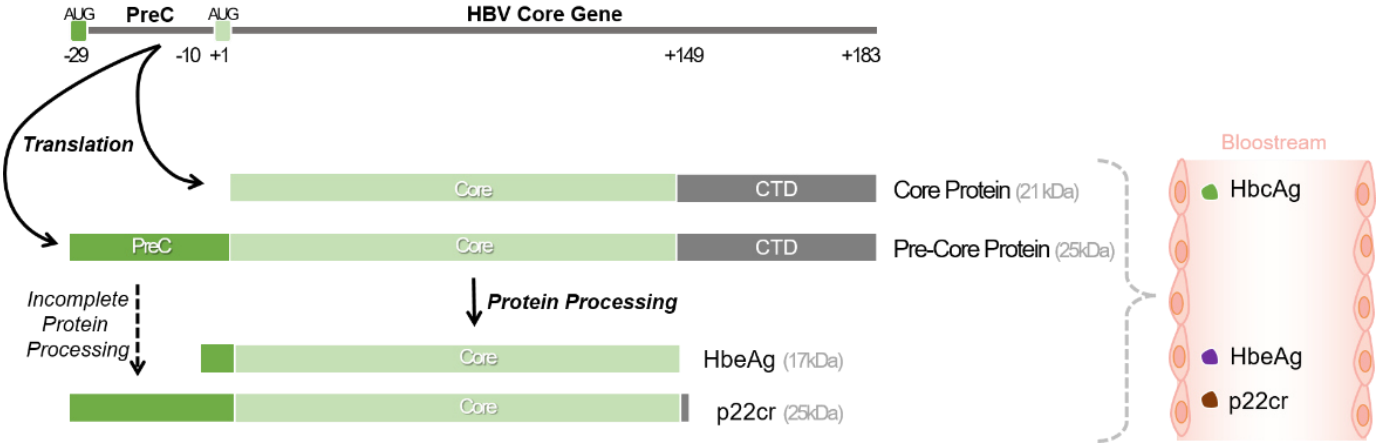

Figure 10.HBc and HBeAg processing. HBcAg, HBeAg and p22cr (collectively known as hepatitis B core-related antigen (HBcrAg)), produced from translation of different starting codons of the preC core gene and differential protein processing afterwards.

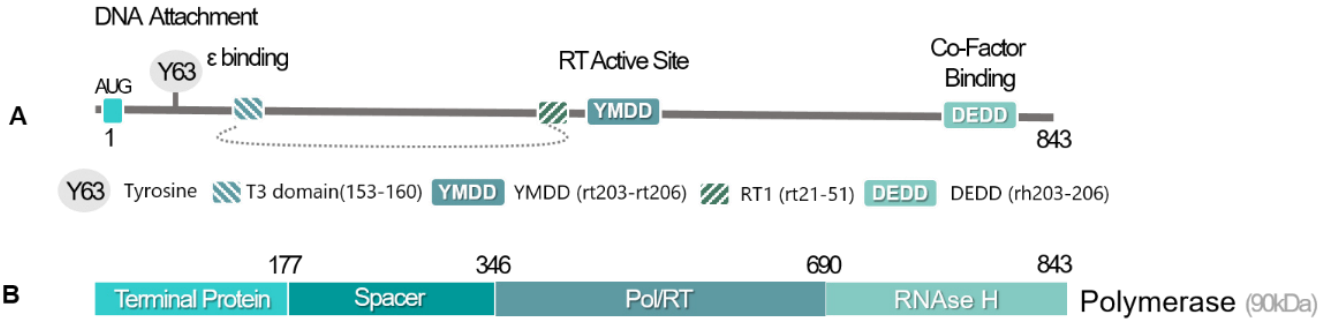

Figure 11. Viral polymerase. The attachment to DNA is made through the Y63 residue. T3 motif is important in ε binding, RNA packaging and protein. The conserved tyrosine, methionine, two aspartate (YMDD) motif coordinates the binding of two magnesium ions and is the enzyme's active site. The RT1 motif is thought to interact with the T3 motif in TP to facilitate ε binding and protein priming. The RNase H domain contains a conserved DEDD box motif, which is important for metal ion co-factor binding (Clark & Hu, 2015).

Pre-Core protein and HBeAg

HBeAg is a soluble antigen and an important diagnostic tool that is used to determine the status of ongoing HBV infections. With an extension of 29 residues in its NTD, HBeAg shares the same sequence and domains as HBc (Fig. 10). The NTD hydrophobic sequence of 19 residues directs the 25-kDa HBeAg precursor to the rough ER where it undergoes two successive cleavages to be fully mature. The first cleavage leads to a 22 kDa protein, which can either be cleaved a second time in the Golgi network in its CTD to produce the secreted form of HBe of 17 kDa (Messageot et al., 2003), or can traffic to the cytosol, forming the p22 viral protein (Dandri & Locarnini, 2012). The secreted HBeAg is not required for viral replication but exhibits immune-modulating roles that contribute to viral persistence.

Polymerase (Pol)

The viral polymerase, designated as Pol, is 843 aa long and is the only enzymatic viral protein encoded by HBV genome. This protein is translated from the pgRNA and contains four different domains, listed below beginning from the N-terminal extremity (Fig. 11):

Terminal protein (TP) domain : The TP domain connects the viral polymerase to the 5' end of the DNA (-) strand through its Y63 residue, leading to a primase activity that allows initiation of pgRNA RT by synthesizing a 3 or 4 nucleotide primer (Lanford et al., 1997; Zoulim & Seeger, 1994). Moreover, the TP domain is also required for pgRNA packaging by interacting with the pgRNA 5' "epsilon" ε-loop by its T3 domain.

Spacer domain: The spacer domain can tolerate amino acid insertion or deletion. The role of this genetically variable region is still unclear and appears to overlap with the PreS domain of the S protein, suggesting a role in environmental adaptation and providing flexibility in conformational changes (P. Chen et al., 2013).

Reverse-transcriptase (RT) domain: The RT domain harbors polymerase/retro-transcriptase activity and is therefore responsible for pgRNA retro-transcription into (-) strand DNA with subsequent DNA (+) strand synthesis.

RNase H domain: The CTD carries RNase H activity and drives pgRNA degradation after retro-transcription of the DNA (-) strand. It is also important for generating the short RNA primer required for (+) strand DNA synthesis (Villa et al., 2016).

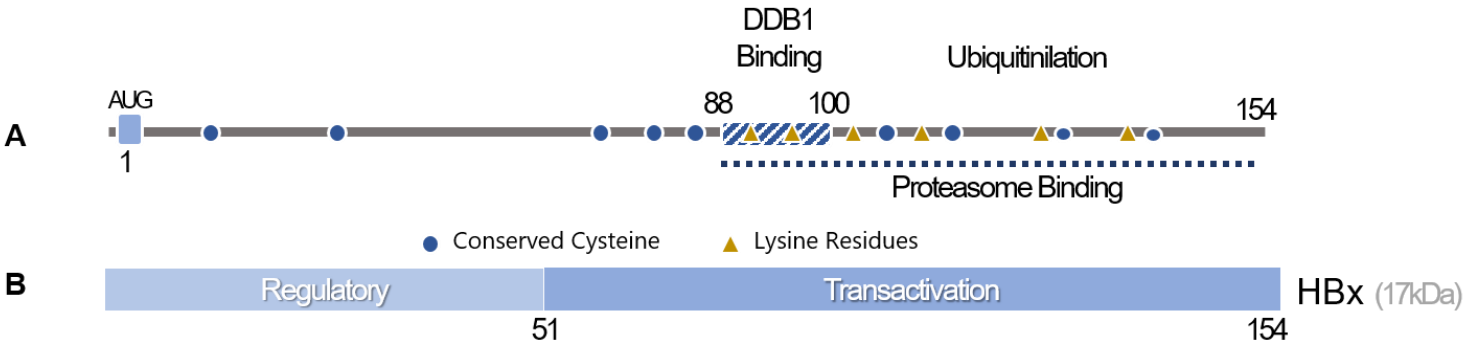

Figure 12. Schematic representation of HBX. Functional domains shown include the regulatory domain (1–50), the transactivation domain (50–154), and the DNA-damage binding protein 1 (DDB1)-binding domain (88–100; hatched area). The proteasome binding domain (90–154) spans the DDB1 binding domain. Conserved cysteine residues have an unknown function and are indicated by blue circles. Six conserved lysine residues, which may be targets for ubiquitination, are indicated by filled triangles (Minor & Slagle, 2014).

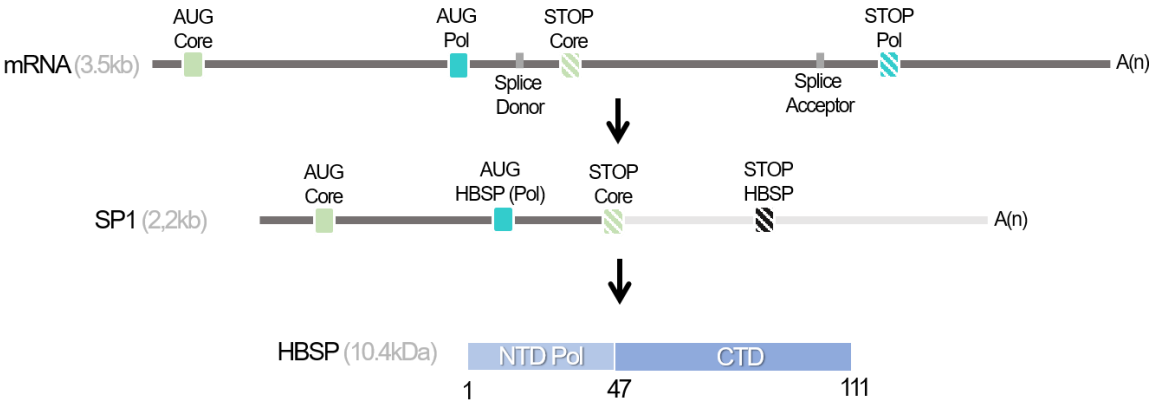

Figure 13. Schematic representation of singly spliced HBV-RNA and HBSP translation product.

X protein

HBx is a 154 aa long, nonstructural protein that has been extensively studied in the last decades, with several roles attributed to it depending on the experimental model. Despite still not having a fully elucidated function, two main roles have been identified: i) a role during viral replication and ii) a role in hepatic carcinogenesis.

HBx is required to initiate and maintain HBV replication in HepaRG cells (Decorsière et al., 2016; Lucifora et al., 2011) and human-liver-chimeric mice (Tsuge et al., 2010) and WHx is required for WHV replication in woodchucks (Zoulim et al., 1994). In the nucleus, HBx interacts with cccDNA and the host transcriptional machinery (Belloni et al., 2009). In the cytoplasm, HBx stimulates signal transduction pathways to benefit virus replication, including factors that affect cell survival, metabolism, proliferation, and transcription pathways (Slagle & Bouchard, 2016). Many other roles of HBx have been identified and extensively reviewed and will not be described further in this manuscript (Slagle & Bouchard, 2016).

Hepatitis B splicing-regulated protein (HBSP)

Translated from SP1, the major HBV spliced variant, HBSP protein is a 10.4 kDa protein present in HBV-infected livers (Soussan et al., 2000). This protein corresponds to the fusion of 47 aa of the HBV polymerase NTD to a 64 aa polypeptide synthesized from a new ORF generated after the splicing event.

Circulating anti-HBSP antibodies have been detected in the serum of patients with different viremia, however, no correlation was established between anti-HBSP antibodies and HBV viral load in chronic carriers. At first, HBSP expression was associated with severe liver fibrosis but not with liver necroinflammation or other histological disorders. In addition, patients having anti-HBSP antibodies showed an increased level of tumor necrosis factor alpha (TNF-α) (Soussan et al., 2003). Then, Pol et al. suggested that this mechanism is related to a down-regulation of immune response, notably through the inhibition of NF-κB activity (Pol et al., 2015). Finally, the immune-modulatory role of HBSP has been evidenced through the downregulation of C-C motif chemokine ligand 2, CCL2 by Duriez and colleague (Duriez et al., 2017). However, these studies were conducted in HBSP-transgenic mice upon artificial TNF-α stimulation. More physiological studies remain necessary to fully elucidate the role of HBSP in HBV-associated pathologies.

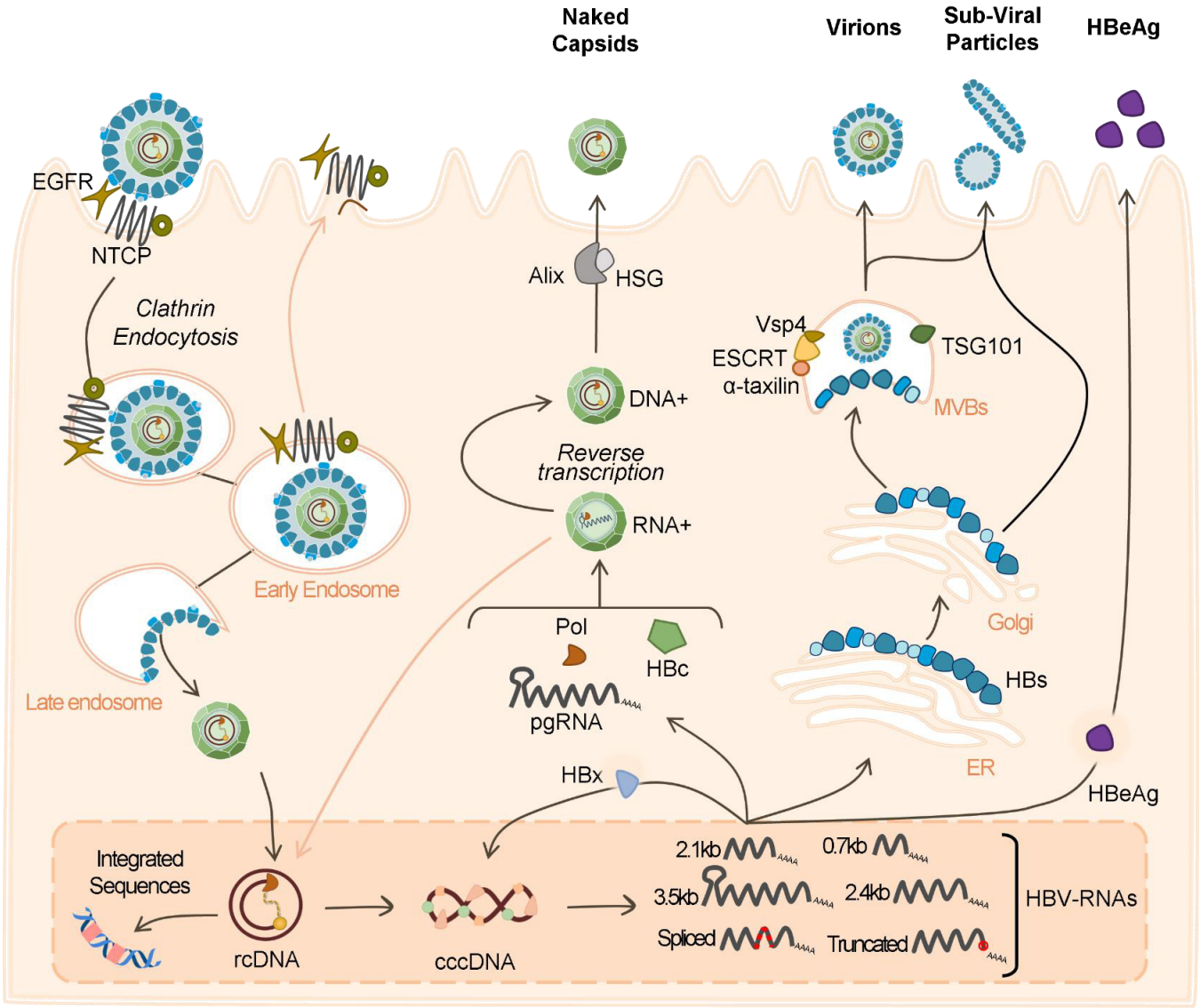

Figure 14. Schematic overview of the HBV cycle. See the main text for a precise description of the HBV cycle.

1. Viral Cycle

Before going into a detailed description, it is important to note that HBV cycle particularity is its ability to secrete a variety of viral particles. Whether infectious or not, each of them has a dedicated role in HBV establishment and replication process. These particles have attracted interest in the past decades as they could be used as a biomarker of viral replication in the serum of patients. As depicted below, HBV heavily relies on the host machinery for most of the replication steps that are described in the following section.

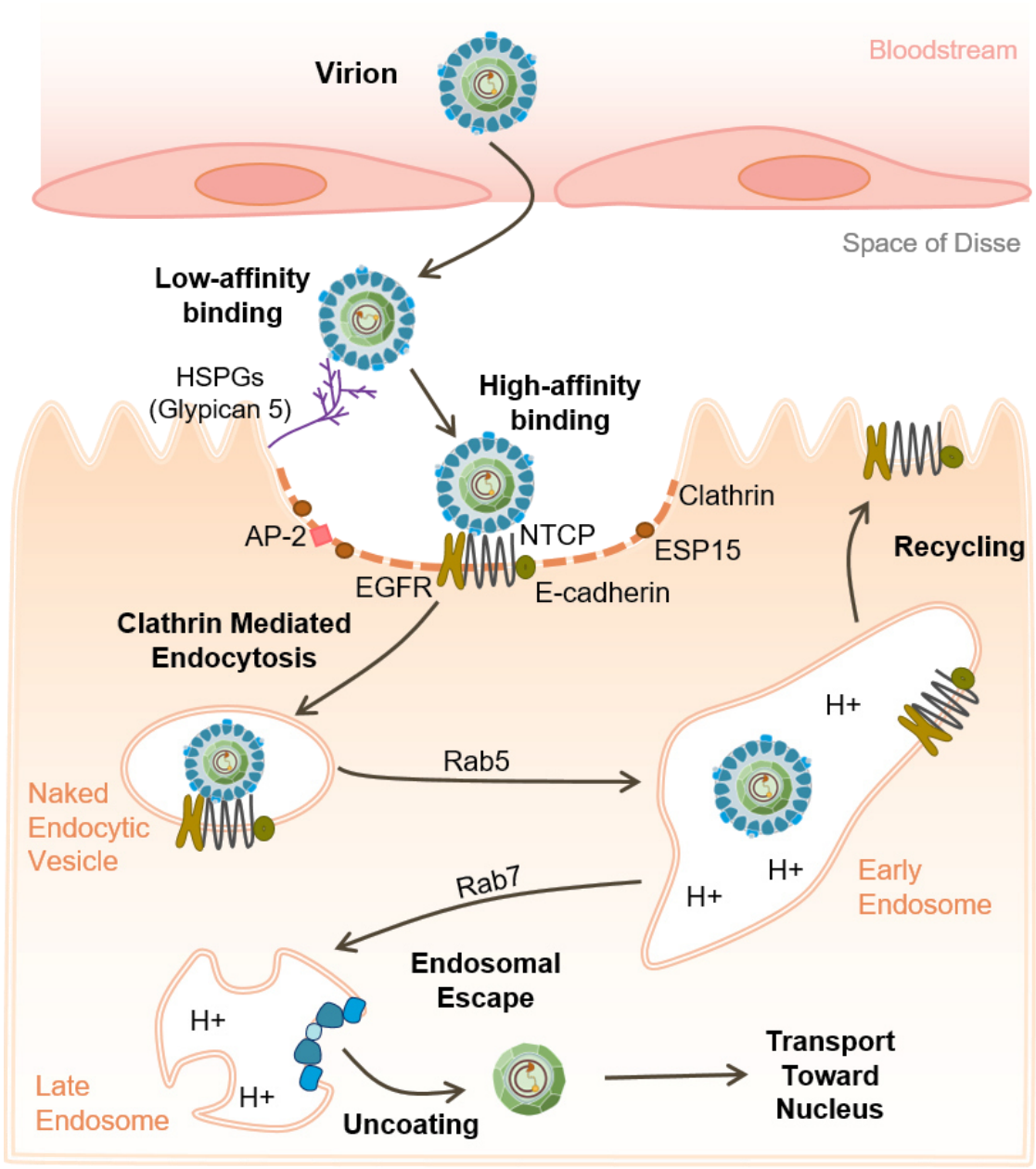

Figure 15. Viral entry adapted from (Herrscher et al., 2020).

i. Viral Entry: Attachment to the hepatocyte surface

In 2012, Yan et al. identified NTCP as the cellular HBV receptor (Yan et al., 2012). However, NTCP overexpression in non-hepatic cells is not sufficient to promote their infection by HBV and silencing of NTCP in primary human hepatocytes (PHH) does not completely inhibits HBV infection, suggesting that other factors are required for HBV infection (R. Xu et al., 2021).

In addition to the well-known NTCP, other cofactors play important roles in efficient and productive HBV infection. Firstly, Verrier et al. reported that HSPGs, in particular **Glypican 5,** binds to the surface of HBV particles prior to NTCP binding, thereby assisting in host cell entry (Verrier et al., 2016). In addition, **E-cadherin** acts as a novel host factor that facilitates HBV entry. Mechanistic studies suggested that E-cadherin regulates cell-surface distribution of NTCP, thus promoting HBV binding to its receptor (Q. Hu et al., 2020). The overexpression of the hepatitis B **surface antigen binding protein** (SBP) in HepG2 cells induces susceptibility to HBV infection. SBP was shown to interact directly with HBV envelope proteins (Y. Sun et al., 2018).

HBV attachment to the hepatocyte surface involves initially a low-affinity interaction with **HSPGs**, followed by a high-affinity interaction between the myristoylated N-terminal preS region of L-HBs and NTCP (Fig.15) (Sureau & Salisse, 2013; Yan et al., 2012). Endocytic pathways regulated by clathrin or caveolin-1 have been proposed for HBV uptake in PHH or differentiated HepaRG cells, respectively (H.-C. Huang et al., 2012; Macovei et al., 2010). Notably, HBV internalization is accompanied by host cellular **Rab GTPases**. Rab GTPases control all aspects of intracellular vesicle trafficking by acting as regulator proteins that can recruit effector molecules when in their active GTP-bound form. By using the HepaRG model combined with inducible gene knockdowns (KDs), HBV infection has been shown to require **Rab5A and Rab7A**, suggesting that HBV is transported from early endosomes (EE) to late endosomes (LE) (Macovei et al., 2013). Conversely, in the same study the authors used shRNA to deplete Rab9 and Rab11, two factors responsible for movement of endocytic vesicles to the trans Golgi network or the recycling endosome, respectively. Interestingly, this was reported to have no effect on viral infection, indicating that LEs are the final destination for HBV particles. In addition, interference with the lysosomal activity by pH elevation had no effect on HBV infection, suggesting that viral uncoating takes place in a compartment preceding the lysosomes (C. N. Hayes et al., 2016).

A recent report described that the machinery for endocytosis of epidermal growth factor receptor (**EGFR**) coordinates the transport of incoming HBV virions to the endosomal network. This process involves EGFR phosphorylation and the subsequent recruitment of adaptor molecules such as AP2 and Eps15. The EGFR-sorting machinery coordinates HBV transport in the endosomal network (early and late endosomes and lysosomes). Accordingly, suppression of EGFR ubiquitination impairs HBV infection (Iwamoto et al., 2020). These observations imply that translocation of the virus to late endosomes is critical for a successful infection. However, how the viral particles deliver their nucleocapsids from endosomal compartments into the cytoplasm has not been clearly elucidated.

ii. HBV Particles Intracellular Trafficking

After escape from the endosomal compartments, nucleocapsids have been generally assumed to be delivered to the nucleus via **microtubule-mediated transport** (Rabe et al., 2006), a mechanism exploited by many viruses, including retroviruses, herpesviruses, parvoviruses, and adenoviruses. The intracellular localization of capsids showed a very close correspondence to the intracytoplasmic distribution of **tubulin**, a major protein of the microtubule network. Moreover, destabilization of microtubules with nocodazole blocked nucleocapsids from reaching the nucleus and the generation of cccDNA. Unfortunately, chemical compounds disrupting microtubule polymerization have severe side effects, limiting the clinical impact of these results. Follow-up investigations showed that **dynein light-chain LL1 (DYNLL1)** works as a functional interaction partner linking capsids to the dynein motor complex, providing molecular details of HBV translocation through the cytoplasm. It is assumed that the CTD of HBc is relevant for DYNLL1 binding (Osseman et al., 2018). In addition, the relevance of **actin filaments** for intracellular nucleocapsid transport has been described. However, the experimental investigation is challenging, as during the infection process the number of viral particles entering the cell is very low and the number of nucleocapsids released to the cytoplasm is even smaller.

iii. Uncoating and Nuclear Import

The HBV cycle requires transport of the viral genome to the nucleus. The rcDNA containing nucleocapsid need to be transported towards the nucleus. However, with a 32 - 36 nm diameter, the size of the nucleocapsid is close to the upper limit for transport

through the nuclear pore. It has been a matter of debate whether the capsid is imported into the nucleus or not.

The HBV capsid protein contains NLS in the CTD (H.-C. Li et al., 2010). The NLS binds to the nuclear pore complex (NPC) via an interaction with nuclear transport factors (importins or karyopherins α and β) in digitonin-permeabilized mammalian cells (Kann et al., 1999). Cryo-electron microscopy showed that CTD is not surface-exposed in the capsids, however, it is noteworthy to mention that capsids undergo topological changes under several conditions, including phosphorylation. However, the physiological relevance of the use of such drugs is controversial as they act on a broad range of intracellular mechanisms.

Further studies showed that once at the NPC, the capsid dissociates and releases the rcDNA complexed with the viral polymerase together with core dimers in the nucleus (Brandenburg et al., 2005). This dissociation occurs on the cytoplasmic site of the NPCs, and once in the nucleus, core dimers are able to reassembly into capsids (Gallucci & Kann, 2017). However, rcDNA is covalently-linked to the polymerase that is about 90 kDa, preventing its simple diffusion in the nucleus (restricted to peptides <42 kDa). This suggests an active transport into the nucleus in opposition to simple diffusion. This transport seems to rely on casein kinase II (CKII)-dependent phosphorylation (Lupberger et al., 2013).

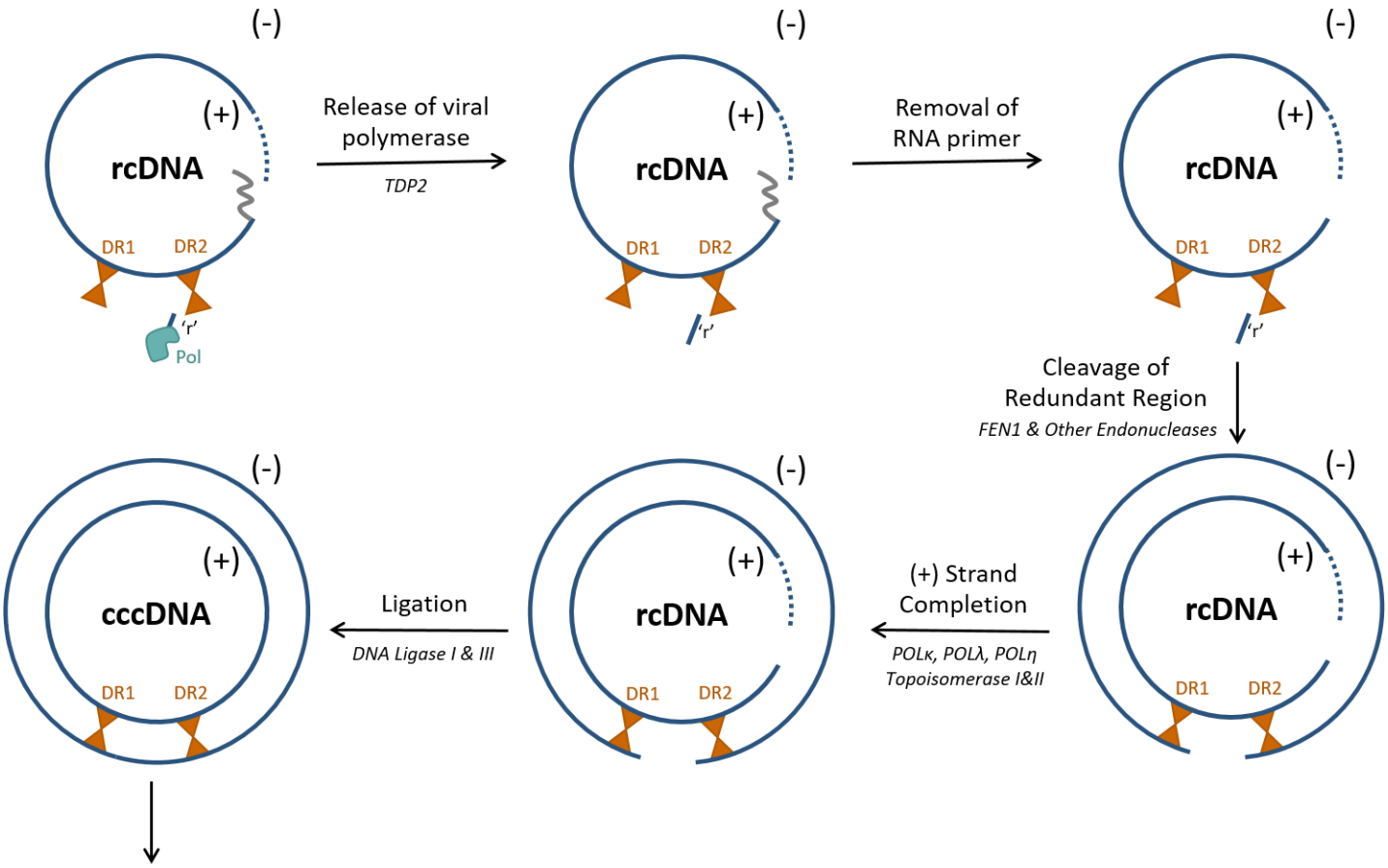

Figure 16. cccDNA formation. Formation of HBV cccDNA involves i) release of viral polymerase, which may be mediated by tyrosyl-DNA-phosphodiesterase 2 (TDP2) or its related proteins; ii) removal of the RNA primer from the (+) strand by some yet unknown enzymes; iii) cleavage of terminally redundant sequences (r) from the (-) strand, which may require flap structure-specific endonuclease 1 (FEN1) activity; iv) repair of the (+) strand, with the help of DNA polymerase κ or polymerase α, δ and ε, and DNA topoisomerase I and II; v) ligation of (-) strand and (+) strand DNA separately or simultaneously by DNA ligase 1 and 3 and finally vii) chromatinization, which involves histone chaperones, chromatin remodelers, transcription factors and viral proteins. Adapted from (Xia & Guo, 2020).

iv. cccDNA Formation and Regulation

Once in the nucleus, rcDNA is converted into cccDNA, which is the persistent form of HBV DNA in the nucleus of infected hepatocytes and is the crucial intermediate of viral replication. This conversion is a multi-step process that strongly relies on cellular protein activity requiring the following steps (Fig. 16):

1) Covalently-linked polymerase is removed from the 5' end of the (-) strand together with the redundancy terminal region "r".
2) Then, RNA oligomer is degraded from the 5' end of the (+) strand.
3) The (+) strand is completed.
4) Finally, DNA extremities are ligated.

Cellular proteins are involved in the conversion of rcDNA to cccDNA, although not all the steps have been yet clearly elucidated, mainly due to technical limitations. In addition, whether the abovementioned steps occur in parallel or in a specific chronological order remains to be elucidated. Recent genetic studies have implicated **tyrosyl-DNA-phosphodiesterase 2** (TDP2) (Königer et al., 2014), **DNA polymerase kappa** (POLκ) (Qi et al., 2016), **DNA polymerase alpha** (POLα) (Tang et al., 2019), **DNA ligases 1 and 3** (LIG1, LIG3) (Long et al., 2017), and **flap endonuclease 1** (FEN1) (Kitamura et al., 2018) in cccDNA formation. However, direct evidence of the involvement of these proteins in rcDNA repair has been hindered by the lack of a biochemical system for reconstituting cccDNA formation. Recently, Wei and Ploss established a biochemical system that fully support the repair of various HBV rcDNA substrates to form cccDNA. They identified five core factors involved in DNA lagging-strand synthesis as essential for cccDNA formation in yeast extracts (Wei & Ploss, 2020). Moreover, Feng and al. reported that that lncRNA PCNAP1 enhances the HBV replication through modulating miR-154/PCNA/HBV cccDNA signaling and the PCNAP1/PCNA signaling drives the hepatocarcinogenesis (Feng et al., 2019).

Besides, these enzymes belong to DNA repair pathways, assumed to be involved in rcDNA conversion to cccDNA (Gómez-Moreno & Garaigorta, 2017). A comprehensive understanding of how rcDNA is repaired to form cccDNA is critical for creating novel targeted therapies. Altogether, the previously mentioned findings support the notion that HBV relies on host cell machinery to successfully accomplish its replication cycle.

To overcome the host restriction mechanisms of cccDNA transcription, HBV encodes the transactivator protein HBx (Lucifora et al., 2011; Slagle & Bouchard, 2016). A

key function of HBx is to redirect the **DNA-damage binding protein 1** (DDB1)-CUL4 E3 ubiquitin ligase to target **Smc5/6** for degradation and thus relieve this suppression (Decorsière et al., 2016; Murphy et al., 2016).

Epigenetic modifications of HBV cccDNA minichromosome, such as DNA methylation and histone modifications are implicated in regulating its transcriptional activity (Hong et al., 2017; Mitra et al., 2018). HBV chromatin has been reported to be associated with histone proteins. All the **canonical histones** (H3, H4, H2A and H2B) compose the core nucleosome associated with cccDNA (Bock et al., 2001). The chromatinized structure of the cccDNA suggests a transcriptional regulation mediated by posttranslational modification of histones such as methylation and acetylation. *In vitro* specific cccDNA chromatin immunoprecipitation (cccDNA-ChIP) revealed the presence of **histones acytransferases** (CPB, p300 and PCAF/GCN5) and **deacetylases** (HDAC1 and Sirt1) on cccDNA minichromosome (Belloni et al., 2009; Pollicino et al., 2006).

Host proteins can bind to cccDNA and regulate its transcriptional activity. Among them, **hepatocyte nuclear factors** (HNFs) are liver-enriched factors known as key regulators of numerous hepatocyte processes. Notably, HNF1α controls cccDNA regulatory elements to favor transcription activation, while HNF3β and HNF6 have been reported to inhibit HBV gene expression in hepatocytes (D. H. Kim et al., 2016). Other factors, which are not liver-enriched, also regulate HBV transcription. **TARDBP** and **PUF60** were reported to positively regulate HBV core promoter activity (Makokha et al., 2019; Y. Sun et al., 2018). On the contrary, **TIP60** complex and **Sirt3** negatively regulate HBV transcription (Nishitsuji et al., 2018; Ren et al., 2018).

v. pgRNA transcription, encapsidation and retro-transcription

The next crucial step during viral replication is the specific packaging of pgRNA together with the reverse transcriptase into newly forming capsids. It contains specific features that are necessary for its retro-transcription and encapsidation in progeny capsids that can be either enveloped and secreted to form new infectious particles or recycled to the nucleus to maintain the cccDNA pool (Fig. 17).

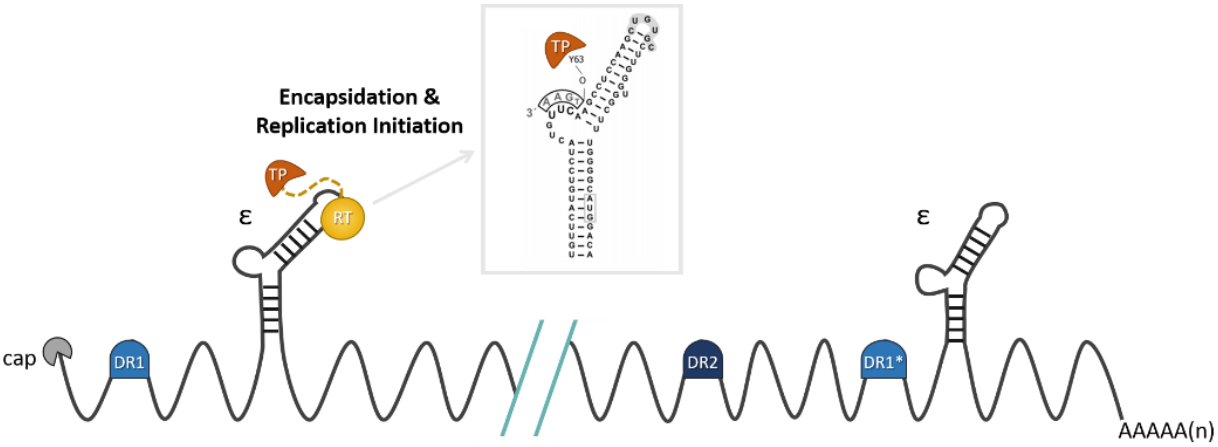

Figure 17. pgRNA secondary structure. pgRNA has two epsilon loops: one in its 5' and the other on the 3' end. Direct repeat sequence (DR1) are present twice while DR2 is only present once. pgRNA is capped and polyadenylated. Adapted from (Beck & Nassal, 2007).

In contrast to its still poorly characterized tertiary structure, the secondary structure of pgRNA is well known (Pollack & Ganem, 1993). First, pgRNA harbors ε loops at its 5' and 3' end. ε is a stem-loop highly conserved in *hepadnaviruses*, harboring a bulge region and an apical loop. Only 5' ε loop serves as encapsidation signal. Noteworthy, the 3' ε loop is shared by all the viral transcripts and is not sufficient to mediate encapsidation (Nassal & Rieger, 1996). Moreover, pgRNA contains the φ sequence, which is complementary to the 5' half of ε. Finally, due to the transcript length, pgRNA also contains two copies of the Direct Repeat 1 (DR1) sequence, while only bearing one copy of the DR2 (J. Hu & Lin, 2009).

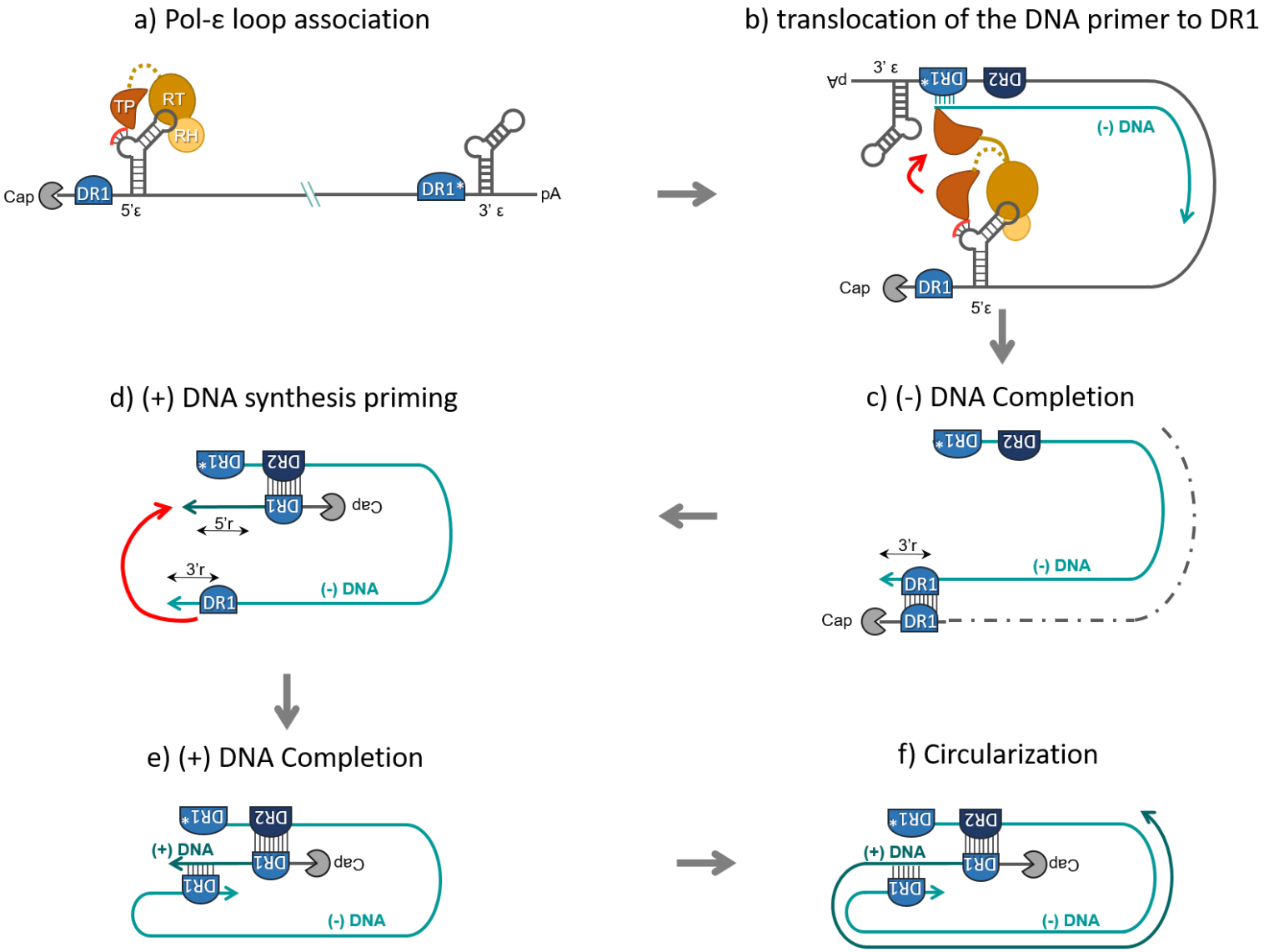

Figure 18. From pgRNA TO rcDNA: retrotranscription. The first step of pgRNA retro-transcription is the protein priming leading to the synthesis initiation of the (-)-DNA strand, followed by the negative strand elongation. After pgRNA partial degradation by the RNase H, the RNA primer is translocated to the DR2 sequence. The RNA priming leads to the completion of the (+)-DNA strand and the circularization allows the proper rcDNA synthesis.

pgRNA retro-transcription and encapsidation is a multi-step process, requiring structural reorganizations and cis- and trans-acting factors (Fig.18).

1) First, the TP domain of the viral polymerase interacts with the 5' ε loop resulting in a stable **Pol-ε loop association**, which mediates the recruitment of HBc dimers leading to packaging initiation (Nassal & Rieger, 1996).

2) Once pgRNA and Pol are encapsidated, this same complex initiates reverse transcription. In the meantime, protein priming to pgRNA 5' ε-loop drives the synthesis of a **small (-)-DNA sequence of 4 nt in length**. Pol will remain covalently bound to this DNA primer via Y63 until its removal during cccDNA formation.

3) At this step, the first template switch occurs with the **translocation** of the neosynthesized 4-nt DNA primer (3'-AAGT-5') to the 3' DR1 sequence (5'-UUCA-3'), by sequence complementarity, together with the covalently-attached viral polymerase.

To help translocation, pgRNA folding may be facilitated by i) the sequence complementarity of φ to the 5' half of ε (Shin et al., 2004); ii) host factors, such as elongation initiation factor 4G (eIF-4G) that can bind both 5' cap and polyA tail (Mangus et al., 2003).

4) Then, **(-)-DNA completion** subsequently occurs through the 3' DR1 to the 5' end of the pgRNA, and pgRNA is concomitantly digested by the RNase H domain of the viral polymerase.

The fate of the non-retro-transcribed 3' end of pgRNA, from downstream 3' DR1 sequence to the polyA tail, is still unknown. RNase H-mediated pgRNA degradation is not complete, leaving about 15-18 nt in pgRNA 5' end, including 5' DR1 sequence, spared from digestion, probably protected by RT/RNase H domains steric encumbrance (Loeb et al., 1991).

5) This 5'-capped RNA oligo is essential for (+)-DNA synthesis priming. It can be either extended from its initial location (10% of cases), leading to the so called "*in-situ* priming", and initiating the synthesis of a dsL-DNA (Staprans et al., 1991); or can be translocated to the DR2 sequence.

This second template switch, essential for complete rcDNA synthesis, is mediated by complementarity to the 5' DR1 sequence, remaining in the RNA primer. From its new

location, RNA primer is extended toward the viral polymerase bound in 5' end of the (-)-DNA, including the 4-nt linker to Pol (Beck & Nassal, 2007).

6) A third template switch is finally required to fully synthesize rcDNA: **circularization**. Indeed, after having synthesized the (+)-DNA strand until the 5' end of the (-)-DNA strand, (i.e. where Pol is still attached), the growing (+)-DNA is transferred from the 5' end to the 3' redundant ("r") sequence of the (-)-DNA from where it can be fully synthesized into mature rcDNA (Beck and Nassal, 2007).

Although identity between 5' and 3' redundant sequences is important to fully achieve circularization, it is assumed that supplemental cis-acting elements are required to ensure proper RNA primer translocation and circularization. Noteworthy, the synthesis of (+)-DNA strand is partially achieved and is heterogeneous in length, leading to the so-called "gap" that is further completed during cccDNA formation. This phenomenon could be explained by two hypotheses: i) a limited quantity of deoxyribonucleotide triphosphates (dNTPs) trapped in the capsid shell, resulting in a more or less filled gap; ii) a space restriction constraint due to the capsid shell. However, it is important to note that the capsid has a considerable structural plasticity (Böttcher et al., 2006). Recently, pgRNA ε-loop has been demonstrated to be N6-methyl adenosine (m6A)-modified. Moreover, m6A modification of 5' ε-loop, but not of 3' ε-loop, has been proposed as regulator for pgRNA retro-transcription (Imam et al., 2018). However, the precise molecular mechanisms involved in rcDNA synthesis have not been fully elucidated yet.

Finally, it is important to note that Core proteins undergo multiple phosphorylation/dephosphorylation modifications during pgRNA retro-transcription and encapsidation. These dynamic dephosphorylation processes play an essential role in pgRNA packaging and concomitant DNA synthesis (J. Hu & Lin, 2009, p. 200). Besides, the phosphorylation status of the capsid is closely linked to rcDNA formation (Gallucci & Kann, 2017). Indeed, during packaged (-)-DNA synthesis, HBc CTD is released outside the capsid shell, and exposed to phosphorylation by Protein kinase C (PKC) (Kann & Gerlich, 1994).

vi. Fate of mature nucleocapsids: Envelopment & Secretion

HBV is an extremely successful pathogen confronting the infected host with distinct particle types that assemble and bud at specific intracellular locations. Once assembled in the cytoplasm, mature nucleocapsids have three alternative fates: i) either they are enveloped with surface proteins and release as viral particles or ii) they are secreted as naked capsids, or iii) they can disassembly to deliver their rcDNA into the nucleus to replenish the nuclear cccDNA pool, in a mechanism called “intracellular recycling” that will not be further described here.

Envelopment & Secretion of progeny virions

Once assembled in the cytoplasm of infected hepatocytes, rcDNA-containing nucleocapsids, considered as mature, will acquire the host derived lipid bilayer containing envelope proteins. L-HBs and S-HBs are essential for the capsid envelopment (Bruss & Ganem, 1991). As described in the above section (see: HBV Proteins), HBs PreS1/PreS2 domain has a dual membrane topology. The region facing the cytoplasm was shown to be involved in capsid envelopment (Prange & Streeck, 1995). Deeper analysis by point mutation suggested that CTD of PreS1 and NTD of PreS2 are essential for HBV envelopment (Bruss, 1997), whereas the NTD of PreS1 is assumed to be dispensable.

In addition to the PreS1/S2 domain that participates in the envelopment, a cytosolic S loop between TM1 and TM2 was shown to bind to the nucleocapsid relying mostly in a structural conformation (Poisson et al., 1997). In addition, specific regions of nucleocapsid are involved in nucleocapsid envelopment. Indeed, a direct interaction between capsid and surface proteins is suggested by a structural model based on electron microscopy analysis of HBV particles derived from patients (Dryden et al., 2006). However, it has been the only study able to report this direct interaction. Besides, several core amino acids are crucial for direct interaction with L-HBs. These are Y132 and residues L60, L95, K96 and I126. However, the relevance of Y132 is questionable, as this mutant adopts a non-canonical structure (Pastor et al., 2019).

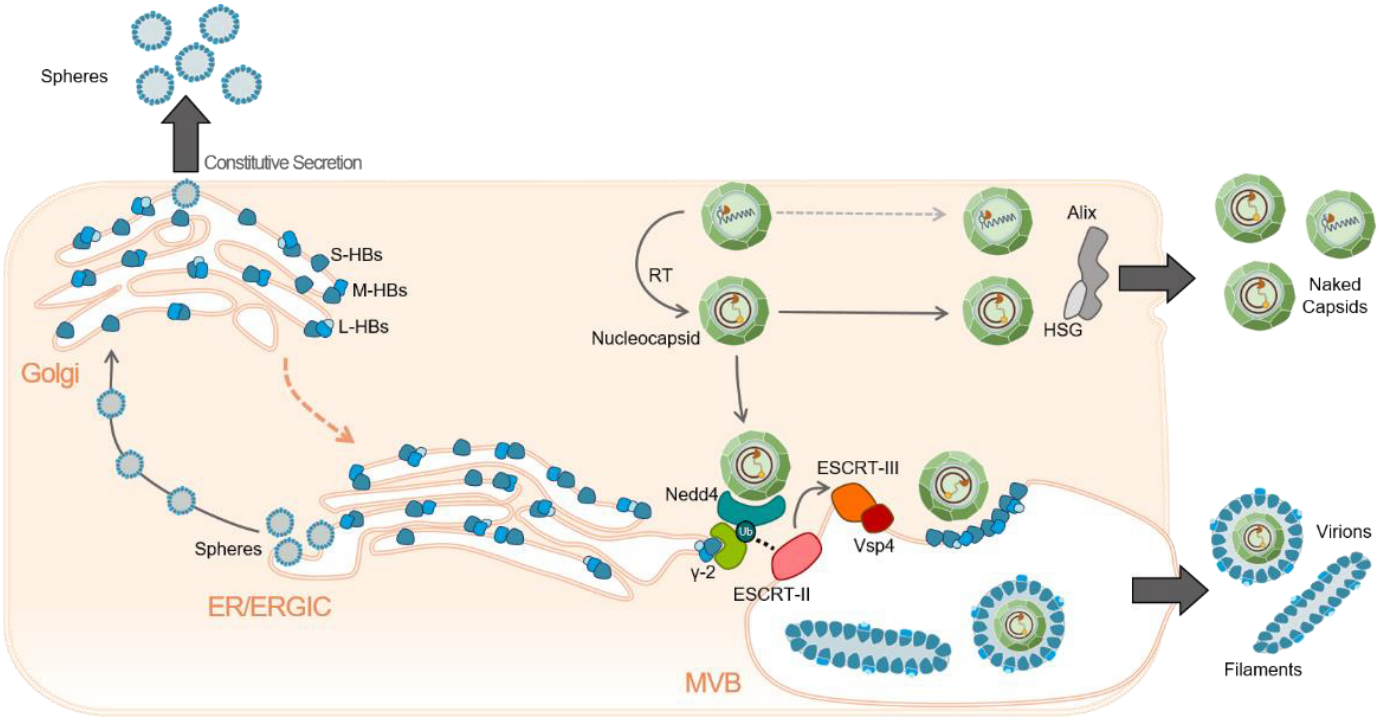

Figure 19. Model for HBV viral and subviral particle morphogenesis. The S, M, and L- HBs are synthesized at the ER membrane. Following oligomerization of envelope chains, spherical SVPs bud into the lumen of the ER/ERGIC and are exported through the constitutive secretory pathway, thereby traversing the Golgi complex. For virus assembly, the envelope proteins are transported to the budding site that may involve MVBs. Transport may be facilitated by γ2-adaptin(γ2) that interacts with the i-preS form of L. Viral nucleocapsids (NC) assemble and mature in the cytosol where they are recognized by Nedd4. Ubiquitinated (Ub) Nedd4 in turn is recognized by the ubiquitin-interacting motif of γ2-adaptin thereby bridging the viral substructures. The Ub moiety of the HBV/Nedd4/γ2-pre-assembly complex may then recruit the ubiquitin-binding ESCRT-II complex followed by the recruitment of ESCRT-III and Vps4 that mediate intraluminal budding and membrane fission of viral particles. MVBs and/or MVB-derived exosomes then fuse with the plasma membrane in order to release HBV. Alternatively, pre-assembled capsids (C) and nucleocapsids (NC) can be recognized by Alix that shunts naked capsids into an ESCRT-independent exit route. The mechanisms underlying the non-vesicular exocytosis of capsids are currently unknown but may involve the membrane-deforming ability of Alix. Adapted from (Prange, 2012).

To study HBV production and egress rather than entry, transfection of hepatoma Huh7 or HepG2 cell lines with a replication-competent HBV genome appears to be convenient model systems. These cells are refractory to infection due to low NTCP receptor levels but allow all steps of viral replication. Those systems have been used in several studies documenting the ESCRT requirement for HBV egress (Jiang et al., 2015; Lambert et al., 2007; Stieler & Prange, 2014; Watanabe et al., 2007). The ESCRT-MVBs pathway components consist of the ESCRT adaptors, **ESCRT-I, -II, and -III complexes**, together with the **Vps4 ATPase** and other associated proteins (Fig.19). The ESCRT-dependency of HBV supports the hypothesis of MVBs serving as HBV budding sites.

Even if several studies have been conducted in recent years, the crucial transport of HBs proteins from the Golgi to the MVB to form progeny virions remains enigmatic. L-HBs is essential for virus assembly as it interacts both with **γ2-adaptin**, a member of the clathrin protein family that guides antero- and retrograde trafficking between the Golgi network and endosomes (Jürgens et al., 2013; Rost et al., 2006) and with **α-taxilin** – another factor that may control virus trafficking (Hoffmann et al., 2013). γ2-adaptin interacts exclusively with the i-PreS topology of L-HBs and recognizes the HBV core protein (Hartmann-Stühler & Prange, 2001). This is mediated by **Nedd4**, which interacts with γ2-adaptin after ubiquitination and binds to the PPAY motif of core protein (Rost et al., 2006). Finally, it has been reported that ESCRT-III complex-forming CHMP proteins and the Vps4 ATPases are involved in the release of HBV virions. Co-expression of dominant-negative mutants of **CHMP or Vps4 ATPases** significantly blocks the budding of virions (Lambert et al., 2007).

In addition, some studies suggested that HBV could subvert cellular autophagy processes for virus envelopment (J. Li et al., 2011; Sir et al., 2010). Consequently, HBV envelope proteins could use the autophagy pathway to reach the endosomal system and then escape through the MVB budding platform. Interestingly, this secretion pathway is the major exosome secretion pathway, a process that requires **Rab GTPases**, in particular Rab27 family members (Blanc & Vidal, 2018). Other hepatitis viruses such as hepatitis C virus (HCV) and hepatitis E virus (HEV) are released through exosomes via a Rab27A-dependent pathway, suggesting that HBV could also hijack Rab GTPases to bud from the cells (Nagashima et al., 2014; Shrivastava et al., 2016).

Naked Capsids secretion

To date, the mechanism relative to NCs release remains elusive. In contrast to virions, the budding of NCs was described to be independent from the ESCRT-machinery (Bardens et al., 2011). The search for dependency factors revealed that **HGS** (HRS, hepatocyte growth factor-regulated tyrosine kinase substrate), a component that belongs to the ESCRT-0 complex was shown to enhance the release of NCs together with **Alix** (apotosis-linked gene 2 [ALG-2]-interacting protein), a protein with multifaceted roles in membrane biology (Chou et al., 2015a). Further analysis showed that Alix binds to core through the Bro1 domain and mediates capsid release (Bardens et al., 2011). Host cell components are necessary for efficient packaging, trafficking, and shedding of nascent HBVs particles. Among them, Ninomiya and colleagues highlighted the role of the tetraspanin CD63, in this process. Interestingly, CD63 depletion results in an increase of TSG101 levels, a key member of the ESCRT complex, on late endosomes. This increase may compensate for the loss of the CD63 protein, as these cells secrete similar numbers of small EVs with a preserved HBV genome copy number but, importantly, less infectious (Ninomiya et al., 2021).

Rab GTPase silencing studies suggested that NCs seem to avoid the MVB territory along with associated ESCRT-, Rab7- and Rab27-controlled pathways to augment their extracellular release. Unlike Rab7 and Rab27, the Rab33B GTPase proved to be an HBV-dependency factor, as its KD blocked naked capsid egress. This study provided evidence that **autophagosome-associated Rab33B, Atg5, Atg12 and Atg16L1** are involved in capsid assembly and egress, suggesting a link between capsid formation and autophagy (Döring & Prange, 2015).

vii. Release of Subviral Particles: Spheres and Filaments

It has been assumed for a long time that SVPs (spheres and filaments) and viral particles self-assemble in the lumen of the ER and are exported using the same route as spheres. However, recent work suggests that the release pathway of HBV viral particles is different from spheres but not from filaments.

Release of Filaments

Filament-like viral particles are characterized by a significantly higher content of L-HBs than spheres. Filaments are estimated to contain LHBs, MHBs and SHBs in the ratio of 1:1:4. The shape and the efficiency of the release of filaments depend on the relative

amounts of S-HBs and L-HBs. A low level of L-HBs results in the production and secretion of spheres containing L-HBs, while a higher level of L-HBs leads to the formation of filaments (Molnar-Kimber et al., 1988).

Filaments, like virions, enter into MVBs, as interruption of the MVBs biogenesis or silencing of α-taxilin inhibits the release of filaments. Thus, filaments like infectious viral particles are released via the ESCRT/MVB pathway. The adaptors concentrate vesicle cargoes and recruit the early-acting ESCRT factors such as ESCRT-I/-II complexes, which can bind ubiquitin and recruit late-acting ESCRT-III subunits. ESCRT-III subunits then form filaments and recruit Vps4 ATPase, which together constrict membranes and mediate fission (Raiborg & Stenmark, 2009).

Release of Spheres

Even if spheres are mainly composed of S-HBS, they also contain variable amounts of M-HBs and very little of L-HBs. It was shown that the assembly of HBsAg into spherical particles occurs within the ER, and the particles accumulate and remain within the ER for most of the time before secretion (Patzer et al., 1986).

In contrast, HBsAg was shown to form the dimer rapidly in the ER and then to be transported to a pre-Golgi compartment to complete the assembly process (Huovila et al., 1992). Ultrastructural analysis of cells producing only S-HBs showed that transmembrane dimers initially assemble in a filamentous form, progressively increase in size and are transported to the **ER-Golgi intermediate compartment** (ERGIC), where they are released and converted into spheres (Patient et al., 2009). Then, the spheres are transported through the constitutive secretory pathway, thereby traversing the Golgi complex.

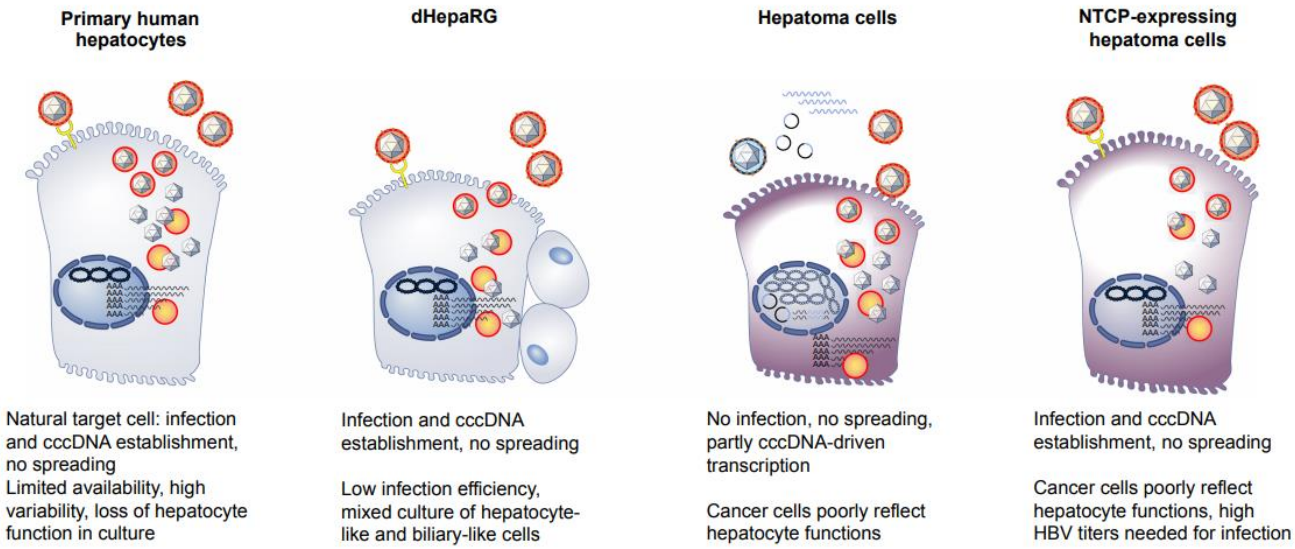

Figure 20. Human cell culture systems for the study of HBV infection. The figure schematically summarizes the four main cell culture systems based on human cells currently available for HBV research and antiviral drug testing. Being the natural host of HBV, PHH support HBV infection through its entry receptor NTCP leading to a full replication cycle including entry, cccDNA establishment, cccDNA transcription, morphogenesis and egress. dHepaRG cells also support HBV infection and the full replication cycle. However, in vitro differentiation prior to infection leads to the formation of hepatocyte-like and non-permissive biliary-like epithelial cell populations. Hepatoma cell lines such as Huh7 or HepG2 are non-susceptible to infection but can be transfected with overlenght HBV containing plasmids, full-length monomeric HBV genomes or can be transduced with genetically engineered HBV-expressing viruses. Hepatoma cells stably expressing HBV are also available. The formation of high levels of cccDNA has been observed with monomeric HBV genome transfections and viral vector-based transductions. Hepatoma cell lines genetically modified to express the human entry receptor NTCP are permissive for HBV infection and replication. The accompanying text provides essential information about the respective models. From (Allweiss & Dandri, 2016a)

2. Models for the study of human HBV infection

For years, HBV research has been limited by the lack of experimental models allowing a complete HBV cycle. This is mainly due to a high liver tropism and species specificity. Chimpanzees are the only nonhuman primates fully susceptible to human HBV infection; however, ethical limitations hamper experimentation in this model. To overcome this limitation, *in vitro* and *in vivo* experimental models have been developed over the years, allowing a better understanding of the HBV cycle.

i. *In vitro* models

HBV only infects fully differentiated hepatocytes. PHH are the gold standard to study HBV replication *in vitro*. However, due to their low availability in laboratories and the fast loss of hepatocyte markers and infection, there was an urgent need to find more accessible cell lines (Gripon et al., 1988). In this regard, hepatoma-derived cell lines have been widely used to study HBV. HepG2 and Huh7 cells are the most used; however, they only partially reproduce physiological conditions and do not express NTCP receptor. Transient or stable transfection were done to allow HBV expression in these models (Sureau et al., 1986). For example, HepG2.2.15 and HepAD38 are two hepatoma-derived cell lines stably expressing HBV genome and commonly used for HBV infectious particle production and studies on viral replication and antiviral drugs (Ladner et al., 1997; Sells et al., 1987).

HBV research was still missing models that could reproduce the entry steps on the virus and cccDNA formation. In 2012, Yan et al. discovered HBV entry receptor allowing the development of new infection models rather than transfection models (Yan et al., 2012). Stable human NTCP-overexpressing cells such Huh7-NTCP and HepG2-NTCP are now commonly used to study HBV infection allowing a full characterization of the HBV cycle (Yan et al., 2013). Even if those cells are a reliable model for HBV cycle study, non-transformed cells are often preferred to get closer to physiology. That is why HepaRG cells can also be used; these are non-transformed hepatic-derived progenitors from an HCV-induced tumor. In a long-term dimethyl sulfoxide (DMSO) treatment (more than two weeks), they start to differentiate into cholangiocytes and hepatocyte-like cells. They support HBV infection and cccDNA establishment. dHepaRG cells have been shown to express a similar pattern of functional Toll-like and RIG-I-like receptors as compared to PHHs, qualifying them as a surrogate model to study hepatocyte-intrinsic innate immune responses. In this regard, dHepaRG cells are often used to investigate innate immune responses to HBV infection *in*

vitro (Luangsay et al., 2015). However, only 50% of the cells are differentiated hepatocytes consequence of low infection rates (10%) (Cerec et al., 2007). Investigating the release of viral and non-viral particles upon infection has been challenging. Most of the studies have been conducted using producing cell lines (e.g., HepAD38 or HepG2.2.15). The use of infection models is hampered by the need to accumulate large quantities of supernatant in order to obtain reasonable levels of extracellular vesicles.

ii. *In vivo* models

Among the *in vivo* systems, monkey species are very attractive, and chimpanzees were the first animals described for their ability to develop an acute HBV infection after the inoculation of sera from HBV-infected patients (Maynard et al., 1972). However, as this species is now protected, chimpanzees no longer represent an appropriate model for an antiviral research program. More recently, it was shown that macaques could represent a useful new primate model for the study of HBV since transfection of HBV-DNA induces hepatitis in cynomolgus macaques, and primary macaques hepatocytes support a complete HBV replication cycle associated with the secretion of Dane particles (Lucifora et al., 2010). The only non-primate animals experimentally susceptible to HBV infection are tree shrews (C. Yang et al., 2015). Although in vivo infection of adult animals results in a mild and transient infection with low levels of viral replication. Mice are the best characterized and most convenient small laboratory animals but they cannot be infected with HBV (Dandri & Lütgehetmann, 2014). Mice with humanized livers support HBV infection and their immune reconstitution allows studying HBV-related immunopathogenesis. Several other models have been developed, each of them having advantages and limitations (for more information refer to (Allweiss & Dandri, 2016b)).

3. Chronic Hepatitis B (CHB)

i. Classification of patients with HBV infection

Chronic hepatitis B phases

The natural history of chronic HBV infection has been classified into five major phases according to European Association for the Study of the Liver (EASL) clinical practice guidelines on the management of HBV infection (European Association for the Study of the Liver. Electronic address: easloffice@easloffice.eu & European Association for the Study of the Liver, 2017) , which takes into account the presence of HBeAg, serum levels of HBV DNA and alanine aminotransferase (ALT) and also the presence or absence of liver inflammation.

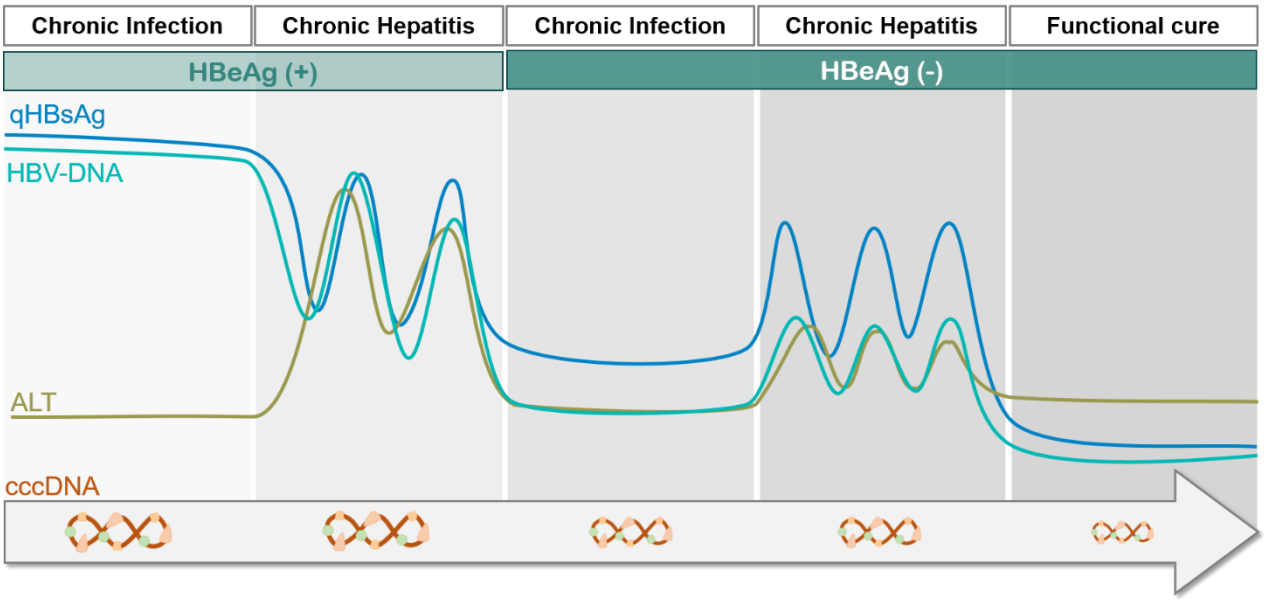

Figure 21. DIFFERENT STAGES OF HBV CHRONIC INFECTION (Adapted from (Fanning et al., 2019))

- **Phase 1: the HBeAg-positive chronic HBV infection** phase formerly called immune-tolerant phase, characterized by HBeAg positivity and very high levels of HBV DNA and normal ALT. In the liver, there is minimal or no liver necroinflammation or fibrosis.
- **Phase 2: the HBeAg-positive chronic hepatitis** phase formerly called the HBeAg-positive immune-active phase, characterized by the presence of serum HBeAg, high levels of HBV DNA and elevated ALT. In the liver, there is moderate or severe liver necroinflammation and accelerated progression of fibrosis.
- **Phase 3: the HBeAg-negative chronic HBV infection** phase formerly called the inactive carrier phase, characterized by the presence of serum antibodies to HBeAg (anti-HBeAb), undetectable or low HBV DNA levels and normal ALT according to traditional cut-off values.
- **Phase 4: the HBeAg-negative chronic hepatitis** phase formerly called HBeAg-negative immune-active phase, is characterized by the lack of serum HBeAg usually with detectable anti-HBeAb,

and persistent or fluctuating moderate to high levels of serum HBV DNA, as well as fluctuating or persistently elevated ALT values. The liver histology shows presence of necroinflammation and fibrosis.

- **Phase 5: HBsAg-negative phase** also known as ‘‘occult HBV infection” is characterized by undetectable viral load, serum negative HBsAg and positive antibodies to HBcAg (anti-HBc), with or without detectable antibodies to HBsAg (anti-HBsAb).

Nevertheless, in a significant number of patients, a single determination of HBV replication markers as well as disease activity markers does not allow an immediate classification into one of the phases. Serial monitoring of serum HBeAg, HBV DNA and ALT levels is required in most instances but even after a complete assessment, some subjects fall into an indeterminate grey area and management needs to be individualized. The development of additional biomarkers could significantly help in the classification of patients and in their monitoring.

Definition of HBV Cure

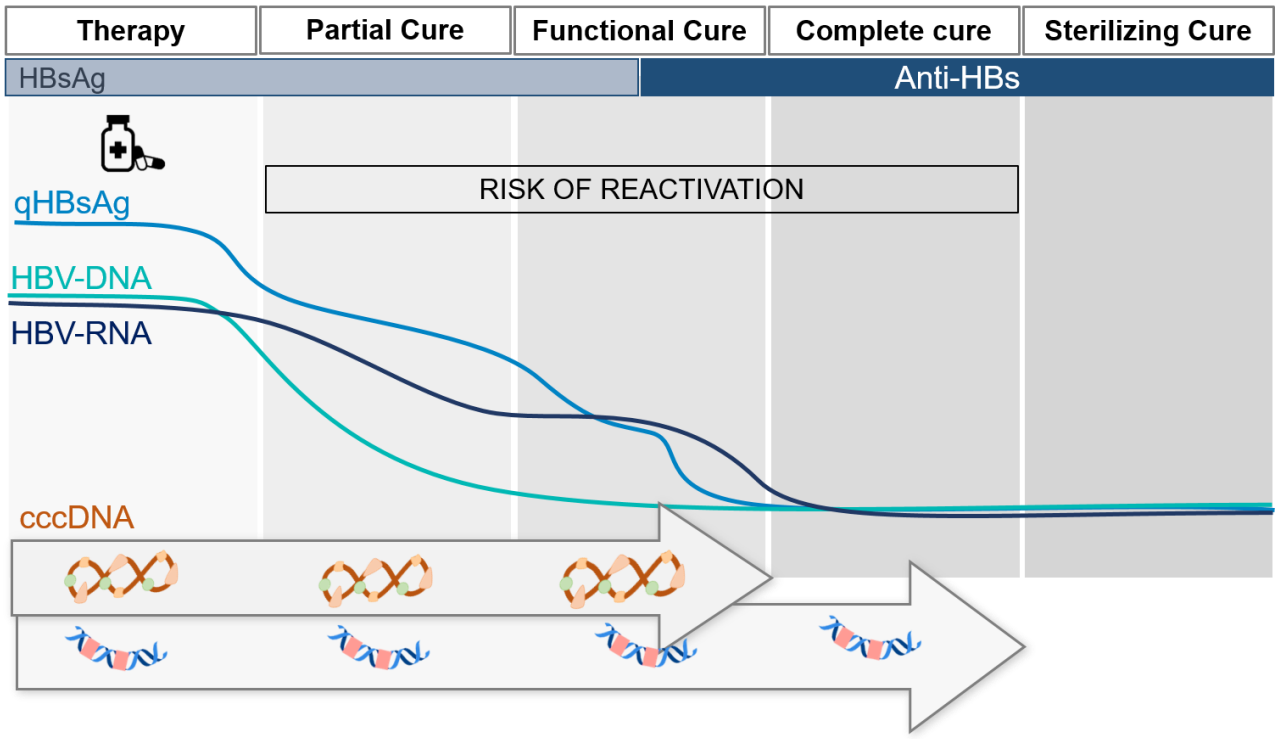

Figure 22. HBV Cure (Adaptated from (Charre et al., 2019)

Although the term "cure" is being increasingly used in HBV-infected patients, several concepts around the definition of a cure of HBV infection need to be clarified. True "complete cure" of HBV would require the total clearance of intra-nuclear cccDNA from all infected hepatocytes, thereby allowing treatment cessation and preventing the risk of reactivation in case of a loss of immune control (Lok et al., 2017).

As an intermediate step, but still relevant toward HBV cure, there is consensus on aiming at reaching a functional cure, equivalent to a resolved acute infection: durable HBsAg loss (with or without anti-HBs seroconversion), undetectable serum HBV DNA, persistence of cccDNA in a transcriptionally inactive status and the absence of spontaneous relapse after treatment cessation. These definitions do not take into account the possible presence and persistence of integrated HBV DNA in the host genome. Clonal expansions of hepatocytes containing unique virus-cell DNA junctions formed by the integration of HBV DNA can be detected in patients at various stages of chronic infection. Terms like HBV eradication or sterilizing therapies, although evocative, should be avoided so far.

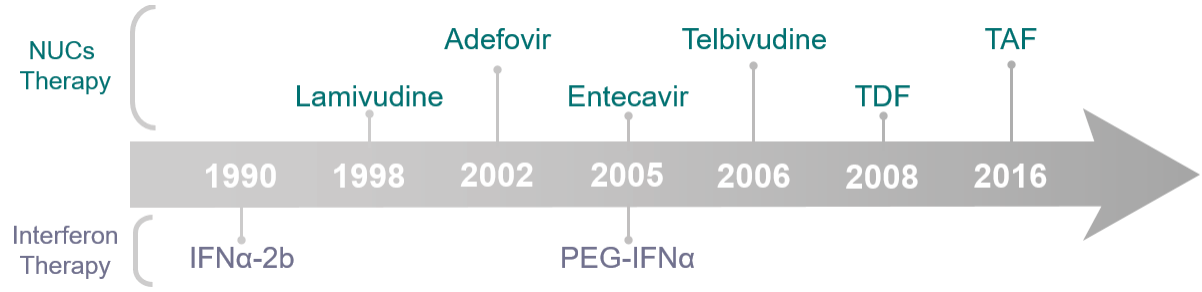

Figure 23. Timeline showing the year of US FDA approval for individual HBV treatment agents. The upper part refers to nucleo(s)tide analogs (NAs), and the lower part refers to interferon-based therapies.

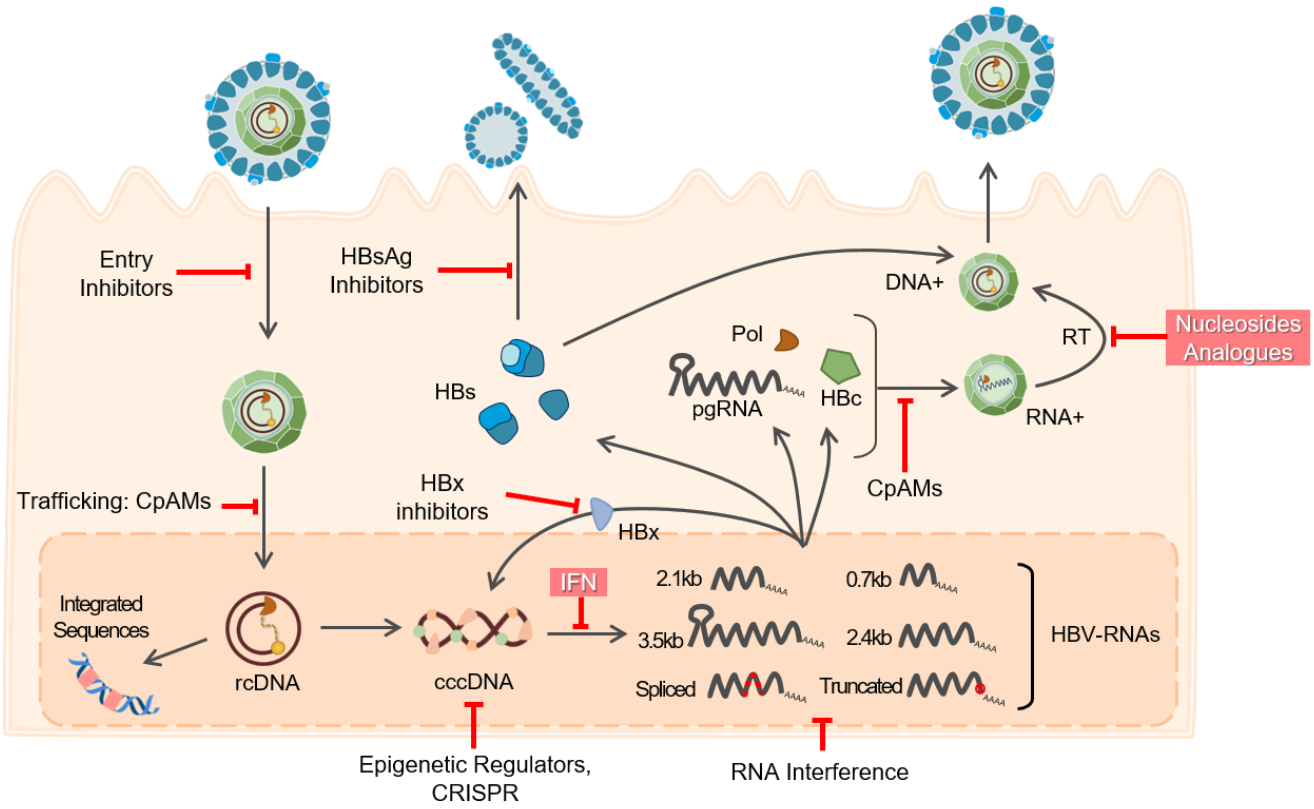

Figure 24. Schematic representation of the HBV cycle and the targets of direct-acting antivirals. Viral entry can be prevented, either by disrupting viral interaction with heparan sulfate proteoglycans or by inhibiting high-affinity binding to NTCP receptor. Strategies targeting covalently closed circular DNA (cccDNA) include prevention of cccDNA formation, cccDNA degradation or destabilization, gene-editing tools to cause sequence-specific damage, and epigenetic manipulations to functionally silence cccDNA. Inhibition of the interplay between hepatitis B virus (HBV) X protein and host proteins leads to transcriptional silencing. Therapeutics based on RNA interference target viral transcripts and block HBV protein expression. Nucleoside or nucleotide drugs are approved inhibitors of reverse transcriptase. Core protein allosteric modulators interfere with the kinetics of nucleocapsid assembly/disassembly and can affect the various functions of the core protein. Hepatitis B surface antigen (HBsAg) release inhibitors limit the circulating HBsAg load. Legend: pegylated interferon α-2a (pegIFN-α), tenofovir disoproxil fumarate (TDF) and tenofovir alafenamide (TAF). Adapted from (Yuen et al., 2018).

ii. Treatments

Antiviral Drugs

At present, there are two main classes of antiviral drugs approved for the treatment of CHB: i) **Pegylated interferon-alpha (pegIFN-α)**, inducing viral suppression but accompanied by severe side effects, and i) new generation **NAs**, with both high antiviral potency and barrier to resistance, that achieve strong viral suppression in most patients.

Pegylated Interferon-alpha (pegIFN-α):

IFN-α is an immune modulator that induces, in a nonspecific manner, the expression of interferon-stimulated genes (ISGs) encoding intracellular or secreted proteins with direct or indirect antiviral properties in both infected and non-infected cells, and promotes the differentiation/activation of immune cells (Sadler & Williams, 2008). Concerning HBV, the IFN-α antiviral activity results from a complex mode of action including the activation of natural killer (NK)/NKT cells, inhibition of viral genome transcription, destabilization of viral nucleocapsid, but also, as recently suggested, degradation of cccDNA via the activation of APOBEC3A in infected cells (Lucifora et al., 2014; Thimme & Dandri, 2013).

Nucleo(s)tide analogs (NAs)

NAs directly inhibit the reverse transcriptase activity of the HBV polymerase. To date, FDA-approved NAs belong to one of the three structural groups:

- L-Nucleosides including Lamivudine (3TC) and Telbivudine.
- Alkyl phosphonates includes adefovir dipivoxil (ADV) and the structurally similar tenofovir (TFV).
- D-cyclopentane including entecavir and having the most potent anti-HBV drug discovered to date.

NAs therapy represents the first line of treatment of CHB. In chronically HBV-infected hepatocytes, NAs inhibit viral polymerase activity, resulting in decreased production of virions, reduced recycling of viral nucleocapsids to the nucleus of infected cells, and theoretically a decline of viral cccDNA, although the latter can only be observed after many years of treatment (Gish et al., 2012; Lai et al., 2017; Lebossé et al., 2020; Werle-Lapostolle et al., 2004). Therefore, NA therapies require long-term treatment. In addition, NAs do not inhibit *de novo* formation of cccDNA in newly infected cells, implying that persistent residual viremia during antiviral therapy can lead to infection of new hepatocytes

and reestablishment of viral cccDNA reservoir. A decrease of the total amount of intrahepatic cccDNA is observed during long-term therapy as a consequence of i) the inhibition of intracellular recycling pathway, ii) dilution of cccDNA via hepatocyte turnover, as cccDNA may be lost through cell division, and iii) decreased rate of infection in new cells (Hagiwara et al., 2018; Vachon & Osiowy, 2021; Werle-Lapostolle et al., 2004; Wong et al., 2006). Long-term inhibition of HBV DNA by antiviral treatments such as NAs has been confirmed to slow down the progression of liver cirrhosis and significantly reduce the risk of HCC (J. H. Kim et al., 2017).

Drugs in development

The search for new antiviral drugs to cure HBV is a highly dynamic field that has grown considerably in recent years thanks to the close collaboration between academic research and industry. Ongoing efforts are made to develop novel direct-acting antivirals (DAAs) and host-targeting agents (HTAs) for HBV infection.

Based on the particularities of the HBV viral cycle, DAA-based therapeutic strategies can be classified according to the process they target. They can either target HBV replication cycle (i.e., entry inhibitors, capsid assembly modulators, strategies targeting cccDNA (by either elimination or transcriptional silencing), agents targeting viral RNAs (siRNAs, ASO, and LNA) or HBs secretion inhibitors or reverse transcriptase) or drugs targeting HBV gene expression aiming at decreasing the level of viral transcripts and antigens. Both of these classes indirectly target cccDNA. Immunebased strategies under evaluation include i) boosters of innate immunity: TLR-7 and TLR-8 agonists, ii) check-point inhibitors: programmed-death 1 (PD1) and programmed-death ligand 1 (PDL1) blockers, and ii) specific immune stimulation by therapeutic vaccines. All these strategies are being evaluated in combination with NAs in Phase 1b and Phase 2a studies (Roca Suarez et al., 2021).

To better follow the impact of these drugs during clinical studies, a reliable and non-invasive biomarker is needed. Hence, the following part will give an overview of the currently available but also new and promising biomarkers. HBV markers are essential for the clinical evaluation of the anti-HBV treatment and the identification of CHB stages.

iii. Biomarkers in CHB

What is a good biomarker?

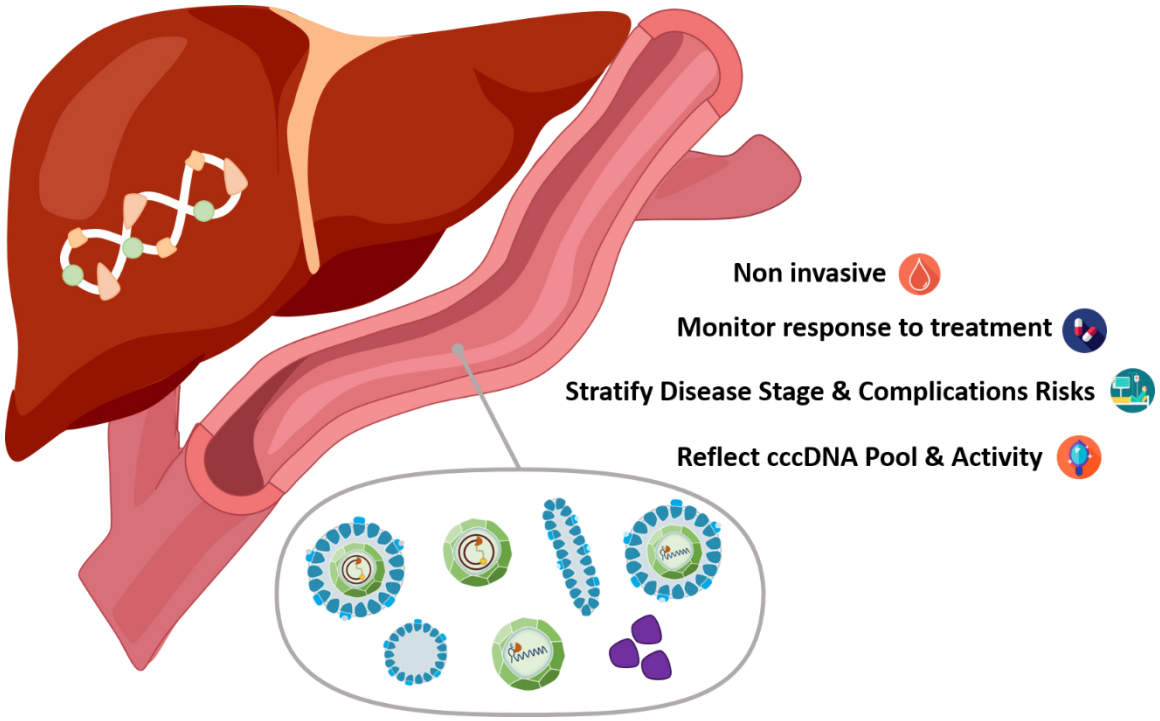

Figure 25. What is a good biomarker?.

The basic definition of a biomarker is deceptively simple: *"A defined characteristic that is measured as an indicator of normal biological processes, pathogenic processes or responses to an exposure or intervention"* (Cagney et al., 2018). However, the question is what should we expect from the ideal HBV biomarkers? At best, it should fill the following criteria:

- Noninvasive in order to minimize risk for the patient.
- Helpful to identify treatment response before or early during treatment.
- Able to stratify by disease stage and risk for complications (e.g., reactivation, cirrhosis, HCC).
- Helpful in the management of patients.
- Reflect intrahepatic cccDNA pool and transcriptional activity.

The gold standard to determine the level of virus in the liver is to quantify intrahepatic cccDNA from liver biopsy, albeit liver biopsies are impractical as a routine diagnosis as non-invasive techniques are preferred.

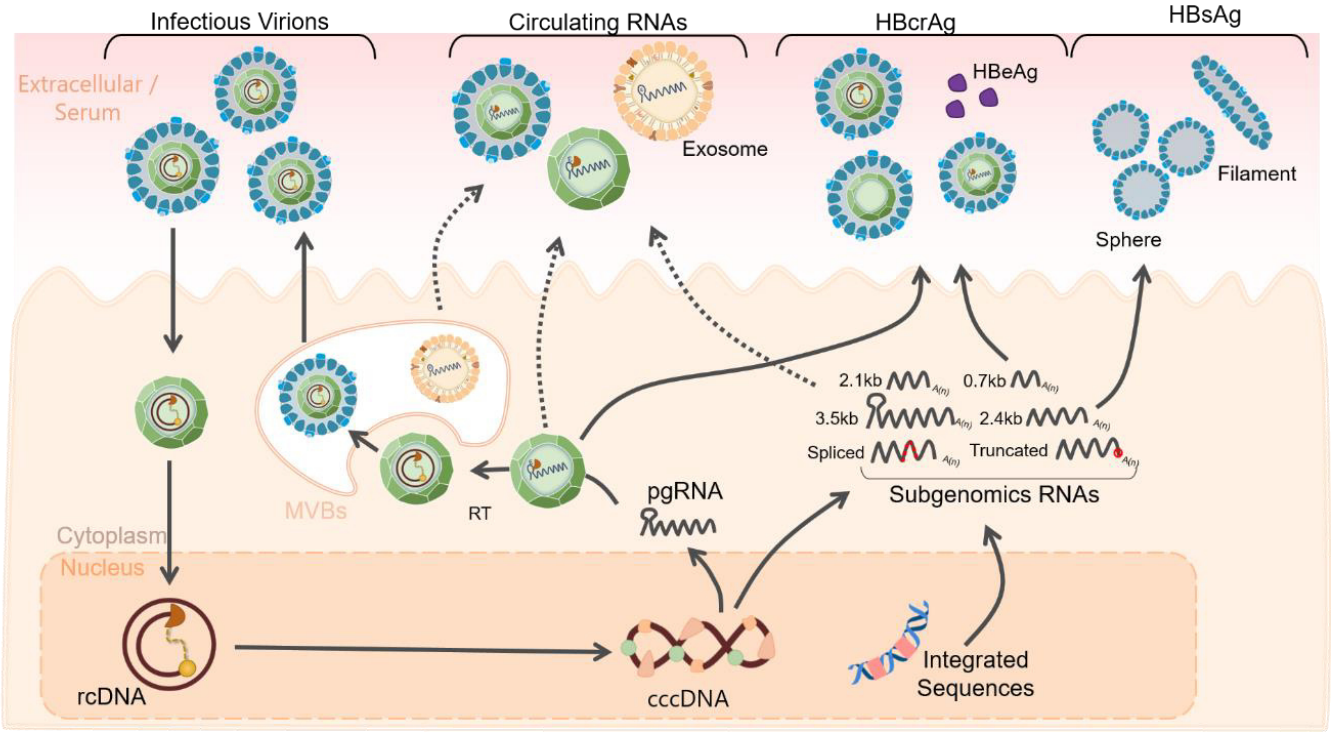

Figure 26. HBV BIOMARKERS.

Biomarker	Advantages	Limitations
qHBsAg	• Monitoring of response to treatment and seroconversion • Prediction of HBsAg loss • Prediction of liver fibrosis and HCC	• Transcription from HBV integrants = poor correlation with cccDNA in HBeAg (-) patients
Serum HBV-DNA	• Monitoring of response to treatment	• Undetectable in long-term NA-treated patients, thus not useful to reflect intrahepatic cccDNA
HBcAb	• Correlates with ALT during treatment • Prediction of development liver fibrosis and necroinflammation • Monitoring treatment and SVR • Identification of occult HBV	• Narrow range of quantification
HBcrAg	• Correlates with cccDNA activity • Levels can distinguish between active and inactive disease • Prediction of HBeAg or HBsAg seroconversion, development of cirrhosis • Monitoring of response to treatment	• Limited availability of assays • Should be further investigated with larger and more diverse cohorts • Improvement of the sensitivity
Serum HBV-RNA	• Surrogate of cccDNA transcriptional activity • Serum HBV RNA levels can be used to differentiate HBeAg-negative phases of CHB • Prediction of HBeAg seroconversion • Prediction of SVR in patients on pegIFN and/or NAs	• Depends on HBeAg status • Larger cohorts and improved sensitivity required • No standardized assay so far

Table 1. Advantages and limitations of HBV biomarkers

What are the current biomarkers used during HBV infection?

While some serological markers are useful in the diagnosis of HBV (e.g., HBsAg and anti-HBc antibodies), others help identify the phase of CHB (e.g., HBeAg, anti-HBe, anti-HBs, and serum HBV DNA) (Fig.26) (Table.1).

Quantitative HBsAg (qHBsAg)

Coating the surface of SVPs and virions, HBsAg is the first recognized biomarker of HBV infection. Routinely used in patient's management, serum HBsAg quantification correlates with the immune stages of CHB, predicts progression of liver fibrosis and HCC and the outcome of antiviral treatment (Seto et al., 2014).

Variability in the protein composition of the HBsAg protein was reported and studies suggested that the composition might be correlated with specific phases of HBV infection (Petit et al., 1990; Stibbe & Gerlich, 1982). In 2018, Pfefferkorn et al. designed a monoclonal ELISA assay against the different HBs proteins and used it to specially quantify M-HBs and L-HBs in serum samples. In this study, they showed that composition of HBsAg was distinct in different well-defined clinically phases of HBV infection and that ratios of L-HBs and M-HBs were better predictors of inactive carriers and HBeAg-negative CHB than total HBsAg levels (Pfefferkorn et al., 2018). Subsequently, they reported a decrease in L-HBs and M-HBs proportions prior to total HBsAg loss during NAs and pegIFN treatment, suggesting that changes in these proportions could be useful to predict HBsAg loss (Pfefferkorn et al., 2021).

Unfortunately, HBs can be produced from both cccDNA and integrated HBV sequences in the host genome, the latter source can introduce a bias in the direct correlation of intrahepatic cccDNA pool and transcriptional activity (Pollicino & Caminiti, 2021). Furthermore, mutations within the PreS1, PreS2 or HBsAg coding regions may result in altered HBsAg quantification due to secretion or expression defects (C.-C. Wu et al., 2018).

Serum HBV DNA

Serum HBV DNA (or viral load) is a key indicator during HBV management and is quantified by real time PCR assay in patient's serum. Several manufacturers provide real time PCR platforms and reagents that are clinically approved for medical diagnostic. According to the American Association for the Study of Liver Diseases (AASLD) guidelines for treatment of chronic hepatitis B (Terrault et al., 2018) and the EASL clinical practice

guidelines, the required sensitivity for HBV DNA detection is 10 IU/mL. The PCR assays that are commonly used demonstrate a limit of detection that is usually lower than the limit of quantification thereby emerging detectable but not quantifiable HBV DNA results. The genetic variability of different HBV genotypes and subgenotypes appears to have minimal, if any, effect in HBV DNA quantification. Nonetheless, mutations in the primer or probe binding regions may lead to underestimation of the viral load.

The measurement of serum HBV DNA is widely used to evaluate HBV replication. In general, HBV DNA level is considered to be an important indicator to start antiviral therapy and monitor patients under such regimes. HBV-DNA becomes undetectable in long-term NA-treated patients. However, most of the long-term suppressed patients still have cccDNA in the liver. In this regard, HBV-DNA is not a suitable biomarker to assess cccDNA pool in treated patients.

Hepatitis B core antibody (HBcAb)

Antibody to the HBV core protein (HBcAb) is a diagnostic marker indicating past exposure or current infection. Quantitative anti-HBc antibodies (qHBcAb) levels can be measured using several commercially available ELISA-based assay and have been found to be a sensitive and specific indicator of the host immune response against HBV (Vanwolleghem et al., 2020). After acute HBV infection, HBcAb-IgG remains in the serum of HBV patients for rather a long time. In general, the quantitative concentration of serum HBcAb in hepatitis B remains at the higher level than that of HBV carriers. Unlike qHBsAg, qHBcAb testing is not routinely used in management and still requires international standardization.

Emerging biomarkers

Hepatitis B core-related antigen (HBcrAg)

Hepatitis B core-related antigen (HBcrAg) is represented by three separate proteins, HBeAg, HBcAg and p22cr, that all share a common 149 aa sequence, with the latter being a posttranslational product similar to HBeAg but retaining the NTD (Hong et al., 2017) (Fig. 10). HBeAg is the major component of HBcrAg (72%), with HBcAg and p22cr both present at approximately 10–15% of total HBcrAg composition in the serum of HBeAg-positive patients (Hong et al., 2021).

HBcrAg levels in serum are measured using a chemiluminescent enzyme immunoassay (CLEIA) involving a series of monoclonal antibodies specific to the different

protein targets (F. Suzuki et al., 2009). Being a promising biomarker for predicting HBV infection status, HBcrAg levels reflect viral replication as it correlates with serum HBV-DNA, as well with serum qHBsAg in HBeAg-positive but not in HBeAg-negative patients. HBcrAg is strongly correlated with intrahepatic total HBV-DNA, cccDNA and pgRNA levels, both in HBeAg+ and HBeAg− patients. Notably, qHBsAg and serum HBV-DNA correlations with the same intrahepatic markers are much weaker. Moreover, cccDNA transcriptional activity, calculated by pgRNA/cccDNA ratio, is only correlated to HBcrAg and not to qHBsAg in HBeAg-negative patients, suggesting that HBcrAg is a better surrogate marker of cccDNA transcriptional activity than qHBsAg (Testoni et al., 2019). Nonetheless, improvement of the sensitivity of this test is required prior to its use in evaluating novel antiviral compounds under clinical development, since only 30–50% of HBeAg-negative patients are currently identified as positive for HBcrAg. A version of the assay (iTACT-HBcrAg) with increased sensitivity has been recently developed and awaits validation in patients (Inoue et al., 2021).

Serum HBV-RNA

It was in 1984 that Miller and colleagues first observed HBV RNA in serum as HBV DNA-RNA hybrid molecules (Miller et al., 1984). Few years later, Kock et al. confirmed the presence of circulating polyadenylated HBV RNAs in the sera of HBV-infected patients by using rapid amplification of complementary DNA (cDNA)-ends (RACE) (Köck et al., 1996). HBV pgRNA has been detected in cultured hepatocytes, patient liver biopsies and serum (van Bömmel et al., 2015; J. Wang, Yu, et al., 2017; M.-L. Wang et al., 2021). It is now widely accepted that HBV RNAs can be found in patient's circulation in proportions ranging between 0.1 and 1% of HBV DNA levels in the absence of antiviral treatment. However, the precise species of circulating RNAs and the molecular entities they are associated with (either free RNA, exosome containing RNA or viral particle containing RNA) remain a matter of debate.

- **What HBV RNA species are circulating in patient's serum?**

Serum HBV-RNA species are heterogeneous in size and sequences. This variability may depend on treatment and the different stages of CHB. In addition, HBV-RNA characterization suffers from a lack of standardized methods for extraction, detection and quantification, raising discrepancies in the literature. The following section gives a state of art of circulating HBV-RNA species over the last decades (see Table 2 for an overview).

HBV-RNA species	Where?	Experimental Model		Reference
		In vitro	*In vivo*	
pgRNA	-	-	CHB Patient	Hacker HJ, Ann N Y Acad Sci 2004
	-	HepG2.2.15	CHB Patient	Jansen L, J Infect Dis 2016
	-	HepaRG, PHH	-	Lam AM, Antimicrob Agents Chemother 2017
	-	-	CHB Patient	Prakash K, Virol J 2018
	VLPs	HepAD38, HepG2.2.15, PHH	TG-mouse, CHB patient	Wang J, J Hepatol 2016
	VLPs, NCs	HepAD38	CHB Patient	Bai L, J Virol 2018
	VLPs	HepG2-NTCP, HepAD38, PHH	CHB Patient	Stadelmayer B, J Hepatol 2020
Spliced Isoforms	-	HepaRG, PHH	-	Lam AM, Antimicrob Agents Chemother 2017
	VLPs	HepAD38, HepG2.2.15, PHH	TG-mouse, CHB patient	Wang J, J Hepatol 2017
	VLPs	HepG2-NTCP, HepAD38, PHH	CHB Patient	Stadelmayer B, J Hepatol 2020
3' Truncated	-	-	CHB Patient	Hacker HJ, Ann N Y Acad Sci 2004
	VLPs	HepAD38, HepG2.2.15, PHH	TG-mouse, CHB patient	Wang J, J Hepatol 2017
HBx mRNA	**Exosome**	-	CHB Patient	Yang Y, Cell & Mol Immunol 2016
	Exosome	HBx-Huh7	-	Kapoor NR, Virus Res 2017
	-	HepAD38, HepG2-H1.3x	CHB Patient	Niu C, PLoS One 2017
	VLPs	HepG2-NTCP, HepAD38, PHH	CHB Patient	Stadelmayer B, J Hepatol 2020

-; Not identified, **VLPs**; Virions Like Particles, **NCs**; Naked Capsids, **PHH**; Primary Human Hepatocytes, **CHB**; Chronic HBV, **TG-mouse**; Transgenic Mouse

Table 2. Overview of the literature about circulating HBV-RNAs

Historically, it was considered that all circulating HBV-RNA were only pgRNA. Therefore, it came as a surprise when later on it occurred that intermediates and other mRNAs could also be secreted. In 2016, Wang et al. used a RT-qPCR assay with specific primers targeting the 3.5 kb RNA or HBx region and obtained similar copy numbers. In addition, they designed primers to discriminate pcRNA from pgRNA and did not detect any pcRNA in serum, meaning that 3.5 kb RNA could be only **pgRNA** (J. Wang et al., 2016a). However, by using droplet digital PCR (ddPCR), a technique which gives absolute quantification and is more sensitive than conventional RT-qPCR, Prakash et al. detected **small amounts of pcRNA** in patients' serum (Prakash et al., 2020a). Even if some discrepancies can come from varying specificity and/or sensitivity from the different assays, it seems that secreted HBV-RNAs predominantly derive from pgRNA. Although pgRNA or viral RNA derived from pgRNA are the major species currently described, other viral RNA may circulate in the bloodstream. For example, **HBx mRNA** was recently detected in sera of patients with CHB (Niu et al., 2017). Furthermore, Stadelmayer et al. later supported this observation using 5'RACE technique by finding **shorter than canonical HBx transcripts** in patients' serum (Stadelmayer et al., 2020).

Next, the question was to know if those RNAs could undergo alternative splicing or if they are full-length pgRNA. *In vitro*, over a dozen **splice-derived variants** have been recognized (Günther et al., 1997), SP1-RNA representing over 30% of the total pgRNAs (H. L. Wu et al., 1991). Spliced cDNA variants resulting from reverse transcription of the spliced RNAs were found in the blood of CHB patients (J. Chen et al., 2015). This question was answered in several studies by the use of different techniques. 5'RACE analysis on patient's serum identified different spliced variants (Stadelmayer et al., 2020). Furthermore, Lam et al. detected both full length pgRNA and spliced forms, even if in lesser proportion, in the supernatant of infected HepaRG cells treated or not with lamivudine as well as in patient's sera (Lam et al., 2017). Another study from Wang et al. reported numerous shorter than full-length pgRNA species detected by PCR and identified them as spliced variants or **3'-truncated forms** (J. Wang et al., 2016a). Finally, it seems that circulating HBV RNAs are a mixture of full-length pgRNA and derived species but also HBx RNA, including shorter forms.

To get a full characterization of HBV-RNAs, the 3' terminal region of HBV RNAs needs to be better characterized. Indeed, using multi-PCR identification or CAGE, Altinel et al. highlighted that circulating HBV-RNAs were mainly pgRNAs that could be devoid of poly A

tail supporting the existence of an additional termination site (Altinel et al., 2016). So far, the major form of described RNA is full-length transcripts (flRNA) ending at the canonical polyadenylation signal "TATAAA" motif located downstream of the HBx ORF. However, truncated RNAs were also identified in HCCs by Hilger et al., who described a cryptic polyadenylation signal CATAAA located within the HBx ORF (Hilger et al., 1991). Kairat et al. used RACE-based quantitative PCR (RACE-qPCR) to selectively quantify serum 3' full-length poly-A HBV RNA and 3' internally truncated poly-A HBV RNA (Kairat et al., 1999). This finding was supported by Van Bömmel et al. who also found that RNAs could be 3′ end-truncated in serum of patients (van Bömmel et al., 2015). This cryptic polyadenylation site is usually used upon transcription from viral integrated sequences (Breitkreutz et al., 2001). Circulating truncated RNAs (trRNAs) may thus reflect the reservoir of integrated viral sequences. Accumulation of circulating 3′-truncated polyA-free pgRNA has also been observed in sera of CHB patients under NAs treatment (J. Wang, Du, et al., 2017). Moreover, NAs treatment can also give rise to virions containing 3' end-truncated pgRNA between DR1 and DR2 or upstream DR2 in serum from telbivudine-treated patients (Shen et al., 2020a).

It is important to keep in mind that other RNA fragments are not excluded. In fact, during retro transcription, abortive RNase H degradation of pgRNA may occur, resulting in residual pgRNA sequences present in the (-) strand as DNA-pgRNA hybrids. These hybrids mimicking double-stranded DNA may then be released from hepatocytes according to state of advancement of reverse transcription and DNA maturation (J. Hu & Liu, 2017). In addition, a distribution of pgRNA fragments with receding 3' ends was observed in treatment-naïve HBV-infected patients and in the supernatant of HBV-replicating stably transduced cell lines (HepAD38) (Bai et al., 2018). These results suggest that circulating HBV-RNAs may also include replicative intermediates of pgRNA according to reverse transcription advancement.

- **Circulating particles containing viral RNA**

Similar to the exact composition of circulating RNA species, the nature of circulating RNA-containing particles (e.g., virion-like particles, naked capsids, extracellular vesicles) remains controversial. *In vivo*, the association between hepatic cytolysis and the level of circulating RNAs (Bai et al., 2018; van Campenhout et al., 2018) led to the hypothesis that

RNA release might be passive, resulting at least partly from the lysis of infected cells. However, other reports suggest an active release mechanism.

Rokuhara et al. speculated that serum HBV-RNA could be incorporated into viral particles. By using a sucrose density gradient, serum RNAs were co-purified with HBV DNA and core protein suggesting a composition similar to DNA virions, however they didn't discriminate virion-like particles from naked capsids because of a lack of HBs characterization (Rokuhara et al., 2006; J. Wang et al., 2016a). Later, immunoprecipitation with HBs and HBc antibodies revealed that the majority of HBV-RNAs were present in virion structures (Jansen et al., 2016a). Finally, pgRNA was also detected after anti-HBc immunoprecipitation in the plasma of three treatment-naïve HBeAg-positive patients with CHB, demonstrating an association between pgRNA and the capsid. The detection was enhanced using a detergent treatment to remove the HBV envelope, suggesting that pgRNA may be both encapsidated and enveloped (Jansen et al., 2016a). This observation is consistent with the protection of serum viral RNA from exogenous RNAses (Prakash et al., 2018).

Wang et al. further investigated the nature of HBV-RNA containing particles. Using HepAD38 supernatant, they concluded that HBV-RNA is encapsidated pgRNA without distinguishing virions from naked capsids. Surprisingly, naked capsids seemed to be enriched in cell culture supernatant, whereas they are barely detected in patient's circulation. In this same study, they used GW4869 to inhibit exosome secretion and observed no decrease in the total 3.5 kb RNA level (J. Wang et al., 2016a). However, GW4869 inhibits ceramide pathway-derived exosomes, which is the minor exosome secretion pathway. Thus, it is not excluded that exosomes secreted through the ESCRT pathway could carry circulating HBV-RNAs.

This hypothesis is supported by the detection of truncated RNAs in the supernatant of infected hepatocytes in the absence of proteins of the capsid or the envelope which could be explained by the release of HBV-RNA associated with extracellular vesicles or by cell lysis (Q. Su et al., 2001; van Bömmel et al., 2015). Finally, Yang et al. identified HBV-RNA associated with exosomes in CHB patient's serum as well as in HepG2.2.15 cell supernatant (Y. Yang et al., 2017).

In accordance with *in vitro* experiments showing the presence of HBV-RNA in NCs (Ning et al., 2011a), Bai et al. recently found HBV-RNA naked capsids as an immune

complex form in the plasma from four CHB patients (Bai et al., 2018). *In vitro*, extracellular HBV-RNAs are preferentially loaded in naked capsids rather than in virions (Chou et al., 2015a). The RNA population detected in naked capsids is heterogeneous in length. Detection of RNA-containing naked capsids is not restricted to *in vitro* systems as analysis of sera from HBV patients revealed the presence of RNA-containing naked capsids (Bai et al., 2018). The factors regulating HBV-RNA incorporation into these capsids is still enigmatic and seems to rely on CTD domain phosphorylation of capsid protein. In normal conditions, the CTD domain of HBcAg is highly phosphorylated, impairing the packaging of non-specific RNA. However, some conditions might lead to a hypophosphorylated state of the CTD (Q. Zhao et al., 2018), resulting in unspecific packaging of RNAs in naked capsids (Ludgate et al., 2016).

Altogether, these observations suggest a wide heterogeneity of circulating HBV-RNA containing viral and non-viral particles that may vary depending on different stages of chronic HBV infection.

- **Measurements of circulating viral RNAs**

Methods of quantification of serum HBV-RNA differ across studies. There are two main strategies to detect and quantify HBV transcripts. The first one is based on a 5' amplification especially targeting 3.5 kb transcripts (i.e., pgRNA and preC mRNA), whereas the other one is based on a 3' end amplification targeting most of HBV transcripts as they share the same 3' end. However, quantification of circulating truncated RNAs by using primers targeting the cryptic or canonical polyadenylation site is possible and could reflect the termination profile of these RNAs.

Assays based on amplification techniques generally use a low input volume, ranging from 100 to 300 µL of plasma or supernatant. However, their sensitivity remains to be improved: currently the limit of detection (LOD) ranges from 1.85 log copies/mL (Jansen et al., 2016a) to 3.4 log copies/mL (van Bömmel et al., 2018a). A high-throughput HBV RNA test developed recently (Abbott m2000 RNA) claimed a LOD of 1.65 logU/mL, where 1 U HBV RNA = 1 IU HBV DNA (Butler et al., 2018a) corresponding to around 150 copies/mL. More recently, Roche Diagnostic (Pleasanton, CA, USA) proposed a new HBV RNA investigational assay for use on the Cobas® 6800/8800 system with a limit of quantification of 10 copies/ml (Scholtès, 2020).

Of note, there is currently no direct standardization of HBV-RNA quantification. In most assays, viral RNA is indirectly estimated after the reverse transcription step. cDNA is then quantified by interpolating signals to an HBV-DNA standard curve. Results should be carefully interpreted depending on the assay and especially primers used. Furthermore, quantification of circulating RNA seems to depend on the HBV genotype but also on the presence of basal core promoter mutation and pre-core mutation (Prakash et al., 2018; van Campenhout et al., 2018).

Standardization of quantification is thus needed to rigorously compare results from different studies with the aim of using circulating RNA as a new biomarker to assess efficacy of new compounds or to be used as a new treatment endpoint. DNase digestion conducted to remove viral DNA before RNA detection might not be sufficient to completely remove all viral DNA. Indeed, in some cases, residual HBV-DNA may be measured instead of or in addition to viral RNA, leading to conflicting results between studies.

- **Correlation between serum HBV RNA and other HBV markers and clinical significance**

NAs therapy can reduce serum HBV-DNA to undetectable levels by blocking reverse transcription without directly influence HBs and HBcrAg levels and HBV-RNA coming from cccDNA transcription. In this case, decline kinetic of circulating HBV-DNA differs from serum makes HBV-RNA more direct biomarker for cccDNA pool.

HBV-RNAs do not correlates with HBsAg in HBe-negative patients as the majority of HBsAg in these patients can hail from integrated sequences rather that from cccDNA. Nevertheless, Rokuhara et al. showed that serum HBV-RNA levels correlated with HBcrAg in treated or untreated patients. However, more studies are needed to better assess this correlation (Rokuhara et al., 2006). Several studies showed that serum HBV-RNA poorly or don't correlate with intrahepatic cccDNA but this may differ according to treatment, disease stage and even detection methods (Y. Gao et al., 2017; H. L. Huang et al., 2000; J. Wang, Du, et al., 2017). Notably, Giersch et al corroborated Wang et al. data highlighting serum pgRNA as a potentially useful clinical surrogate marker to estimate the intrahepatic activity of cccDNA in HBV-infected patients. In their study, Wang et al. demonstrated that serum HBV RNA correlated with intrahepatic cccDNA only in HBeAg-positive patients (Pearson $r = 0.39$, $p = 0.002$). These results suggested the potential influence of HBeAg status to the correlation between serum HBV RNA and cccDNA. Giersch et al. assessed the relationship

between pgRNA in the blood and the amounts of pgRNA and cccDNA molecules in the liver of HBV-infected humanized mice (Giersch et al., 2017a). Levels of serum pgRNA clearly correlated with intrahepatic pgRNA (Spearman r = 0.82, p <0.0001) in non-treated mice but also in NA- or pegIFN-α-treated rodents. In untreated HBV-infected animals, levels of serum pgRNA (copies/mL) also significantly correlated with cccDNA (Spearman r = 0.89, p <0.0001), indicating that serum pgRNA indeed may serve as a suitable serological marker for the persistence of active cccDNA molecules. It is noteworthy that all mice used in this study were infected with HBeAg positive, wild-type HBV.

Thus, future studies will be needed to assess the impact of the HBeAg status on the levels of circulating pgRNA as suggested previously by Wang et al.

III. Extracellular Vesicles (EVs) and viruses

Extracellular vesicles (EVs) are a heterogeneous group of cell-derived membranous structures comprising exosomes and microvesicles, which originate from the endosomal system or shed from the plasma membrane, respectively. EVs are present in biological fluids (e.g., plasma, saliva, breast milk, semen, urine) and are involved in multiple physiological and pathological processes. Now considered as an additional mechanism for intercellular communication, EVs allow cells to exchange proteins, lipids and genetic material. Knowledge of the cellular processes that govern extracellular vesicle biology is essential to shed light on the physiological and pathological functions of these vesicles as well as potential clinical applications involving their use and/or analysis. Upon release from the donor cell, EVs can either be taken up by neighboring cells or travel through body fluids for cargo delivery into recipient cells at distant sites. Although many details are missing, cellular uptake of some EVs appears to depend, at least in part, on specific ligand-receptor recognition (Gonda et al., 2019), and can be mediated by direct fusion of the EVs with the plasma membrane or by endocytotic uptake (Maas et al., 2017). Cells have been reported to secrete highly specified EVs after infectious exposure or under various cell activation conditions. Through the packaging and transfer of functional proteins, mRNA/miRNA, and other cytosolic components, microvesicles have been found to be beneficial either to the host cell or to the infectious agent.

The study of EVs and the mechanisms that govern their generation and functions in multicellular organisms spans from physiological tissue regulation to pathogenic injury and organ remodeling. Research in this field is stimulated by the potential of EVs as diagnostic and therapeutic tools for the treatment of various diseases, including neurodegeneration, cardiovascular dysfunction, and cancer. Increasingly, EV research is aimed at classification of EVs, isolation methods, and cataloging their putative functions in disease progression and therapy. The utility of EVs as liquid biopsies is particularly promising because of their presence in all biological fluids and their potential for multicomponent analyses.

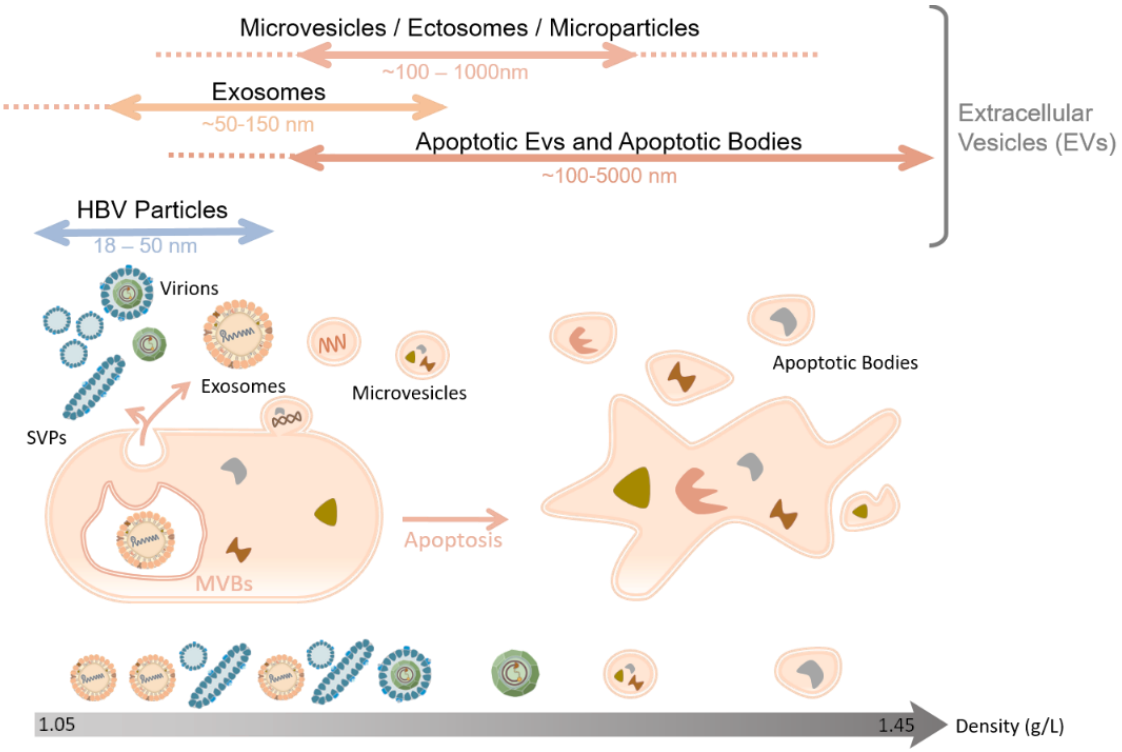

Figure 27. Physical characteristics of different EVs subtypes.

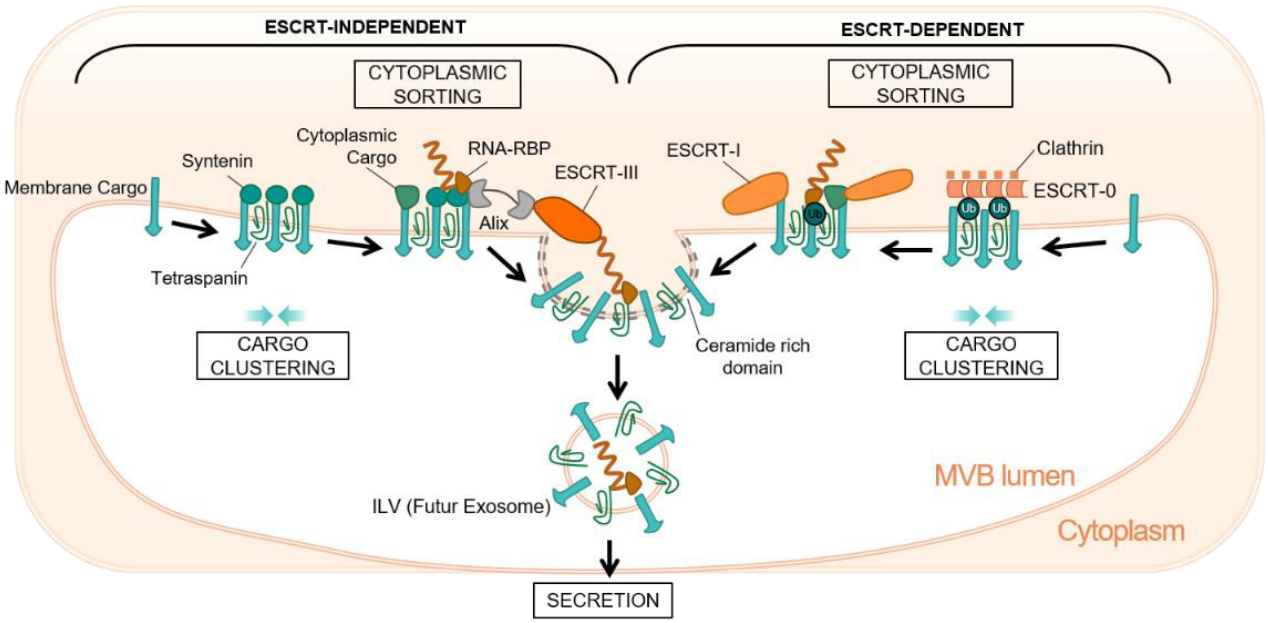

Figure 28. Sorting machineries involved at different steps of exosome biogenesis.

1. Generalities about EVs

i. What are EVs?

Although the classification of EVs is continuously evolving, they are now classified into the following three types based on their mechanism of release and size: exosomes (less than 150 nm in diameter), MVs/shedding particles (100~1000 nm), and apoptotic bodies (>1000 nm) (Théry et al., 2018). Exosomes are carriers of several molecules, such as DNA, RNA, proteins, and lipids, and their contents directly reflect the metabolic state of the cells from which they originate. In this manuscript, we will focus on exosomes, which are also called small EVs (Fig.27).

ii. Exosome Biogenesis

Exosome biogenesis consists of three different stages, including i) the formation of endocytic vesicles by invagination of the plasma membrane; ii) the formation of MVBs by inward budding of the endosomal membrane; and finally, iii) the fusion of MVBs with the plasma membrane and release of the vesicular contents, called exosomes. The biogenesis of exosomes is a tightly regulated process. It begins with the inward budding of endosomes, which in turn forms MVBs that contain intra-luminal vesicles (ILVs) (Hessvik & Llorente, 2018).

During this process, cargo proteins are incorporated into the invaginating membrane, while the cytosolic components are englobed and enclosed within the ILVs. Evidence has revealed that the formation of ILVs requires the endosomal sorting complex required for transport (ESCRT) function (Fig.28). It is an intricate protein machinery composed of four separate protein ESCRTs (0 through III) that work cooperatively to facilitate MVB formation, vesicle budding, and protein cargo sorting. Interestingly, recent evidence favors an alternative pathway for sorting exosomal cargo into MVBs in an ESCRT-independent manner, which seems to depend on raft-based microdomains for the lateral segregation of cargo within the endosomal membrane. These microdomains are thought to be highly enriched in sphingomyelinases, from which ceramides can be formed by hydrolytic removal of the phosphocholine moiety (Mathieu et al., 2019; van Niel et al., 2018).

Several proteins are involved in the origin and biogenesis process of exosomes (e.g., Rab GTPase, Sytenin-1, TSG101, ALIX, ESCRT), although their precise rate-limiting actions and functions in exosome biogenesis require further in-depth exploration (Bebelman et al.,

2018). An intersection of the exosome biogenesis pathway with other molecular pathways associated with the trafficking of intracellular vesicles has confounded the interpretation of functional studies. Distinct cell types, culture conditions, and genomic health of the cells may affect some of the putative key regulators of exosome biogenesis *in vivo*. The potential inconsistencies in identifying regulatory elements associated with exosome biogenesis could also result from different methods for exosome production, enrichment, and concentration (Willms et al., 2018).

iii. Biological function of exosomes

The biology, function, and heterogeneity of exosomes depend on the cell/tissue of origin and its status at the time of exosome generation. Firstly considered as garbage bags of the cells, recent studies claim that exosomes play a significant role in various biological processes, such as angiogenesis, antigen presentation, apoptosis, coagulation, cellular homeostasis, inflammation, and intercellular signaling. These roles are inherent to their cargo role and results from their ability to transfer RNA, proteins, enzymes, and lipids, thereby affecting physiological and pathological processes in various diseases, including cancer, neurodegenerative diseases, infections, and autoimmune diseases (Théry et al., 2002). Below are some examples:

- So far, one of the best-characterized physiological roles of exosomes is their capacity to enhance coagulation and thus participate in **hemostasis.** This capacity seems to be amplified in several pathological processes, for example, in EVs generated by cancer cells (Olejarz et al., 2020).

- Exosomes, in their strict sense, were originally termed and described in reticulocytes where they allow the remodeling of the plasma membrane during **erythrocyte maturation**. During their maturation to erythrocytes, reticulocytes selectively remove proteins, noticeably the transferrin receptor, as well as membrane-associated enzymes, through the formation of reticulocyte-derived exosomes (Blanc et al., 2005).

- Various cell types of the innate immune system have been shown to release exosomes. Exosomes are known to be involved in **inflammatory processes** that play a pivotal role in many pathologic states, including cancer, inflammatory bowel diseases, type 2 diabetes, obesity, rheumatoid arthritis, and neurodegenerative

diseases (Console et al., 2019). Exosome-mediated inflammatory responses are involved in all stages of tumor development, immune surveillance, and resistance to therapy (Colotta et al., 2009).

- Exosomes secreted by antigen-presenting cells (APCs) can confer therapeutic benefits by attenuating or stimulating the immune response by **carrying and presenting** functional major histocompatibility peptide complexes that modulate antigen-specific T cell responses. Dendritic cell (DC)-derived exosomes show immunostimulatory properties by activating T and B cells and exosomes derived from macrophages, and DCs show immunosuppressive properties (Shenoda & Ajit, 2016).

Exosomes can also have a significant role during infection by a pathogen. Reflecting the state of originating cells, they could also play a crucial role in the monitoring of diseases. This molecular function of the exosomes will be discussed in subsequent sections.

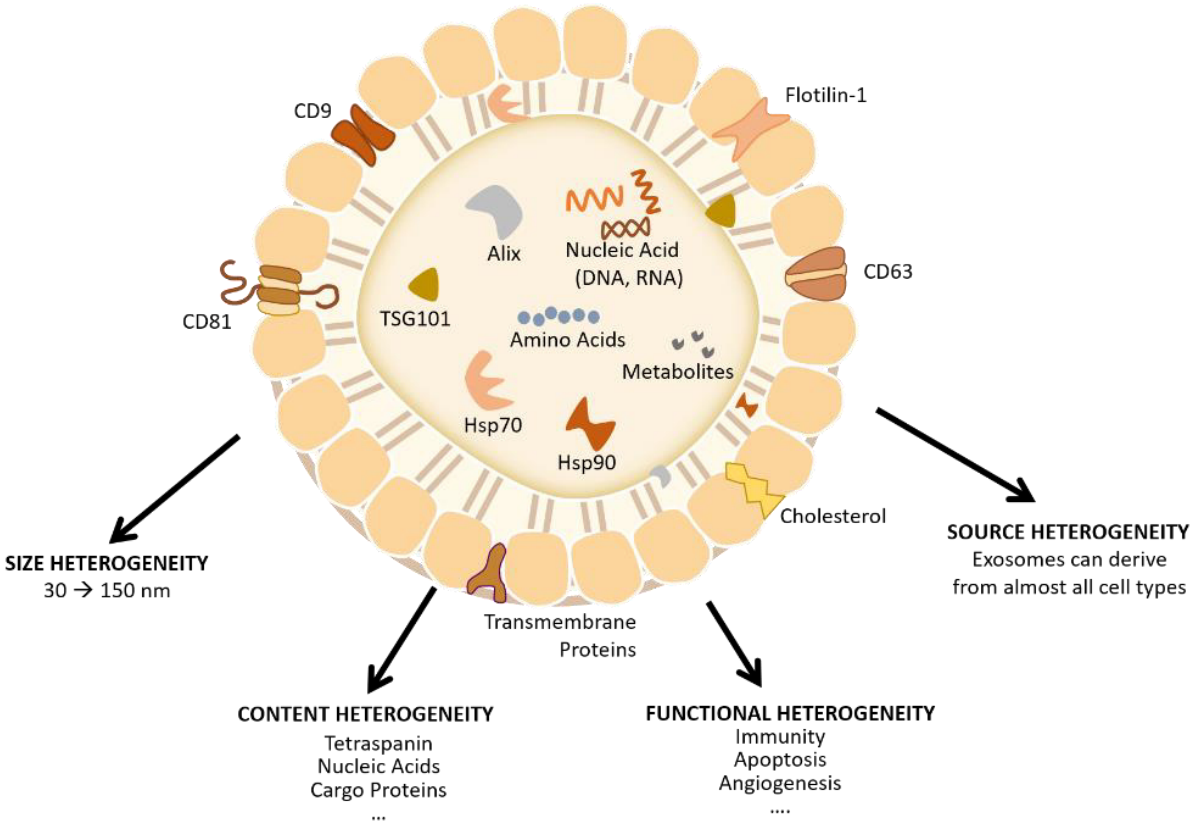

Figure 29: IDENTITY AND THE HETEROGENEITY OF EXOSOMES.

2. Molecular Characteristics

i. Exosome heterogeneity

The heterogeneity of exosomes is likely reflective of their size, content, functional impact on recipient cells, and cellular origin (Fig.29). The microenvironment and the inherent biology of the cells may influence the content of exosomes and their biological markers. Heterogeneity can also be based on the organ and tissue of origin of exosomes, including whether they are from cancer cells (Wen et al., 2019), giving them distinct properties such as tropism to certain organs and uptake by specific cell types. Although it is not surprising that the proteome of the exosomes reflects the proteome of the originating cell, exosome protein cargo from cancer cells can be altered (L. Chen, Chen, et al., 2018; Conde-Vancells et al., 2008; H. Liu & Li, 2018)

ii. EV-specific proteins?

Exosomes contain proteins that are considered to be pan-exosome markers (i.e., common for most exosomes), and their proteins and protein posttranslational modifications specifically reflect the vesicle localization, cellular origin and mechanism of secretion. In general, exosomes are highly abundant in cytoskeletal-, cytosolic-, heat shock- and plasma membrane proteins, as well as in proteins involved in vesicle trafficking. Intracellular organelle proteins are less abundant. Proteomic profiles obtained have been found to be highly dependent on how exosomes are isolated.

Due to small differences in physical properties and composition, discrimination between different EV subgroups after their cellular release remains difficult. Furthermore, the same cell type may secrete different subgroups of vesicles depending on environmental factors (e.g., oxygen tension), cell topography (e.g., from basolateral or apical cell surfaces) or activating stimulus (e.g., apoptosis or autophagy). Furthermore, a given cell may contain different types of MVBs characterized by differential exosome content.

Characterization of EV protein content is commonly conducted by, for example, immunoblotting, immuno-gold labelling combined with electron microscopy and antibody-coupled bead flow cytometry analysis. Proteins enriched in EV sub-populations that are often used as markers (although not necessarily specific) include **tetraspanins** (e.g., CD9, CD63, CD81 and CD82), **14-3-3 proteins**, **major histocompatibility complex** (e.g., MHC) molecules and cytosolic proteins such as specific **stress proteins** (e.g., heat shock proteins;

HSPs), **Tsg101** and the Endosomal Sorting Complex Required for Transport (ESCRT-3) binding protein **Alix**. Tetraspanins CD9, CD63 and CD81 were previously considered to be specific markers for exosomes; however, these proteins have now also been observed in apoptotic bodies and microvesicles. Conversely, some studies indicate that CD63 (and Tsg101) is only present in certain EV subgroups (Deng & Miller, 2019b).

How to find proteomic data?

Proteomic studies of EVs released by primary cell cultures, cell lines, tissue cultures or isolated from biofluids have yielded extensive catalogues describing protein abundance in different types of EVs. Public on-line databases are available that catalogue EV-associated components. These include Vesiclepedia (www.microvesicles.org/), EVpedia (www.evpedia.info) and ExoCarta (www.exocarta.org).

iii. RNAs contained within exosomes

Extracellular RNA exists in different forms, for example, they can be loaded in exosomes, bound to protein complexes or circulate freely. The presence of functional RNA in exosomes derived from murine stem cells was first described in 2006 (Ratajczak et al., 2006). While cellular mRNAs vary in size from 400 to 12,000 nt, RNA detected in exosomes has a predominant size of 700 nt. Since the discovery of RNA in exosomes, increasing evidence suggests that RNAs are not passively loaded into EVs, but that certain populations of RNAs are willingly enriched in exosomes compared to parental cells. Although this enrichment could occur because of a size restriction, there is a specific repertoire of miRNAs selectively exported to EVs even among small RNA species, whereas other miRNAs are usually excluded indicating that an active sorting mechanism occurs at the RNA level. An enrichment of RNA containing specific nucleotide motifs has been documented in EVs (Batagov et al., 2011; Villarroya-Beltri et al., 2013). In contrast to RNA, the presence of DNA associated with exosomes has been less explored.

3. Isolation Techniques

Specific characteristics have been proposed for EVs subgroups in some instances, but currently there is still a lack of widely accepted specific markers to distinguish these populations. This may partly be explained by the lack of standardization of both isolation procedures and methods for the characterization of EV subgroups. In addition, isolation procedures typically do not unequivocally purify specific types of vesicles but, instead, yield complex mixtures. Exosomes have been successfully purified from cell culture conditioned

medium or bodily fluids such has saliva, urine, semen and cerebrospinal fluid (Properzi et al., 2013). The specific method used to isolate EVs is critical to the success of the isolation and there have been efforts to improve and standardize these methods (Théry et al., 2006). After isolation, vesicles can be analyzed by immunoblotting, immuno-staining or proteomic techniques. Several conventional methods such as **differential ultra-centrifugation**, **ultrafiltration, size exclusion chromatography, precipitation, and immunocapture** are used to isolate exosomes (Clayton et al., 2001). Among these methods, differential ultra-centrifugation is the most widely used approach to extract exosomes from cell culture media and body fluids. However, to overcome the limitations of time and sample volume of the conventional methods, several companies have developed quick and easy isolation kits even if purity yields can be less optimal in comparison to those obtained with conventional methods. Recently, several characterization and validation methods have been developed for both research and clinical purposes, aiming to analyze exosome purity and to quantify exosomal cargo. These methods include **transmission electron microscopy** (TEM), **scanning electron microscopy** (SEM), **nanoparticle tracking analysis** (NTA), **enzyme-linked immunosorbent assay** (ELISA), **flow cytometry, fluorescence-activated cell sorting** (FACS); etc (Dragovic et al., 2011; Théry et al., 2006).

IV. Exosomes and viruses

Recent studies have shown that exosomes play an important role in infectious disease by mediating the transfer of pathogen-derived antigens and virulence factors. Exosomes derived from virus-infected cells contain viral proteins and viral RNA. Being enclosed in a cellular membrane structure, the contents of these vesicles is protected, thus enabling viruses to evade host immune response. Furthermore, EVs from hepatitis A virus (HAV) or HCV–infected hepatocytes permit the respective viruses to invade and replicate within host hepatocytes. However, the role of EVs in HBV infection is still largely unknown. Specifically, the lack of viral culture systems for HBV has hampered the evaluation of EV-mediated transmission of HBV infection.

1. Viral impact on EV content

Several lines of evidence indicate that viruses can modify both the quality and the quantity of EVs released by infected cells and that these EVs can be beneficial for either the host or the pathogen. Epstein Barr virus (EBV), herpes simplex virus (HSV) and human

immunodeficiency virus (HIV) are some of the most intensively studied viruses with respect to exosomal release.

Exosomes released by **EBV**-infected B cells were shown to deliver EBV latent membrane protein 1 (LMP1) protein to surrounding uninfected cells, thereby contributing to virus latency and tumor progression. In addition, exosomes derived from EBV-infected cells were shown to carry EBV-encoded mature miRNAs in their lumen (Hatton et al., 2014).

HIV has also been shown to encode its own miRNAs. A prominent HIV miRNA, the trans-activation response element (TAR), was found to be present in EVs secreted from HIV-infected cells. Exposing uninfected cells to EVs derived from HIV-infected cells resulted in an increased susceptibility to HIV infection, through TAR-regulated inhibition of apoptosis in the recipient cells. Also, the presence of HIV co-receptors in EVs derived from HIV-infected cells may confer an increased susceptibility to infection in recipient cells that are otherwise non-permissive (L. Chen, Feng, et al., 2018).

Infection of hepatocytes with **HCV** leads to the incorporation and export of viral genomic and sub-genomic RNA sequences in exosomes and can induce a strong IFN response (Thakuri et al., 2020). In addition, coxsackie virus B1, HAV and HCV were shown to package their viral genomes in exosomes for release in the extracellular milieu (Inal & Jorfi, 2013; Longatti, 2015). Based on these observations, it can be hypothesized that EVs could serve as vehicles that mediate intercellular transmission of viruses. The use of cellular secretion and vesicular trafficking and targeting pathways may allow viruses to disseminate and gain access to a pool of potential target cells that are otherwise non-permissive for virus entry, while escaping immune surveillance.

2. Evading Immune Responses

During primary viral infection, humoral and cell-mediated host immune responses such as production of neutralizing antibodies and cytotoxic T-cell attack on infected cells are employed to contribute to viral destruction. Early evasion strategies adopted by viruses interfere with complete elimination of the virus, allowing it to persist. During HSV-1 infection the release of microvesicles, formerly known as L-particles containing viral tegument proteins and glycoproteins, can prime surrounding cells for productive infection and reduce immune rejection (Deschamps & Kalamvoki, 2018). Another evasion strategy observed for HSV-1 is targeting of the MHCII molecule-processing pathway by viral envelope glycoprotein B. In the case of HIV, EVs packaging and spread of the virus encoded Nef protein impairs

proper endocytosis of the immature MHCII/invariant chain, antibody class switching, and lysosomal degradation of viral peptides, allowing HIV to evade immune recognition (Rucevic et al., 2014).

3. Invasion and Replication within the Host Cell

Exosomes can incorporate elements from the cell, as well as from the intruding virions. In the case of the human cytomegalovirus (HCMV), exosomes derived from infected cells harbor the C-type lectin family molecule expressed on DCs that is used in capture and internalization of pathogens in complex with the HCMV glycoprotein B (Plazolles et al., 2011). This complex can be subsequently delivered to other cells, thus increasing the susceptibility of these cells to HCMV.

A similar mechanism is found in the case of HCV. In HCV-positive patients, the cellular membrane protein CD81 associates with one of the HCV envelope glycoproteins, E2. Extracellular release of the E2/CD81 complexes within exosomes allows to increase virus-fusing ability and infectivity of naïve cells. Exosomes bearing the E2/CD81 complex and containing HCV RNA are of notable importance as they have been reported to be infectious even in the presence of neutralizing antibodies (Masciopinto et al., 2004) (Bukong et al., 2014).

4. Exosomes Contribute to Host Immunity against Viral Infection

In contrast to the above-mentioned examples, exosomal release can also contribute to the host immune response against viruses. For example, in the early steps of CMV invasion, CMV antigens are transferred from infected epithelial cells (ECs) via EC-derived exosomes to APCs and induce an innate immune response (Walker et al., 2009).

Exosomes can promote the innate immune response to other viruses as observed for HIV, where transfer of a particular antiviral cytidine deaminase via exosomes inhibits HIV replication (Khatua et al., 2009). In addition, virus-like vesicles can be used as vaccination strategy, and recently chimeric virus-like vesicles were engineered using a mixture of coronavirus and influenza proteins functioning as a potential severe acute respiratory syndrome (SARS) virus vaccine (Y. V. Liu et al., 2011).

Viral Component	Species	Exosome Source	Reference
HBV-DNA	rcDNA	Serum of CHB Patients	Yang Y, Cell & Mol Immunol 2017b
	cccDNA (discutable)	HepG2 (co-cultured with HBV-positive serum)	Liu D.X, Oncol. Lett. 2019
HBV-RNA	HBx mRNA	Serum of CHB Patients	Yang Y, Cell & Mol Immunol 2017b
		HepG2.2.15	Yang Y, Cell & Mol Immunol 2017b
	HBs/p	Serum of CHB Patients	Yang Y, Cell & Mol Immunol 2017b
HBV proteins	HBsAg	Serum of CHB Patients	Yang Y, Cell & Mol Immunol 2017b
	HBeAg	-	
	Core Protein	HepAD38	*Jia X.,* Mol. Cell. Proteomics 2017
	L-HBs	-	
	HBx	HBx-Huh7	Kapoor NR, Virus Res 2017
	Polymerase	-	
HBV miRNA	HBV miR-3	Serum of CHB Patients	Yang Y, J. Virol 2017a

-; Not identified, **HBs/p;** Primers located in S and Core region (position 412 to 723 on HBV genome with nt1: EcorI)

Table 3. HBV components in exosomes derived from HBV-infected cells and CHB patients (from (J. Wang et al., 2020)).

V. Exosomes and HBV

1. Exosomes Participate in HBV Replication

Several studies have been conducted regarding the role of exosomes in context of HBV infection and are listed in table 3.

HBV nucleic acids (DNA and RNA) have been detected in exosomes derived from HepG2 cells transfected with HBV (Kouwaki et al., 2016). Exosomes isolated from serum of CHB patients also contained both HBV-DNA and RNA, as well as HBsAg, while the presence of cccDNA is highly debated. These exosomes were shown to deliver HBV components to naïve hepatoma cells. HBs and HBc proteins were detected in hepatoma cells after incubation with CD63-exosomes derived from CHB patients. Furthermore, exosomes derived from CHB patients suppress NK cells cytotoxicity and decrease the production of IFN-γ and TNF-α (Y. Yang et al., 2017). These data suggest that exosomes derived from CHB patients' serum could contribute to the spreading of HBV infection but also induce NK-cell dysfunction.

Several proteins encoded by the HBV genome, including large S, core and P proteins, were found to be associated with exosomes isolated from HepAD38. Furthermore, differences of protein content in exosomes secreted by the HepAD38 cell line with or without HBV replication were evaluated by label free proteomic analysis. In this study, 1412 protein groups were identified and bioinformatic analysis revealed that 32.98% of exosomal proteins were plasma membrane-associated, as well as some proteins participating in the regulation of cytokine production or signaling transduction. These data may provide insights into the potential function of exosomes in HBV-host interaction and their immunomodulatory effect during HBV infection (Jia et al., 2017a).

Another example that illustrates the variety of cargo that exosomes can have in context of HBV infection is the case of *HBV-miR-3*, an HBV-encoded miRNA that was identified by deep sequencing. *HBV-miR-3* expression was detected in patients with HBV infection, and its expression level was significantly higher in the sera of patients with HBV infection in the acute phase than in those presenting chronic infection. This miRNA was identified in exosomes isolated from HepG2.2.15 supernatant. This miRNA can target a unique site of HBV transcript to reduce the level of HBV pgRNA and HBc and finally resulting in replication inhibition (X. Yang et al., 2017).

HBx is required for viral infection and replication, and it is closely associated with HCC development. Moreover, Kapoor and colleagues identified HBx mRNA and protein in exosomes isolated from HBx-expressing hepatoma cells (Kapoor et al., 2017). They suggested that HBx could increase the production of exosomes through the induction of nSMnase2, a protein involved in the ceramide exosome biogenesis pathway. HBx can modulate the biogenesis of host exosomes and alter neighboring liver cells.

2. Exosomes Modulate Immune Responses during HBV Infection

Exosomes can modulate immune responses during HBV infection. Exosomes released from pHBV-transfected hepatocytes were shown to induce NKG2D ligand expression in macrophages via MyD88, TICAM-1, and MAVS-dependent pathways. These data suggest the importance of exosomes for macrophage function (Kouwaki et al., 2016).

Moreover, exosomal *miR-21* and *miR-29a*, as well as other immunosuppressive miRNAs, were markedly increased in HBV infected HepG2-NTCP cells. *miR-21* downregulates *IL12A* mRNA expression and *miR-29a* is known to suppress *IL12B* mRNA expression. These exosomal miRNAs may inhibit the activity of NK cells via impaired IL-12 expression. These observations indicate that exosomes play a crucial role in the innate immune response against HBV and that exosomes would mediate viral escape from host immune response by downregulating IL-12 (Kouwaki et al., 2016).

Co-culture of NK cells from healthy donors with exosomes derived from CHB patient's serum show transmission of rcDNA and HBV-RNA into NK cells. These transmitted HBV components could lower cytotoxicity and proliferation of NK cells (Y. Yang et al., 2017). Therefore, the intricate relationships among various viral components and host factors could determine whether viral clearance or persistence occurs. Besides, exosomes can deliver proteasome subunits to monocytes, as suggested by HepAD38-derived exosomes containing higher levels of proteasomal activity proteins. This leads to the suppression of IL-6 expression in monocytes (Jia et al., 2017a). Altogether, these data demonstrated that HBV-induced exosomes might influence the production of proinflammatory molecules in the recipient monocytes.

In addition, exosomes isolated from HepAD38 cells with HBV replication can strongly upregulate PDL1 expression in monocytes compared to exosomes secreted from HepAD38 cells without HBV replication (Kakizaki et al., 2018). In this regard, HBV-induced exosomes

might promote HBV infection by suppression of T cells. Type I IFNs, mainly IFN-α and IFN-β, present an important role in controlling viral replication during the initial stages of infection. IFN-α can induce the transfer of resistance to HBV from non-permissive liver non-parenchymal cells (LNPCs) to permissive hepatocytes via exosomes. Some specific antiviral activity molecules can be sorted into exosomes from IFN-α-treated LNPCs. These antiviral molecules can be transferred via the internalization of exosomes to hepatocytes, where they can attenuate HBV replication (J. Li et al., 2013). Additionally, viral antigen expression and DNA quantification studies have indicated that exosomes isolated from IFN-α-treated macrophages can efficiently transfer IFN-α-induced anti-HBV activity to HepG2.2.15 cells (Yao et al., 2018). As mentioned, exosomes and HBV are mutually influenced and stimulated, and the function of exosomes during HBV infection can be compared to a double-edged sword.

3. Exosomes as Markers for HBV Diagnosis or monitoring?

As described above, exosomes are involved in multiple steps during HBV infection. Quantitative and qualitative analyses related to differences in the composition of exosomes from healthy and infected patients have been extensively reported. These observations, together with the practicality of isolation and relative storage stability, make exosomes promising biomarker reservoirs with potential applications for diagnosis or monitoring (Devhare & Ray, 2018). Recent studies have identified several exosome-specific cargos as biomarkers for different liver diseases (Bala et al., 2012).

The levels of *hnRNPH1* mRNA and *miR-21* in serum exosomes isolated from HCC patients were remarkably higher than in CHB group. Receiver operating characteristic (ROC) curve analyses showed that exosomal *hnRNPH1* mRNA level can discriminate HCC from CHB. The detection of serum exosomal *miR-21* is also more sensitive than in serum, so *hnRNPH1* mRNA and *miR-21* in exosomes may serve as sensitive and specific biomarkers to diagnose HCC and distinguish CHB (H. Xu et al., 2018).

The interest in using miRNAs within circulating exosome as noninvasive biomarkers has increased rapidly, considering that within the exosomal lipid bilayer membrane miRNAs are protected from degradation and kept stable in body fluids. Despite the great benefits of exosomal miRNAs in diagnosis, several issues still need to be addressed. Firstly, the selection of suitable reference genes as normalization factors is necessary to accurately compare exosomal miRNA transcripts. In particular, *U6* (CCG-1) or *miR-181a* (RG-5d) had

lower sensitivity for the comparability of *miR-21* expression between CHB patients and HCC patients. The combination of *miR-221*, *let-7a*, *miR-191*, *miR-26a*, and *miR-181a* (RG-5d) was the optimal reference gene set, for the comprehensive investigation into the progression of CHB to HCC (Y. Li et al., 2015). These findings highlight the importance of validating reference genes before quantifying target miRNAs. Secondly, biological body fluids are a rich source of exosomes with different origins, which makes it difficult to isolate HBV-induced exosomes. The specificity of exosomal miRNAs still needs to be validated. For example, exosomal *miR-21* is also highly expressed in glioblastomas, pancreatic, colorectal, breast and colon cancer (Nedaeinia et al., 2017). Therefore, large-scale studies of HBV and HCC patients would determine the value of differentially expressed exosomal miRNAs as potential biomarkers for distinguishing HBV patients from HCC. CHB patients on long-term treatment with NUCs are at risk of selecting drug-resistant HBV mutation strains. In two cases of HBV-infected patients whose treatment with entecavir (ETV) and tenofovir (TDF) is ineffective, rtS78T mutation was found in the reverse transcriptase gene of the HBV genome. The mutation causes a premature stop codon at sC69 and thereby deletes almost the entire small HBV surface protein in viral particles and exosomes. These changes facilitate replication and resistance to ETV and TDF treatment (Shirvani-Dastgerdi et al., 2017). Further studies are needed to predict drug resistance according to specific changes in exosomal contents. With the deep study of these correlations between exosomal components and diseases, it is expected that exosomes will gradually become useful diagnostic and prognostic tool.

RESEARCH PROJECT

I. Scientific Background

Currently, therapy of chronic HBV infection relies on two treatment regimens: PEG-IFN and NAs. PEG-IFN reduces viral transcription, yet it is responsible for severe side effects. On the other hand, NAs are well tolerated and often used in a long-term treatment. Indeed, by inhibiting reverse-transcription, NAs prevent the formation of new virions but not intrahepatic cccDNA which is the key determinant of chronicity of HBV infection in the hepatocytes. An accurate monitoring of intrahepatic cccDNA levels and activity is essential to stratify and monitor patients and to take decisions on treatment strategies, but it is hampered by the need for invasive liver biopsy procedures. Therefore, there is an unmet need for the identification and characterization of new non-invasive markers for the evaluation of intrahepatic cccDNA pool. In this regard, HBV-RNAs, which were identified in patients' serum, could be useful in the evaluation of new antiviral therapies aiming at a functional cure of HBV infection either by directly or indirectly targeting the intrahepatic cccDNA pool. Despite the growing literature on the subject, circulating HBV-RNAs still remain not fully characterized. Isolation, detection, and quantification methods differ from one study to another, hampering a consistent and solid knowledge of the different RNA species and their association with circulating particles. In this study, we took advantage of relevant in vitro models of HBV infection to establish a sound experimental strategy to characterize HBV-RNA species and associated extracellular particles in the supernatant of infected hepatocytes that could be translated to clinical samples. To this aim, the research project was divided in three main axes:

1) **Distribution of the viral nucleic acids released by infected hepatocytes across density gradient: a characterization of the physical entities carrying extracellular HBV-RNA.**

HBV infected hepatocytes release viral particles and non-viral EVs upon infection. However, the mechanisms underlying HBV-RNA secretion and the physical entities in which they are transported are still poorly characterized. Recent reports suggest that HBV-RNA are present in virion-like particles and naked capsids in the cell supernatant and patient's serum. Thus, as HBV uses the host ESCRT secretion machinery for its own secretion, we hypothesized that non-viral extracellular vesicles such as exosomes could also be involved

in HBV-RNAs secretion. To explore this hypothesis, we determined the distribution of HBV-RNAs in the different physical entities present in cell supernatant after a specifically adapted density gradient separation strategy. ELISA, western blotting, EVs tracking were employed to define EVs and viral particles repartition, while sensitive droplet digital PCR (ddPCR) was used to detect and quantify secreted HBV-RNAs.

2) **Identification of the nature of secreted HBV-RNAs and the impact of NAs treatment on the composition of these RNAs.**

It was proposed that extracellular HBV-RNAs mostly consisted of pgRNA. However, HBV spliced isoforms and HBx mRNA were also detected in culture supernatant of HBV stably replicating cells as well as in sera of CHB patients. In this study, we used a dual approach to clarify the picture of extracellular HBV-RNA species in the divers EVs populations (viral particles or exosomes) and assess if NAs treatment could affect the nature of secreted viral RNA. In particular, 5'end extremities were characterized by coupling 5' RACE and long read single molecule sequencing using Oxford Nanopore Technology (ONT) MinION. In parallel, custom primers and probes assays for ddPCR were designed to detect and quantify truncations at 3'end of HBV transcripts.

3) **Profiling of the proteins associated with exosomes secreted by hepatocytes: effect of HBV infection and NAs treatment.**

As the exosome biogenesis has a considerable overlap with the assembly and egress of viral particles, it is suggested that some viruses can hijack the exosomal pathway for cell-to-cell spread to avoid immune surveillance. It is reasonable to assume that exosome associated proteins could be modulated by a pathological state such as HBV infection. The profile of the proteins which are packaged in the exosomes may give a proteomic signature that could be informative upon infection. To date, only few publications have documented the implication of exosomes in HBV infection and the effect of HBV infection on the proteomic signature of the exosomes. To get a comprehension analysis of these two aspects, we performed a mass spectrometry study in collaboration with the EDyP facility in Grenoble (France). The main goal of our study was to get insight on the modulation of exosomes-associated proteins secretion upon infection (with or without NAs treatment) and identify key factors that could be involved in the cargo of HBV-RNAs in exosomes.

II. Context of the project

My thesis was conducted within Pr. Zoulim's team working on the molecular mechanisms responsible for cccDNA establishment and persistence. In 2017 the CirB-RNA project was funded by the French National Research Agency (ANR) (https://www.cirb-rna.fr/main/fr_FR/). The aim of this project is to develop a new diagnostic tool based on circulating HBV-RNA quantification as a reliable biomarker to monitor viral infection and persistence. Our specific objective in this project is to characterizing HBV-RNA both in patient's serum and in cellular model. The project is shared by an industrial partner: Roche diagnostic (Pleasanton, California) who oversees the industrial development of the above-mentioned test. Two post-doctoral researchers are also contributing to the RHU project: Dr. Doohuyn Kim studies circulating HBV-RNA in patient's sera on different phases of the disease and during treatment. Dr. Kim's work represents the counterpart of my own project, since we share the same methodology and we cross-validate the results in samples derived from both *in vitro* models and patients. Dr. Hyoseon Tak focuses on the identification of intracellular RNA binding proteins that could be responsible for the shuttling of HBV RNA into secreted non-viral particles. Altogether, we aim at providing a complete characterization of extracellular HBV-RNA that could be used in the future for correlation studies and the design of a new assay in the serum of chronic infected patients.

Results

Part I. Characterization of the Physical Entities carrying HBV-RNAs

Part II. Identification of the Nature of secreted HBV-RNAs

Part III. Secretion Profile of the Exosomes- Associated Proteins

PART I.

DISTRIBUTION OF THE VIRAL NUCLEIC ACIDS RELEASED BY INFECTED HEPATOCYTES ACROSS DENSITY GRADIENTS: CHARACTERIZATION OF THE PHYSICAL ENTITIES CARRYING EXTRACELLULAR HBV-RNA.

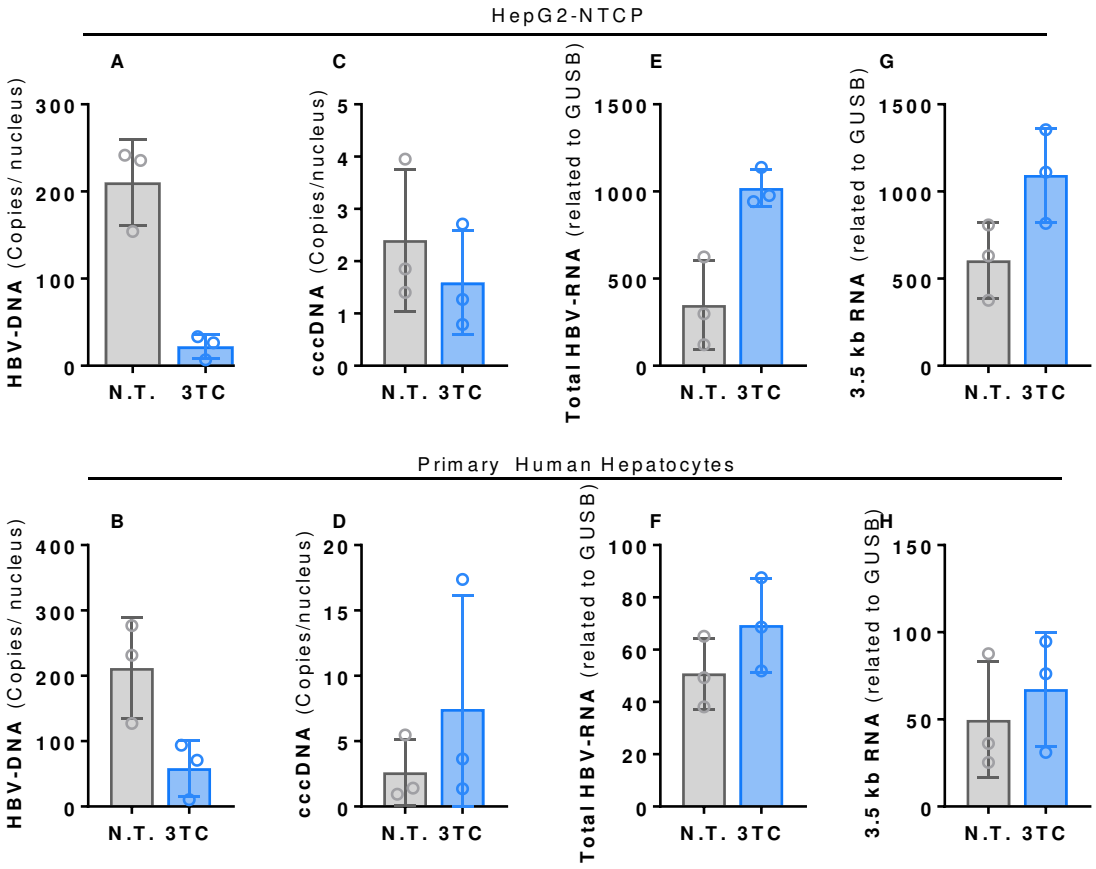

Figure 30 : Evaluation of Lamivudine treatment (3TC) effect on intracellular viral parameters. HepG2-NTCP cells (top) or Primary Human Hepatocytes (bottom) were infected with HBV at MOI 250 and treated or not with 3TC (10µM) 3- and 5-days post infection (dpi). Cell pellets were collected 7dpi and nucleic acids were extracted. Total HBV DNA (A and B), cccDNA (C and D), total HBV RNA (E and F) and 3.5kb-RNA (G and H) were quantified by qPCR with HBV specific primers. HBV-DNA and cccDNA were normalized over β-Globin and HBV-RNA was normalized over GUSB expression. Graphs show the mean ± SD of 3 independent experiments.

RESULTS: PART 1

For this experiment, HepG2-NTCP cells and Primary Human Hepatocytes (PHH) were infected with HBV at a MOI of 250 for 7 days and treated (labelled as 3TC) or not (labelled as NT) with NA (lamivudine) for 4 days after cccDNA establishment at 3 dpi. First, a global characterization of the intracellular parameters was done in all the biological replicates to ensure the reproducibility of HBV infections and the expected effects of NA treatment.

I. Quantification of intrahepatic viral markers after NAs treatment using a qPCR method

Intrahepatic total HBV-DNA (tHBV-DNA), cccDNA, total HBV-RNA (tHBV-RNA) and 3.5 kb RNA (preC/pgRNA) were first quantified using a qPCR method with specific primers already described for intrahepatic HBV markers quantification (Primers are listed in methods section)(Lebossé et al., 2020). HepG2-NTCP cells or PHH were treated or not for 4 days beginning at day 3 post infection with 10µM of lamivudine (3TC), a nucleoside analogue frequently used in HBV infection (Fig.30). HBV-DNA levels after 3TC treatment were significantly decreased in both cell types (respectively 90% and 72% reduction in HepG2-NTCP and PHH) confirming the efficacy of 3TC, since this drug blocks reverse transcription step and consequently rcDNA production. Intrahepatic cccDNA level was not affected by 3TC treatment; indeed, levels were consistent in both cell types with around 2 copies per cell. In contrast to tHBV-DNA, intracellular levels of tHBV-RNA and 3.5 kb RNA were slightly increased after 3TC treatment (in HepG2-NTCP: 977 vs. 347 copies/nucleus and in PHH: 69 copies/nucleus vs 47 copies/nucleus for tHBV-RNA). A greater increase was observed for 3.5kb RNA, as expected following the inhibition of the retro transcription by 3TC inducing accumulation of pgRNA. Altogether, these results confirm that 3TC treatment is efficient in both HepG2-NTCP and PHH with reproducible results across independent experiments.

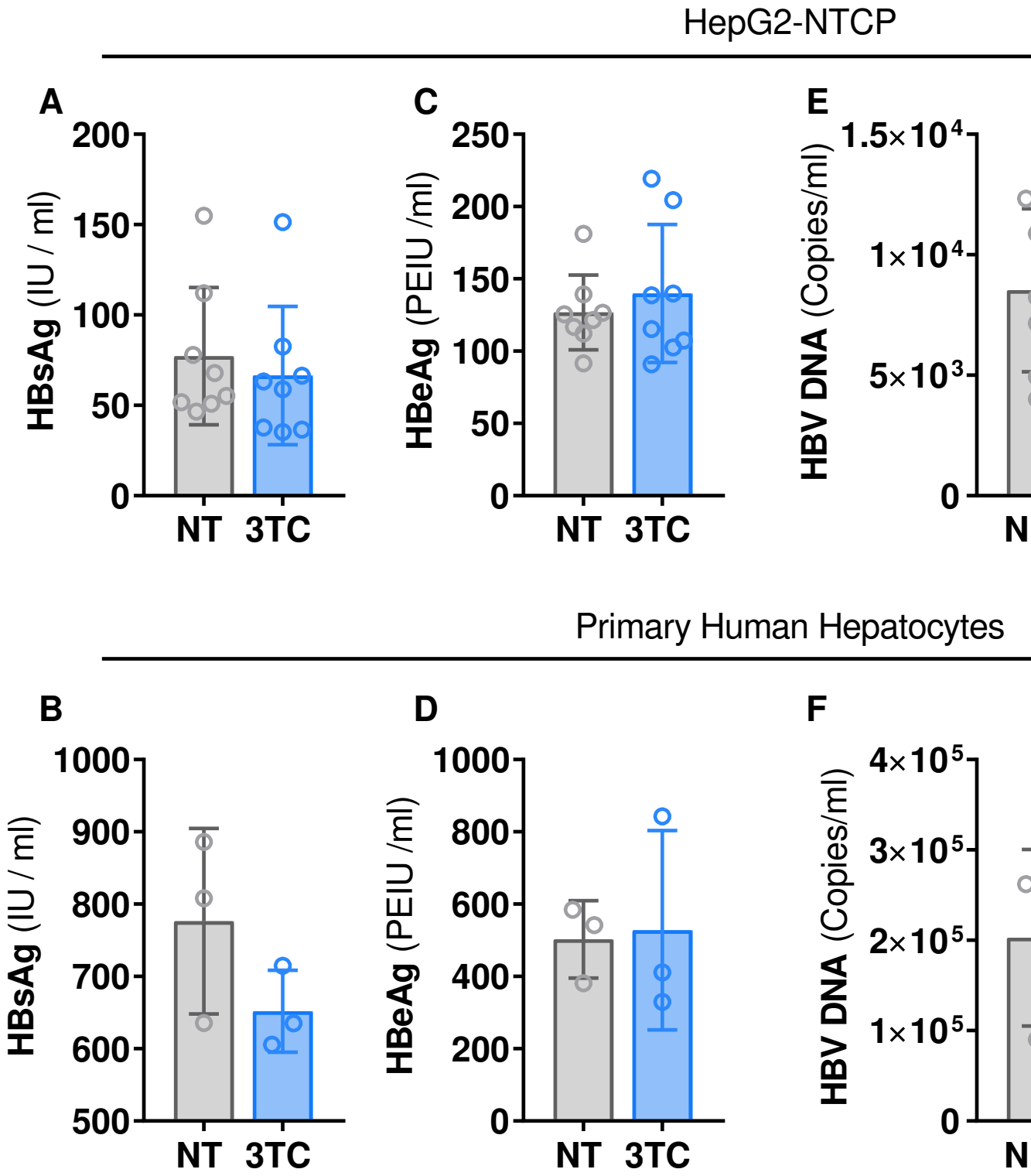

Figure 31 : Evaluation of Lamivudine treatment (3TC) effect on extracellular viral parameters. HepG2-NTCP cells (top) or Primary Human Hepatocytes (bottom) were infected with HBV at MOI 250 and treated or not with 3TC (10µM) 3 and 5 dpi. Supernatant were collected 7 dpi. HBsAg (A and B) and HBeAg (C and D) were measured by ELISA. Total HBV-DNA (E and F) and 3.5kb HBV-RNA (G and H) were respectively quantified by ddPCR. Graphs show the mean ± SD of 8 (HepG2-NTCP) or 3 (PHH) independent experiments.

II. Quantification of secreted viral markers in supernatant of infected hepatocytes

Since we observed a clear effect on intrahepatic viral parameters upon 3TC treatment, we investigated the effect in cell supernatant. Firstly, HBsAg and HBeAg were detected by ELISA (Figure 31). As expected, no difference was observed between treated and untreated samples since 3TC does not affect mRNA transcription and, as a result, HBV proteins production. Then, DNA and RNA were extracted from 200µl of supernatant and tHBV-DNA and 3.5kb RNA were quantified by ddPCR using specific primers and probes. We decided to use ddPCR which has been recently shown to be more sensitive than qPCR in detecting HBV nucleic acids in low-level HBV infected samples. Moreover, it allows an absolute quantification avoiding efficiency bias and the use of a standard, making ddPCR the ideal technique for HBV nucleic acids quantification in patient's serum or cell supernatant. We observed a great reduction of tHBV-DNA (>70% both in HepG2-NTCP and PHH), and a slight increase in 3.5kb RNA in the supernatant under 3TC treatment, consistently with the previous results in intracellular samples. In addition, tHBV-DNA levels were approximatively 2Log higher than HBV-RNAs as described in the literature in cell supernatant and patient's sera (Butler et al., 2018b). The analysis of secreted HBV viral parameters in the supernatant of infected cells confirmed the direct correlation between intra and extra cellular viral parameters and confirmed the sensitivity and specificity of ddPCR technique as reference for the study of circulating HBV RNAs.

Recently, it was shown that viral RNAs are circulating in the bloodstream of chronically infected patients and in the supernatant of infected cells (Giersch et al., 2017b; Jansen et al., 2016b; Shen et al., 2020b; van Bömmel et al., 2018b; van Campenhout et al., 2020; J. Wang et al., 2016b). To gain more insight into the particles that transport viral-RNAs and the nature of those RNAs, we performed a density gradient with gradual concentrations of iodixanol and sucrose and analyzed each fraction separately.

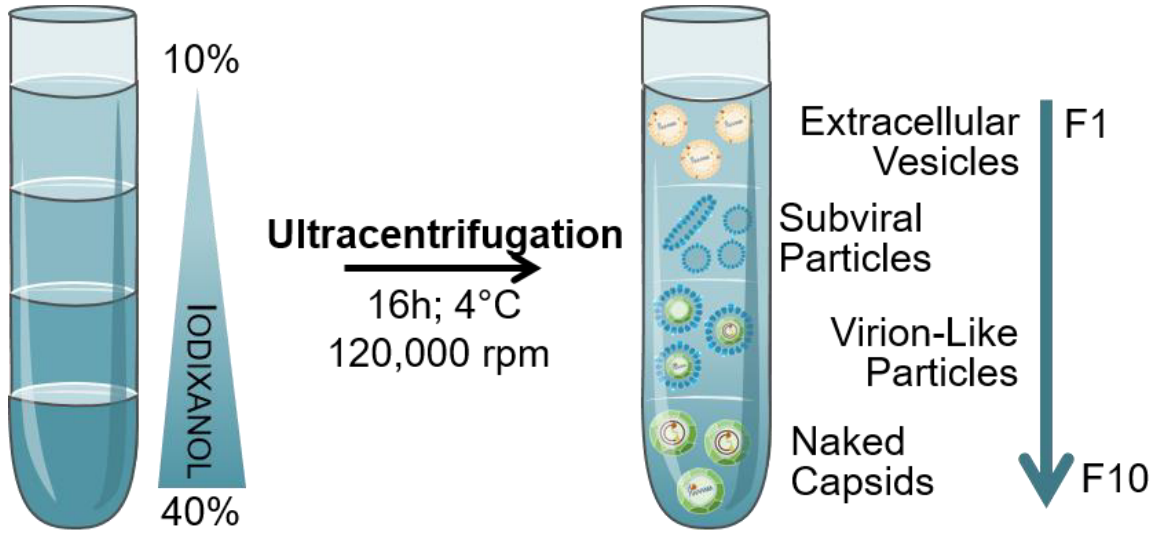

Figure 32: Scheme of Iodixanol / Sucrose density gradient. Gradual concentration of iodixanol (Optiprep) was diluted in STE buffer (see composition in M&M) then solutions of iodixanol/STE from 10 to 40% were layered sequentially. Pelleted supernatant, containing small extracellular vesicles and viral particles was mixed with the lightest fraction and layered on the top of the gradient. After overnight full-speed ultracentrifugation, 12 fractions were collected and analyzed separately. This gradient allows a theoretical separation of particles according to their buoyant density instead of their size.

Figure	Experiments & Content	Experimental model
Figure 33	- HBsAg (ELISA) - Density - CD9, Flot-1 & HBc (WB)	**HepG2-NTCP** (4 independent replicates)
Figure 35	- HBV-DNA, tHBV-RNA & 3.5kb-RNA (ddPCR)	
Figure 34	- HBsAg (ELISA) - Density - CD9, Flot-1 & HBc (WB)	**PHH** (3 independent replicates)
Figure 36	- HBV-DNA, tHBV-RNA & 3.5kb-RNA (ddPCR)	
Figure 37	- HBsAg (ELISA), HBV-DNA, tHBV-RNA & 3.5kb RNA relative abundance in each fraction (n=4 in HepG2-NTCP and n=3 in PHH)	**HepG2-NTCP & PHH** (pool)

Table 4. Table listing the number of repetitions of the experiments and the corresponding model.

III. HBV-RNA are associated with viral and non-viral particles in the supernatant of infected hepatocytes

EVs secreted from HBV infected hepatocytes include viral (subviral particles, naked capsids and virions) and non-viral particles (exosomes, microvesicles). However, all EVs (including exosomes and viral particles) share approximatively the same size range (between 18 to 100nm) preventing separation by size exclusion methods. To overcome this problem, we used Iodixanol/Sucrose density gradient, which allow a theoretical separation of EVs according to their buoyant density as schematized in Figure 32.

Sharing the same composition as the plasma membrane, i.e. lipids rich, exosomes are located at the top of the gradient followed by sub viral particles. Virions, which are composed by proteins and less lipids than exosomes, are heavier and found in the middle fractions of the gradient. Finally, devoid of any lipid envelope, naked capsids lie at the bottom of the gradient. Evidently, this repartition is theoretical and can be affected by the quality of the samples and the technical processing, raising some differences between theory and practice. Set-up experiments were conducted with HBV producing cell lines such as HepAD38, a model that allows a constant and fast HBV particles production in the supernatant (data not shown). However, to be closer to the physiology, all experiments were subsequently performed in *in vitro* HBV infection models, more relevant for comparison with patient's serum. As a result, experiments shown below were repeated 4 times in HepG2-NTCP cells then 3 times in PHHs. Figures related to this section are listed in Table 4. Table listing the number of repetitions of the experiments and the corresponding model. .

We separated EVs into exosomes, SVPs , virion and NCs using a density gradient. Twelve fractions were recovered and analyzed for the presence of exosome markers, CD9 and Flot-1, and viral proteins, HBsAg and HBc.

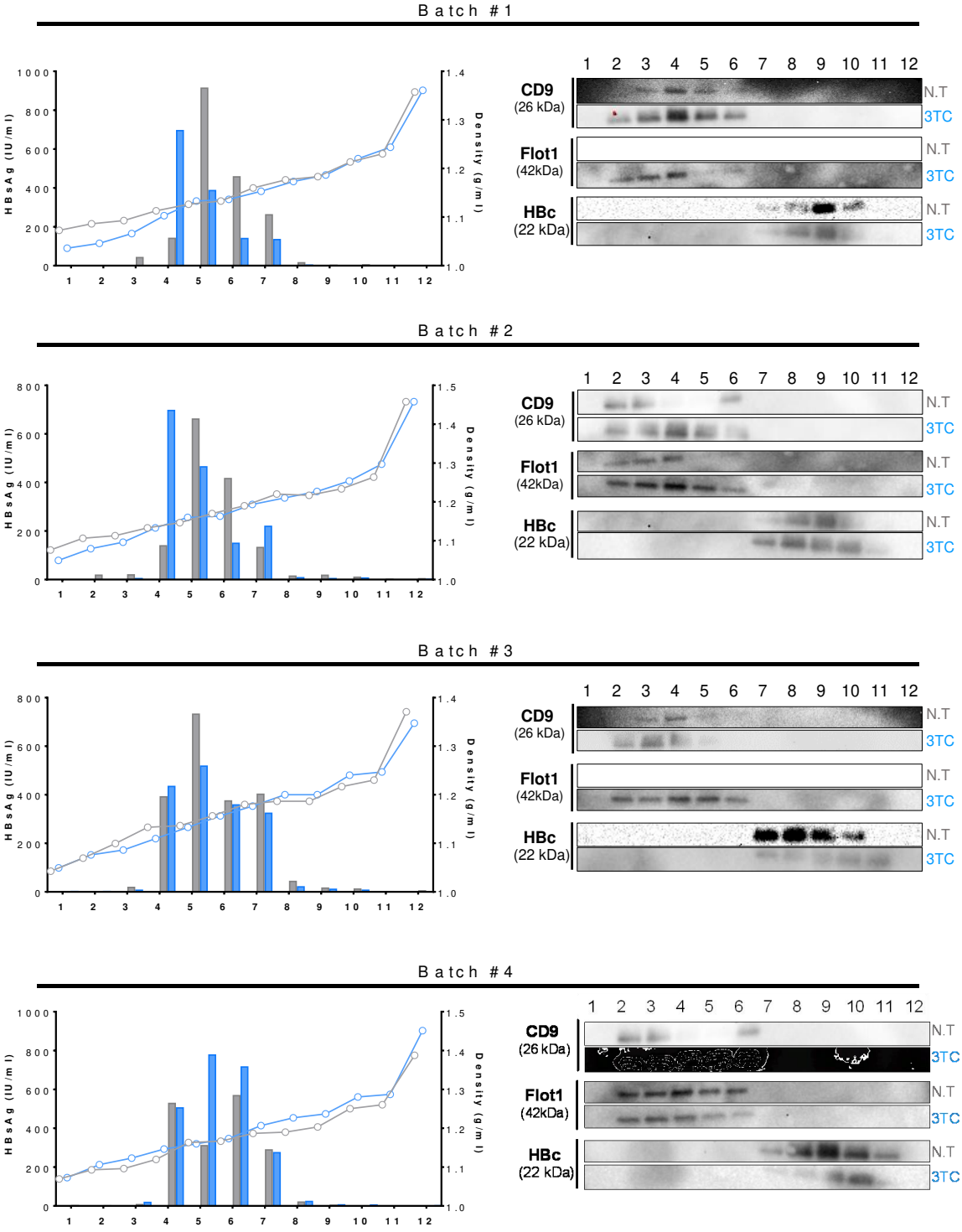

Figure 33. Analysis of viral and non-viral proteins across density gradient separation of exosomes, subviral particles, and virions in HepG2-NTCP. Extracellular vesicles (EVs) were collected by ultracentrifugation from 1L of culture supernatant of infected HepG2-NTCP with (blue) or without (grey) 3TC treatment. Pelleted EVs were fractionated by a density gradient separation using iodixanol/sucrose (see Fig.3). Twelve fractions were collected, and the presence of CD9, flotillin-1, and the viral proteins (HBsAg and HBc) in each fraction was analyzed by western blotting and ELISA. Experiment was repeated 4 times and noted from batch 1 to batch 4.

As shown in Figure 33 and Figure 34, exosomes were found in fractions 2 to 6 (F2 to F6) as witnessed by the presence of CD9 and flotillin-1, commonly accepted exosome markers. Unfortunately, due to low proteins quantities we were not able to make the western blot for Flot-1 in all the conditions in HepG2-NTCP and in none of them in PHH. Subviral particles were found in F4 to F7 in HepG2-NTCP and F5 to F6 in PHH, they were identified by the presence of high levels of HBs but lack of HBc signal in western blotting. Finally, virions were found in F7 (combining HBs and HBc) and naked capsids were found in F8 to F10, devoid of HBs.

No significant changes in exosomes markers or viral protein levels and repartition were observed under 3TC treatment. However, due to the difficulties to obtain a signal for the exosomes markers because of low proteins quantities in the samples, we observed variability across the replicates, although the global repartition remains consistent. Altogether, these experiments gave us an approximate repartition of the EVs across the gradient and indicated that exosomes, SVPs, NCs and virions were successfully separated from initial supernatants obtained from infected cells. However, we did not achieve a strict separation between exosomes and SVPs. This may be due to the similar composition and, by result, concordant density with small EVs. A lower iodixanol percentage would have allowed a better separation; nevertheless, we would have lost the efficient separation between the others viral components.

In the future, it could be interesting to pellet F2 to F6 and layer those fractions on a density gradient with iodixanol concentration between 5 to 15% in order to obtain a more resolute gradient repartition.

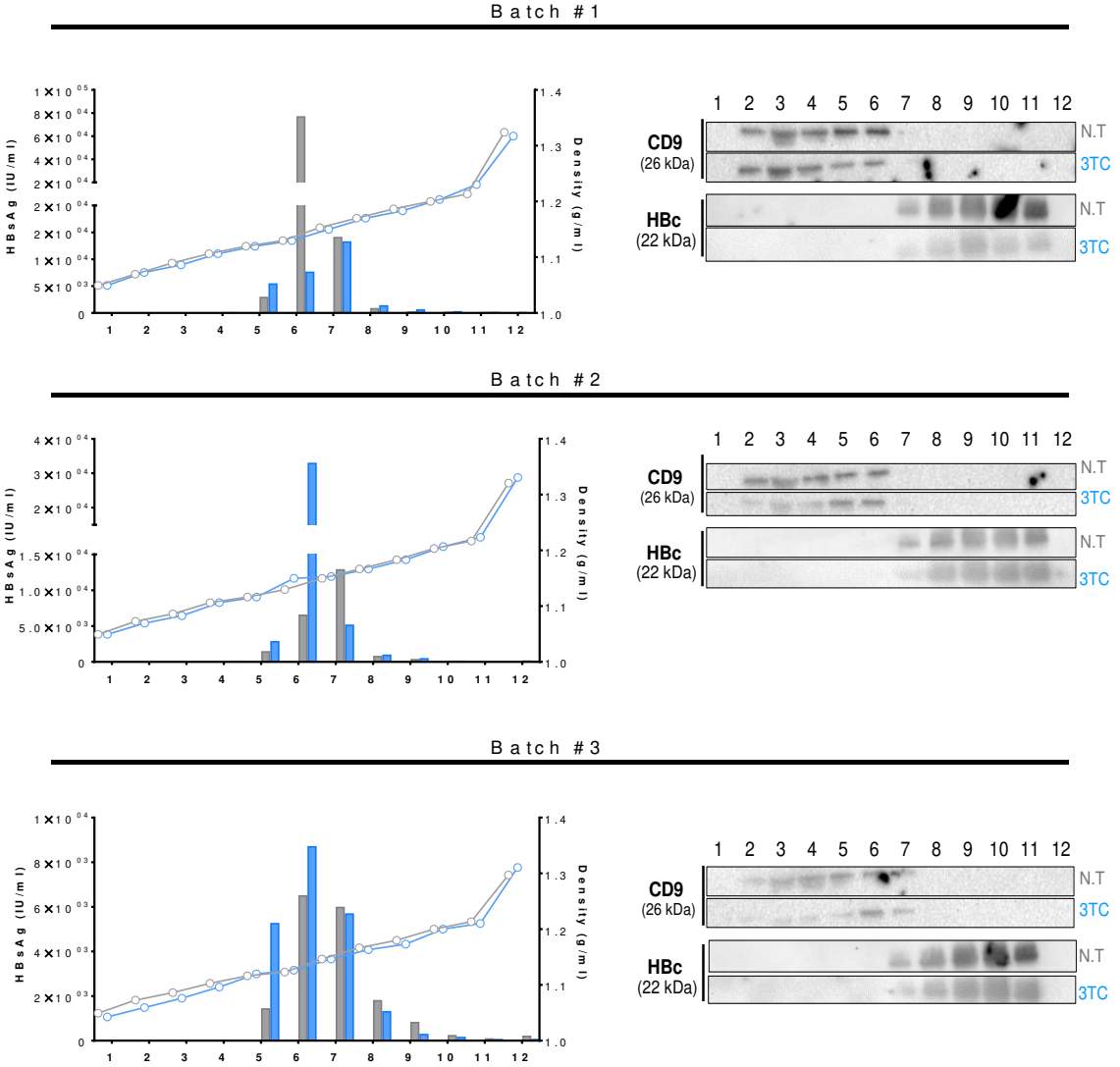

Figure 34. Analysis of viral and non-viral proteins across density gradient separation of exosomes, subviral particles, and virions in PHH. Extracellular vesicles (EVs) were collected by ultracentrifugation from 1L of culture supernatant of infected PHH with (blue) or without (grey) 3TC treatment. Pelleted EVs were fractionated by a density gradient separation using iodixanol/sucrose (see Fig.3). Twelve fractions were collected, and the presence of CD9, flotillin-1, and the viral proteins (HBsAg and HBc) in each fraction was analyzed by western blotting and ELISA. Experiment was repeated 3 times and noted from batch 1 to batch 3.

Next, to further examine the composition of the gradient, nucleic acids were extracted in each fraction and quantified by ddPCR. As mentioned before, this technique allows an absolute quantification of nucleic acids.

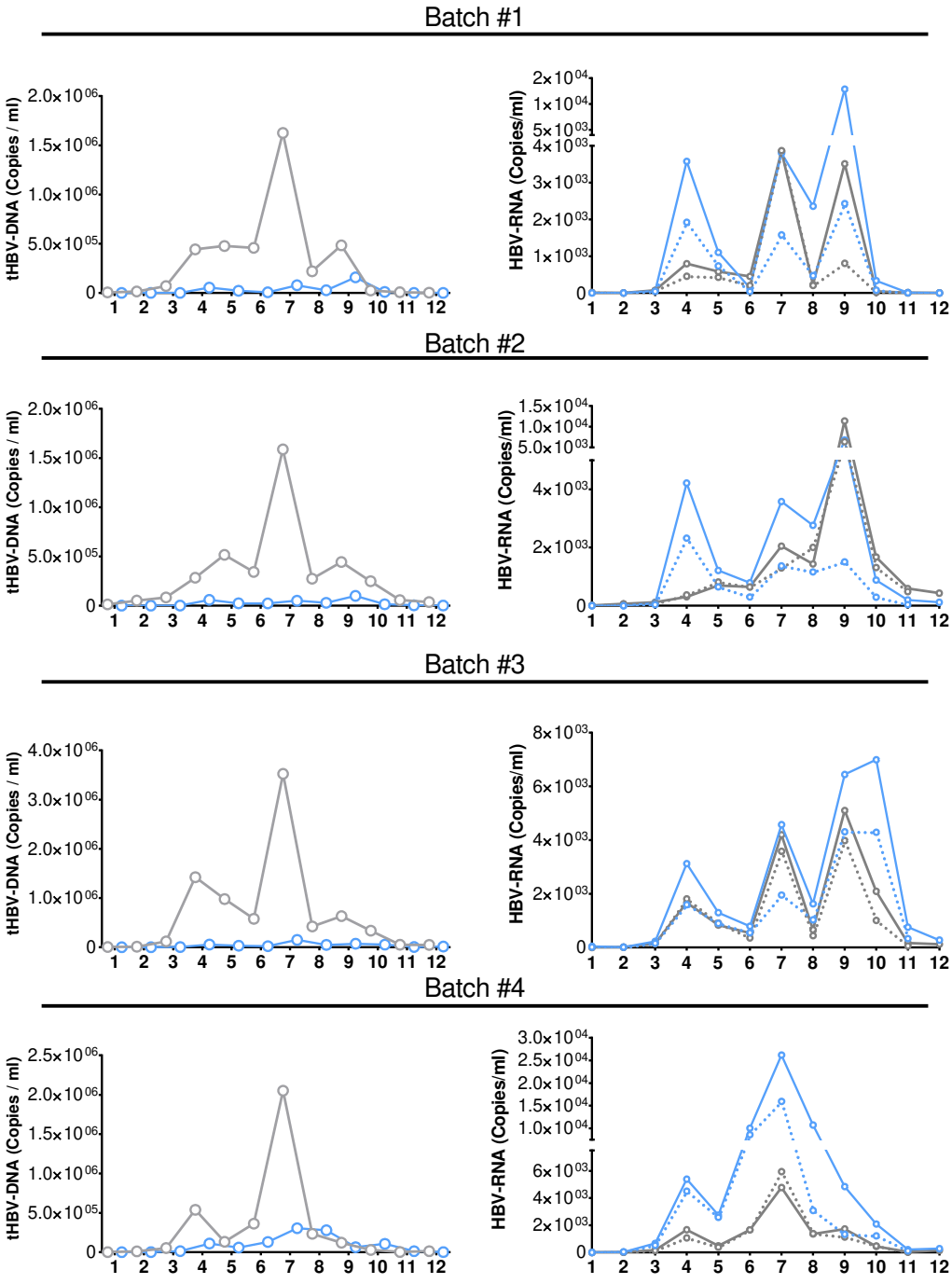

Figure 35. HBV-DNA and RNAs repartition across fraction in each individual replicate in HepG2-NTCP. Nucleic acids from HepG2-NTCP infected cell supernatant after density gradient were extracted from supernatant fraction and detected by specific assays using droplet digital PCR in 4 independent replicates. On the left: total HBV-DNA in replicate 1 to 4 respectively. On the right: Total HBV-RNA (full lines) and 3.5kb RNA (dotted line) in replicate 1 to 4 respectively. Grey lines: Non treated samples and blue lines: 3TC treated samples.

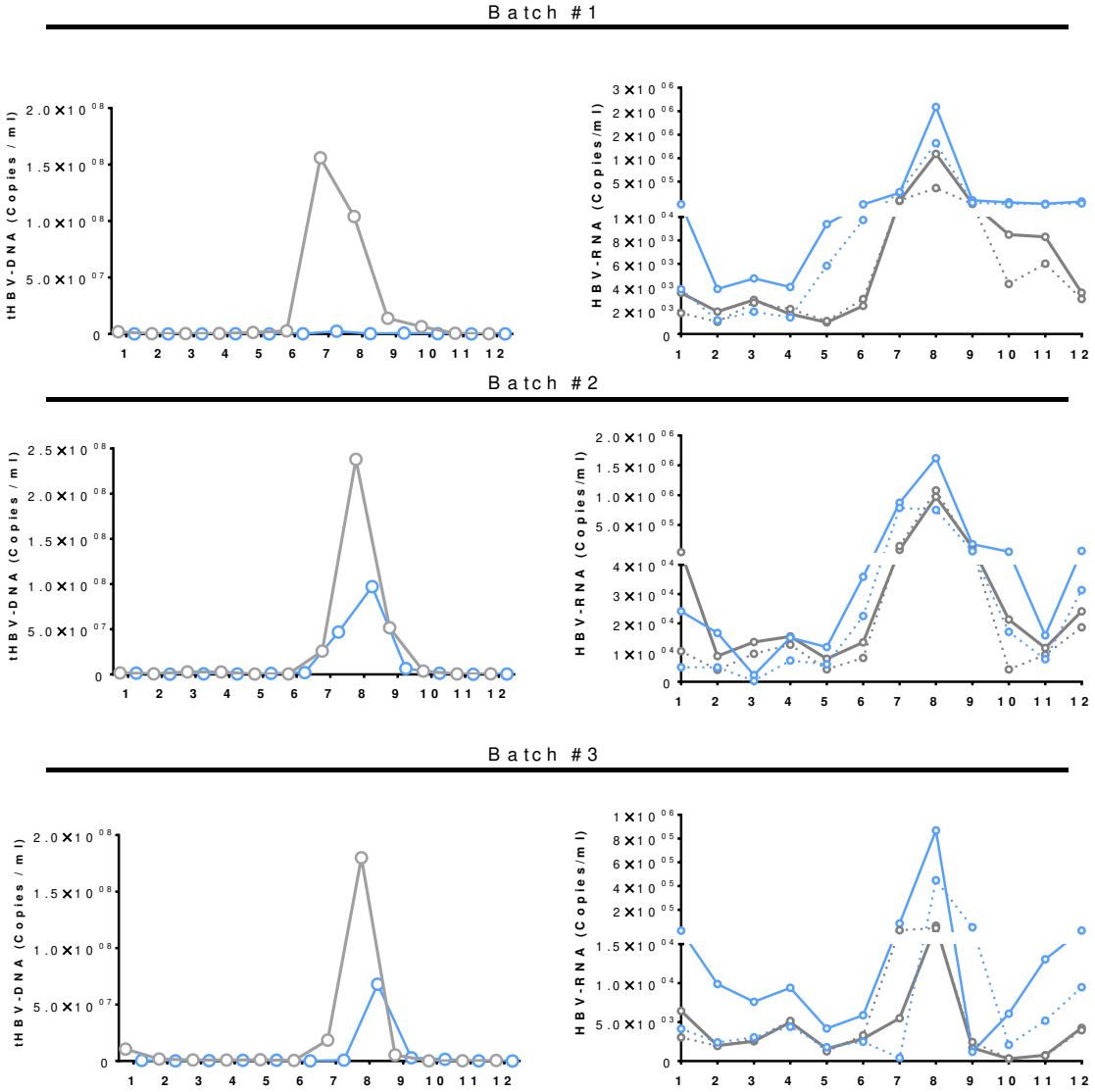

Figure 36. HBV-DNA and RNAs repartition across fraction in each individual replicate in PHH. Nucleic acids from PHH infected cell supernatant after density gradient were extracted from supernatant fraction and detected by specific assays using droplet digital PCR in 3 independent replicates. On the left: total HBV-DNA in replicate 1 to 3 respectively. On the right: Total HBV-RNA (full lines) and 3.5kb RNA (dotted line) in replicate 1 to 3 respectively. Grey lines: Non treated samples and blue lines: 3TC treated samples.

Figure 35 and Figure 36 shows tHBV-DNA, tHBV-RNA and 3.5kb RNA repartition across the fractions of each individual replicate. Experiments were repeated four times in HepG2-NTCP and three times in PHH.

We observed that tHBV-DNA is mainly found in F7 corresponding to virions. There are two additional DNA peaks in fraction 5 and 9 corresponding to exosomes and naked capsids, respectively, in HepG2-NTCP but not in PHH. Under 3TC treatment, tHBV-DNA was dramatically decreased in all fractions.

Regarding extracellular HBV-RNAs, their repartition is more heterogeneous than DNA. Indeed, tHBV-RNA and 3.5kb RNA were mainly present in F4, F7 and F9, respectively corresponding to exosomes, virion-like particles (VLPs) and NCs fractions. RNAs were mostly identified in VLPs. In PHH, RNAs were mainly present in VLPs and much less represented in F4 and F9 associated to exosomes or NCs, respectively.

tHBV-RNA and 3.5kb RNA were increased in almost all the fractions following 3TC treatment, except for F9. tHBV-RNA levels were higher than 3.5kb suggesting that pgRNA would not be the only RNA species that is secreted upon infection, in contrast to most of the data published so far on the subject. Surprisingly, tHBV-RNAs and 3.5kb RNA were also found in fractions corresponding to the mixture of SVPs and exosomes, with the bigger increase under 3TC treatment was seen in these same fractions in HepG2-NTCP but not in PHH. As SVPs are devoid of HBV genome and F4 is composed of a mixture of SVPs and exosomes, it is reasonable to assume that HBV-RNAs are indeed associated with exosomes.

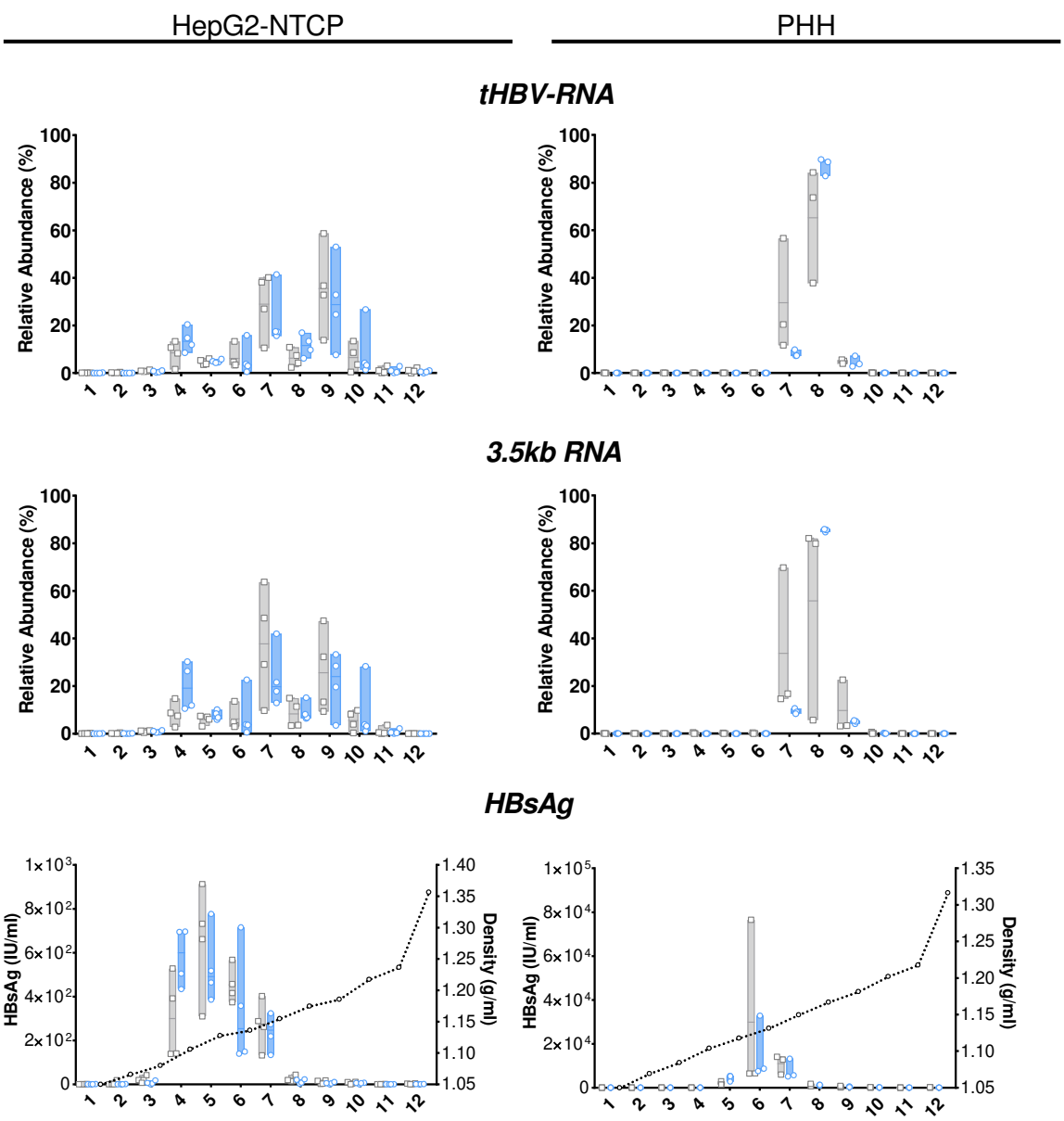

Figure 37. EVs collected from HepG2-NTCP cells supernatant treated or not with 3TC were fractionated by density gradient separation using iodixanol. Twelve fractions were collected, nucleic acids were extracted and quantified by ddPCR. Relative abundance of tHBV-RNA and 3.5kb RNA was calculated in each fraction in comparison with input values (n=4 for HepG2-NTCP on the left and n=3 for PHH on the right). From the top to the bottom: Boxplot of the mean value of the relative abundance of 1) total HBV-RNA and 2) 3.5kb RNA. 3) HBsAg absolute quantification by ELISA.

Figure 37 shows the relative abundance of tHBV-RNA and 3.5kb RNA in each fraction normalized on the input quantity. This representation gives the global distribution of the RNAs across the gradients and by extension in each particles subtype. This repartition shows that HBV-RNAs were indeed enriched in NCs (F9, ≈40% in HepG2-NTCP) where there was no increase under treatment and in F7 (≈30%), the virions corresponding fraction. As mentioned above, we also found that approximatively 15% of the tHBV-RNAs in the FR4, maybe transported by exosomes, which increased up to 20% under 3TC treatment. Altogether, our study was the first to give a complete characterization of the repartition of secreted HBV nucleic acids across density gradient of infected hepatocytes supernatant.

Interestingly, DNA & RNAs distribution was slightly different across the gradient in PHH supernatant. Indeed, DNA & RNA were also found in F1, fraction devoid of CD9 or HBs. This fraction could correspond to lipid particles floating at the surface of the gradient because those particles are produced in large amount by hepatocytes. A better characterization of those particles by western blot (ApoB, ApoC…) could shed a light on the composition of this fraction. In addition, infection rates were higher in PHH than in HepG2-NTCP and there was a bigger variability between the replicates probably due to the inter-individual variability of the donors. However, nucleic acids were still found in low density fractions corresponding to exosomes and the repartition of the markers (fig.5) was not different from the one on HepG2-NTCP cell supernatant.

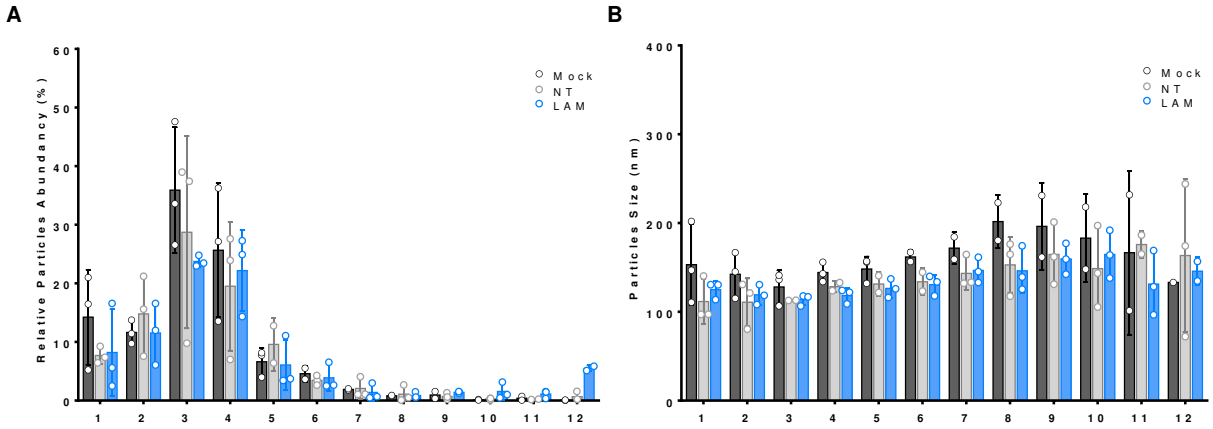

Figure 38: (A) Concentration and (B) Size measurement of EVs in each fraction after density gradient. 100ml of supernatant from non-infected, infected or infected + 3TC HepG2-NTCP cells were concentrated by ultracentrifugation and layered on a density gradient as described previously (n=3). Graphs show the mean ± SD of 3 independent experiments

To get a better insight on exosome repartition across the gradient, we looked for a method that could allow their quantification in each fraction. Some teams are using Bradford Protein assay to give an approximate quantification of exosomal proteins, however, in our study design, this method presents two major limitations: i) upon infection, HBV secretes proteins could introduce a bias in the protein quantification because subviral particles are secreted in large excess in patient's circulation and cell supernatant, ii) extracellular proteins levels are most of the time not quantifiable because too low concentrated. As a result, we decided to opt for a different and more refined approach that allows the quantification of nanoscale particles in suspension.

Nano-particle tracking is a method that estimates particle size distribution by tracking the movements of individual particles, using multiple images of particles moving under Brownian motion. Nanoparticle Tracking Analysis (NTA) is commonly used to determine EVs concentration and diameter. To further characterize EVs distribution across the fractions, we analyzed each gradient fraction by NTA.

We compared three conditions in HepG2-NTCP cells: i) non-infected, ii) infected or iii) infected and treated for 4 days with 3TC. This experiment was independently reproduced three times only in HepG2-NTCP cells, because it requires a huge quantity of material that was not available in PHH model. In fig. 38A, we confirmed the previous results observed in western blot with CD9, marker for exosomes. Indeed, exosomes were mainly present in the light fractions of the gradient with a peak in F3 and F4 containing approximatively 30 and 25% of the total exosomes in the gradient, respectively. In addition, it is noteworthy that neither HBV infection nor 3TC treatment seem to affect particles concentration, suggesting that exosomes secretion is not enhanced upon infection or treatment. Next, fig. 38B shows the size measurement of the particles in the fractions, with equal values along the gradient and not affected by the infection and treatment. All particles had a diameter of ~100nm corresponding to small EVs and attesting that we were able to remove bigger EVs such as apoptotic bodies in our samples. It is important to note that NTA allows quantification of particles but fails at quantify particles under 60 nm of diameter, excluding very small EVs or viral particles.

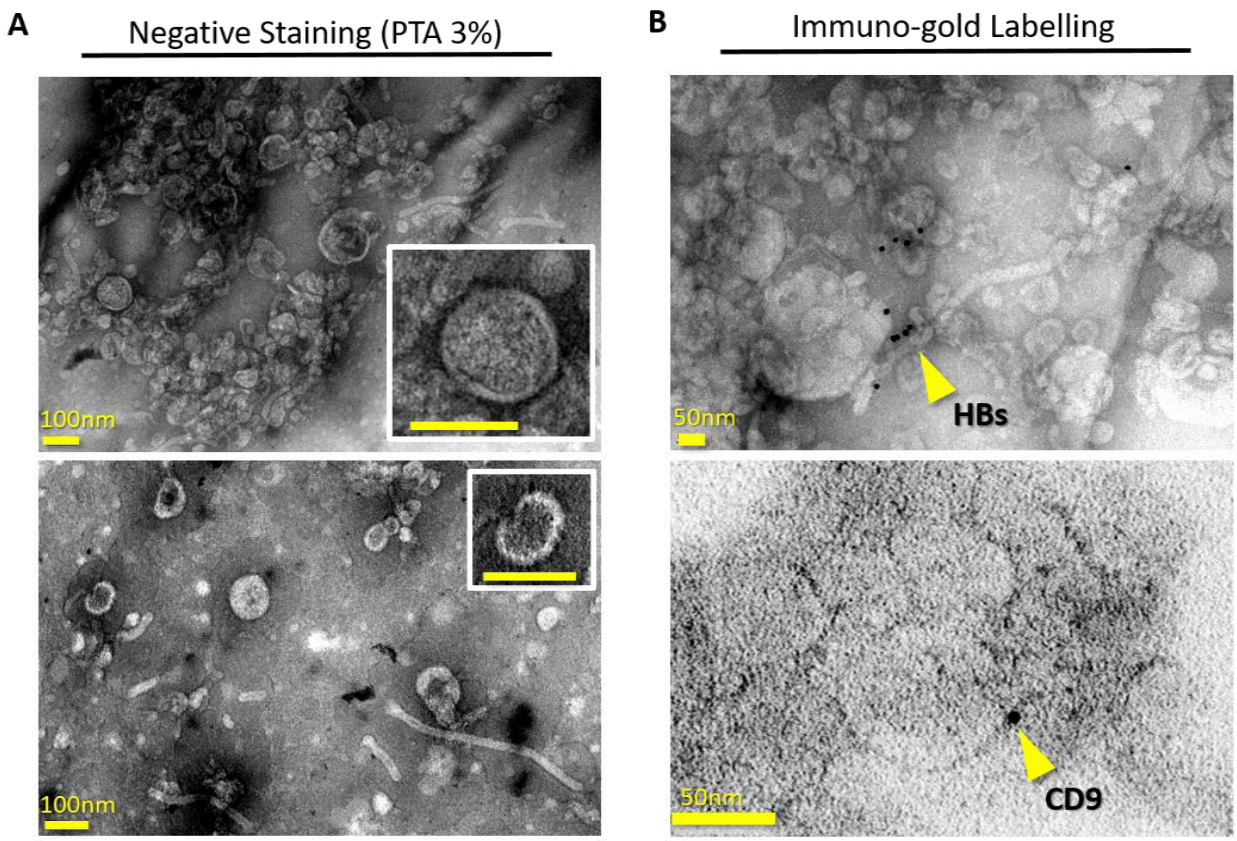

Figure 39 : F4 is mainly composed of exosomes and SVPs. Electron microscopy was performed in fraction 4 by (A) Negative Staining with PTA 3%) or (B) specific immunogold labelling with HBs antibody (left) or CD9 antibody (right).

As mentioned above, by the combination of CD9 and HBs in F4, we were not able to clearly determine the exact composition of this fraction. We stated two hypotheses: i) or F4 is composed by both exosomes and subviral particles, and/or ii) HBs could be incorporated in the membrane of the exosomes. To answer this question, we decided to perform transmission electron microscopy (TEM) in our samples. Indeed, early in biomedical EV research, TEM was used to visualize EVs and viral particles that are undetectable by standard light microscopy due to their small size and low refractive index. That is why we visualized F4 from HepG2-NTCP density gradient in TEM after negative staining with 3% PTA.

Fig.39A confirmed the presence of both exosomes and SVPs in F4. Exosomes were cup shaped structure of ~100nm of diameter and containing a double membrane. On the contrary, SVPs were found as spheres of 22nm diameter or filaments of 18nm width and up to 400nm long. As simple negative staining could not inform us about the presence of HBs at the surface of the exosomes, we performed immunogold labelling with HBs antibody or CD9 antibody (Fig. 39B). We observed that HBs was localized at the membrane of the sphere and filaments but not on the surface of exosomes whereas CD9 was found at the surface of the exosomes. HBs and CD9 were not co-localizing in our experimental conditions. This result suggests that F4 is composed by two entities: exosomes and SVPs. It is necessary to keep in mind that these experiments do not exclude the potential presence of HBs protein at the surface or incorporated inside the exosomes. However, neither western blotting nor TEM are able to give us this information.

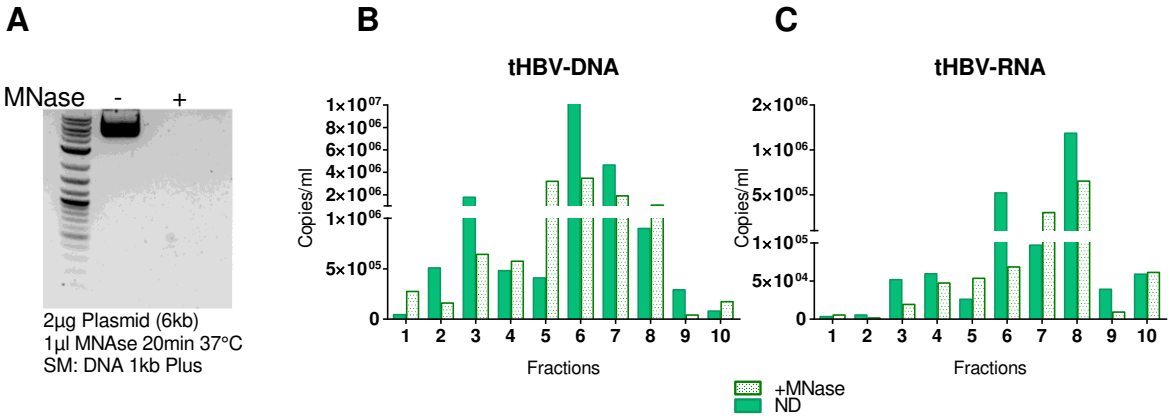

Figure 40 : MNase protection assay. Supernatant from HepAD38 was concentrated and separated through density gradient. MNase digestion step was added and reaction was stopped by trizol addition. (A) DNA Plasmid was added to monitor MNase digestion. (B) DNA and (C) RNA were quantified by ddPCR.

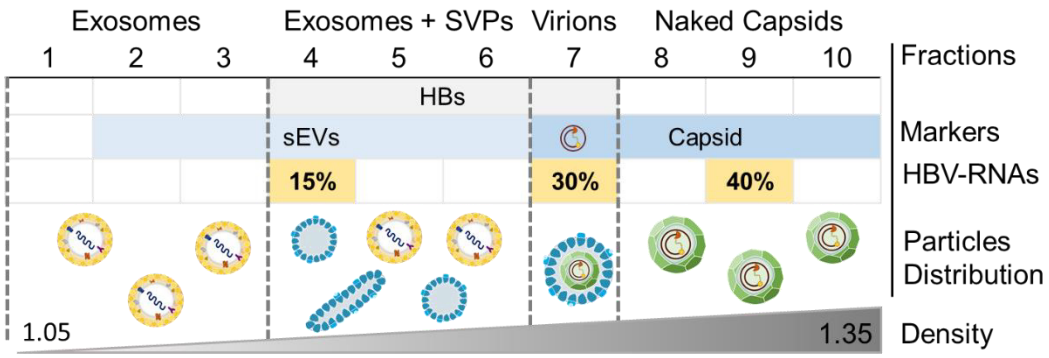

Figure 41. EVs and HBV-RNAs schematic repartiton across density gradient

IV. Circulating RNAs are contained within EVs in the supernatant of infected hepatocytes

Exosomes acts as a cargo for the transport of nucleic acids, lipids and proteins either by transporting their content in their inside compartment or by including them in their membrane. Concerning HBV-RNAs associated with exosomes, we performed a MNase digestion assay to assess if these RNAs were loaded inside the exosomes.

Micrococcal nuclease (MNase) is derived from Staphylococcus aureus and is a relatively non-specific endo-exonuclease. It is purified from a recombinant *E. coli* strain that digests double-stranded, single-stranded, circular and linear nucleic acids. For this experiment, each fraction of the gradient was digested and DNA and RNA were extracted before and after digestion. Supernatant from the HBV producing cell line, HepAD38, was accumulated, concentrated and processed through density gradient as described previously. Each fraction was digested with MNase and reaction was stopped by trizol addition and nucleic acids were extracted and quantified by ddPCR. A digestion control was done by adding 2µg or pcDNA6 DNA plasmid and digestion efficiency was controlled on an agarose gel (Fig.40a). Across the gradient, we observed that neither DNA nor RNAs levels were significantly affected by MNase digestion in F4 suggesting that HBV RNAs are mostly contained inside the exosomes in the supernatant of infected hepatocytes. We observed small variations in other fractions but the distribution of DNA and RNA remains similar after digestion, suggesting the presence of very few amount of free HBV nucleic acids in the supernatant of HepAD38 cells.

Altogether, these results showed that in addition to VLPs and NCs, HBV-RNAs are also loaded in exosomes (Fig. 41). Exosomes pathway have been extensively described to be hijacked by viruses like HPV and HCV to export their viral content and communicate to neighboring cells or modulate immune response. Many studies have discussed the vehicles for HBV-DNA and RNA, however no studies yet gave a full description of the repartition of these nucleic acids in the supernatant of infected cells. In addition, the presence of HBV-RNAs has been poorly observed to be associated with exosomes yet and this novelty could open a new axis of research in the understanding of HBV-RNAs as a biomarker for intrahepatic cccDNA activity.

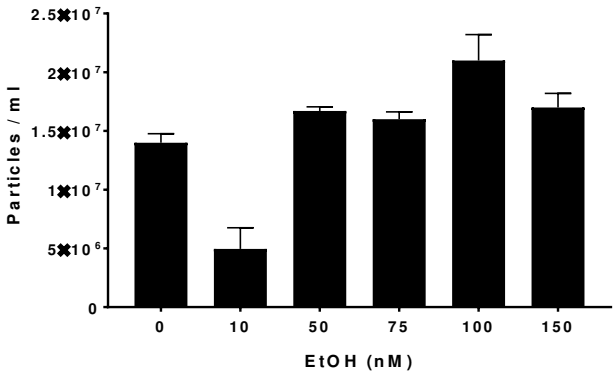

Figure 42 : Different doses of EtOH were added to HepG2-NTCP cells and particles were quantified by NTA. Graphs show the mean ± SD of 3 NTA acquisition of one experiment.

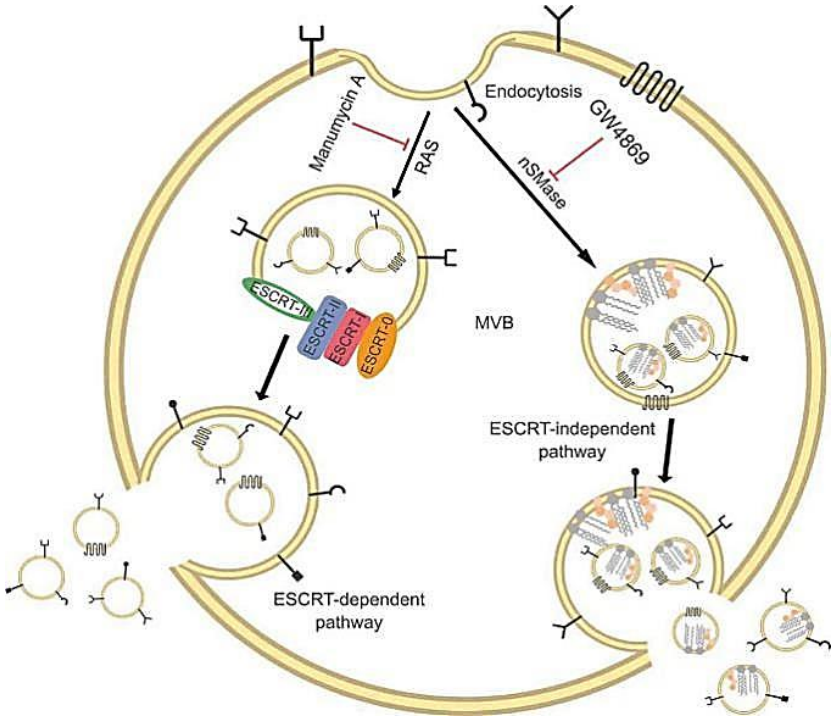

Figure 43 : Manumycin A and GW4869 inhibit exosomes secretion by blocking two independent pathways. (Catalano & O'Driscoll, 2020)

V. Modulation of exosome secretion

To confirm the presence of HBV-RNAs in exosomes rather than in other particles types in F4 even if up to date no nucleic acids have ever been described in SVPs, we tried to modulate exosomes secretion by the use of different drugs. Different approaches were tested but none of them was conclusive.

Firstly, as described by Momen-Heravi and al., ethanol treatment was shown to increase exosomes secretion in Huh7.5 cells, which are an hepatoma cell line, similar to our model of HepG2-NTCP (Momen-Heravi et al., 2015). They claimed that 25nm of ethanol for 72h was sufficient to get a significant increase of exosomes secretion by these cells. As a result, we tried to reproduce this experiment by accumulating HepG2-NTCP cell supernatant with the addition of increasing ethanol concentration. We accumulated 100ml of supernatant and concentrated it in order to quantify the particles with NTA. We did not infect the cells this time because it was a pilot study and we did not know at this time if HBV could alter exosome secretion.

In Figure 42, we did not observe a dose response as shown in the previously mentioned publication with Huh7.5 cells. In fact, we observed a decrease with 10nM of EtOH, followed by a slight increase (from $1{,}5.10^7$ to 2.10^7 particles/ml) with 100nM of EtOH. However, this increase was poorly reproducible and not sufficiently ample to ensure the detection of a difference in secreted HBV RNAs levels that associates with exosomes.

As we did not get conclusive results, we chose another approach by testing drugs which inhibit exosomes secretion. As a read-out, a decrease or change in gradient fraction distribution of the HBV RNA previously found in F4 could confirm the hypothesis that HBV RNA are indeed transported by exosomes.

To this aim, we tested two inhibitors of exosomes secretions: i) GW4869 which inhibits nsmase and, as a consequence, blocks the ceramide-dependent exosome secretion pathway or ii) Manumycin A that blocks Ras GTPases which associate with the ESCRT complex (Figure 43). It is noteworthy that only 20% of the exosomes are secreted through the ceramide associated secretion pathway. As a result, even if GW4869 inhibits at 100% this pathway, 80% of the exosomes will still be secreted by the ESCRT complex. However, it is important to keep in mind that HBV hijacks the ESCRT pathway for the secretion of viral particles and that using Manumycin A could also affect HBV secretion. If this is the case, we won't be able to clearly decipher if RNAs are decreased because of

inhibition of exosomes secretion or because of repression of global HBV secretion. Despite the limitations in the use of these drugs, we nevertheless decided to test these their efficiency, since they are commonly used as modulators of exosomes secretion. Firstly, we did a dose response study for Manumycin A and GW4869 and check if there was an effect on intracellular exosomes associated proteins (flotillin-1 and CD63) by western blotting.

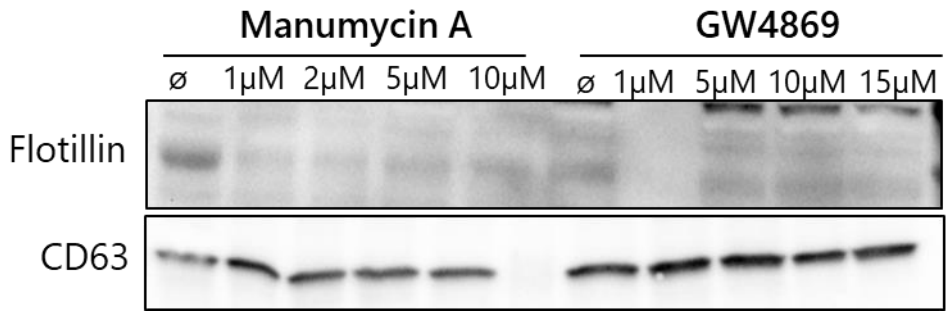

Figure 44 : Manumycin A and GW4869 dose response. HepG2-NTCP cells were treated with increasing doses of exosomes inhibitors and intracellular exosome associated proteins were detected by western blot.

We observed a slight reduction of flotillin signal following drug treatment, however we did not observe any significant change in CD63 levels, which is a more specific exosomes-associated proteins (Figure 44). Both drugs did not have any effect on cell survival (data not shown). We investigated additional exosomes-associated markers and HBV surface protein expression upon GW4869 addition.

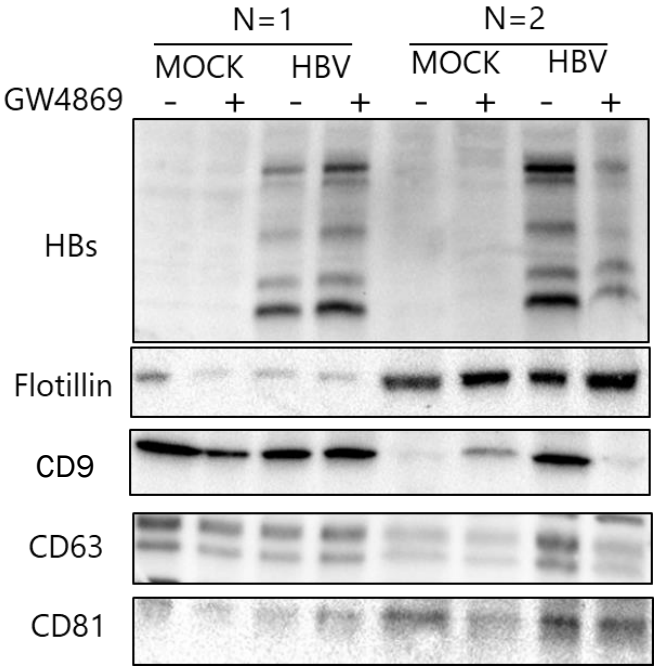

Figure 45: Exosomes associated proteins and HBs detected by western blot. HepG2-NTCP cells were infected or not (mock) with HBV and treated with GW4869 at 10µM.

Once again, we observed a decrease of Flot-1 but not CD63 in the first replicate (Figure 45). In addition, we observed a reduction of CD9 and HBs in GW4869-treated sample after infection but this observation was not reproducible between the replicates. In the end, we concluded that GW4869 did not have a significant effect on intracellular exosomes associated proteins in our experimental model. We still wanted to confirm our observation by quantifying exosomes in the supernatant this time.

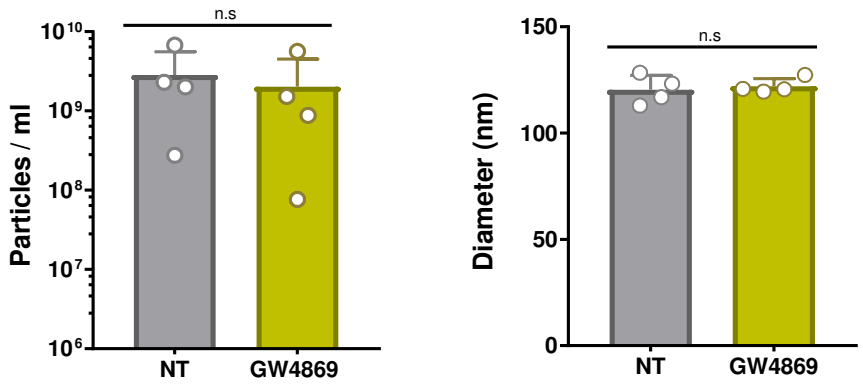

Figure 46: NTA quantification and size distribution of the particles treated or not with 10µM of GW4869. Graphs show the mean ± SD of 3 independent experiments

In the same experiment of Figure 45, this time we collected the supernatant and analyzed the particles by NTA (Figure 46). Cells were treated with 10µM of GW4869 which is a dose commonly used in the literature. GW4869 did not affect particles size distribution or exosome concentration across four independent replicates.

Facing these results, we wondered how to modulate exosome secretion with alternative approaches. We considered using silencing approaches, but, as there is no clear distinction in the secretion pathways between HBV and exosomes, silencing one of the gene involved in these pathways would have also affect HBV secretion (Chou et al., 2015b). In addition, exosome secretion is essential for cell survival and a complete knock out would probably be toxic for the cell. In this regard, we decided to quit this approach and focus a bit further on the characterization of the exosomes-associated proteins during HBV infection (Results Part III).

PART II.

IDENTIFICATION OF THE NATURE OF SECRETED HBV-RNAS AND THE IMPACT OF NA TREATMENT ON THE COMPOSITION OF THESE RNAS.

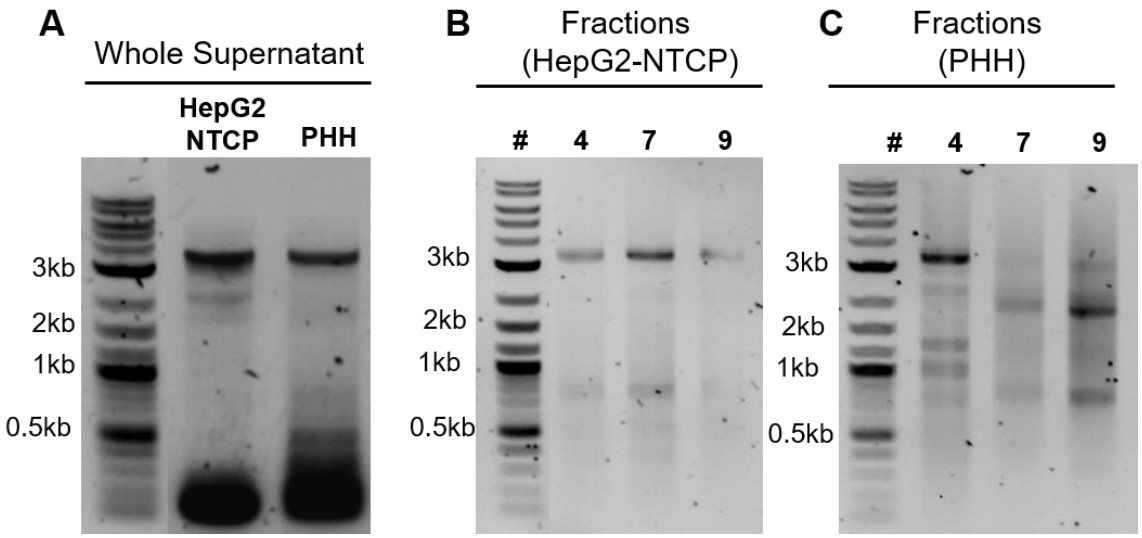

Figure 47: 5'RACE analysis of RNA secreted by infected hepatocytes. HepG2-NTCP or PHH were infected at MOI 500 and RNA was extracted using Trizol reagent from (A) concentrated whole supernatant; (C) Fraction F4, F7 and F9 of density gradient (see Results Part I and Material & Methods) of (B) HepG2-NTCP or (C) PHH.

RESULTS: PART 2

I. Various HBV-RNAs species are secreted in the supernatant of infected hepatocytes

With the aim of identifying HBV-RNAs species present in the different fractions of the gradient, we used a dual approach. First, we used the 5'RACE method recently published by Stadelmayer et al (Stadelmayer et al., 2020). 5'RACE for "rapid amplification of cDNA ends" was used to characterize all major intra- and extracellular HBV RNAs during viral infection of cultured hepatocytes. Even if 5'RACE allows discrimination between HBV RNA species, information about 3' truncation is lacking (see Mat&Met). Therefore, to get a full characterization of circulating HBV RNA species, we also designed a ddPCR assay with specific primers able to picture HBV-RNA 3'end termination signal.

As mentioned earlier, 5'RACE is a semi-quantitative technique that allows a good discrimination between HBV RNA species. This method has previously led to the identification of short HBX transcripts and spliced variants in infected cells and in CHB patients' serum samples (Stadelmayer et al). In Figure 47, secreted RNAs found in the different fractions across the gradient were compared to whole supernatant of infected HepG2-NTCP cells and PHH at 7 days post-infection. This experiment was performed by Dr. D. Kim, a post-doctoral researcher in our lab. Regarding extracellular RNA in whole supernatant of infected cells, pgRNA was found in both cell types. Bands corresponding to spliced isoforms were also found but at a higher level in HepG2-NTCP cell supernatant. Several HBx RNA forms seem to be present according to the migration profile. These results further suggest that extracellular RNAs are not only constituted by pgRNA. Finally, selected fractions representing exosomes+SVPs (FR4), Dane particles (FR7) and NCs (FR9) were analyzed separately. In HepG2-NTCP (Fig.47B), pgRNA was present in the three fractions. In addition, spliced variants were also present, mostly in F7 corresponding to virion-enriched fraction. No HBx transcripts were identified but this may be due to sensitivity issues given the low quantity of RNA used for this experiment. In PHH, (Fig. 47C), the distribution of the RNAs species across the fractions was more heterogeneous. Indeed, pgRNA was found in F4 and F9 corresponding to exosomes and NCs respectively, but the signal was weak for pgRNA in F7 corresponding to virions. While the migration profile

corresponding to spliced variants was similar in F7 and F9 (bands around 2.5kb), they seemed to be different in exosomes (around 1.5kb).

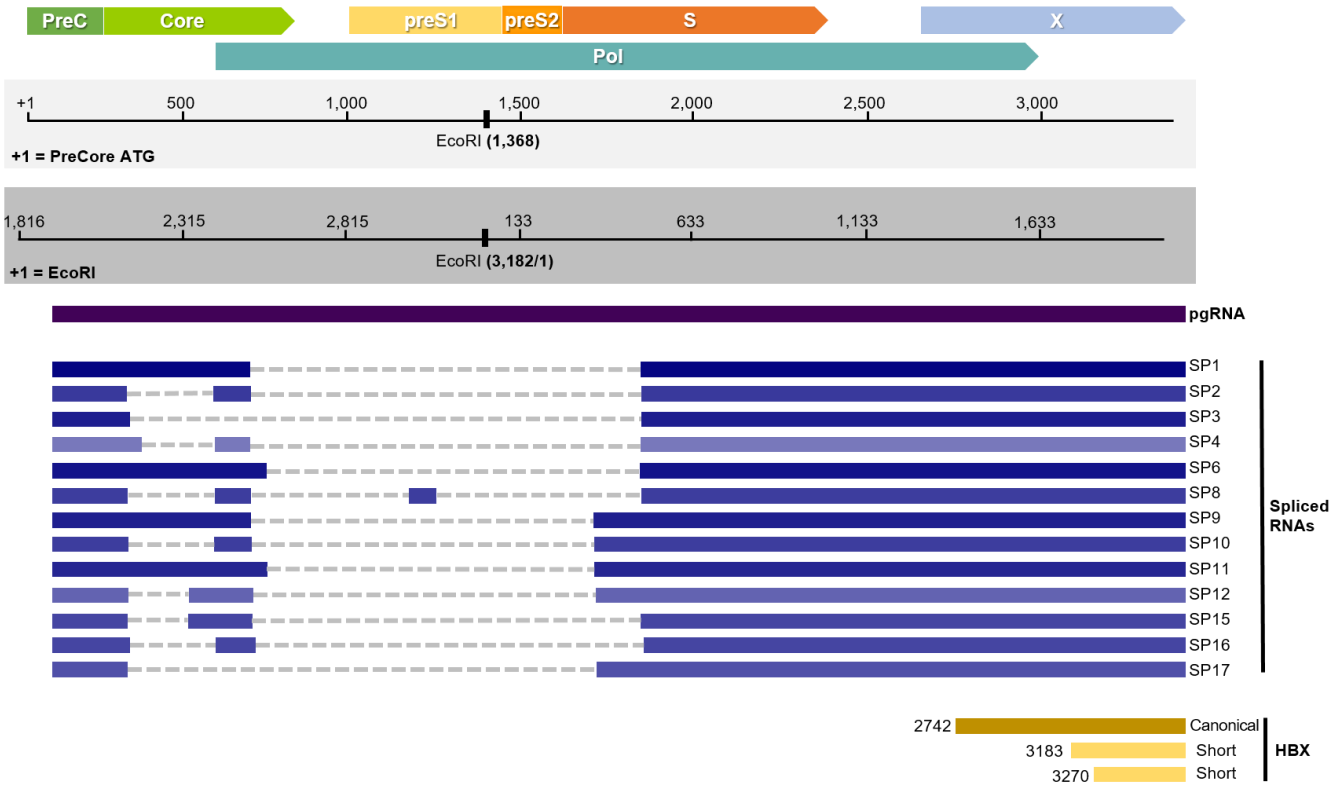

Figure 48. Alignment of sequenced amplicons with respect to HBV genotype D (reference sequence GenBank U95551.1). Sequence were aligned on HBV genome where +1 corresponds to ATG of PreCore (light grey square).

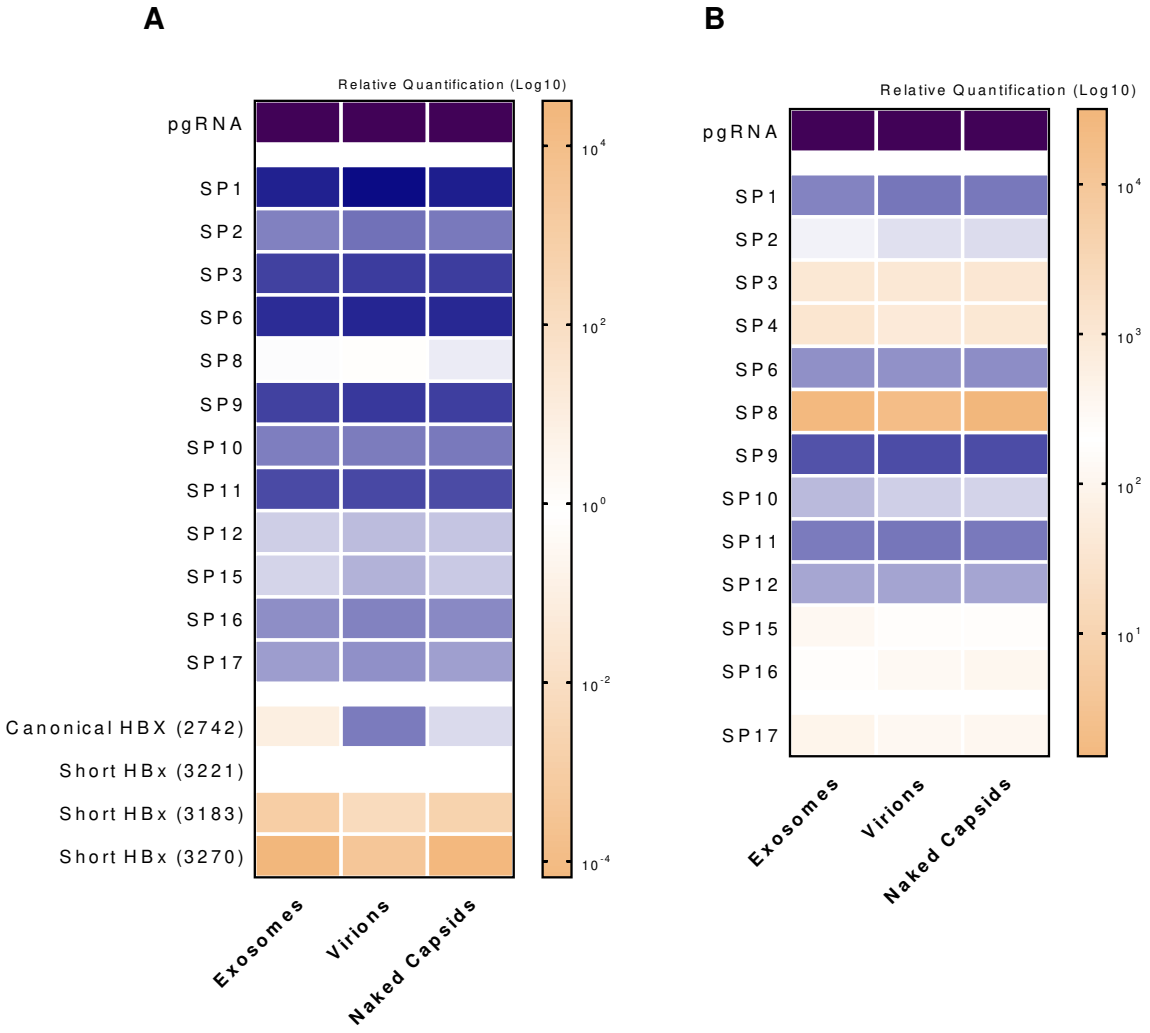

Figure 49. Heatmap of the RNAs species found in each fractions of the gradients in (A) HepG2-NTCP and (B) PHH. Quantification according to Log10 of FPKB values (Fragments per kilo base per million mapped reads). Purple squares correspond to very high values out of the scale (around 6Log FPKB)

Then, PCR-products from 5'RACE were sequenced by long-read Oxford Nanopore Technology (ONT).

Analysis of ONT MinION sequencing results identified high levels of pgRNA in all fractions both in HepG2-NTCP and PHH (Fig.49A and B, respectively). As expected, pgRNA was the main RNA specie reaching up to 30% of the total reads in each fraction. In HepG2-NTCP the more abundant spliced variants were SP1, SP3, SP9 and SP11 while in PHH they were SP1, SP6, SP9 and SP11. Slight variations in the quantity of the spliced variants were observed across the fractions in both cell types. In HepG2-NTCP, canonical and short HBx mRNAs were found in all fractions with a predominance in the virions associated fraction

(F7). HBx mRNA was not found in the fractions derived from PHH supernatant, probably due to sensitivity issues.

Altogether, these results support our previous observation made in Fig.35 and 36, i.e. that HBV-RNAs in the supernatant of infected hepatocytes are constituted by other species besides pgRNA.

To get further insight on 3'end of secreted HBV RNA, we designed a ddPCR assays with specific primers as described in fig.50A.

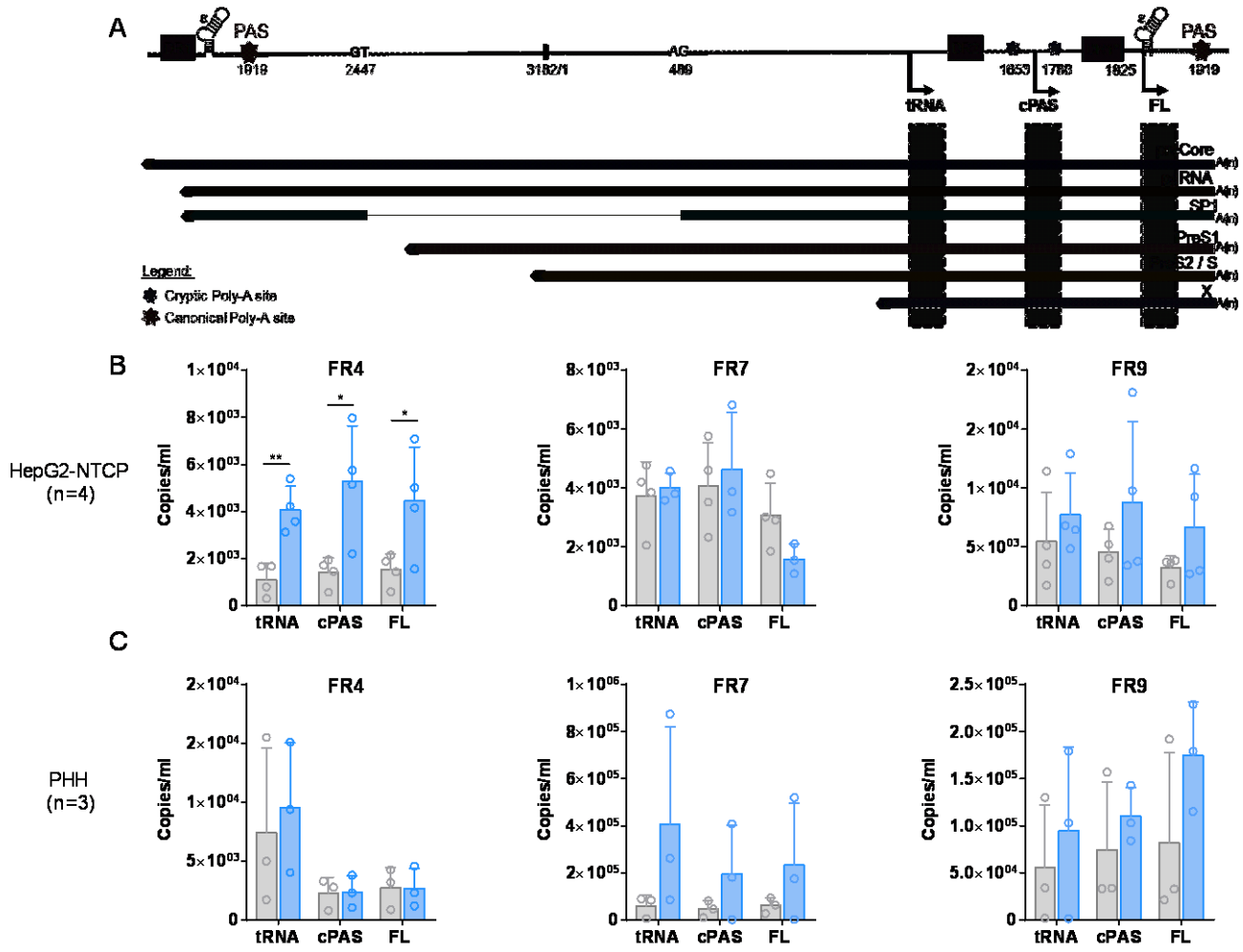

Figure 50. Characterization of HBV-RNA species contained in extracellular compartments of infected HepG2-NTCP cells and PHH. (A) HBV-RNA specific ddPCR assay design. This assay allows an absolute quantification of HBV-RNA species using assays located at the 3' end region. Results are expressed in copies/ml. grey bars= HBV infected; blue bars= HBV infected+3TC treatment. Graphs show the mean ± SD of 4 independent experiments in HepG2-NTCP (B) and 3 independent experiments in PHH (C). F4,F7 and F9 correspond to small EVs, VLPs and NCs fractions, respectively. tRNA = total HBV-RNA located in HBx region; cPAS= cryptic poly-adenylation site located before TATAA box; FL = Full Length located in the extreme 3'-end just before ε –loop.

tRNA (for total RNAs) is located before DR2 and all the cryptic polyadenylation sites, however, it only quantifies long HBX transcripts. cPAS is located between the two cryptic polyadenylation sites and allows the quantification of short HBX transcripts. Finally, FL for Full Length, is located after the cryptic polyadenylation sites but before the canonical one. By the combinatorial analysis of this amplicons, and the absolute quantification inherent to the ddPCR technique, this assay should shed a light on HBV-RNA 3' variability in cell supernatant. We performed this assay on the three main fractions containing HBV-RNAs: F4, F7 and F9, coherently with the previous 5'RACE experiment.

In HBV-infected non treated HepG2-NTCP cells, tHBV, cPAS and FL were approximatively equal in each fraction, suggesting that all HBV-RNA contained in exosomes should end at the canonical poly A signal. On the contrary, results were a bit different under 3TC treatment. Firstly, we observed a clear increase of secreted HBV-RNA under 3TC treatment, mainly in F4 associated to exosomes. In F7, there is clearly less signal for FL under NAs treatment, supporting the observations made by Shen et al, claiming that NAs treatment could increase the early truncation of HBV-RNAs (Shen et al., 2020b). Finally, in F9, there was a slight accumulation of HBV-RNAs with 3TC but not change in the composition according to treatment.

In PHH, the profile of the secreted RNA was hardly conclusive, given the considerable variability between the replicates. However, no significant increase of secreted RNA was observed in F4 under 3TC treatment compared to HepG2-NTCP cells.

Altogether, these results clearly demonstrated that in addition to pgRNA, other viral mRNA e.g. spliced isoforms and different HBx transcripts are also found in cell supernatant. In addition, we identified 3'truncated HBV-RNA using the two cryptic PAS located between DR2 and the second DR1.

PART III.

STUDY OF THE SECRETION PROFILE OF THE PROTEINS ASSOCIATED WITH EXOSOMES: EFFECT OF HBV INFECTION AND NA TREATMENT (MASS SPECTROMETRY)

RESULTS: PART 3

We showed that HBV-RNAs are associated with exosomes in the supernatant of HBV-infected hepatocytes by using two different cell models: HepG2-NTCP and PHH. We observed an increase of secreted HBV-RNAs under NAs treatment, mainly in density fractions enriched for exosomes. Unfortunately, our attempts to modify exosome secretion using drugs were unsuccessful.

As exosomes biogenesis has a considerable overlap with the assembly and secretion of viral particles, we hypothesized that exosome content could be modulated by HBV infection. The main goals of the mass spectrometry study were to get insight on i) if and how HBV regulates exosomes-associated proteins secretion, ii) key factors involved in the sorting of HBV-RNAs into the exosomes and finally iii) the potential presence of HBV proteins associated with exosomes secreted by infected hepatocytes.

I. General Experimental Design

We accumulated supernatant from non-infected (N.I), HBV infected or HBV infected + lamivudine HepG2-NTCP cells. Cells were infected with HBV at a MOI of 250 for 7 days and treated or not with lamivudine for 4 days after cccDNA establishment at 4 dpi. As detailed in Material and Methods section, after a pilot experiment to assess the protein quantity and purity requirement for MS analysis, we performed 4 experiments and selected 3 samples to be analyzed by MS according to their profile for viral parameters (HBeAg, HBsAg, HBV-DNA & HBV-RNA) (See Materials and Methods, Fig. S7). 1 liter of supernatant was accumulated and concentrated by differential ultracentrifugation. The EVs pellet containing both exosomes and viral particles was layered on an iodixanol/sucrose density gradient and twelve fractions were recovered, as described in Results Part I. The fractions were separately analyzed for viral and exosomal markers as wells as viral DNA and RNA. According to their characteristics, fractions were pooled in four subgroups:

I. Small EVs (sEVs) group including F1 to F3, containing exosomes markers but no HBs
II. Small EVs + Subviral particles (sEVS+SVPs) group including F4 to F6, containing both exosomes markers and HBs. This fraction was composed of both exosomes and subviral particles as shown by electron microscopy (Results Part I).

III. F7 containing virions

IV. Naked Capsids (NCs) group including F8 to F10 containing neither exosomes markers nor HBs, but only the capsid protein.

The following analysis will focus on the first two groups (sEVs and sEVs+SVPs), which were processed by MS in three independent replicates. Since proteins quantity was very low in the virions and naked capsids groups, a pilot experiment involving only one replicate of each was sent to MS to test the feasibility of the analysis and will not be described in this manuscript.

Sub-Groups		sEVs	sEVS+SVPs
Tetraspanin	CD9	x	x
	CD63	x	x
	CD81	N.F	
Flotillin-1		x	x
TSG101		x	x
HSP70		x	x
LAMP2		x	x
HSP90 Complex	HSP90AA1	x	x
	HSP90AB1	x	x
	HSP90B1	N.F	x
	CDC37 (HSP90 co-chaperone)	N.F	x

Table 5. Commonly recognized exosome-associated proteins. The cross indicates that the proteins were identified in all the experimental conditions in all the replicates of the same group. When the protein was not present in the data set the mention "not found" (N.F.) appears.

II. Exosomes enrichment and characterization

The MS experiment was technically successful and a total of 735 and 2369 proteins were identified in all biological replicates of each experimental conditions in sEVs and sEVs+SVPs groups, respectively (see Methods for details). Firstly, a preliminary analysis was conducted by pooling the proteins identified in all the experimental conditions and replicates within sEVs or sEVs+SVP group.

Before going deeper into the analysis, we listed all the proteins that were commonly identified in the three experimental conditions (N.I, HBV, HBV+3TC) of each group and compared them to an already published database of exosome-associated proteins in order to get insight in the specific particles composition of sEVs and sEVs+SVPs groups.

To ensure the purity of the preparation, we looked over different parameters. Indeed, a successful purification of the exosomes is characterized by the lack of possible contamination by cellular debris. sEVs and sEVs + SVPs groups were devoid of the early endosome antigen (EEA1), the mitochondrial marker CoxIV, the endoplasmic reticulum marker (Grp94) and the Golgi apparatus marker (GM130), indicating absence of relevant cellular contamination in the samples. We detected serum albumin (ALB) which is not surprising because hepatocytes can produce large amount of albumin. In addition, we detected histone subunits (H1 to H4) in the samples. This could be due to a contamination of the samples by nuclear material, even if it seems unlikely, since other common intracellular contaminants were missing in the samples. It could be explained by the sorting of the histone proteins out of the nucleus and the cell, as H3 was recently found to correlate with liver dysfunction (Novruzov et al., 2021).

On the contrary, a standard panel of proteins associated to exosomes was used as a reference to estimate the presence of exosomes in the same samples (Deng & Miller, 2019, Table 2).

We were able to detect the most common markers used to identify exosomes in both sEVs and sEVs+SVPs groups (Table 5). The tetraspanins family including CD9 and CD63 was abundantly detected in the samples, however we didn't detect any CD81. Besides tetraspanins, other exosomal markers such Flotillin-1, the tumor susceptibility gene 101 (TSG101), the lysosome-associated membrane protein 2 (LAMP2), heat shock proteins 70 and 90 were abundantly detected in the samples. Finally, the subunit HSP90B1 and the HSP90 chaperone, CDC37, were only detected in sEVs + SVPs group.

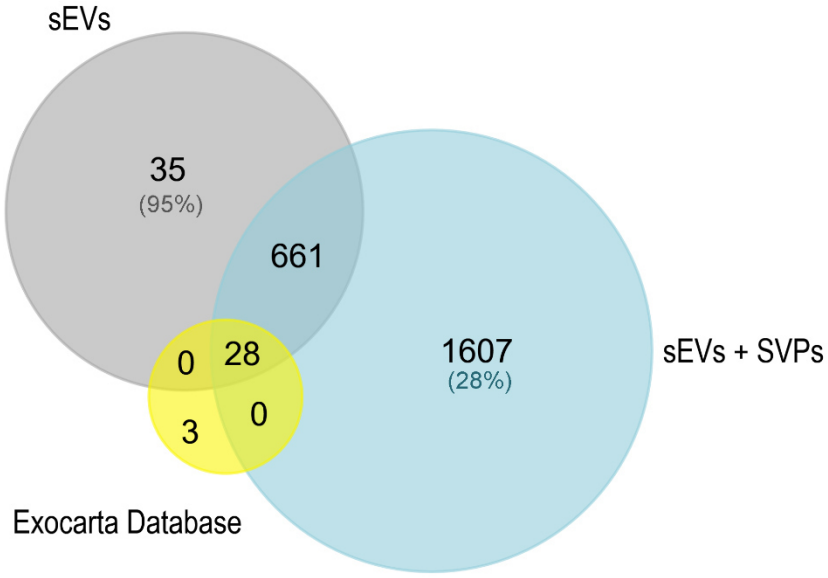

Figure 51. Venn diagram of proteins identified in HegG2-NTCP exosomes by mass spectrometry. All the proteins identified in the three replicates and all the conditions of each group were divided in two protein sets: sEVs or sEVs + SVPs. The two protein sets were compared to the 31 most common exosome associated proteins. Percentage represents the proportion of protein which are common in the two proteins sets compared to the total number of proteins.

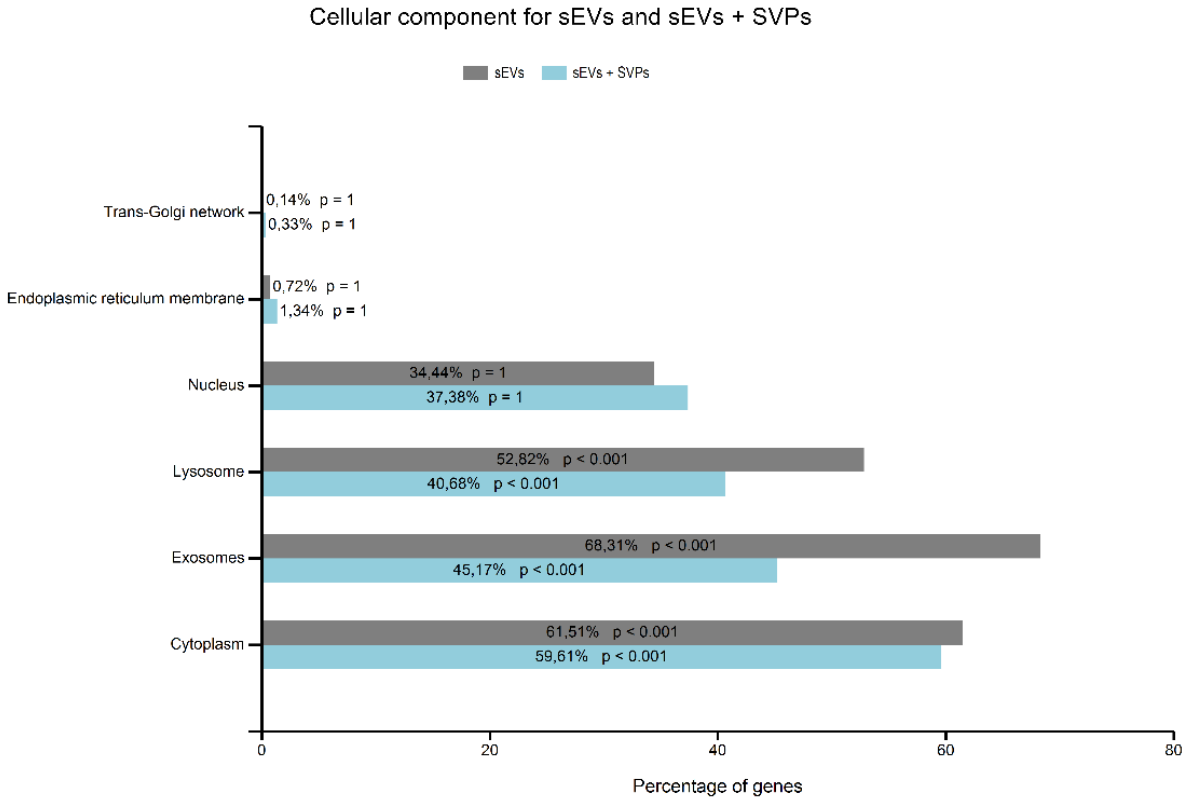

Figure 52. Gene enrichment according to cellular components. Gene ontology was performed on the two data sets. The X-axis shows the percentage of genes of the specific cellular compartment that are found in the data set. P-value is the probability of seeing at least x number of proteins out of the total n genes in the list annotated to a particular GO term, given the proportion of genes in the whole genome that are annotated to that GO Term.

689 proteins were common to the two groups, representing 95 % (689/735) of the proteins identified in sEVs and 28 % (689/2369) of sEVs + SVPs (Figure 51). The two protein sets were crossed with the Exocarta database which gather results of published exosomal proteins (Simpson et al., 2012). 28 of the 31 (90 %) most exosome-associated proteins according to Exocarta were present in both sEVs and sEVs+SVPs.

To confirm the enrichment in exosomes in the two groups, we performed a gene ontology bio statistical analysis according to cellular compartments.

Gene ontology according to cellular compartments confirmed that exosomes are one of the most enriched compartments with up 68% of the sEVs and 45% of the sEVs + SVPs proteins belonging to exosomal category (Figure 52). Unsurprisingly, proteins belonging to cytoplasm and lysosome were also significantly enriched in both groups. Indeed, exosome associated protein list has a considerable overlap with lysosome and cytoplasm associated proteins which could explain this significant enrichment in our protein sets. On the contrary, endoplasmic reticulum, nucleus and Golgi associated proteins were not significantly enriched in our groups confirming the specificity of our samples for extracellular compartment. Altogether, these findings further indicated that the preparation of the exosomes secreted from infected and/or treated HepG2-NTCP cells was enriched in exosome-associated proteins and showed minimal contamination by cellular debris.

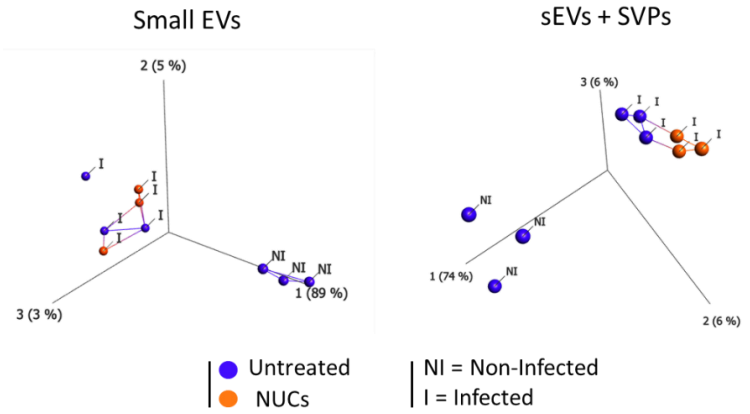

Figure 53. PCA of sEVs and sEVS + SVPs samples. Each dot represents an individual replicate of each experimental condition.

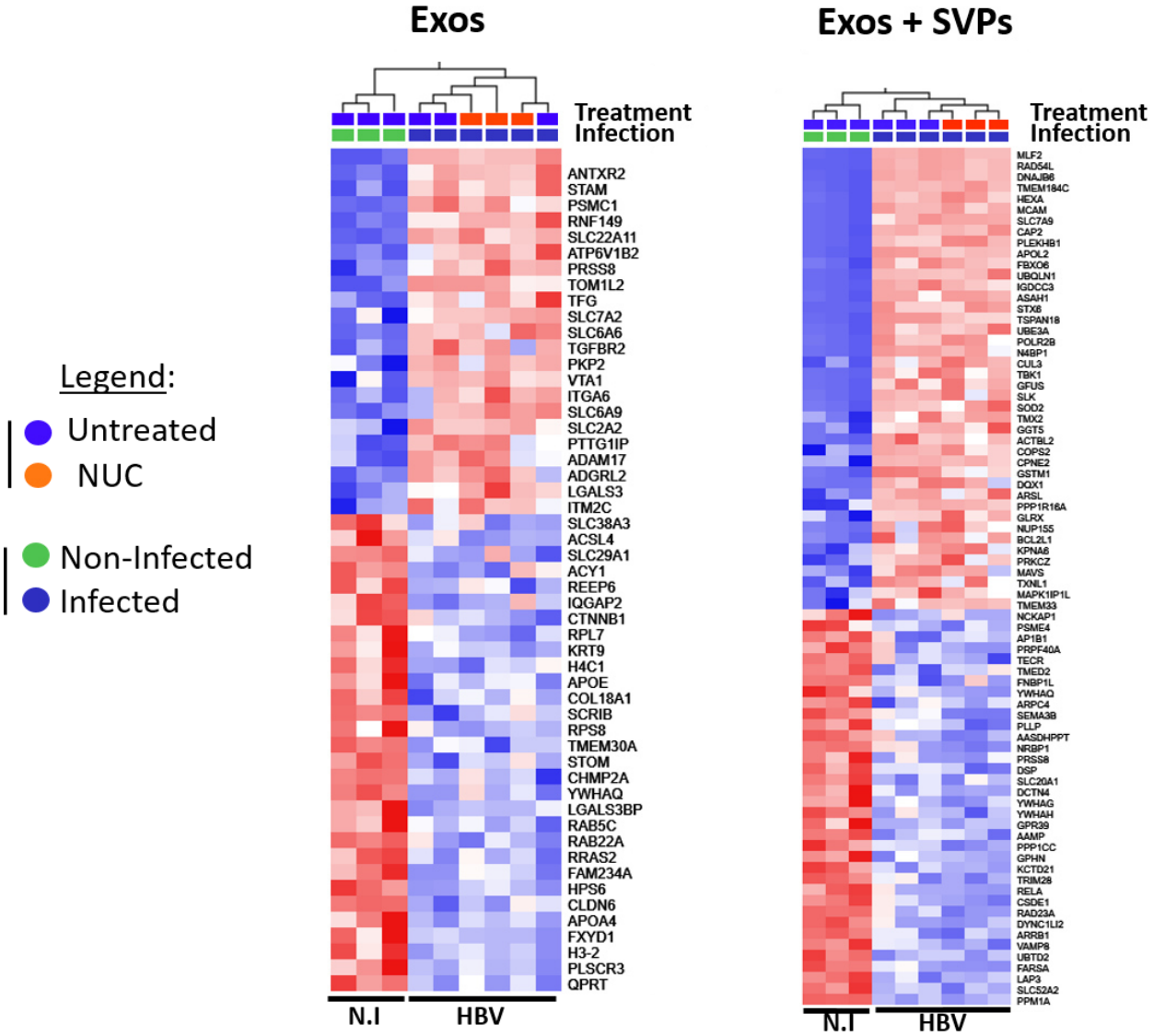

Figure 54. Heatmap visualization of protein secretion profiles in each sample preparation. A dendrogram of three experimental conditions and on the replicates is shown at the top. Protein secretion values were z-score normalized prior to clustering. (p-value <0,05)

III. Differential profiling of HBV infected HepG2-NTCP derived exosomes

Global profiling of proteins content in exosome secreted by rat hepatocytes and human HCC cell lines have been reported (He et al., 2015; Jia et al., 2017b; X. Zhao et al., 2014). These studies reported a putative effect of HBV on exosomal content but none of them were conducted in models of infection or were aiming at finding factors that could be involved in the viral RNA sorting through exosomes. To get insight on the effect of HBV infection on secreted proteins, we performed principal component analysis (PCA) on the protein identified in each experimental condition of all the replicates in sEVs and sEVs+SVPs groups.

PCA analysis revealed that secreted protein profile is significantly different upon infection but not upon 3TC treatment in the two groups (Figure 53). A similar observation was previously done by Jia et al. in exosomes derived from HepAD38 cell line where HBV replication was induced or not by doxycycline treatment. It is noteworthy that the authors did not looked at the potential effect of NAs treatment in this study.

To corroborate our previous observation, we used Qlucore Omics software to picture the modulation of extracellular proteins secretion during HBV infection in the presence or not of 3TC (Figure 54). In both sEVs and sEVs+SVPs groups, we observed a clear hierarchical clustering of the samples according to the infection status but not according to 3TC treatment. We could easily make two panels, one with proteins that were more secreted upon infection and, in contrast, one with proteins that were less secreted. It is clear that HBV can affect secreted protein profile; however, it might be interesting to see if in these proteins we can identify key biological processes or molecular function, highly modulated upon infection.

Amongst the most differentially secreted proteins, none of the subgroups was harboring proteins belonging to the top 100 proteins associated with exosomes according to Exocarta database.

To gain insight on the potential role that secreted proteins could play in the modulation of HBV infection, GO enrichment analysis in term of biological process was performed on the proteins set that were differentially secreted according to the experimental conditions and the groups. Indeed, six subgroups were created. Indeed, in sEVs and sEVs + SVPs groups, each condition was compared to each other raising three

new proteins sets: i) HBV-infected versus non-infected (N.T vs N.I), ii) HBV-infected and 3TC treated versus non infected (3TC vs N.I) and iii) HBV-infected and 3TC treated versus HBV-infected non treated (3TC vs N.T). While classification according to groups i) and ii) could inform on the effect of the virus on the proteins secretion, subgroup number iii) could shed a light on a potential modulation by 3TC treatment during infection. We didn't make any distinction between the proteins which were significantly more or less abundantly found among the different conditions.

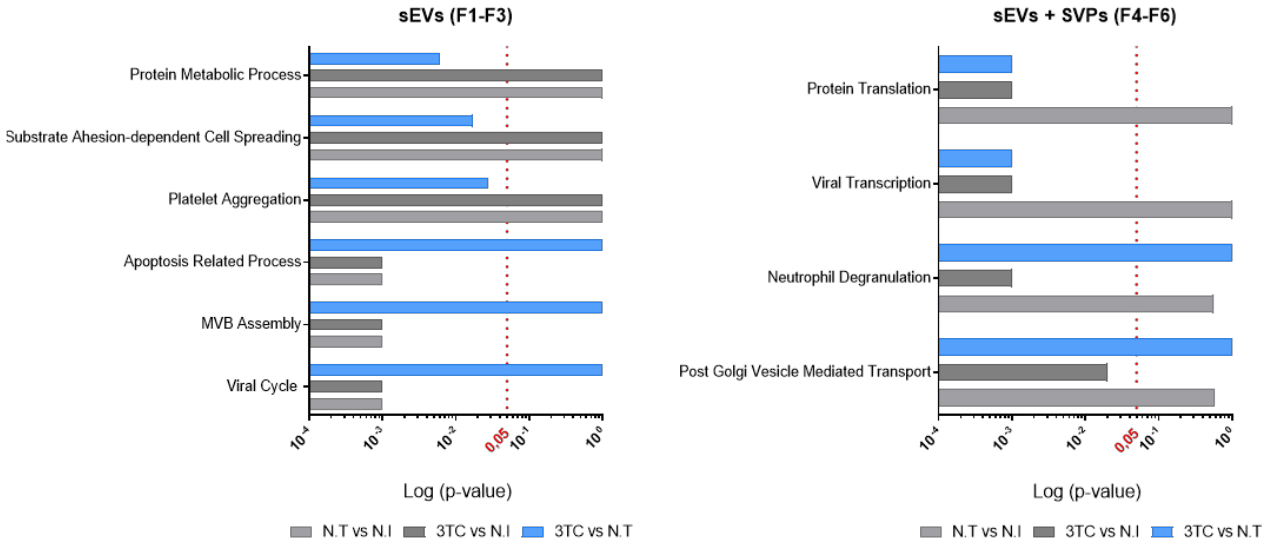

Figure 55. Gene ontology analysis in term of biological process was done on the differentially secreted host proteins. X-axis represents the log (p-value) which illustrates the probability of the proteins listed in the dataset to belong to the mentioned biological process. P-value cut-off is set at 0.05.

Biological processes are vital for the cell and shapes its ability to interact with its environment. In the case of proteins associated with hepatocyte derived-exosomes, we wondered if HBV infection and/or 3TC treatment could affect some of these processes. In this regard, we made gene ontology analysis in the different subgroups that were previously listed (Figure 55).

In the sEVs group, the analysis suggests that the proteins which were more or less secreted upon HBV infection were mostly belonging to processes related to viral replication, MVB assembly and apoptosis related reactions. This observation suggested that HBV could modulated the secretion of the proteins involved in its replication cycle and egress and that 3TC treatment has significant effect on these functions. On the contrary, we observed that proteins which were differentially secreted in response to 3TC treatment during infection belong to platelet aggregation, positive substrate adhesion-dependent spreading and

protein metabolism. It suggests that the secretion of proteins associated with these biological processes could be affected by 3TC treatment during infection.

This analysis was also done in the sEVs + SVPs group corresponding to the fractions mixing exosomes and SVPs. In this group, we were not able to establish a clear phenotype of the differentially secreted proteins in response to HBV infection and/or 3TC treatment. The proteins that were differentially secreted in 3TC vs N.I and 3TC vs N.T belongs to protein translation and viral transcription processes illustrating a potential effect of 3TC.

The last question we asked was about the presence of HBV proteins in the different groups.

Protein ID	Enrichment Score (Relative to Non Infected)			
	Small EVs		**sEVs + SVPs**	
3TC	**-**	**+**	**-**	**+**
Surface (HBs)	31,08	19,31	539,23	427,00
Capsids (HBc)	ND	ND	549,38	416,58
Polymerase	ND	ND	3,33	3,64
HBX	ND	ND	ND	ND

ND = Not Detected

Table 6. Relative Abundancy of HBV proteins in sEVS and sEVS + SVPs group

HBV proteins were found in sEVs and sEVs + SVPs group. Only HBs was detected in the sEVs group in a relatively small abundance and these values don't seem to be affected by 3TC treatment. The peptides that were identified were in S-HBs and across PreS1 and PreS2 domain suggesting the possibility of the presence of L-HBs in the extracellular compartment were exosomes are found. In the sEVs + SVPs group, HBs and Capsid protein were largely represented by a high relative abundance. Concerning HBs, peptides have been identified in S-HBs but also in PreS1 and crossing PreS1 and PreS2 domain suggesting once again the presence of L-HBs more likely in SVPs. It was not surprising that HBs was largely found in this fraction as these fractions contain both exosomes and SVPs, but did not expect to find the capsid protein. Yet, we do not know if HBc found in this group are HBc dimer proteins that are transported by the exosomes and could act as a decoy for viral immunity hijacking the role of antigen presentation of the exosomes or simply due to a lack of separation between these fractions to the virion fraction. In addition, very few

peptides corresponding to polymerase were found in this group; however, the significance of these results is still unknown and more studies are needed to confirm this observation. No peptides corresponding to HBx protein were detected in any of the groups.

In conclusion, MS study is a good approach to screen actors that are involved in the sorting of HBV RNA in the exosomes, processes that was never described before. However, these results must be analyzed with caution, as mass spectrometry is a technique which heavily relies on the quality of the samples. In our case, variability can occur depending on several experimental biases as the purification of exosomes from HBV infected cells is a long and labored process. All the results presented in this third part should be confirmed by ELISA, western blotting or silencing assays.

Discussion & Perspectives

DISCUSSION & PERSPECTIVES

In the context of the global HBV cure research programs, the evaluation of the intrahepatic cccDNA amount and its transcriptional activity will be instrumental for the assessment of the efficacy of the novel antiviral strategies under clinical investigation. However, this is strongly hampered by the need of invasive biopsy procedures, by sampling bias due to potential focal differences in the infected tissue and by technical constraints in specific detection and quantification of cccDNA. Therefore, there is an unmet need for the development of non-invasive biomarkers reflecting the levels and the activity of the intrahepatic cccDNA pool. Recently, it was suggested that the extracellular or circulating HBV-RNAs could serve as such a surrogate marker (Giersch et al., 2017a; Jansen et al., 2016a; Rokuhara et al., 2006; J. Wang et al., 2016a).

I. Objectives of the research project

My research project was divided in three main axes. **First**, I identified the physical entities carrying HBV-RNAs in the supernatant of infected cell. **Second**, I wanted to determine which RNA species are released by HBV infected cells. Indeed, several HBV-RNAs species were identified in literature; however, none of these studies gave a complete characterization of both 5' and 3'end of the RNAs as well as their nature upon NAs anti-viral treatment. **Third**, I used mass spectrometry to get more insight on the factors involved in HBV-RNA sorting through EVs.

II. Experimental Models

Numerous studies about HBV-RNAs were conducted in patients' serum or in cell supernatant from HBV-inducible cell lines. On our side, we decided to use a relevant and accessible model of *in vitro* infection that could be the closest to the physiology. For sure, patient's serum is the gold standard but hard to obtain and does not allow to test drugs. Therefore, these experiments were conducted on two different *in vitro* infection models. On one hand, **PHH,** which are the best physiological model, however, their supply is limited as they are isolated from patient's liver resection. They are easy to use, provide high infection rates but have high inter individual, technical dependent and time dependent variability that can lead to difficulties on the reproducibility of the experiments. On the other hand, we chose **HepG2-NTCP** cell line, a hepatocellular carcinoma cell line susceptible to HBV

infection and cccDNA establishment. This model is reliable, easy to handle and can be highly amplified to accumulate consequent quantities of supernatant, necessary for quantitative exosomes isolation. Indeed, as exosomes *in vitro* are produced by a single cell type, their quantity is limited compared to serum, where all cells are able to deliver them in the circulation, including immune cells which produce large amounts of exosomes. For a matter of availability, some experiments could not have been performed in PHH model and were consequently only repeated in HepG2-NTCP. Our model has two limitations. First, HepG2-NTCP are carcinoma-derived cells in which the exosome biogenesis and production could be different from non-transformed hepatocytes (Gudbergsson et al., 2016; Kalluri, 2016; Z. Sun et al., 2018; Zhang & Yu, 2019). Second, HepG2-NTCP cells are cultured in DMSO to reach a quiescent state necessary for HBV-infection. Nevertheless, it is known that exosomes are mostly released while cells are proliferating (O. Hayes et al., 2005; Steinman et al., 2003). In addition, no data is available on a potential effect of DMSO on exosome secretion.

We did not use HepaRG-cells, which are closer to PHH than carcinoma cell lines because after differentiation, hepatocytes represent only 10 % of the cell population. The remaining 90 % is composed by cholangiocyte-like cells, which are not susceptible to HBV infection. Thus, working with this model would provide a mixture of exosomes from two different cell types with only one replicating HBV. In addition, we did not use rodent models such as liver humanized mice for their poor accessibility and the low quantities of circulating blood, in which it would have been tricky to isolate a suitable quantity of exosomes to perform downstream analysis.

It is important to specify that studying exosomes derived from a single cell type compared to whole serum exosome is not equal. Indeed, serum derived-exosome preparation consist in a mixture of different population of exosomes, released in the body fluids by almost all the cells of the organism whereas exosomes derived from hepatocyte supernatant represents only the hepatocytes derived exosomes (Willms et al., 2018). Exosomes have a specific signature that correspond to the cell they are derived from so we wanted to look at this specific signature and the mechanism responsible for the secretion of HBV-RNAs and might be useful as a potential biomarker. In this regard, similar experiments were concomitantly carried out in patient's serum Dr D. Kim.

III. Which particles carry HBV-RNAs in cell supernatant?

During viral replication, HBV infected hepatocytes shed several extracellular vesicles – e.g. viral and non-viral particles- with different structural and genetic components, including the infectious DNA-virions, genome-free virions, SVPs, and NCs that could carry viral RNAs (J. Hu & Liu, 2017). Several studies report that HBV-RNAs are carried by VLPs and NCs; however, we also found that 15% of viral RNAs are carried into exosomes. While the presence of HBV-RNAs in NCs and VLPs is well-recognized in the HBV field, the presence of HBV-RNAs with exosomes is still a matter of debate since studies have been contradictory on this subject. On one hand, three different reports claimed that exosome could not likely carry HBV-RNAs. First, Jansen et al observed no difference in the total quantity of HBV-RNAs in cell supernatant after treatment with GW4869, an inhibitor of exosome secretion. However, it has to be noted that GW4869 only affects a pathway involved in the minority of exosome secretion (Jansen et al., 2016a). Then, in their study, the group of Kohara et al. claimed that only DNA was present in exosomes isolated from HBV-infected PXB cells (Sanada et al., 2017). Finally, Bai and colleagues only observed little quantity of HBV-RNAs in fractions associated with exosomes in serum of CHB patients even if they did not excluded the fact that exosomes could serve as HBV-RNAs carriers (Bai et al., 2018). On the other hand, in 2017, Yang et al showed that HBV-DNA and HBV-RNA, as well as HBsAg, were identified in exosomes derived from the serum of CHB patients. Regarding this divergent literature, our study is the first to give a first in depth characterization of the association of HBV-RNAs with hepatocytes-derived exosomes.

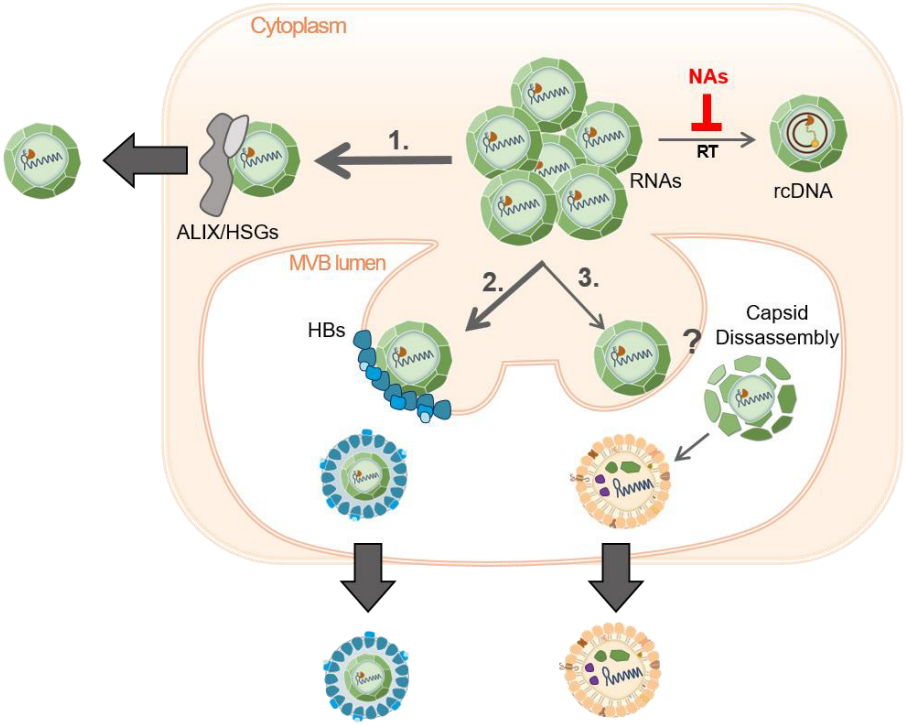

Figure 56. Proposed model for the increase of HBV-RNAs secretion under NAs therapy. We hypothesized that NAs treatment could induce an accumulation of RNA containing capsids in the cytoplasm, which could be released in the supernatant by three different pathways: 1) Most of the RNA containing nucleocapsids are secreted as naked capsids. 2) They enter the lumen of MVB to be secreted as virions like particles. 3) if the two latter pathways are overwhelmed, they could be redirected towards the exosomes secretion where the capsids could be disassembled and both RNAs and HBc could be incorporated in exosomes.

In our experimental conditions, while HBV-DNA was dramatically decreased under NA treatment, HBV-RNAs where increased, mostly in the fraction associated with NCs and exosomes. Since no studies so far reported the effect of NAs on the content of exosome derived from infected cells, our study brings new insights on this process. However, several studies have reported the effect of NAs treatment on circulating or extracellular HBV-RNAs. Indeed, Wang and colleagues observed that the levels of virions containing pgRNA increased in a dose-dependent manner when HepAD38 cells were treated with ETV and 3TC, accompanied by a significant decrease in the level of HBV DNA. This effect was also observed in HepG2.2.15 cells. They suggest that following NA-treatment, reverse transcription would be inhibited, and the pgRNA in core particles would still be enveloped and released into the serum, thereby increasing the level of pgRNA containing virions (Wang et al., 2016). However, this study only reports the presence of pgRNA associated with VLPs, excluding the potential presence of other viral mRNAs or other particles types.

Contrary to these results, in our experimental model, we observed a reproducible decrease of 3.5kb RNAs, including both precore and pgRNA, compared to the total HBV-RNAs in fractions enriched in VLPs upon NA treatment. We cannot exclude that this

difference might be due to the different model, natural infection vs HBV-replicating cells, or by different experimental approaches in identifying HBV-RNA associated to VLPs. On the other hand, both total HBV-RNAs and 3.5Kb RNAs level were increase in NCs and exosomes-enriched fractions, suggesting a change in the secretion profile of HBV-RNAs following 3TC treatment. We may speculate that, in a condition where 3TC induces the accumulation of pgRNA following the blocking of retrotranscription, the RNAs containing capsids might be redirected to the MVBs were they would be disassembled. HBc could then be loaded into exosomes while viral RNAs could be shuttled by RNA binding proteins towards the exosomes particles. This process could prevent an accumulation of capsids containing viral RNAs in the cytoplasm, explain the increase of their secretion in exosomes and favor HBV spreading. However, since the peptide that we identified in MS overlaps with both HBc and HBe proteins, we cannot exclude the presence of HBe instead of HBc in exosomes enriched fractions. In addition, a direct effect of the NAs on exosome secretion and therefore the loading of HBV-RNAs into exosomes is also possible. Even if we did not observe a significant effect of NAs treatment on the secretion of proteins associated with exosomes, it could be interesting to quantify exosome secretion on non-infected cells with or without NAs to check this hypothesis.

IV. How are HBV-RNAs shuttled into exosomes?

Mechanism leading to secretion of HBV-RNAs is still poorly characterized. Through specific interactions with their cognate RNA molecules, RNA binding proteins (RBPs) regulate RNA processing, nucleocytoplasmic transport and maturation, intra-compartmental localization and turnover (Glisovic et al., 2008; König et al., 2012). As a result, RBPs could serve as key players in this mechanism, by making complexes with RNAs and transporting them into exosomes during their biosynthesis. In fact, RBPs can bind to both single-stranded as well as double-stranded RNA; demonstrating an ability to interact not only with mRNAs but also with small non-coding RNAs which may form RNP complexes. Such a compendium of interactions can be long lasting and is considered driving factor in several aspects of cellular metabolism and pathology. Currently, there is no consensus regarding the respective mechanisms, by which RBPs contribute to the precise regulation of selective release of RNAs from cells into exosomes. However, the application of biochemical, cell-based, and computational approaches revealed in several models the enrichment of transcript sequences, defining ‘RNA motifs’, recurrently found in transcripts associated to EVs and validated as consensus substrate for RBPs.

Heterogeneous nuclear ribonucleoproteins (hnRNPs) represent a large family of 20 major and minor proteins in humans with differential RNA-binding capacities (Dreyfuss et al., 1993). hnRNPs are characterized by a typical structure of four unique RNA-binding domains (RBDs): the RNA recognition motif (RRM), the quasi-RRM (qRRM), a glycine-rich domain constituting an RGG box, and a KH domain. Six members of this RBP family emerged in association with EVs: hnRNPA2B1, hnRNPC1, hnRNPG, hnRNPH1, hnRNPK, and hnRNPQ. Most of these hnRNPs were identified in both sEVs and sEVs+SVPs groups in our MS study. In this regard, we could hypothesize that one of these hnRNPs might responsible for HBV-RNAs sorting in exosomes. By checking if their binding motif is present on HBV-RNAs sequence we could study the close association between this specific RBP and HBV RNAs. This work is currently successfully done by Dr Hyoseon Tak, a post-doctoral researcher in the group in charge of this part of the project. She identified HNRPA1 to be the best candidate to associate with HBV RNAs.

Besides hnRNPs, other RBPs are thought to be involved in RNA sorting in exosomes (reviewed in (Fabbiano et al., 2020)). The majority of these proteins was also identified in our MS study, however, deeper studies are needed to decipher their implication in viral RNA transport. Among them, the apoptosis-linked gene 2 (ALG-2)-Interacting protein X (ALIX) is one of the established protein markers enriched in exosomes (Vanessa et al., 2019). This protein has a pivotal role in regulating functions such as the endocytic membrane trafficking (Odorizzi, 2006), the virus entry process (Martin-Serrano et al., 2003) or the extracellular matrix assembly (Pan et al., 2008), etc. Of relevance, Iavello et al. evaluated the contribution of ALIX in the packaging of miRNAs in EVs released by human liver stem-like cells (HLSCs) suggesting that ALIX could directly bind RNA to shuttle them into extracellular vesicles (Iavello et al., 2016). This observation is particularly interesting because ALIX was identified to be associated with exosomes derived from HBV-infected cells and ALIX is also thought to be involved in naked capsids secretion, which carry the major proportion of viral RNAs secreted in cell supernatant (Bardens et al., 2011). An analysis of its RNA-dependent interactome might contribute to understand its role in RNA sorting.

Finally, it is well known that HBV hijacks the host cellular secretion machinery ESCRT to release its viral content. Thus, it is not surprising to observe that HBV could also incorporate its genetic material in exosomes rather that in viral particles. Several mechanisms could explain the presence of HBV-RNAs in exosomes:

i) Exosomes and viral particles sharing the same secretion pathway, viral RNAs could be loaded in exosomes in order to increase viral spreading or target immune response. This RNAs could directly shuttle towards MVBs with the help of RBPs or could derive from nucleocapsids that are disassembled in MVBs to release their content in exosomes.

ii) Alternatively, viral RNAs incorporation in exosomes could be a natural cell process to eliminate the viral intrude or a way for the virus to discharge RNA fragments after RNAse H hydrolysis or viral mRNAs that are not transported to ribosomes for translation.

V. What could be the role of exosomes derived from HBV-infected hepatocytes?

In addition to HBV, other viruses can hijack vesicular trafficking and assimilate viral constituents into exosomes for their own benefit, such as HCV, Zika virus (ZV), West Nile virus (WNV), and DENV (Hamel et al., 2015; Liu et al., 2014; Ramakrishnaiah et al., 2013; Smit et al., 2011). The presence of viral antigens in exosomes is known to maximize the persistence of the virus by hiding their genomes, entrapping the immune system, and increasing viral infection in uncontaminated cells.

1. Dual role in the regulation of immune responses

Exosomes derived from HBV-infected cells or CHB patients' serum are thought to modulate immune response (Figure 57). Several studies report that HBV components may induce dysfunction of immune cell with the assistance of the exosomes (R. Chen et al., 2017; Kakizaki et al., 2018; Shi et al., 2019; Y. Yang et al., 2017). For example, exosomes derived from HBV infected cells can be endocytosed by monocytes and results in the increase of PDL1, which inhibits the activation of the T cells by repressing CD69 (Kakizaki et al., 2018). In addition, exosomes derived from serum of CHB patients target NK cells by TGF-β pathway and consequently decrease NK cells proliferation and stability but also inhibit the production of IFN-γ (Y. Yang et al., 2017)

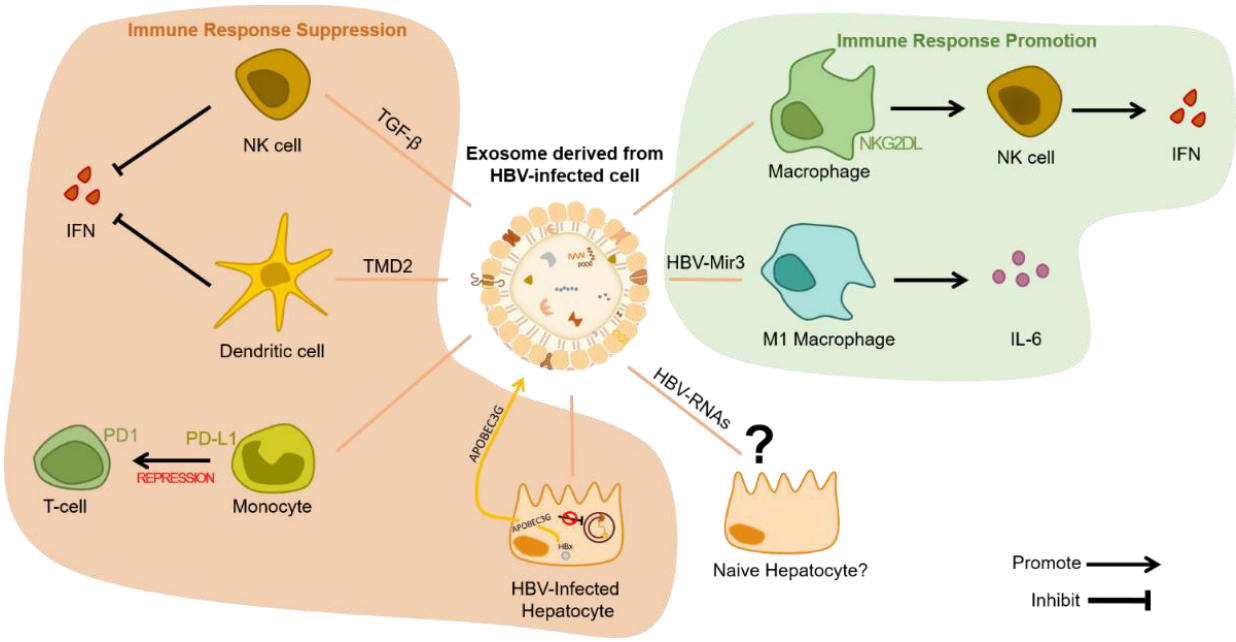

Figure 57. *Exosome have a dual effect on the modulation of antiviral response. I) HBV-associated exosomes may create an immune tolerant microenvironment that favors HBV survival and replication by preventing the innate antiviral immune responses (Orange) or ii) exosomes promote the adaptive antiviral immune responses by activating macrophages and transfer antiviral materials to hepatocytes to enhance the immune response (green). NK cell, natural killer cell; DCs, dendritic cells; IFN, interferon; IL-6, interleukin-6; APOBEC3G, apolipoprotein B messenger RNA-editing enzyme catalytic polypeptide-like 3G; PD-1, programmed-death protein 1; PD-L1, programmed death-ligand 1; NKG2DL, NKG2D ligands; rc DNA, relaxed circular DNA; TMD2, transmembrane protein 2.*

In contrast with the previously mentioned effect of exosomes derived from HBV infected hepatocytes on the immune system, it was also observed that these exosomes could be able to promote immune response against HBV. Indeed, exosome derived from HBV infected hepatocytes are able to increase NKG2D on macrophages and induce NK cells to produce IFNγ, which will inhibit early steps of HBV replication (Kouwaki et al., 2016). In addition, miR-3 is a micro RNA that is encoded by HBV and harbors antiviral effect. miR-3 was detected in exosomes and is thought to help the polarization of liver macrophages towards M1 phenotype to release IL6, a pro inflammatory and antiviral cytokine (Y. Yang et al., 2017).

In the future, it could be interesting to incubate HBV-RNAs containing exosomes treated or not with antiviral drugs with different immune cell types such as Kupffer cells, dendritic cells, etc. and observe their cytokine secretome. Since exosomes derived from HBV-infected cell were shown to carry genetic material but also presumably HBV proteins, they could play the role of antigen presenting cells on immune cells to generate immune response in favor of the host or the virus.

2. Are exosome derived from HBV-infected hepatocyte able to generate de novo infection on naïve hepatocytes?

In recent years, increasing evidence has shown that HBV utilizes exosomes to greatly improve its transmission efficiency, although the direct role of the population of exosome derived from infected hepatocytes and carrying HBV genetic material is still unclear.

Recently, two studies have been published on this subject. First, Sanada and al. isolated exosomes by differential ultracentrifugation from HBV infected PXB cells, which are human primary hepatocytes isolated from liver-humanized mice (Sanada et al., 2017). They recovered three different fractions and incubated these fractions with or without neutralizing antibodies from serum of HBV-vaccinated patients on naïve PBX-cells. Finally, they measured intracellular HBV-DNA. They were able to detect HBV-DNA in naïve hepatocytes, in presence of neutralizing antibodies suggesting that while inhibiting virions DNA transmission, other particles are able to transmit HBV DNA. However, vaccination triggers only the production of anti-HBs antibodies and not anti-HBc suggesting that NCs could still infect naïve cells.

Then, a similar study was performed recently by the team of U. Prozter (Jung et al., 2020). They purified exosomes from infected patient's serum by size exclusion chromatography followed by affinity-based purification with anti-HBs antibodies. They incubated HepG2-NTCP naïve or infected cells with these EVs and measured HBeAg secretion 5 days post infection. They claimed that naïve cells were infected by these EVs, however, once again, NCs were not withdrawn from the serum. Therefore, residual NCs containing HBV DNA could be responsible for HBV infection. A purification combining anti-HBs and anti-HBc antibodies should have been a better strategy, allowing the clear purification of HBV derived exosomes. It is also important to note that this time, EVs were coming from patient's serum so they were not only infected hepatocytes derived exosomes.

In our study, we showed more specifically that HBV-RNAs were also detected in exosomes, then we wondered if the specific presence of HBV-RNAs could have a role during infection. Packaging of viral RNA within exosomes was also detected in other studies. HCV (Bukong et al., 2014), Epstein-Barr Virus (EBV) (Baglio et al., 2016), Rift Valley Fever Virus (Ahsan et al., 2016) and HIV-1 (Sampey et al., 2016) RNA are packaged within exosomes. An accumulating body of evidence demonstrates that EVs released from virus-infected cells transfer viral RNAs to recipient cells including DCs and macrophages, thereby inducing innate immune responses. In addition, we could think that the presence of viral RNAs such as HBx mRNA could have a role in the dissemination of HBV. Indeed, presentation of viral RNA, DNA or proteins to naïve hepatocytes could prepare the cells for future infection to increase the yield of infected hepatocytes in the liver. Moreover, pgRNA contained in exosomes could increase pgRNA pool in hepatocytes to increase infection or create de novo infection.

In this regard, we tried to test the infectivity potential only of exosomes containing only HBV-RNAs. To this aim, we tested several cellular models such as long-term NA-treated HepAD38 or HBV-RNA producing cell line (data not shown); however, remnant DNA was present in both models, thus preventing their use for such experiments. The best way to study this phenomenon would be to produce synthetic viral particles or exosomes containing pgRNA and viral mRNAs and assess whether they would be able to enter uninfected cells and launch neo-cccDNA formation.

Unfortunately, at this time, it is technically too difficult to isolate pure HBV-RNAs exosome and thus discriminate if a new infection would be triggered by viral DNA or RNA. As a consequence, we decided to restrict our efforts in investigating the ability of exosomes

enriched in HBV-RNAs to enter non-infected cells. HepG2-NTCP and HepG2-WT cells were incubated for 30 min, 2 h or 16 h with either F4 or F7 of concentrated supernatant from 3TC-treated HepAD38 cells or from a cell line producing HBV RNA due to a block in retro transcription in the presence or not of the entry inhibitor Myrcludex. Our read out was to detect HBV-DNA and HBV-RNAs directly after the incubation. Unfortunately, this preliminary study was not conclusive.

3. Role of exosomes derived from HBV-infected cells in the pathogenesis of liver disease

It has been demonstrated that exosomes serve an important role in the formation and progression of tumors, with anti-apoptotic effects in malignant cancer (Kawakubo-Yasukochi et al., 2018; Oushy et al., 2018). Exosomes are involved in the occurrence, development, and metastasis of tumors, including HCC (W. Liu et al., 2015).

Exosomes are also known to shuttle miRNA. Interestingly, an increase of miR-122 was shown to favor the development of HBV related HCC (A. Li et al., 2019), furthermore, this miRNA is known to be associated to liver exosomes (Sohn et al., 2015). Regarding these studies, we could think that exosomes could be involved in this process.

In 2013, Bayliss et al. showed that quantitative changes in circulating splice variants of HBV transcripts were correlated with the occurrence of HCC (Bayliss et al., 2013). Indeed, a double spliced variant, sp10, was isolated from the serum of a patient with HCC and reported to increase HBV replication *in vitro* (Ma et al., 2009). Since increased HBV replication is a major risk factor for development of HCC (Chan et al., 2008), the presence of SP10 is thought to enhance carcinogenesis. Our 5'RACE results showed that spliced pgRNA was carried by exosomes from HBV-infected hepatocytes an in the serum pf CHB patients' (Stadelmayer et al, 2020 and Appendix 1), then we cannot exclude that these spliced RNAs transported by exosomes might play a role in the development of HBV-induced HCC. In addition, Nanopore Long Read Sequencing will help us determining precisely which spliced isoform is present in the exosomes. Since spliced isoforms were identified in both VLPs and exosomes, a comparison of which spliced isoform is present in each particle type would be interesting.

With more research conducted on exosomes, it is believed that exosomes could be successfully used in clinical diagnosis of early stage HCC in near future.

VI. Heterogeneity of extracellular HBV-RNA species and effect of NA treatment

We reported the presence of HBx transcripts of different lengths in NCs and VLPs but also in exosomes; however, their physiological role remains to be determined. This observation was also reported by Lam et al. which demonstrated that HBV-RNAs were mainly carried by NCs and are of heterogeneous lengths, ranging from full-length pgRNA to a few hundred nucleotides (Lam et al., 2017). Interestingly, none of the studies conducted on circulating HBV-RNAs reported the presence of extracellular HBs mRNA.

Moreover, we also observed 3'end truncation of the RNAs associated to VLPs but not NCs or exosomes with NAs. This difference could be explained by the presence of the viral polymerase which could induce the early truncation of pgRNA. Quetier and colleagues, showed that the expression of HBx protein translated from 3' truncated HBx mRNA led to a more rapid onset of HCC than did the full length one. It could be assumed that the expression of truncated forms of HBx may facilitate cell transformation by accelerating the initiation step of carcinogenesis (Quetier et al., 2015). We also identified shorter pgRNA species that could either be pgRNA splicing variants and/or pgRNA with 3' end truncation. 3'end truncation is thought to be induced by NAs treatment (Shen et al., 2020a) and could explain the replication deficiency of progeny virus produced under NAs treatment as particles produced from NAs treated patients fail to produce de novo infection (Y. Liu et al., 2020). Interestingly enough, our ddPCR data failed to found 3' truncated RNAs in exosomes or naked capsids, suggesting that this phenomenon would be specifically associated with RNA packaging into virions.

VII. HBV-RNAs in exosomes as non-invasive biomarker for HBV infection

Knowledge about the physical entities in which HBV-RNAs are contained could inform on their stability in the circulation and by extent after sampling for routine analysis. Indeed, being packed into viral or non-viral particles could prevent from nucleases digestion and enhance their stability. If circulating HBV-RNAs are stable, automated assay and processing could be easier with more flexible storage conditions.

In the frame of the scientific objectives of the CirB-RNA RHU program, a post-doc in the laboratory, Dr. D. Kim, performed similar experiments in serum from CHB patients. His

results demonstrated that circulating HBV-RNAs distribution in serum of patients was overall similar to the one described in supernatant from infected cells with slight differences. A joint manuscript gathering in vitro and in vivo data is in preparation and can be found in Appendix 1. In serum, HBV-RNAs are contained in VLPs but also in low-density fractions, corresponding to exosomes. Yet, unlike in vitro model, only few RNAs where found in NCs. In 2018, Bai and colleagues hypothesized that due to their strong immunogenicity, NCs rather form immune complexes with specific anti-HBcAg antibodies than circulate as free particles (Bai et al., 2018). Besides, they did not observe major differences in the abundance of RNA in NCs fractions in HepAD38 supernatant compared to CHB patient's serum, contrary to our observations. We hypothesized that the fast turnover of NCs in the bloodstream could be responsible for this difference and that NCs secretion and content could depend on the infection stage of the disease. Indeed, it would be interesting to study the correlation between NCs quantities and anti-HBc antibodies in the serum of the patients.

Interestingly, we also observed that in the case of patient with low HBs or non-detectable HBs levels, there is a shift of the RNA contained in the virions fractions towards the exosomes associated fractions. These results suggested that in absence of HBs, VLPs could be replaced by non-viral particles such as exosomes for HBV-RNAs secretion. This observation comforted us in the fact that even if F4 was composed by both exosomes and sub viral particles, in the absence of SVPs (because undetectable levels of HBsAg), HBV-RNAs are still incorporated in exosomes, if not even more. Finally, we got access to serum from the same patients before and after NAs treatment. This follow up study showed that the proportion of HBV-RNAs in exosomes was increasing at the expense of the one in the VLPs 6-months and 1-year after treatment onset, suggesting a dynamic in the secretion of HBV-RNAs that could be affected by antiviral drugs.

Several studies were conducted to identify which circulating HBV-RNAs species are found in patient's serum. Although the discrepancy among different studies might be due to the variable specificity and/or sensitivity of different assays, it seems that the detected serum HBV-RNA sequences from CHB patients are predominantly derived from pgRNA ((Bai et al., 2018; Jansen et al., 2016b; Prakash et al., 2020b; Stadelmayer et al., 2020). Similarly, in the study conducted by Dr D.Kim on a cohort of serum from CHB patients, he also observed the presence of pgRNA and spliced variants derived from pgRNA in the fractions corresponding to VLPs, NCs and exosomes. pgRNA and spliced variants will be

sequenced by Nanopore long read sequencing technology to get a deeper characterization of these RNA species. In addition, HBx mRNA were also identified in patient's serum (Kapoor et al., 2017; Niu et al., 2017; Stadelmayer et al., 2020), fact that was also observed in our study. Indeed, HBX transcript of length ranking from 400 to 1000 nucleotides were identified in the serum of patients. While we did not observe any obvious difference in the RNAs species across the different EVs (VLPs, NCs or exosomes) by 5'RACE in the same patient, some differences were found across patients belonging to different CHB phases or under treatment. For example, HBx mRNA was not detected in the serum derived from NAs treated patients or from inactive carriers. This strongly suggest the need of better characterizing circulating RNA species in CHB patients and correlate them with intrahepatic cccDNA pool and transcriptional activity, disease stage and response to treatment.

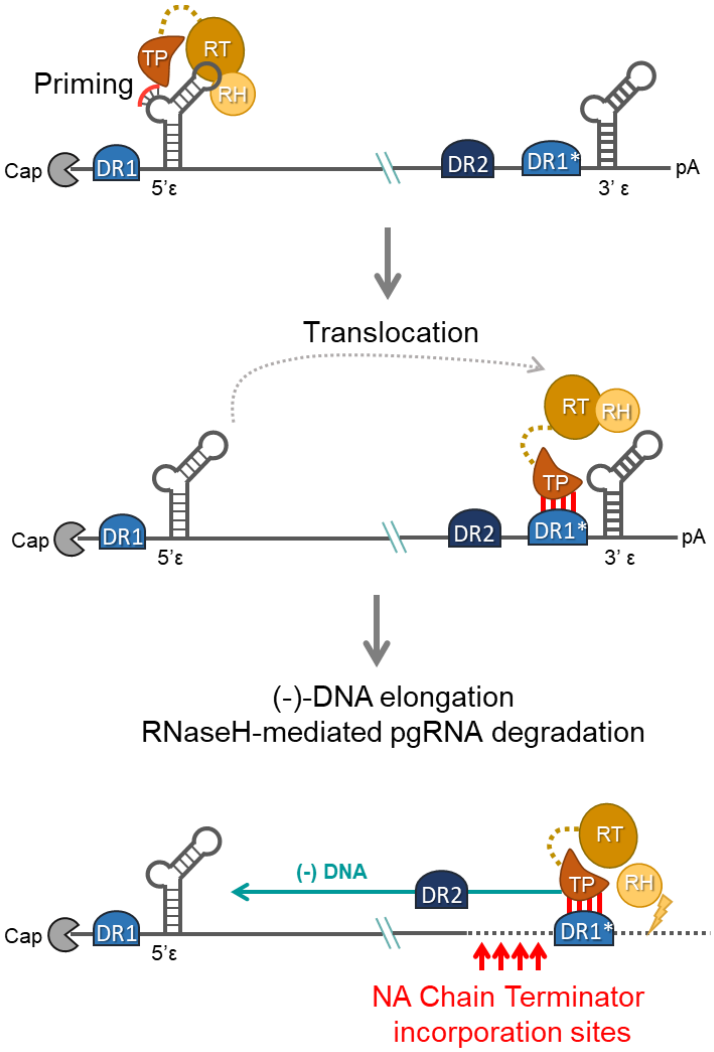

Figure 58. Proposed model for pgRNA 3'truncation.

Then, a critical question that needs to be answered is whether the serum HBV-RNAs are full-length or 3'truncated. This was impossible to determine using by 5'RACE, so it would be interesting to study the termination of HBV-RNAs in the serum of patients by ddPCR or perform direct RNA long read sequencing. As recently suggested by Shen et al. (Shen et al., 2020a) and reported in supernatant from HepG2-NTCP cells, NAs treatment could induce an early truncation of HBV-RNAs in VLPs. They attribute this phenomenon to the degradation of viral RNA catalyzed by the RNaseH activity of HBV polymerase during minus strand DNA synthesis. The incorporation of NAs into the growing minus strand DNA terminates DNA synthesis and also blocks RNaseH-mediated degradation of pgRNA. However, since NAs do not efficiently block minus strand DNA synthesis at the early stage, this could give rise to truncated pgRNA with 3' ends located between DR1 and DR2 or even upstream of DR2 (Figure 58).

In the future, it would be interesting to study the correlation between HBV-RNAs contained in exosomes, specifically isolated from virions, and intrahepatic cccDNA. The effect of different drugs such as NAs or Capsid Assembly Modulators (CAMs) should also be studied. However, using specifically exosome containing HBV-RNAs as a biomarker could introduce a limitation because in cell supernatant, HBV-RNAs in exosome only represents 15 % of the total quantity of secreted HBV-RNAs. As a result, if HBV-RNAs quantities are low, they could be even lower and hamper the detection of HBV-RNAs in low viremia infection. In addition, the kinetics of the release of HBV-RNAs in exosomes must be studied. Indeed, our studies were done in short infection kinetics with only 4-days of NAs treatment. This treatment duration could explain that we poorly observed a shift in the distribution of HBV-RNAs towards exosomes compared to the one in patients' serum after 1-year of tenofovir treatment. In the future, finding a model to study the effect of long-term treatment on exosome derived from HBV-infected hepatocytes could be interesting even though we observed significant changes in the exosome associated proteins secretion profile after only 8-days of infection.

Given that NAs have no or little effect on the transcription of cccDNA, it is possible that viral RNAs may be continuously produced in infected hepatocytes, even if HBV DNA is undetectable. Detection of HBV-RNAS, in particular pgRNA, in cell supernatant and patient's serum may reflect the presence and active transcription of cccDNA in the liver of patients. However, we observed that the proportion of HBV-RNAs in VLPs or NCs could be decreased in long-term NAs treated patients in favor of to the one associated with

exosomes. In this respect, we could think that in case of NA therapy, the presence of HBV-RNAs in exosomes could be a better predictive biomarker informing on the transcriptional state of cccDNA and by extent helping to decide the safe discontinuation of NA-therapy.

Finally, exosomes are found in various body fluids including plasma, semen, urine, amniotic fluid and saliva. It could be interesting to isolate exosomes from different fluids such as urine, for which the sampling is non-invasive and gives access to high quantities and check the presence of viral nucleic acids. Indeed, reports already suggests the presence of HBV-DNA in urine of CHB patients (Jain et al., 2018).

VIII. Perspectives

Accumulating and processing of huge amount of infected cell supernatant took a long time. It took us some time to set up the density gradient separation protocol, however, this protocol does not allow a strict separation of the exosomes and subviral particles. To overcome this problem, we could think of two different strategies. First, FR 1 to 6 which are composed by exosomes and SVPs could be pelleted altogether. This pellet could be layered on a similar density gradient but this time with different percentages of Iodixanol and sucrose. Indeed, inspired by a study published about HIV and exosomes, we could make a gradient with concentration ranking from 8 to 12% of Iodixanol in order to get a more resolute gradient that could probably more segregate between SVPs and exosomes. However, the inconvenient of this method is that we could lose material by adding concentration step and a new gradient but also that it will induce a repartition of the exosomes across the gradient. More precisely, as mentioned in the introduction, exosomes are heterogeneous and could be separated in different population. This gradient could induce the separation of the different categories of exosomes according to their size and density and the global exosome information could be lost. Moreover, infection levels must be high because this segregation implies that we split the F1 to F6 in up to 12 fractions so the RNAs amount in fractions will be twice lower. The other option would be to combine an immune-capture protocol with the gradient approach. Indeed, recently, Jung et. al. published a method paper that could allow the depletion of HBs particles from serum of HBV infected patients. They use a SEC columns follow by an immune-affinity base purification using anti-HBs antibodies. They claim that the remaining particles in the serum are exosomes, however, they did not remove the naked capsids from their samples. But if this experiment is done from the light fractions that contain both exosomes and SVPs but no HBc, the remaining eluate should only be composed by exosomes. Indeed, we detected

only few amounts of HBc peptides which should be interpret with caution because it could be contamination by VLPs or residual HBeAg rather than true incorporation of HBc in exosomes. Another approach would be to directly isolate exosomes from concentrated supernatant before gradient or after gradient on F1 to F6. Antibodies against common markers for exosomes could be used to capture exosomes with magnetic beads. However, a mixture of different exosomes markers has to be used to prevent the isolation of a specific exosome population unless we want to study separately CD63-, CD81- or CD9-exosomes. This experiment is faster than the previous one but request a constant monitoring of efficacy controls. At any rate, those hypotheses must be tested to clearly isolate exosomes from subviral particles and also eliminate the possibility of a contamination by virions in those fractions.

Regarding our mass spectrometry analysis, a deeper analysis will be needed to select candidate proteins that could play a crucial role: i) either in the shuttle of HBV-RNAs in exosomes, ii) or in HBV pathogenesis. Detailed analysis allowed us to identify proteins for which the secretion was highly modified by HBV infection, yet validation of this observation either by WB or siRNA approaches will be needed in the future.

Another criticism would be on the technology that was used long read RNA sequencing. Indeed, RNA was retrotranscribed by HBV specific primers or random primers. For 5'RACE experiments, gene specific primers were used, located in the 3' end of RNA transcripts. The inconvenient of this approach is that the 3'end of the RNA are not sequenced. We could have complemented 5'RACE by 3'RACE sequencing in order to get more information of the termination of HBV RNAs even though it won't allow to have a full sequence of the same transcript. However, direct RNA sequencing is also possible with Nanopore long read sequencing technology. This approach allows to prevent the efficacy bias of the reverse transcriptase but also to get a full information on HBV RNA sequence from 5' to 3' end. This approach will be done in the future and will give us all the information's about the nature of the transcripts, their termination but also the post transcriptional event such as methylations. The inconvenient of this technic is that as we don't amplify RNA into cDNA, we have to work in consequent RNA starting quantities.

To complete our observations before doing direct RNA sequencing and to get a quantification of the transcripts, I designed a ddPCR assay specific for the different viral RNA. Since it is accepted that RT-qPCR is preferred for the detection of circulating HBV-RNAs (Limothai et al., 2020; D. Yang et al., 2018), this technology may represent an ideal

assay for measuring serum HBV RNA levels in research and clinical practice. Quantification of different HBV-RNAs species may be done by northern blot, but this technique is insufficiently sensitive for analysis of small quantities. Alternatively, qPCR assays that target specific parts of the genome may be used. However, a limitation of this strategy is related to overlapping HBV transcripts; for example, an assay that targets the X region unavoidably measures all the different RNA species. Another limitation is that amplification efficiencies may bias the comparison if the RNA levels are assessed by assays, such as real-time PCR, that rely on threshold cycle (Ct) values for quantification. By using an absolute quantification technique, such as ddPCR, this problem can be overcome. Prakash and Colleagues were the first to study HBV RNA in liver tissue by using ddPCR targeting several segments of the genome. They obtained an RNA profile similar to that obtained by RNA sequencing and allows analysis of correlations between the levels of different RNA species (Prakash et al., 2020b). We used a similar approach but we targeted different regions of the genome. Assay targeting the 5' and the 3' extremities of the genome were conclusive and ready to use for routine experiments and test on patient's serum.

In conclusion, our study was the first to give in depth characterization of the association between extracellular HBV-RNAs and exosomes. In concordance with the literature, it seems that exosomes play an important role in viral infection, even if research on the roles of exosomes in HBV replication and hepatitis B infection is still in an early stage. A more extensive and in-depth understanding of the interplay of exosomes and HBV is needed to get more insights on their clinical significance for use as a potential biomarker.

MATERIAL & METHODS

Cellular Culture and Infection Protocol

Cell culture and Infection

The HepG2-NTCP cell line was a kind gift of Dr S. Urban (Heidelberg University, Germany). HepG2-NTCP cells were seeded at 105 cells/cm2 in DMEM medium supplemented with 1% penicillin/streptomycin (Life Technology), 1% sodium pyruvate (Life Technology), 1% glutamine (Life Technology), 5% Fetal Calf Serum (FCS; Cytiva Sérum HyClone™ FetalClone™ II). The day after, medium was renewed and complemented with 2.5% DMSO (SIGMA). After 72h, cells were infected at a multiplicity of infection of 250 in the presence of 4% PEG800 for 16h and then extensively washed with PBS and maintained in complete DMEM medium containing 2.5% DMSO until harvesting (Figure S1A). Non-infected (N.I.) control cells were incubated with 4%PEG800 for 16h without HBV inoculum.

To obtain the infectious inoculum, HBV particles were concentrated (approximately 100-fold) from the supernatant of HepAD38 (genotype ayw) cells by filtering and PEG precipitation (REF). The HepAD38 cell line was a kind gift of Dr C. Seeger (Fox Chase Cancer Center, Philadelphia, USA).

Cell Culture & Preparation of MS samples

Three days after HBV infection cells were treated or not with lamivudine at 10µM with DMEM medium containing 2.5% DMSO and exosome depleted SVF. The exosome depleted SVF was obtained after 2h of full speed ultracentrifugation. Two days after, cells were treated again and wash 3 times with PBS. Medium without SVF was adeed to prevent any contamination by bovine exosomes. Cell viability was measured by Propidium Iodide (FluoroPure™ Grade, Invitrogen) staining in Flow Cytometry (BD FACSCalibur, BD Biosciences) (Fig. S1.B).

PHH Isolation and infection

Primary human hepatocytes (PHHs) were isolated from surgical liver resections as previously described (LeCluyse and Alexandre, 2010) after informed consent of patients and plated in complete William's supplemented with 1% penicillin/streptomycin (Life Technology), 1% glutamine (Life Technology), 5 µg/ml Human insulin (Sigma-Aldrich), 25

µg/mL Hydrocortisone hemisuccinate UPJOHN (SERB), and 5% Fetal Calf Serum (FCS; Cytiva Sérum HyClone™ FetalClone™ II). PHH were maintained in William's medium supplemented with 1.8% DMSO (Sigma, St Quentin, France) and infected within 72h post-plating according to the experimental timeline in Figure S1A. Non-infected (N.I.) control cells were incubated with 4%PEG800 for 16h without HBV inoculum.

Drug treatments of culture hepatocytes

10 µM lamivudine (Sigma Aldrich) was added to cell cultures as detailed in Figure S1A. To modulate exosome secretion three drugs were used: GW4869 (Sigma Aldrich), Manumycin A (Sigma Aldrich) and Ethanol (Normapur, VWR) according to the experimental timeline shown in Figure S1A. Specific concentrations are indicated in each figure of the Results section.

EV isolation

100ml to 1liter of culture supernatants were collected and centrifuged at 1500 ×g for 15 min at room temperature. To thoroughly remove cellular debris, the supernatants were filtered through a 0.22 µm filter (Merck Millipore, KGaA, Darmstadt, Germany). For EV concentration, filtered supernatant was purified using Amicon® Pro Purification System with 100kDa filter. Nest, for EV preparation, the concentrated supernatants were ultracentrifuged at 110,000 ×g for 2h at 4˚C. The pellets were then washed with 8 mL of PBS to remove contaminant proteins and ultracentrifuged again at 110,000 ×g for 2h at 4˚C.

Density Gradient

EV pellets were resuspended in 2.5 mL of 10% iodixanol solution. 10%, 20%, 30% and 40% iodixanol solutions were prepared by mixing Optiprep™ (Axis Shield) with buffer containing 0.25 M sucrose, 10 mM Tris at pH 8.0, and 1 mM EDTA, with a final pH set of 7.4. Resuspended EVs were layered on the top of the gradient and then subjected to ultracentrifugation in a SW41-Ti Rotor tube (Beckman) for 6 hours at 4˚C at 110.000 ×g. Twelve fractions of 1ml were recovered and analyzed separately.

Intracellular DNA and RNA Quantification

DNA and RNA Extraction

Intracellular accumulation of viral RNA and DNA was monitored by RT-qPCR and qPCR, respectively. Total DNA and RNA was purified from infected cells using MasterPure™ Complete DNA Purification Kit (Epicentre) and resuspended in RNase free water. RNA-containing eluates were digested with DNase 1 (RQ1 RNase-Free DNase (Promega) and retro-transcribed into cDNA using SuperScript IV Vilo (SuperScript™ IV VILO™ Master Mix) according to manufacturer's instructions (Invitrogen, Carlsbad, USA)

qPCR and RT-qPCR

cccDNA was quantified after ExoI + ExoIII endonuclease (Epicentre) digestion of total extracted DNA for 2 hours at 37 °C, followed by 20 minutes inactivation at 80 °C. Real-time qPCR for total HBV RNA/DNA and cccDNA was performed using an Applied QuantStudio 7 machine (BioSystem) and TaqMan Advanced Fast Master Mix (primers and probes sequences and concentration in the PCR reaction are listed in Table S1 and S2). Serial dilutions of a plasmid containing an HBV monomer (pHBV-EcoR1) served as quantification standard for HBV DNA and cccDNA. The number of cellular genomes was determined by using the β-globin gene kit (Roche Diagnostics, Manheim, Germany). RT-qPCR were analyzed using the ΔΔCt method, where ΔCt = Ct (target) − Ct (GUS), where GUS is the housekeeping gene used as internal normalizer.

ELISA for viral antigens

Supernatants were diluted 10 times in culture medium and gradient fractions were diluted 100 to 1000 times in PBS prior to ELISA. ELISA tests for HBeAg and HBsAg detection in cell supernatants were performed according to the manufacturer's protocol using the CLIA kits from Autobio Diagnostic.

Extracellular DNA and RNA Quantification

DNA and RNA Extraction

Viral nucleic acids were extracted from 200µl of whole cells supernatant or gradient fractions using QiAmp MinElute Virus spin kit (Qiagen, Germany). RNA was digested with DNase 1 (RQ1 RNase-Free DNase (Promega) and retro-transcribed into cDNA using SuperScript IV Vilo (SuperScript™ IV VILO™ Master Mix) according to manufacturer's

instructions (Invitrogen, Carlsbad, USA). To ensure that DNA was completely digested and that RNA was exclusively measured, a control without reverse transcriptase enzyme was performed in each experiment.

Droplet Digital PCR (ddPCR)

Extracellular HBV-DNA and RNA were quantified using ddPCR platform (QX200; Bio-Rad). A total of 22 µL reaction mixture included 11 µL of 2X ddPCR Supermix (Bio-Rad), 1.1µl of primers and probe 20X premix, 5µl of DNA or cDNA and 4.9 µL of water. Primers and probe premix contains 500nm of forward and reverse primers and 200nm of Taqman probe. The sequences of primers and probes were the same used in qPCR (Table S1). For each ddPCR reaction mixture, 18 µL of droplet generation oil was added to the cartridge and the droplets were produced by a droplet automated generator of the QX200 Droplet Digital PCR system (Bio-Rad). The droplets were then transferred to a 96-well PCR plate for amplification using the C100 Touch Thermal Cycler (Bio-Rad) according to the following amplification protocol: one cycle at 95°C for 10 minutes, 40 cycles at 94°C for 30 seconds and 60°C for 1 minute and one step at 98°C for 10 minutes. Subsequently, a droplet reader was used to quantify the number of both positive and negative droplet events from each PCR reaction mixture. The absolute concentration of template was calculated by QuantaSoft analysis software (Bio-Rad) by calculating the ratio of the positive droplets over the total droplets combined with Poisson distribution. For samples with HBV DNA or RNA levels higher than 10^6 copies, the appropriate dilutions of DNA or cDNA template were performed.

ddPCR Specific RNA Assay

Design

Specific primers and probes were designed to target specific regions of the 3' extremity of HBV-RNAs. The regions that are target are illustrated in Fig.14 and primers and probes are listed in table S1. Different steps of validation of specificity and efficiency of the assays were performed:

1. Primer sets were validated in SYBR Green qPCR by assessing linearity and specificity on an HBV linearized plasmid (Fig. S2)
2. Primers and Taqman probes assays linearity was verified in ddPCR on serial dilution of HBV-linearized plasmid (Fig S3).

3. RNA from supernatant of HepAD38 cells were quantified by Taqman qPCR using the different primer and probe sets and migrated on an agarose gel (1%) (Fig S4) before Sanger sequencing of the products (data not shown).
4. Finally, primer and probe sets were tested on RNA extracted from infected HepG2-NTCP or PHH in three indipendent replicates (Fig S5).

Statistical Analysis

When possible, functional analysis of differential viral parameters was performed using non-parametric student t-test (Wilcoxon) in Prism 7 software (Graphpad).

Transmission Electron Microscopy (TEM)

For TEM analysis, 500µl of selected fractions were diluted in 10ml of PBS and ultracentrifuged at 110.000 x g for 2 hours. Pellet was washed with PBS and centrifuged again. Finally, EVs pellet was resuspended in 20µl of PBS and fixed with 4% of paraformaldehyde (PFA) and 10µl was adsorbed on 200 Mesh nickel grids coated with formar-C. Immunogold labeling was performed by flotation of grids on drops of reactive media. Non-specific sites were coated with 1% BSA in 50 mM Tris–HCL, pH 7.4 for 10 min at RT. Antibody incubation was carried out for 4 hours at 4°C in a wet chamber with mouse monoclonal antibody raised against CD9 or HBs (see Table S3) (dilution 1/50) in 1%BSA, 50 mM Tris–HCL, pH 7.4. Grids were successively washed once in 50 mM Tris–HCL, pH 7.4 and pH 8.2 at RT. They were then preincubated with 1% BSA in 50 mM Tris–HCL, pH 8.2 for 10 min at RT and labeled with a goat anti mouse IgG gold-conjugated 10 nm, (Tebu bio, France) diluted 1/80 in 1% BSA-, 50 mM Tris–HCL, pH 8.2 in a wet chamber for 45 min. Grids were successively washed once in 50 mM Tris–HCL, pH 8.2 then pH 7.4 and once in filtrated distilled water at RT. Grids were then floated on top of drops of silver enhancement mixture (Aurion R-GENT SE –EM) for 30 min. After washing once in filtrated ultra-pure water, suspensions were colored with 2% phosphotunstic acid for 2 min and examined using a JEM Jeol 1400 transmission electron microscope (Tokyo, Japan) equipped with a Orius 600 camera (USA). Particle sizes were determined with the Digital Micrograph software.

Western Blot

16µl of each fraction obtained from density gradient were mixed with Laemmli buffer and heat at 95°C for 5min. 20µl of proteins were migrated in 4-20% mini-PROTEAN@ TGX stain-

FreeTM Precast Gel (Bio-Rab Laboratories) and transferred onto a nitrocellulose membrane (Bio-Rab Laboratories). Membranes were blocked 1 hour with 5% milk or BSA (Sigma) in TBS (1 x Tris Buffer Saline (Sigma)) and stained with primary antibodies in blocking buffer overnight at 4 °C (see Table S3). After primary antibody incubation, membranes were washed 3 times with TBS-T 0.1% (1X TBS with 0.1% Tween 20), stained with HRP-conjugated secondary antibodies (1/50000) for 1 hour at room temperature and washed again 3 times with TBS-T 0.1%. The detection was done using Clarity or Clarity Max Western ECL and the ChemiDoc XRS system (Biorad).

Nano Tracking Analysis (NTA)

100ml of supernatant from non-infected, HBV-infected or infected and 3TC treated HepG2-NTCP cells was accumulated and processed as shown in Figure S1A and subjected to density gradient ultracentrifugation as described above. 1ml of each fraction was fixed for 20min at RT with 4%PFA and EVs were pelleted by ultracentrifugation at 110.000 x g for 2h and resuspended in PBS. For NTA analysis, EVs were diluted 20 times in PBS. Approximately 0.3 ml supernatant was loaded into the sample chamber of an LM10 unit (Nanosight, Amesbury, UK) and three videos of 30 seconds were recorded of each sample. Data analysis was performed with NTA software (NTA 3.4 Build 3.4.003, Nanosight) on Nanosight NS300 (Malvern). Software settings for capture were: Camera level: 14; Temperature: 25 °C, Viscosity: 1.0 cP and syringe pump speed: 100. Software settings for analysis were: Detection Threshold: 13; Blur: auto; Minimum expected particle size: 50 nm. The data obtained are presented as the average and standard deviation of the three video recordings for each replicate. The experiment was repeated in three independent HepG2-NTCP batches.

MNase digestion of HepAD38 supernatants

To digest free viral DNA and RNA, we performed MNase (Micrococcal Nuclease) digestion of the material obtained after density gradient ultracentrifugation of HeAD38 cell supernatant 7 days after plating. Supernatant was proceed as described in “EV isolation” and “Density Gradient” section. MNase is a DNA and RNA endonuclease that degrades double and single-stranded DNA and RNA. MNase buffer and 2µg of non-relevant plasmid (pcDNA6 vector + insert) was added to monitor digestion efficiency. MNase digestion was performed for 20 min at 37 °C using 2000 gel units (New England Biolabs) in a 200µl

reaction. Reactions were stopped by Trizol and nucleic acids were extracted and quantified by ddPCR as detailed before.

5'RACE and Nanopore Long Read Sequencing

5'RACE

5'RACE was performed as previously described in (Stadelmayer et al., 2020). Briefly, RNAs were isolated using a guanidinium thiocyanate–phenol–chloroform extraction protocol (TRI reagent (Sigma)). 5'RACE was essentially performed as described in the GeneRacer Kit manual (ThermoFisher Scientific) except Tobacco Acid Pyrophosphatase was substituted by RNA 5' Pyrophosphohydrolase (New England Biolabs) and SuperScript reverse transcriptase III by SuperScript reverse transcriptase IV (ThermoFisher Scientific). The reverse transcription reaction was performed using 3' HBV specific Gsp1 primer 5'-TTAGGCAGAGGTGAAAAAAGTTG-3'. For the 5'RACE PCR reaction Platinum™ SuperFi™ DNA Polymerase (ThermoFisher Scientific), GeneRacer 5' primer and HBV specific nested primer Gsp2 5'-AGCGTAATCTGGAACATCGTAATGGGTA-3' were used. 5'RACE PCR was run in a C100 Touch thermocycler (Biorad) using the following touch down PCR program: Initial denaturation step 98°C 3 min >5x (98°C 10 s; 72°C 3 min) >5x (98°C 10 s; 70°C 3 min) >25x (98°C 10 s; 64,4 20 s; 72°C 3min) >72°C 10min.

Oxford Nanopore Technology (ONT) MinION DNA sequencing of 5'RACE products

Products of 5'RACE PCR amplification performed with Platinum™ Taq DNA Polymerase High Fidelity (Invitrogen) were prepared for ONT MinION Sequencing using SQK-PBK004 kit, according to the manufacturer's instructions. Analysis was performed similarly to (Pertea et al., 2016) combining HISAT, StringTie and gtf compare tools. Sequences were aligned to a reference HBV genome, corresponding to full-length genome starting at forward PCR primer (position 1814).

Mass spectrometry (MS)-based quantitative proteomics

Preparation of samples - Pilot study

Before sending samples to MS analysis, a pilot study was performed to evaluate the experimental feasibility. Four independent experiments were conducted in HepG2-NTCP cells and processed as described above (Figure S1 and Density Gradient section). The results of this pilot study are recapitulated in Fig. S6. A validation step is crucial to ensure the purity and the quality of the sample before sending more replicates. The MS results

indicated that the samples were indeed enriched in exosomes associated proteins and few cellular or exogenous contaminants were present. However, we were around the limit of detection for most of the proteins, so we increased the quantity of supernatant from 250ml per condition to 1L per condition.

Silver Staining

To ensure that protein was sufficient to be sent to analysis, proteins were quantified by silver staining. Gels were silver-stained according to manufacturer protocol (Silver Quest Staining Kit; Invitrogen). The image of the gels for pilot study (Fig.S6) and the study presented in results parts (Fig.S7) are shown in supplementary figures.

Adjustment of protein quantities

Proteins bands intensity from silver-stained gels were quantified by Fiji Software. Sample volume was adjusted among the replicated to get the closer protein quantity as possible between the different conditions and the replicates. For a reason of quantity homogeneity, one of the four replicates was excluded and F7 and F8 to F10 were not analyzed in mass spectrometry (Table 4).

The proteins were solubilized in Laemmli buffer and stacked in the top of a 4-12% NuPAGE gel (Invitrogen). After staining with R-250 Coomassie Blue (Biorad), proteins were digested in-gel using trypsin (modified, sequencing purity, Promega), as previously described (Casabona et al., 2013).

MS analysis

The resulting peptides were analyzed by online nanoliquid chromatography coupled to MS/MS (Ultimate 3000 RSLCnano and Q Exactive HF, Thermo Fisher Scientific) using a 120 min gradient. For this purpose, the peptides were sampled on a precolumn (300 µm x 5 mm PepMap C18, Thermo Scientific) and separated in a 75 µm x 250 mm C18 column (Reprosil-Pur 120 C18-AQ, 1.9 µm, Dr. Maisch). The MS and MS/MS data were acquired by Xcalibur (Thermo Fisher Scientific).

Peptides and proteins were identified by Mascot (version 2.7.0.1, Matrix Science) through concomitant searches against the Uniprot database (*Homo sapiens* taxonomy, February 2021 download), a database containing HBV protein sequences (homemade), a homemade database containing the sequences of classical contaminant proteins found in proteomic analyses (human keratins, trypsin, etc.), and the corresponding reversed

databases. Trypsin/P was chosen as the enzyme and two missed cleavages were allowed. Precursor and fragment mass error tolerances were set at respectively at 10 and 20 ppm. Peptide modifications allowed during the search were: Carbamidomethyl (C, fixed), Acetyl (Protein N-term, variable) and Oxidation (M, variable). The Proline software (Bouyssié et al., 2020) was used for the compilation, grouping, and filtering of the results (conservation of rank 1 peptides, peptide length ≥ 6 amino acids, peptide score ≥ 25, allowing to reach a false discovery rate of peptide-spectrum-match identifications < 1% as calculated on peptide-spectrum-match scores by employing the reverse database strategy, and minimum of one specific peptide per identified protein group). Proline was then used to perform a compilation, grouping and label-free quantification of the identified protein groups. For samples for which triplicates were analyzed, the quantification of proteins was based on MS1 signals using razor and specific peptides. For samples for which replicates were not available, the quantification of proteins was based on spectral countings.

Statistical Analysis of MS results

Statistical analysis was performed using the ProStaR software (Wieczorek et al., 2017) on the basis of the quantitative data obtained with the three biological replicates analyzed per condition. Proteins identified in the contaminant database, proteins identified by MS/MS in less than two replicates of one condition, and proteins detected in less than three replicates of one condition were discarded. After log2 transformation, abundance values were normalized using the vsn (variance stabilizing normalization) method, before missing value imputation (slsa algorithm for partially observed values in the condition and DetQuantile algorithm for totally absent values in the condition). Statistical testing was conducted with limma, whereby differentially expressed proteins were sorted out using a log2(Fold Change) cut-off of 1 and a p-value cut-off of 0.01, leading to a FDR inferior to 5% according to the Benjamini-Hochberg estimator.

Gene Ontology Analysis, Networks, Functional, and Pathway Mapping

Different set of proteins were created according to the analysis that was conducted. Funrich Software (v3.1.3) was used to map proteins sets to exocarta database (https://exocarta.org/index.html) which contains the list of the proteins frequently identified in exosomes. The overlap between the protein sets was illustrated on a Venn Diagram. Protein-Protein interaction network was generated by STRING 10 (http://string-db.org/) and Funrich Software. Qlucore Omics Explorer (v3.7) was used to generate Principal Component Analysis (PCA) (q-value < 0.15 & p-value < 0.001) and Heatmap

visualization of hierarchical clustering of the proteins that were differentially secreted across the different experimental conditions (q-value < 0.15 & p-value < 0.001). Gene ontology according to molecular function, cellular component and biological process was done on ShinyGO v0.66 with a p-value cut-off of 0.001. KEGG pathway enrichment analysis was also conducted by ShinyGO v0.66

SUPPLEMENTARY FIGURES

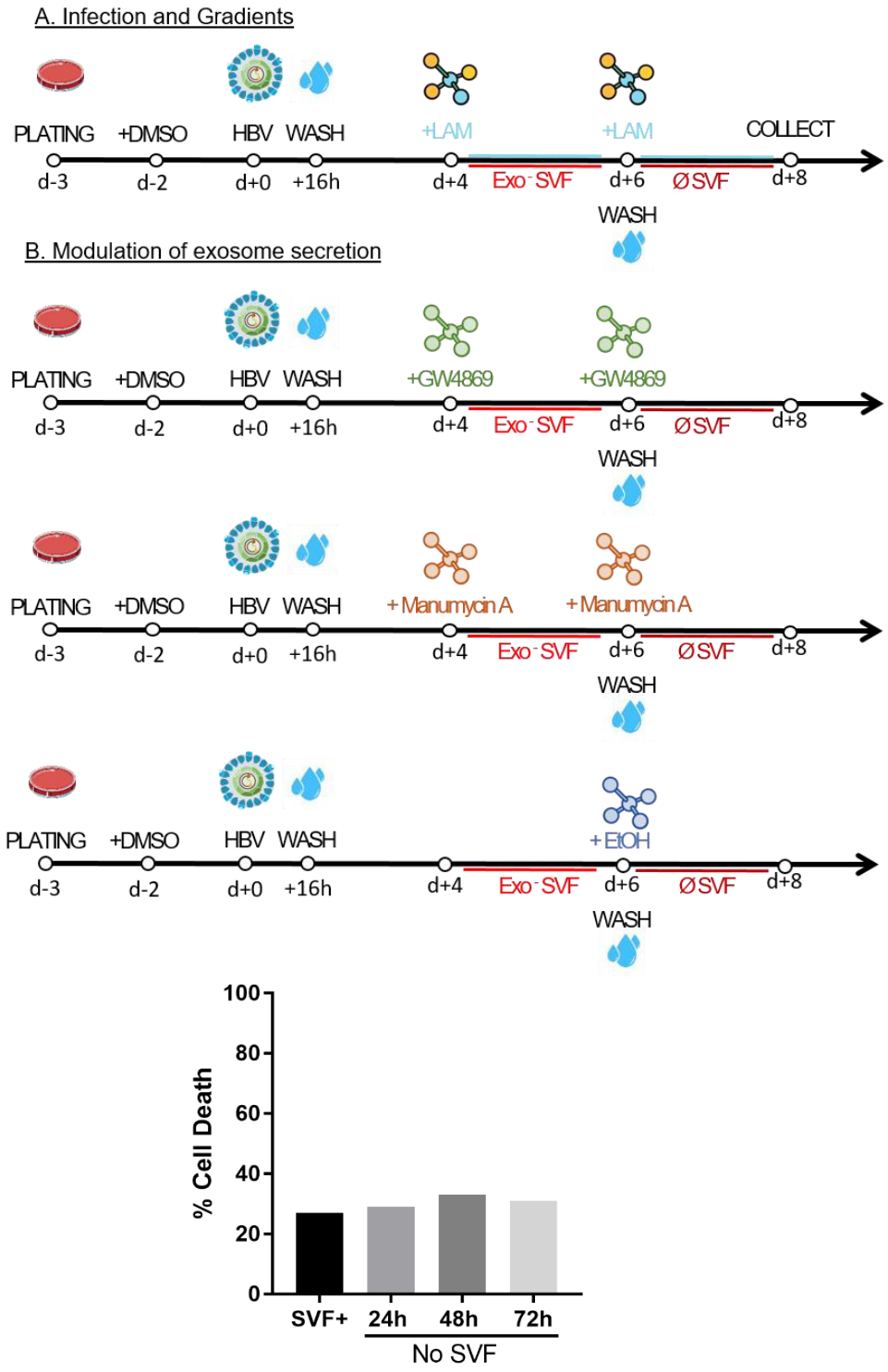

Figure S 1. (A) Cell culture & Drug treatment kinetics. (B) HepG2-NTCP cell viability after 24 to 72h without SVF. Cell death was measured by propidium iodide (PI) straining in flow cytometry (FACS)

FL (1780-1848)	Forward	GGCTGTAGGCATAAATTGGTC
	Reverse	CAAGAGATGATTAGGCAGAGG
	Probe	[6FAM]CGCACCAGCACCATGCAACTTT[BHQ1]
cPAS (1688-1767)	Forward	GACCGACCTTGAGGCATACT
	Reverse	GCCTACAGCCTCCTAATACAAAGA
	Probe	[6FAM]TAATCTCCTCCCC+CAACTCC[BHQ1]
tHBV(1381-1578)	Forward	CTAGGCTGTGCTGCCAACT
	Reverse	ACGGTCCGGCAGATGAG
	Probe	[6FAM]ACTCTCTCGT+CCCCTTCTCC[BHQ1]
3.5kb (FAM /HEX) (2267-2421)	Forward	GGAGTGTGGATTCGCACTCCT
	Reverse	AGATTGAGATCTTCTGCGAC
	Probe	[6FAM]AGGCAGGTCCCCTAGAAGAAGAACTCC[BHQ1]
cccDNA	Forward	CCGTGTGCACTTCGCTTCA
	Reverse	AGATTGAGATCTTCTGCGAC
	Probe	[6FAM]AGGCAGGTCCCCTAGAAGAAGAACTCC[BHQ1]

Table S 1: Sequence of Primers and Probes

Premix (20X)	Stock Solution	Final Concentration	Volume for 100 reactions
Forward Primer	100µM	0,5µM	10µL
Reverse Primer	100µM	0,5µM	10µL
Taqman Probe	50µM	0,2µM	8µL
	Water		72µL

Commercial Mix (Primers + Probes):

- Total HBV-DNA: Life Technologies #Pa03453406_s1
- BetaGlobin: Life Technologies #Hs00758889_s1
- GUSB: Life Technologies #Hs99999908_m1

For cccDNA Only:

Premix (20X)	Stock Solution	Final Concentration	Volume for 100 reactions
Forward Primer	100µM	0,1µM	2µL
Reverse Primer	100µM	0,8µM	16µL
Taqman Probe	50µM	0,2µM	8µL
	Water		72µL

Table S 2. Primers & Probes Premix Concentrations

Target	Specie	Size (kDa)	Reference	Company
CD9	Mouse	25	AHS0902	Life Technologies
Flotilin-1	Mouse	42	610820	BD bioscience
HBc	Mouse	21	ab8637	Abcam
HBc	Rabbit	21	b0586	Dako
HBs	Mouse	25-60	H166	Abbot

Table S 3. Antibodies List

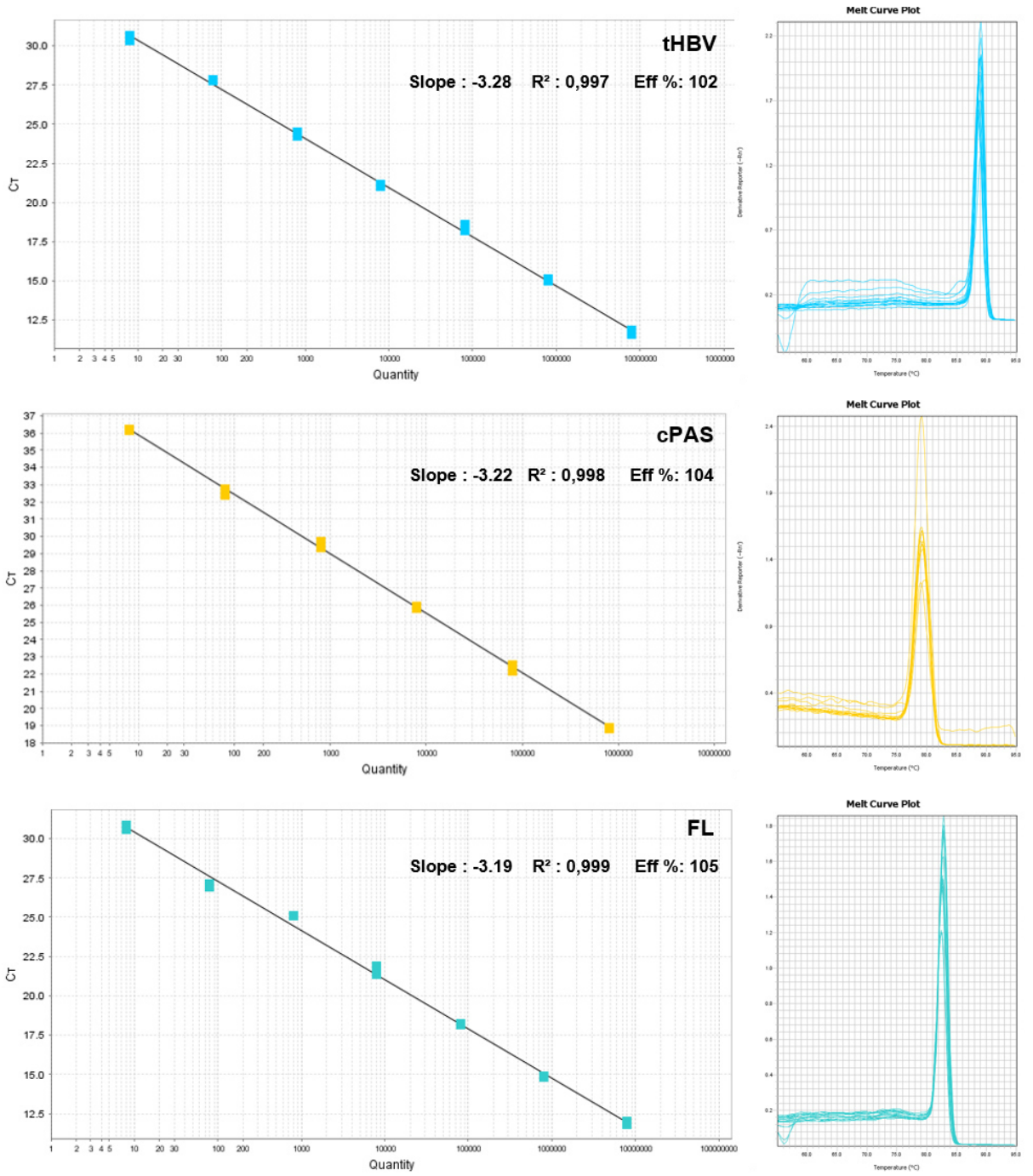

Figure S 2. . Linearity & Specificity: Primers test in SYBR Green qPCR on HBV Standard Plasmid DNA. Serial dilution of linear HBV DNA plasmid currently used as a standard was done. For each couple of primers (tHBV, cPAS and FL) efficacy and melting curve plots were calculated by Quantasoft RealTime software v1.2

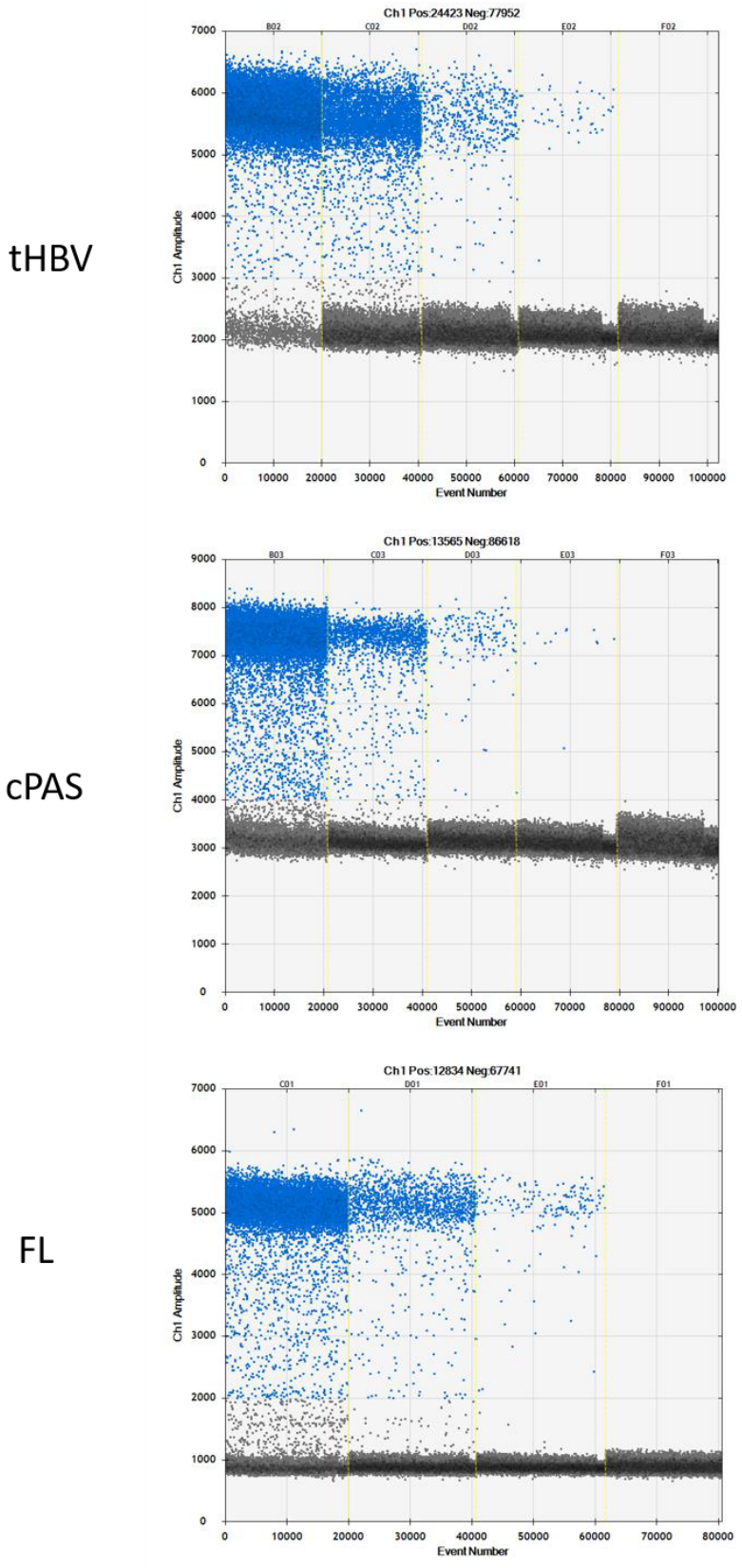

Figure S 3.Linearity & Specificity: Primers and Probes test in Taqman ddPCR on HBV Standard Plasmid DNA

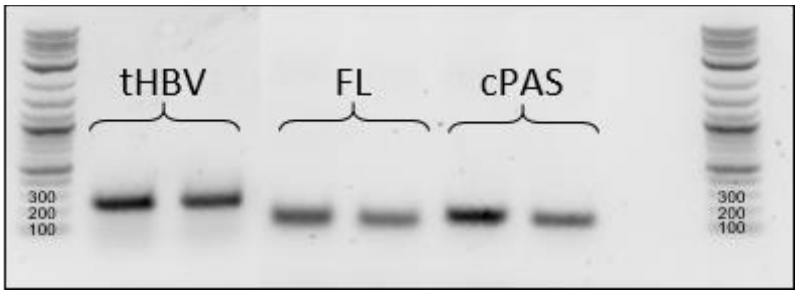

Figure S 4.qPCR Product of Taqman RT-qPCR on RNA extracted from HepAD38 supernatant and migrated on 1% Agarose Gel. These products were sent to Sanger sequencing (data not shown)

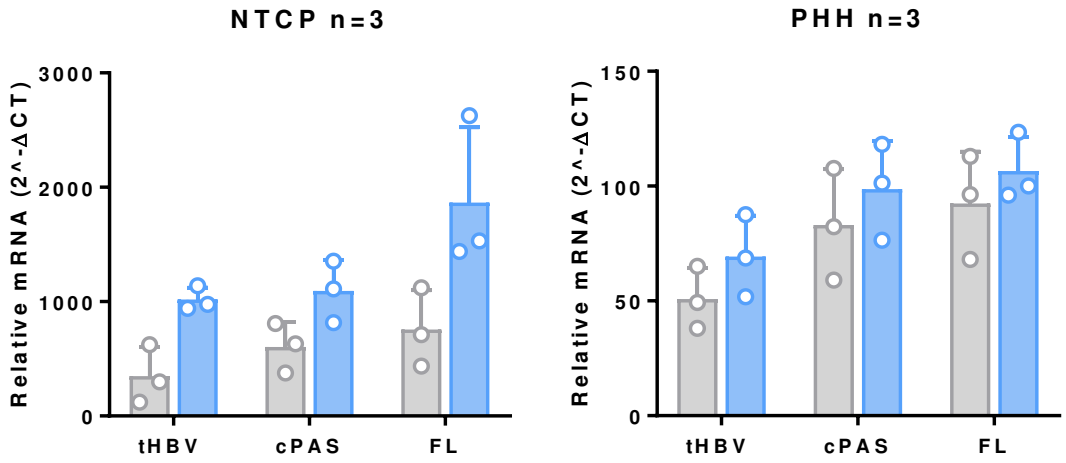

Figure S 5. RNA from infected HepG2-NTCP or PHH were extracted and measured by RT-ddPCR for the presence of the different RNA species. Experiment was repeated 3 times in both cell types. Grey bar represent HBV infected samples and blue bars HBV-infected samples treated with lamivudine (10µM). Results are normalized on housekeeping gene (GUSB)

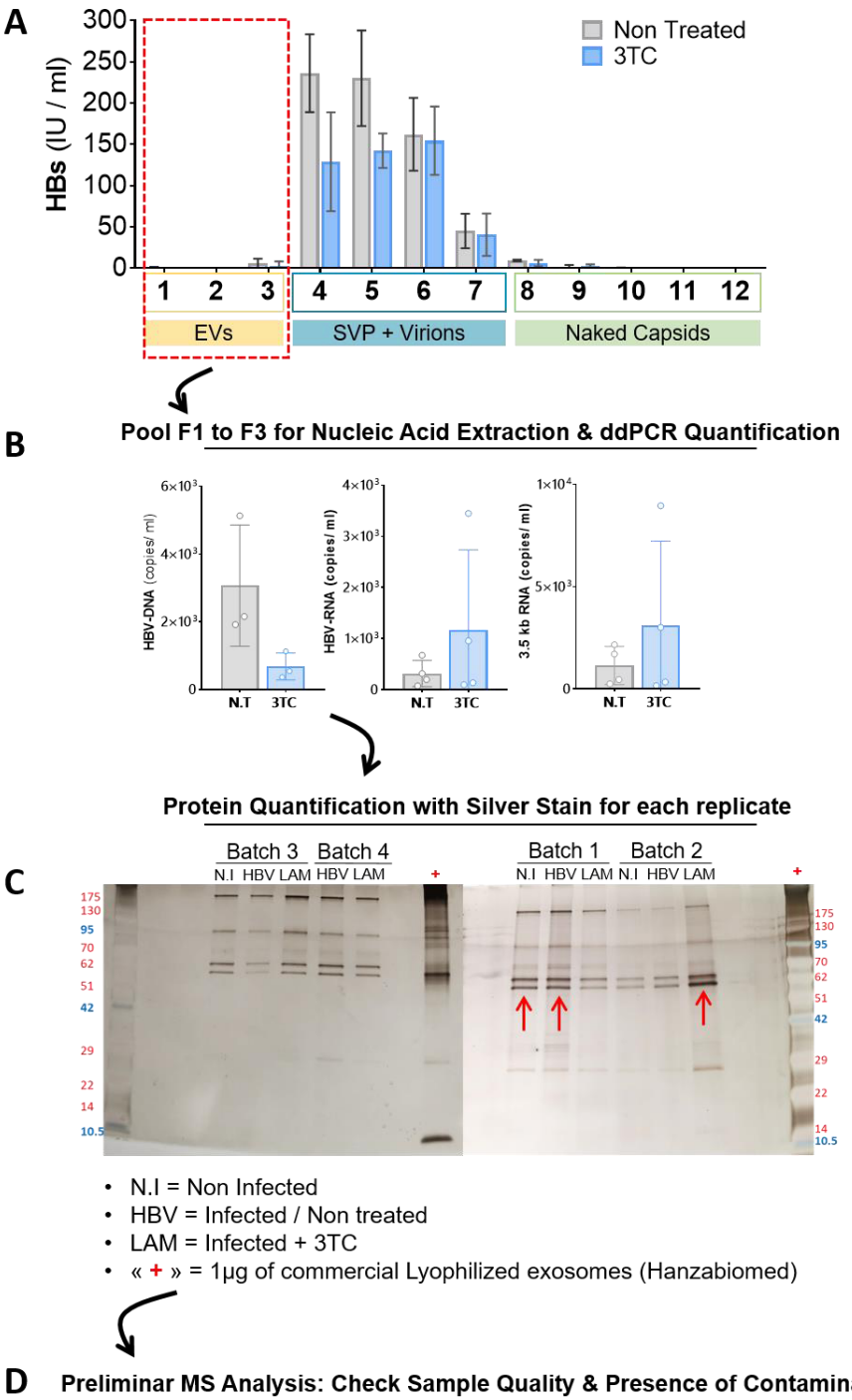

Figure S 6. Mass Spectrometry Pilot Study. Four independent batch of HepG2-NTCP were infected and treated or not with lamivudine (10µM). Supernatant were processed as described in the previous section. (A) ELISA for HBSAg allows to select F1 to F3 which are devoid of HBsAg, (B) F1 to F3 were pooled and concentrated by ultracentrifugation and HBV-DNA and RNA were detected by ddPCR. (C) Protein were migrated on 4-12% NuPAGE gel and stain to appreciate protein quantity. Protein profile was compared to lyophilized exosome derived from HepG2 cells. (D) Finally, samples corresponding to the red arrows were sent for MS analysis.

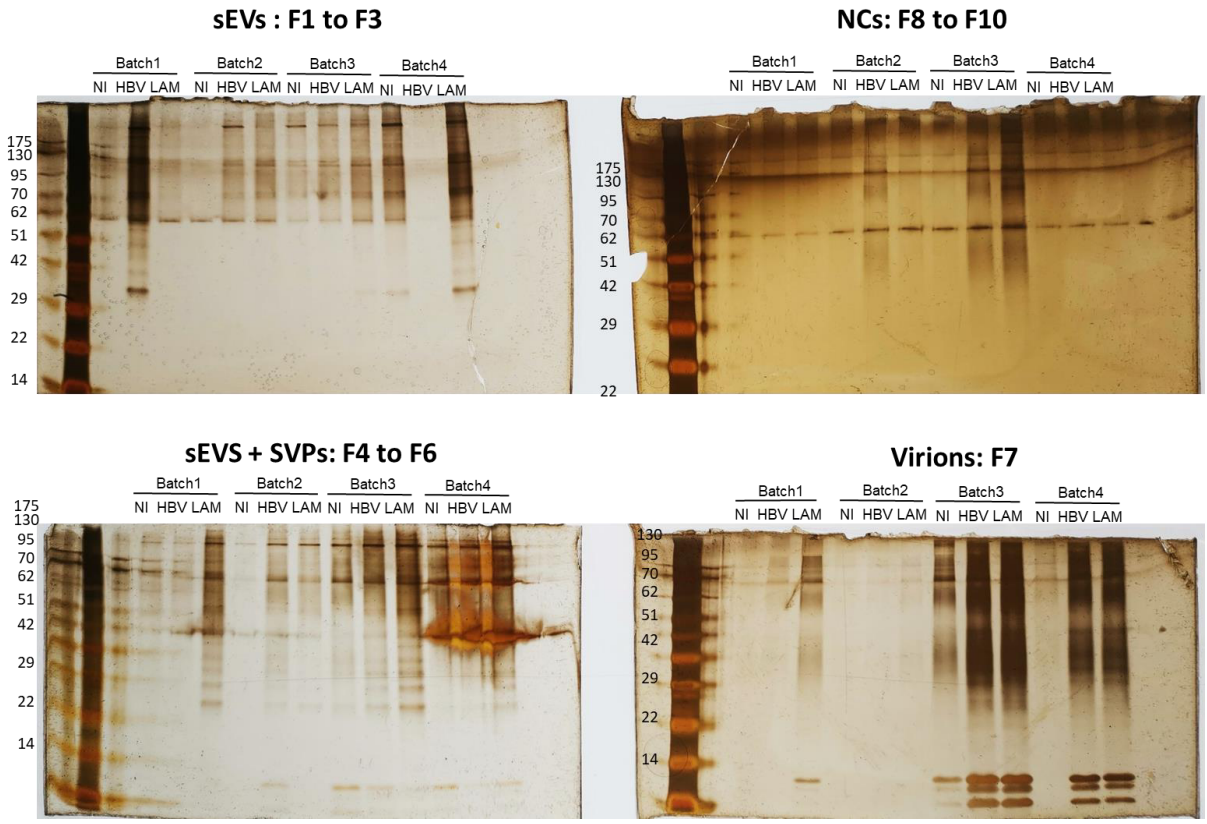

Figure S 7. Mass Spectrometry Final Study. Four independent batch of HepG2-NTCP were infected and treated or not with lamivudine (10µM). Supernatant were processed as described in the previous section. Protein were migrated on 4-12% NuPAGE gel and stain to appreciate protein quantity.

Sample	Volume (µl)	% of Sample on the gel	Silver Stain Quantification	
NI Batch 1 sEVs	42,8	5,8	91558	
HBV Batch 1 sEVs	40,4	6,2	159156	
LAM Batch 1 sEVs	65	3,8	64634	
NI Batch 2 sEVs	46	5,4	49799	
HBV Batch 2 sEVs	54	4,6	57900	
LAM Batch 2 sEVs	49,5	5,1	56076	
NI Batch 3 sEVs	47,2	5,3	35692	
HBV Batch 3 sEVs	47,5	5,3	40277	
LAM Batch 3 sEVs	52	4,8	50946	
NI Batch 4 sEVs	47,8	5,2	71047	
HBV Batch 4 sEVs	38,8	6,4	13433	
LAM Batch 4 sEVs	39,4	6,3	111627	
NI Batch 1 sEVs+SVPs	46	5,4	103395	
HBV Batch 1 sEVs+SVPs	33,6	7,4	90553	
LAM Batch 1 sEVs+SVPs	44	5,7	144278	
NI Batch 2 sEVs+SVPs	35,5	7,0	47332	
HBV Batch 2 sEVs+SVPs	55	4,5	73589	
LAM Batch 2 sEVs+SVPs	50	5,0	53154	
NI Batch 3 sEVs+SVPs	55,4	4,5	75334	
HBV Batch 3 sEVs+SVPs	41	6,1	99536	
LAM Batch 3 sEVs+SVPs	45,5	5,5	154546	
NI Batch 4 sEVs+SVPs	39	6,4	126429	
HBV Batch 4 sEVs+SVPs	39	6,4	154386	
LAM Batch 4 sEVs+SVPs	34	7,4	160183	

Table S 4. Protein Quantification according to band intensity on Silver Staining with Fiji Software. The last columns indicate the samples that were selected for analysis. The three batch are represented by different colors (yellow, green and blue

REFERENCES

La mise à jour automatique des citations est désactivée. Pour voir la bibliographie, cliquez sur Actualiser dans l'onglet Zotero.

ACKNOWLEDGEMENTS

I would like to greatly thank **Pr. Reihnild Prange** and **Dr. Eloi Verrier** for having accepted to review my thesis manuscript. I thank **Dr Lorena Martin-Jaular, Dr Marintha Heil, Pr. Philippe Roingeard and Pr. Massimo Levrero** for having accepted my invitation to participate to my thesis defense. Finally, I thank **Dr. Patrick Soussan and Dr. Mirjam Zeisel** for having followed my work throughout these three years by participating to my thesis evaluation committees and for their essential observations regarding my thesis project.

J'aimerais également remercie **Pr. Zoulim** pour m'avoir chaleureusement accueilli dans son équipe et m'avoir accordé sa confiance. Je ne vous remercierai jamais assez de m'avoir laissé ma chance, moi, étudiante en master cardio qui avait tout à découvrir sur la biologie moléculaire et encore plus sur notre pire ennemi HBV. Je resterai toujours admirative de la pertinence de vos remarques et vos réflexions.

Barbara, je pense qu'un seul merci n'est pas suffisant mais sache que je te serai reconnaissante à jamais pour ton aide. Tu as été un vrai vecteur tout au long ces trois dernières années, tu as été là quand il le fallait, et tu as su me pousser quand je doutais. Ton encadrement m'a aidé à prendre confiance en moi dans ce milieu pour laquelle j'étais totalement étrangère. Je pense ne pas me tromper quand je dis que nous avons réussi à trouver notre équilibre, entre suivi et autonomie. Au-delà de la thèse, je te remercie pour tes qualités humaines. Je n'aurais jamais pensé tomber sur un encadrement aussi maternel, tu es compréhensive, bienveillante et accessible, une nouvelle fois, je te remercie du fond du cœur. Merci d'avoir toujours répondu à mes appels à l'aide et mes idées bizarres ! Tu m'as transformé en petit monstre d'HBV et tu peux en être fière… PS : Merci pour m'avoir fait découvrir le plus merveilleux que j'ai jamais gouté !!!

Fabien et Barbara, d'une manière générale je vous remercie d'avoir veillé à me fournir les conditions idéales pour réaliser ma thèse. Merci d'avoir toujours pris du temps pour discuter avec moi quand j'avais des doutes et des interrogations. Cela m'aura pris du temps de trouver ma place dans ce projet, mais ce dont je suis sûre c'est que c'est grâce à votre encadrement qu'aujourd'hui j'ai un pincement au cœur à l'idée de le quitter.

On dit qu'écrire une thèse n'est pas simple, mais c'est encore moins simple de trouver les mots juste pour tous vous remercier. Vous, les gens du CAT, mes amis, ma famille, vous

avez été la clé de ma réussite. Je ne serais même pas la moitié d'un docteur sans vous, et j'espère que mes mots seront à la hauteur de ma reconnaissance.

La semaine de mon arrivée au laboratoire, 3 doctorants ont soutenus leur thèse. Il pesait à la fois une ambiance mélancolique mais aussi terriblement festive. J'ai été immédiatement baignée dans grand bain des tournages des vidéos de thèse, l'émotion des soutenances et l'euphorie de la célébration. A l'époque, c'était un peu abstrait pour moi ce que pouvait représenter ce moment, mais en voyant ça, je n'avais qu'une envie : que ça soit mon tour ! D'un autre côté, ce qui m'a aussi frappé, c'est la rapidité à laquelle les gens arrivent et repartent au laboratoire, à ce moment, je me suis dit qu'il serait impossible de créer de réels liens, qu'ils seraient éphémères, mais au fil du temps je me suis rendue compte que j'avais tort. Et je n'ai jamais été aussi heureuse de me tromper. Au CAT, j'ai trouvé des amis et une seconde famille. Si vous vous baladez dans les couloirs, vous trouverez forcément quelqu'un pour vous sourire, vous faire une blague ou vous apporter du réconfort quand vous en avez besoin. On ne mesure pas assez le bonheur que peut vous apporter un tel cadre de travail, si je suis arrivée à bout de ce doctorat ça n'est pas juste au terme de centaines de manips, c'est grâce à tous ces petits lutins qui s'affairent dans le labo. Une équipe, un micro environnement, des collègues et amis que je vais quitter avec le cœur lourd. Pour ça, je vous remercie. Je sais que vous avez tous marqué un point dans ma vie qui restera gravé dans ma mémoire.

Aux membres de **l'équipe BT**, pour moi, faire partie de cette équipe c'est être animés de discussions passionnantes au cours de nos meetings, se réunir tous ensemble autour d'une table et découvrir à quel point vous êtes tous passionnants et l'aide volontaire que vous m'avez apporté quand je vous ai sollicité. Non comptant mon amour inconditionnel pour la nourriture, j'ai adoré partager nos fameux lunchs cosmopolites. **Doohyun**, I was pleased to share the project with you, you always have a kind word towards me and I really appreciate that. 감사 해요. **Hyoseon**, you definitely are THE western blot queen. Thanks for your kind words, your WB tricks and your sweetness. Keep on creating all you cute scrapbooking stuff; it brings joy in everyone's life! **Guada**, I think you are the kindest person I have ever met. I learnt a lot with you, you always took time to help me. Your sense of organization and perfectionism is impressive and I am sure you will shine everywhere you will work. I know we will keep in touch. Please do not stop posting pictures of the snoring Herculito! **Guillaume**, tu as toujours répondu à mes appels à l'aide, et pour ça je ne te remercierai jamais assez. HBV a un grand avenir avec un chercheur comme toi c'est

certain. Merci pour ton temps, ta gentillesse, tes textos plus ponctuels que l'horloge atomique elle-même pour les douze coups de midis et bon, il faut le reconnaitre, tu es un peu le dieu des ARNs pour moi… ! **Manu**, qu'en est-il du deuxième petit déjeuner ? Merci pour ton aide, tu es passionné et passionnant, j'espère réellement que l'équipe pourra te garder auprès d'elle car d'après moi tu es une personne indispensable à son bon fonctionnement. J'espère que mon/ma remplaçante partagera aussi des cookies et des pains comté noisette avec toi mais des bananes jamais, ça reste le fruit du démon (beurk pas bon !). **Khadija**, merci pour ta générosité. Du lapin de Pâques à la mère noël, des baklawas au baba ghanouj, toutes tes délicieuses petites attentions m'ont fait chaud au cœur. Tu as toutes les qualités pour faire une très belle thèse, accroches-toi, je te souhaite une très belle continuation. **Andrès**, merci pour ton aide, particulièrement ces derniers jours dans ma rédaction. Tu es un chercheur très talentueux et tu as toujours des questions et des remarques pertinentes. **Xavier,** merci pour ta précieuse aide bioinfo, l'aventure Nanopore ne fait que commencer, on a intérêt à bien s'accrocher ! **Mélanie**, bien que tu sois arrivée il y'a peu, j'ai partagé de bons moments avec toi et tu as une énergie communicative. **Maud**, te voilà dans l'équipe BT, et mon dieu que cette équipe a de la chance de t'avoir. Tu es drôle, bienveillante et pétillante. **Anaëlle**, coucou toi. Je suis heureuse de m'être rapprochée de toi ces derniers mois, les vacances d'été au labo ont du bon après tout ! Nos petites conversations, nos achats compulsifs et nos cahiers de doléance sur nos félins me manqueront beaucoup mais je sais qu'on restera en contact ! **Sarah**, tu viens on va faire une wesh-tern ? Non mais je te jure, à cause de toi on parle comme au bled starfoullah, y'a quoi ?! Mon dieu comme je t'affiche sur mes remerciements, dire que potentiellement les gens les liront… On va opter pour des remerciements plus softs mais non moins sincères. Tu es une personne d'une gentillesse extrême, haute en couleur et vraiment très drôle. Ne change jamais ! **Anaëlle et Sarah**, sérieusement, cette bonne humeur communicative n'a pas de prix. Vous m'avez fait rire, vous m'avez soutenu, vous êtes toujours là pour rire et pour râler et vous aller me manquer…

Aux membres du **RHU**, ce fut un plaisir de faire partir de ce microenvironnement avec vous. **Alexia,** je te remercie pour ta douceur extrême. Ta rigueur et ta perseverance me laissent admirative. J'ai passé de très bons moments à tes côtés et je t'enverrai toutes mes meilleures ondes dans quelques mois ! **Francesca**, (alias l'italienne qui a appris le français le plus rapidement du monde), quelle bonne humeur et gentillesse communicative. Marie-Laure, désolée d'avoir été un petit boulet de plus à gérer. Merci de m'avoir aidé, tant sur

le plan humain qu'en tant que référente officielle SafiR ! **Bernadette**, bravo pour toujours avoir organisé nos réunions d'une main de maître, tu es la femme de l'ombre sans qui rien ne serait possible. **Massimo**, merci pour vos idées, vos conseils et votre énergie débordante. **Françoise,** merci pour m'avoir formé à la ddPCR et avoir répondu à mes appels au secours quand la machine ne voulait plus fonctionner. **Isabelle B.**, merci pour ta gestion du laboratoire, tu es pour tous un rouage indispensable au bon fonctionnement du labo !

Merci aux filles de la **plateforme PHH**, Maud, Anaëlle, Jennifer, pour votre persévérance et les jolies PHH en (GRAAAAANDE) quantité que vous m'avez octroyé pendant cette thèse.

Et enfin, le bureau. **Marion**, Armande, Rusard, merci pour tout. Je n'aurais pu rêver mieux comme alter ego de thèse. Il faut croire que je suis tombée sur le bon bureau ! Je suis heureuse que nos chemins se soient croisés. Tu es passionnée, tu défends les idées qui te tiennent à cœur, tu es cultivée, d'une générosité monumentale et … la meilleure personne pour faire des blagues nulles et citer des répliques de film. Merci d'avoir été là, merci de m'avoir intégrée. J'ai adoré nos sessions répétitions de présentations, tout ce que tu m'as fait découvrir et pas dessus tous les fous rires. Bisou baby, London's calling ;)

Ma petite padawan **Valentine**, merci à toi pour ton aide inestimable. Je n'aurais pas pu rêver mieux comme stagiaire. Je suis fière d'avoir pu t'aider dans ton cursus et comme tu les sais déjà je te souhaite le meilleur pour ce qui t'attend dans le futur. Nos chemins se recroiserons ça c'est certains, alors d'ici là, apprends à faire des plans de plaques easy to read !

Marie-Agnès, un immense merci. En toi j'ai trouvé un grand réconfort. Non comptant que tu es la petite souris qui fait tourner la maison, tu as des qualités humaines innombrables qui font de toi une super personne ! Nos longues conversations vont me manquer mais je sais que maintenant quand tu regarderas ton calendrier et que tu verras qu'on est le 7 du mois tu penseras à moi !

Aux annexiens**, Margot, Caro P., Yasmina, Romain, Florentin, Vincenzo, Claire**, et à **TOUS les autres** membres du CAT, je vous dis un grand merci pour les moments partagés ensemble autour d'un repas ou au détour d'un couloir. Merci d'avoir répondu à mes questions car oui, j'ai surement dû vous en poser des milliers, simplement merci pour votre sourire et je vous souhaite le meilleur à tous pour la suite.

Une pensée pour ceux qui sont partis, sans qui cette aventure n'aurait pas été la même. **Fleurette**, j'ai tant de choses pour lesquelles je dois te remercier. Tu m'as accueilli dans l'équipe, tu m'as TOUS montré, tu m'as pris sous ton aile avec une gentillesse extrême. C'était un déchirement de te voir partir et encore plus d'imaginer la vie du labo sans toi. Comme promis, j'ai fait de mon mieux pour guider les nouveaux de l'équipe BT et c'est à ce moment que j'ai mesuré toute la gentillesse dont tu as su faire preuve. Ne perds jamais confiance en toi, tu es une merveilleuse personne ! **Maëlle** mon dieu quelle énergie et bonne humeur communicative. J'aurais aimé passer plus de temps au labo en même temps que toi, je suis sure qu'on aurait bien rigolé ! **Audrey**, Merci d'avoir été si gentille avec moi, de m'avoir beaucoup aidé (surtout lors de longues extractions) et répondu à mon millier de questions au labo. **Caro C**, mon dieu tu es tellement la chercheuse la plus excentrique et passionnée que je n'ai jamais connue. Tu es une femme épatante et avec un style exceptionnel. Chloe, the Australian good vibe. It was a pleasure to meet you. You are such an amazing and gorgeous woman and of course you have the most beautiful baby sonnie boy ever!

Et enfin, je remercie également ceux qui ne sont pas au labo mais qui ont toujours été là et le seront toujours.

Les copines, Louise, Joëlle et Victoire, vous êtes mes fondations, la dream team des petites aixoises que je n'échangerais pour rien au monde. **Joe**, il est loin le temps des boums dans le sous-sol et des mojitos clandestins effrayées par les grenouilles de la serre. Merci mon petit mochi pour ton soutien sans faille (ta mimolette qui t'aime). **Vic**, on peut ne pas se voir pendant des mois et se retrouver pendant des heures à parler à cœur ouvert de nos vies passées, futures et présentes et ça je ne m'en lasserai jamais. **Ma Loulou**, tu es ma Loulou c'est tout. Ma petite allumette, flamboyante, excentrique qui m'accompagne depuis bien trop longtemps pour le mentionner… Tu m'as accompagné dans de nombreuses épreuves, du primaire au premier jour de PACES, et je suis rassurée de savoir qu'il y en aura bien d'autres à tes côtés.

Clara, mon gourou, que dire. Tu as suivi de très près l'intégralité de mon aventure et je te remercie pour ton oreille attentive, pour les moments improbables qu'on a passés ensemble et ton affection. Tu m'as fait grandir moralement, difficile d'énumérer à quel point tu m'as aidée. Mais tu es là, et je t'en remercie.

Claudia, mon petit chat, comment les gens qui ne te connaissent pas font pour vivre ? Comment on peut vivre sans sa dose de câlins de petit chat ? Je suis heureuse que mon

échec de médecine m'ai conduit jusqu'à toi, pipelette qui s'est jetée sur moi me premier jour de fac. Depuis, on ne s'est pas quittées et je sais que quoi qu'il arrive nous pourrons toujours compter l'une sur l'autre et qu'on passera encore des centaines de moments géniaux ensemble !

Louis, merci d'avoir toujours été là et de m'avoir remonté le moral d'innombrables fois avec des vidéos de Gibsouille ou Pasco qui te mâchouillait où te maltraitait ! Et merci pour les reste, ton temps, tes conseils et ton amitié !

Maman, comment je ferais sans toi. Il paraît qu'à partir de 18 ans on devient adulte, on part faire ses études et on a plus besoin de ses parents… Eh bien, c'est faux, pour moi c'est à partir de ce moment précis qu'on commence à avoir le plus besoin d'une maman. C'est quand on quitte le nid qu'on se rend compte de combien il est difficile de voler de ses propres ailes, mais où qu'on soit, quoi qu'on fasse, on sait que maman n'est pas loin pour nous aider, pour nous écouter ou pour nous rassurer. Merci maman

Papa, une force tranquille qui agit dans l'ombre. Merci papa pour ton soutien, je sais que quoi qu'il arrive je pourrais toujours compter sur toi, et que tu veilleras toujours à mon bonheur. On ne se le dit pas souvent mais ce jour est assez exceptionnel pour te dire que j'aime fort mon papa poule.

Jb, je ne te dirais jamais suffisamment merci d'être toi. Toutes ces années tu n'as jamais arrêté d'être fier de moi, de me soutenir et de m'aider à aller plus loin. Je n'ai pas toujours les mots pour te montrer que je suis reconnaissante mais sache que ma réussite, c'est aussi un peu la tienne. J'ai hâte d'ouvrir le prochain chapitre de notre aventure !

APPENDICES

I. Circulating Hepatitis B Virus (HBV)-RNAs associates with extracellular vesicles (EVs) in cell supernatant and patient's serum (Article in preparation)

Co first author with Dr D.Kim

II. Huh7-3D29 Clonal cell line secretes HBV RNA in excess and low quantities of HBV DNA: the generation of an HBV RNA standard (Article in preparation)

Participation in the characterization of the clonal cell line

III. Communications

1. Oral Presentations

- ISEV 2021: 10 min Presentation
- ANRS AC42 2021: 10 min Presentation
- Poster/Flash Talk for HBV Meeting 2021

2. Poster Presentations

- EASL 2021
- HBV Meeting 2021

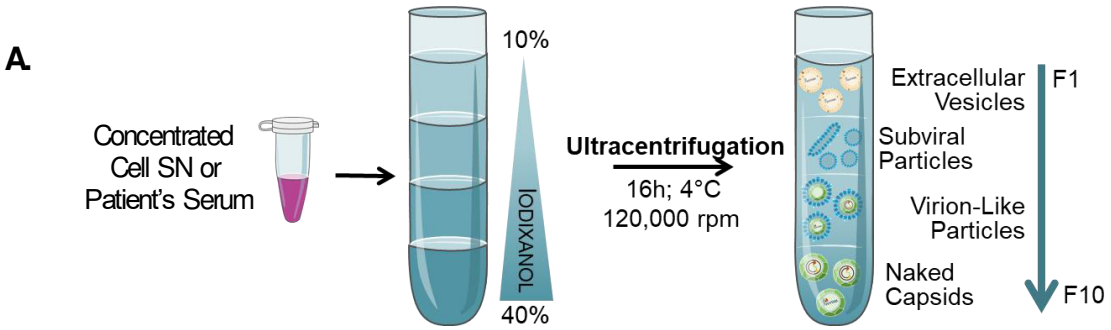

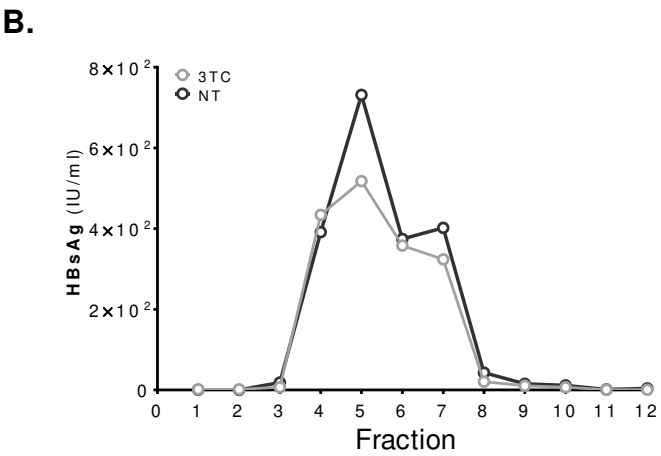

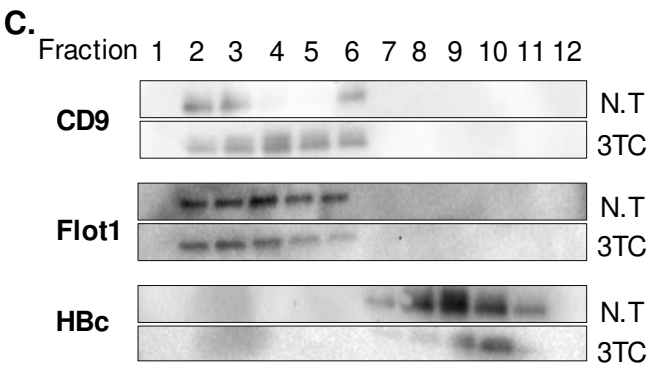

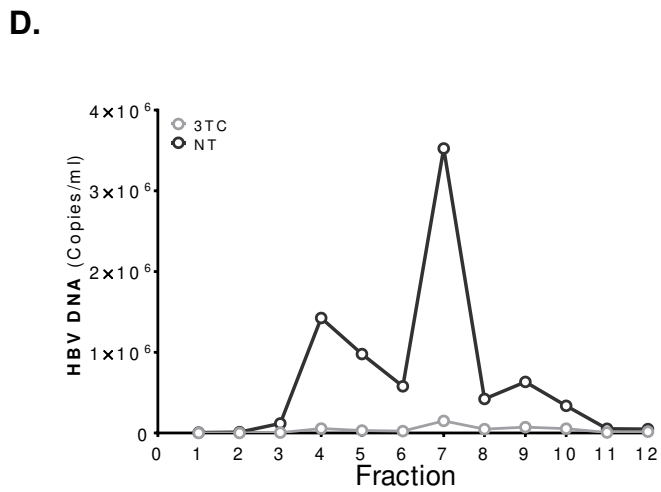

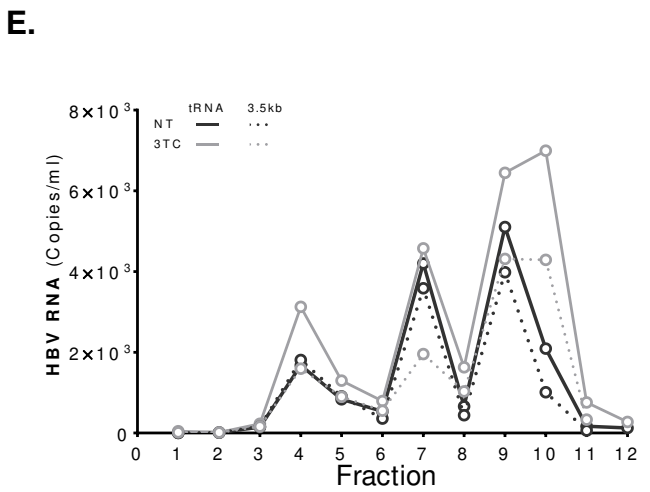

Figure 1. Secreted HBV RNA is associated to small extracellular vescicles in supernatant of HBV-infected HepG2^{hNTCP} cells (A) Scheme of 10-40% Iodixanol/STE density gradient and theorical small extracellular vescicles (Evs) distribution according to their buoyant density. Briefly, HepG2^{hNTCP} cells were infected at MOI 250 and supernatant was collected 8 dpi. Infected cells were treated (3TC) or not (N.T) with lamivudine (3TC) at 10μM for 5 days. (B) HBsAg ELISA was measured in each fraction. (C) Exosome marker, Flotillin-1 (Flot-1) and HBV core protein (HBc) were detected by western blot in each fraction. (D) Total HBV-DNA, (E) total HBV-RNA (tHBV-RNA) and 3.5kb RNA were quantified by ddPCR in each fraction.

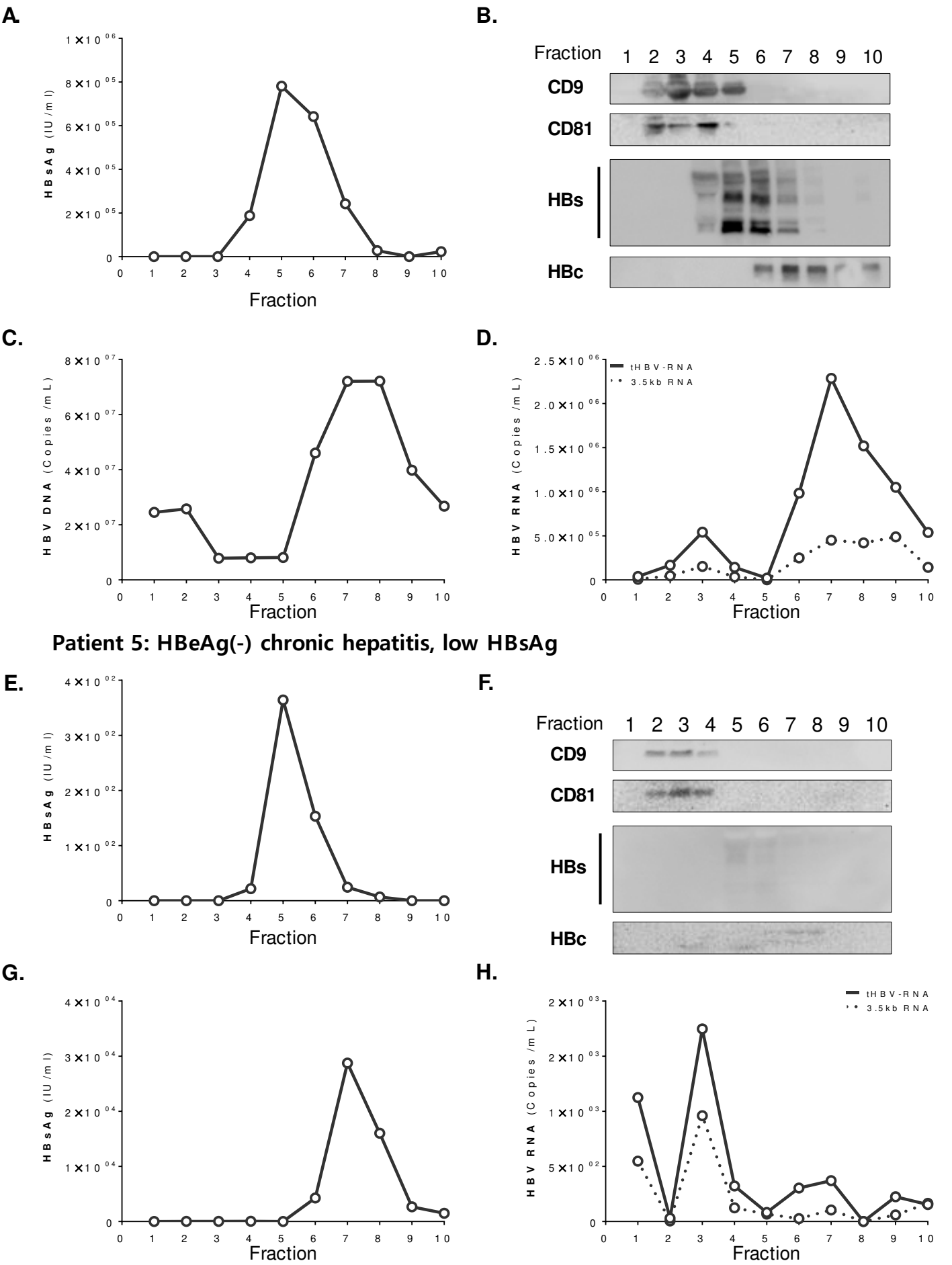
Patient 1: HBeAg(+) chronic infection
A.
HBsAg (IU/ml)
Fraction
B.
Fraction 1 2 3 4 5 6 7 8 9 10
CD9
CD81
HBs
HBc
C.
HBV DNA (Copies/mL)
Fraction
D.
tHBV-RNA
3.5kb RNA
HBV RNA (Copies/mL)
Fraction
Patient 5: HBeAg(-) chronic hepatitis, low HBsAg
E.
HBsAg (IU/ml)
Fraction
F.
Fraction 1 2 3 4 5 6 7 8 9 10
CD9
CD81
HBs
HBc
G.
HBsAg (IU/ml)
Fraction
H.
tHBV-RNA
3.5kb RNA
HBV RNA (Copies/mL)
Fraction

Figure 2.

Figure 2. Analysis of viral parameters and EVs markers in gradient fractions of serum samples derived from patients in different CHB phases.

Gradient fractions were obteined according to the protocol detailed in Method section. a) HBsAg ELISA. b) Representative Western Blot analysis using anti-extracellular vesicle (EVs) markers (anti-CD9 and anti-CD81), anti-HBsAg and anti-HBV core antibody. c) HBV DNA quatification by qPCR. d) HBV RNA quantification by RT-qPCR. HBx ORF common region was used to quantify both HBV DNA and total HBV RNA. pre-Core/pgRNA 5' unique region was used to quantify 3.5kb HBV RNA (Testoni et al. JHep 2019). CHB phases are defined according to 2017 EASL CPGs.

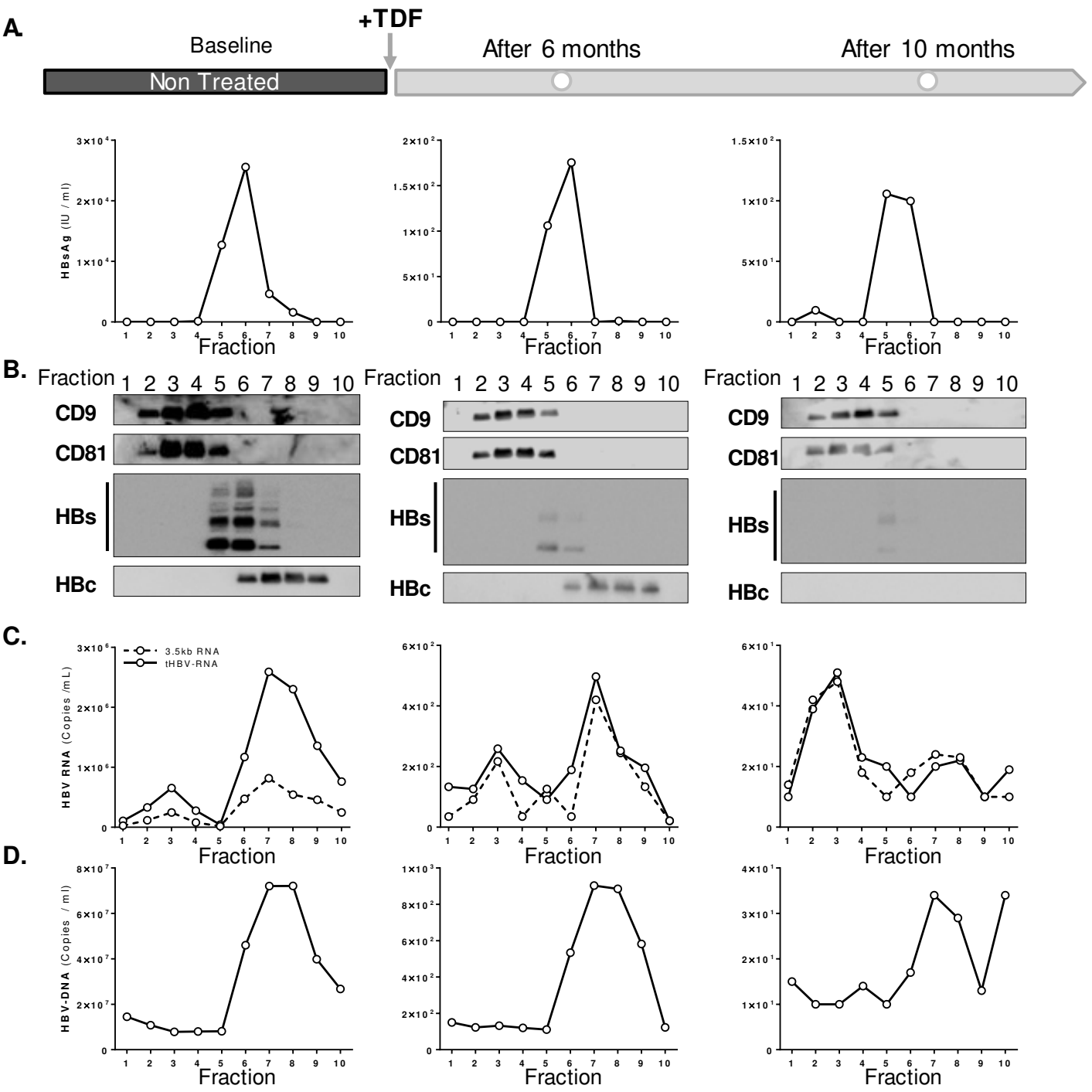

Figure 3. Analysis of viral parameters and EVs markers in gradient fractions of longitudinal serum samples derived from a Tenofovir-treated patient.

Gradient fractions were obteined according to the protocol detailed in Method section. a) HBsAg ELISA. b) Representative Western Blot analysis using anti-extracellular vesicle (EVs) markers (anti-CD9 and anti-CD81), anti-HBsAg and anti-HBV core antibody. c) HBV RNA quantification by RT-qPCR. HBx ORF common region was used to quantify both HBV DNA and total HBV RNA. pre-Core/pgRNA 5' unique region was used to quantify 3.5kb HBV RNA (Testoni et al. JHep 2019). d) HBV DNA quatification by qPCR.

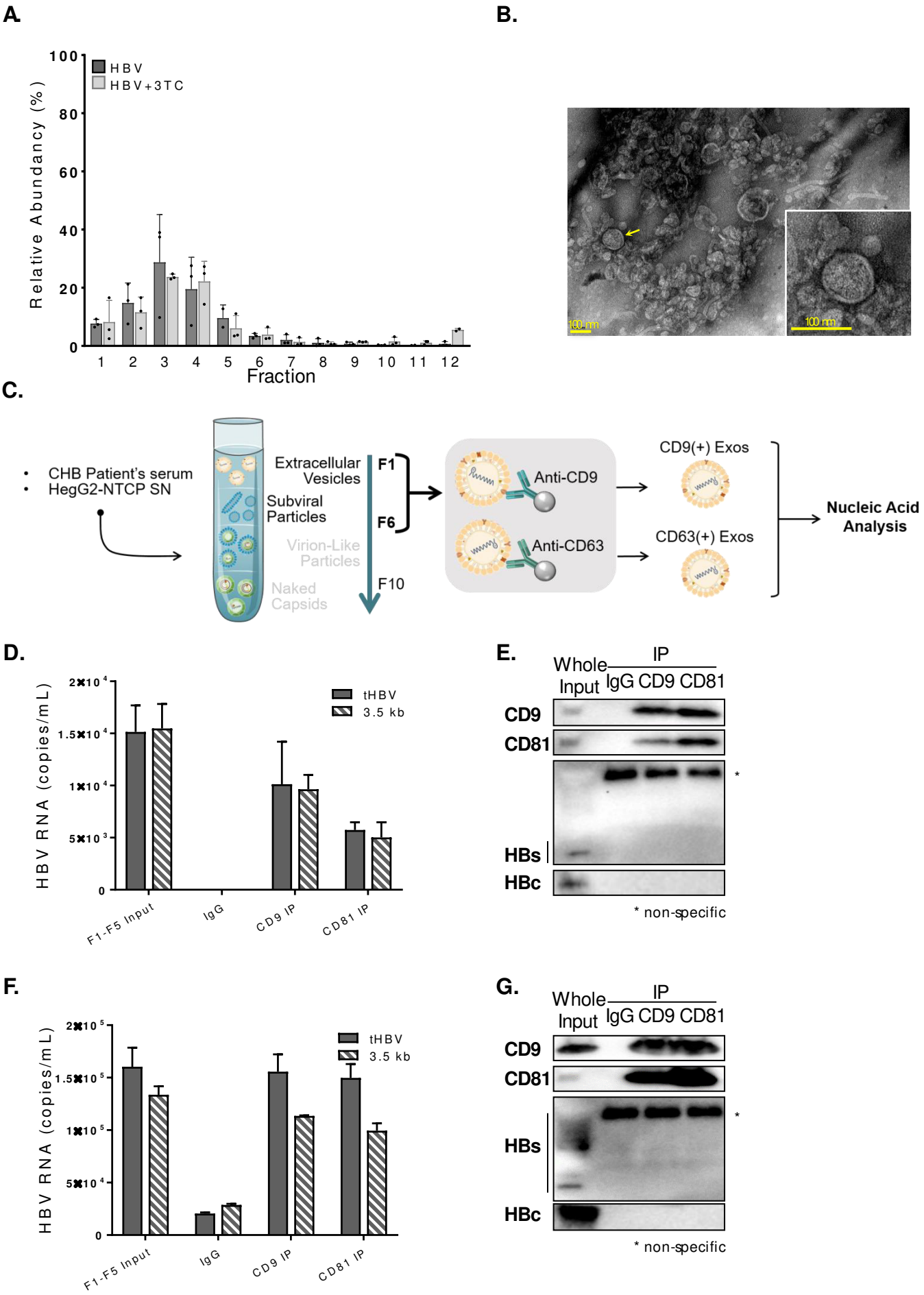
A.
B.
C.
D.
E.
F.
G.
HBV
HBV+3TC
Relative Abundancy (%)
Fraction
100 nm
CHB Patient's serum
HegG2-NTCP SN
Extracellular Vesicles
Subviral Particles
Virion-Like Particles
Naked Capsids
F1
F6
F10
Anti-CD9
Anti-CD63
CD9(+) Exos
CD63(+) Exos
Nucleic Acid Analysis
tHBV
3.5 kb
HBV RNA (copies/mL)
F1-F5 Input
IgG
CD9 IP
CD81 IP
Whole Input
IP
IgG CD9 CD81
CD9
CD81
HBs
HBc
* non-specific

Figure 4.

Figure 4. Characterization of sEVs fraction. Supernatant form HBV-infected HepG2^{hNTCP} cells was separated through density gradient. (A) Particles were quantified and size was assessed in 3TC-treated and non-treated samples by Nanoparticle Tracking Analysis. (B) Negative staining of fraction 4 in electron microscopy (PTA 3%). (C) Schematic protocol of sEVs-Immunoprecipitation (IP) (D-E) sEVS-IP in HBV-infected HegG2^{hNTCP} supernatant (F-G) sEVS-IP in Patient serum. Graphs show the mean ± SD of 3 independent experiments

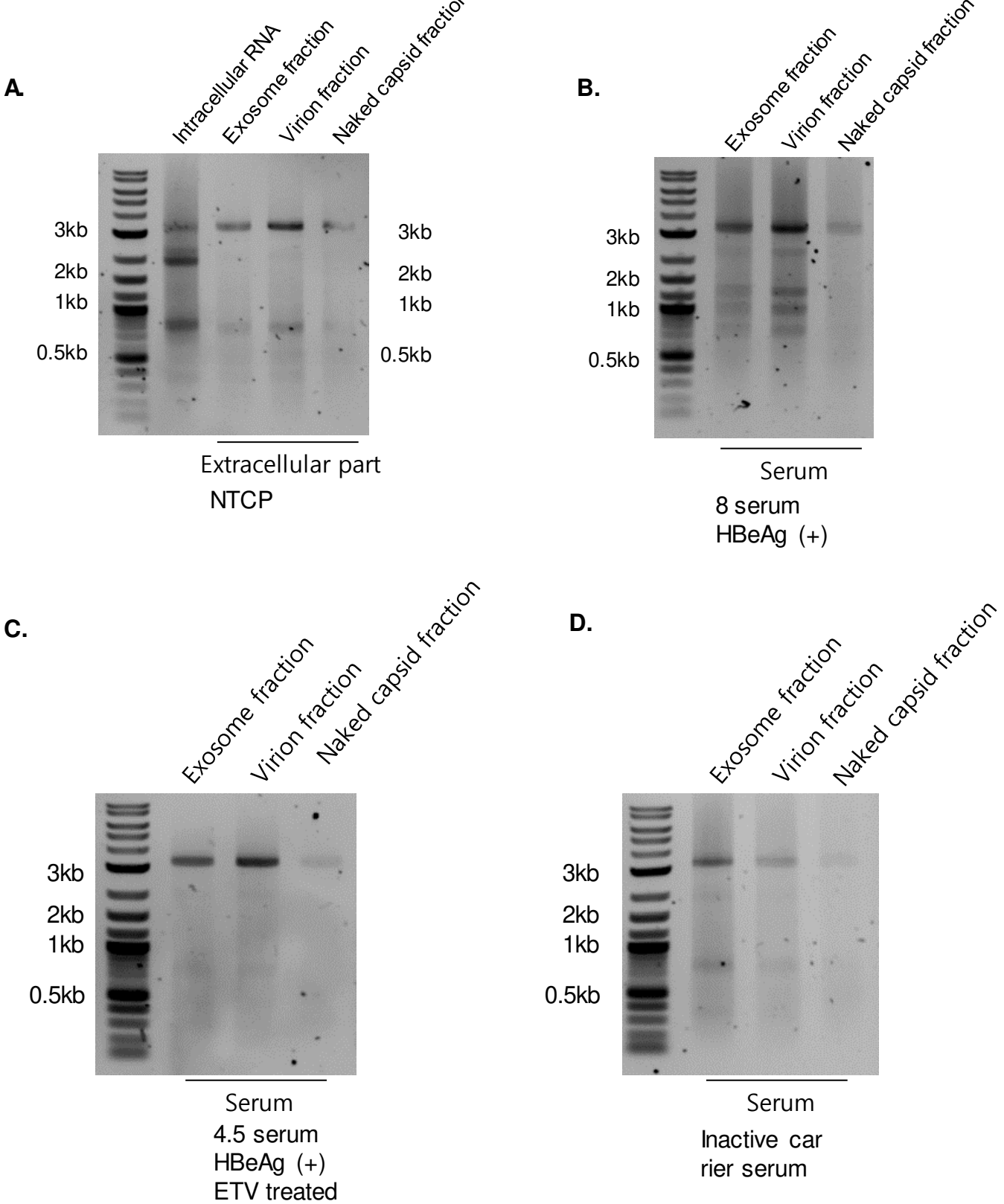

Figure 5. Characterization of RNA in each gradient fraction by HBV 5' RACE. (A) HepG2^{hNTCP} were infected at MOI 500 and RNA was extracted using Trizol reagent from concentrated whole supernatant. Fraction F4, F7 and F9 of density gradient were subjected to HBV-5'RACE. (B-D) RNA from patients' serum was extracted with Trizol reagent and subjected to HBV-5'RACE

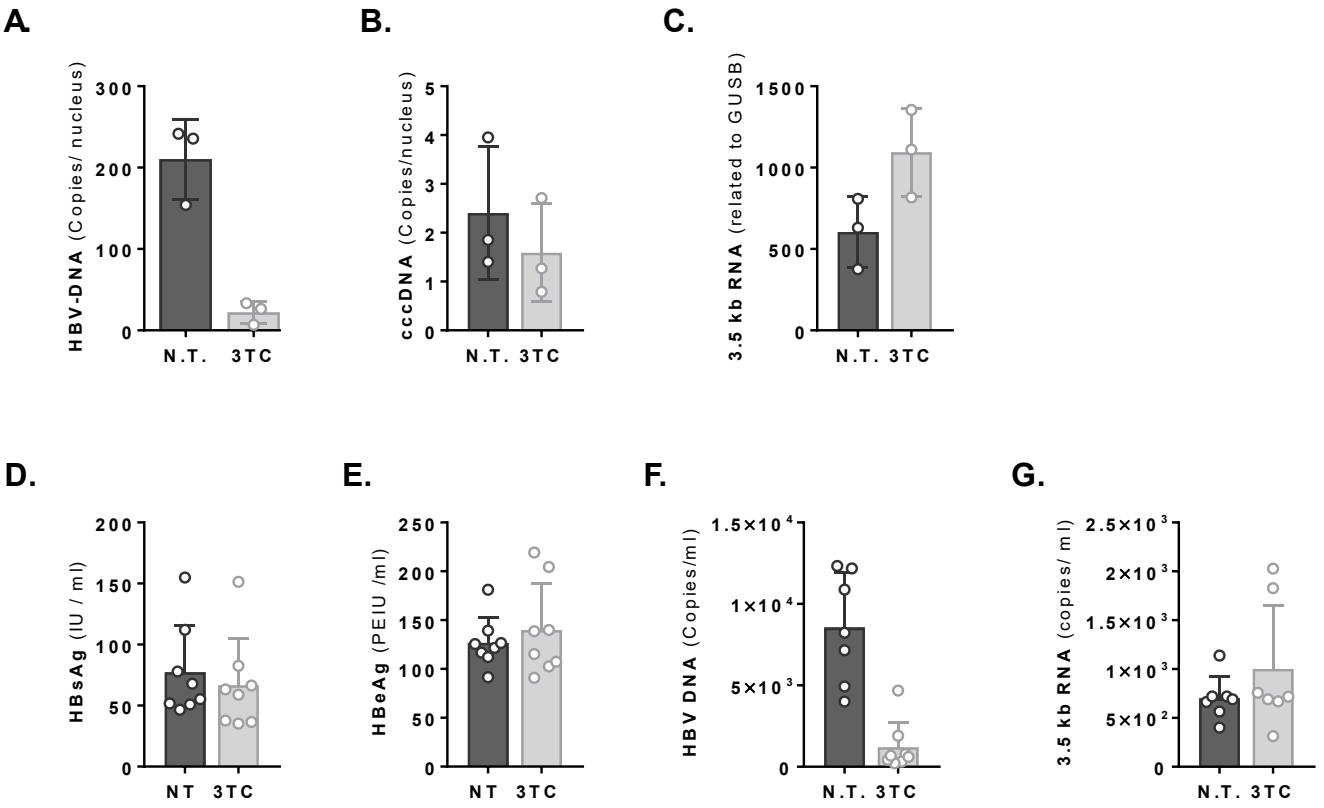

Supplementary Figure 1: Evaluation of Lamivudine treatment (3TC) effect on intracellular and extracellular viral parameters. HepG2^{hNTCP} cells were infected with HBV at MOI 250 and treated or not with 3TC (10µM) 3- and 5-days post infection (dpi). Cell pellets were collected 7dpi and nucleic acids were extracted. Total HBV DNA (A), cccDNA (B), 3.5kb-RNA (C) were quantified by qPCR with HBV specific primers. HBV-DNA and cccDNA were normalized over β-Globin and HBV-RNA was normalized over GUSB expression. Graphs show the mean ± SD of 3 independent experiments. HBsAg (D) and HBeAg (E) were measured by ELISA. Total HBV-DNA (F) and 3.5kb HBV-RNA (G) were respectively quantified by ddPCR. Graphs show the mean ± SD of 7 independent experiments.

Fig. S2

P2 HBeAg(+), HBsAg(high), High viral serum

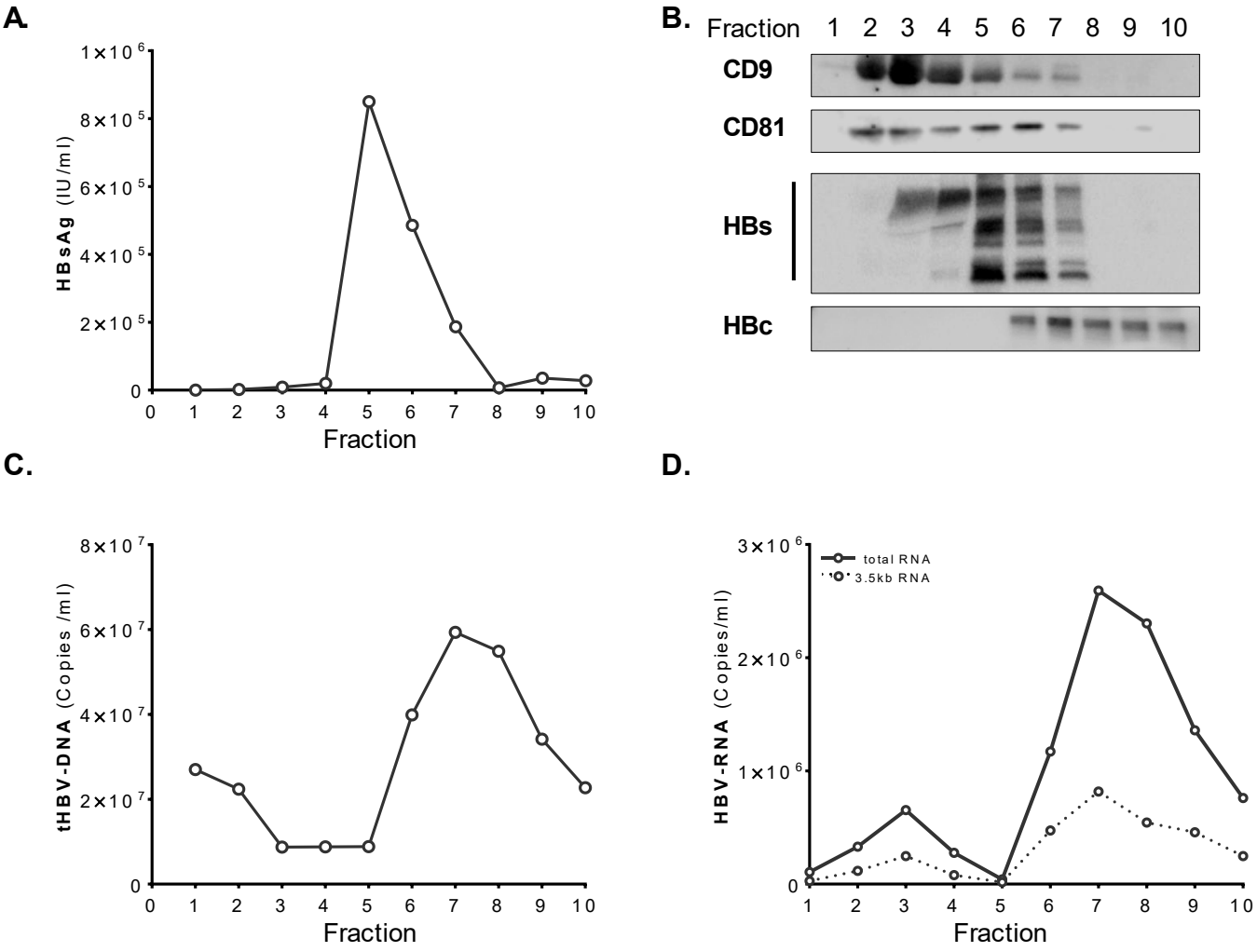

Supplementary Figures 2-11. Analysis of viral parameters and EVs markers in gradient fractions of serum samples derived from patients in different CHB phases.

Gradient fractions were obteined according to the protocol detailed in Method section. a) HBsAg ELISA. b) Representative Western Blot analysis using anti-extracellular vesicle (EVs) markers (anti-CD9 and anti-CD81), anti-HBsAg and anti-HBV core antibody. c) HBV DNA quatification by qPCR. d) HBV RNA quantification by RT-qPCR. HBx ORF common region was used to quantify both HBV DNA and total HBV RNA. pre-Core/pgRNA 5' unique region was used to quantify 3.5kb HBV RNA (Testoni et al. JHep 2019). CHB phases are defined according to 2017 EASL CPGs.

Fig. S3

P3 HBeAg(+), HBsAg(high), High viral serum

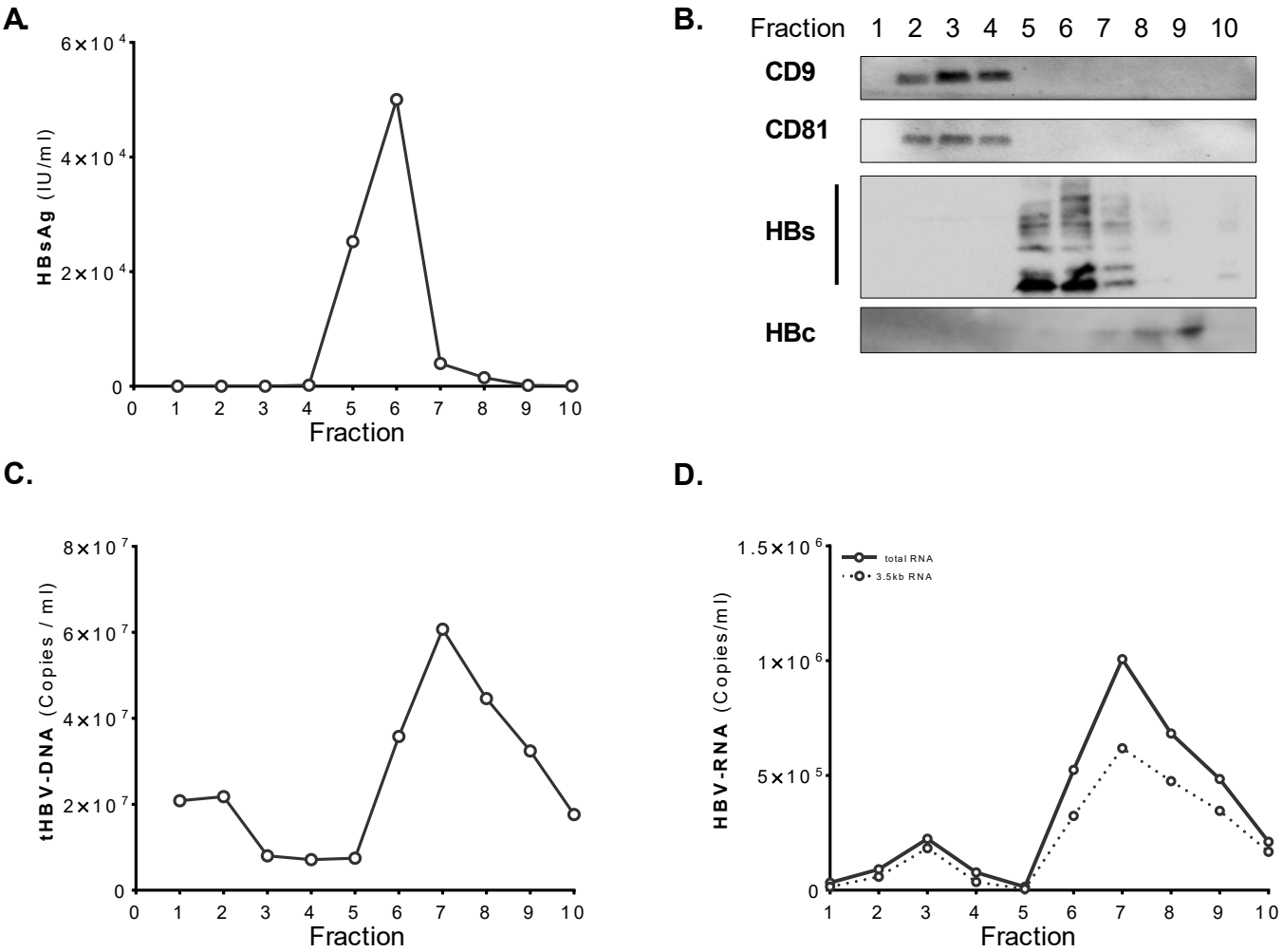

Fig. S4

P4 HBeAg(+), HBsAg(high), High viral serum

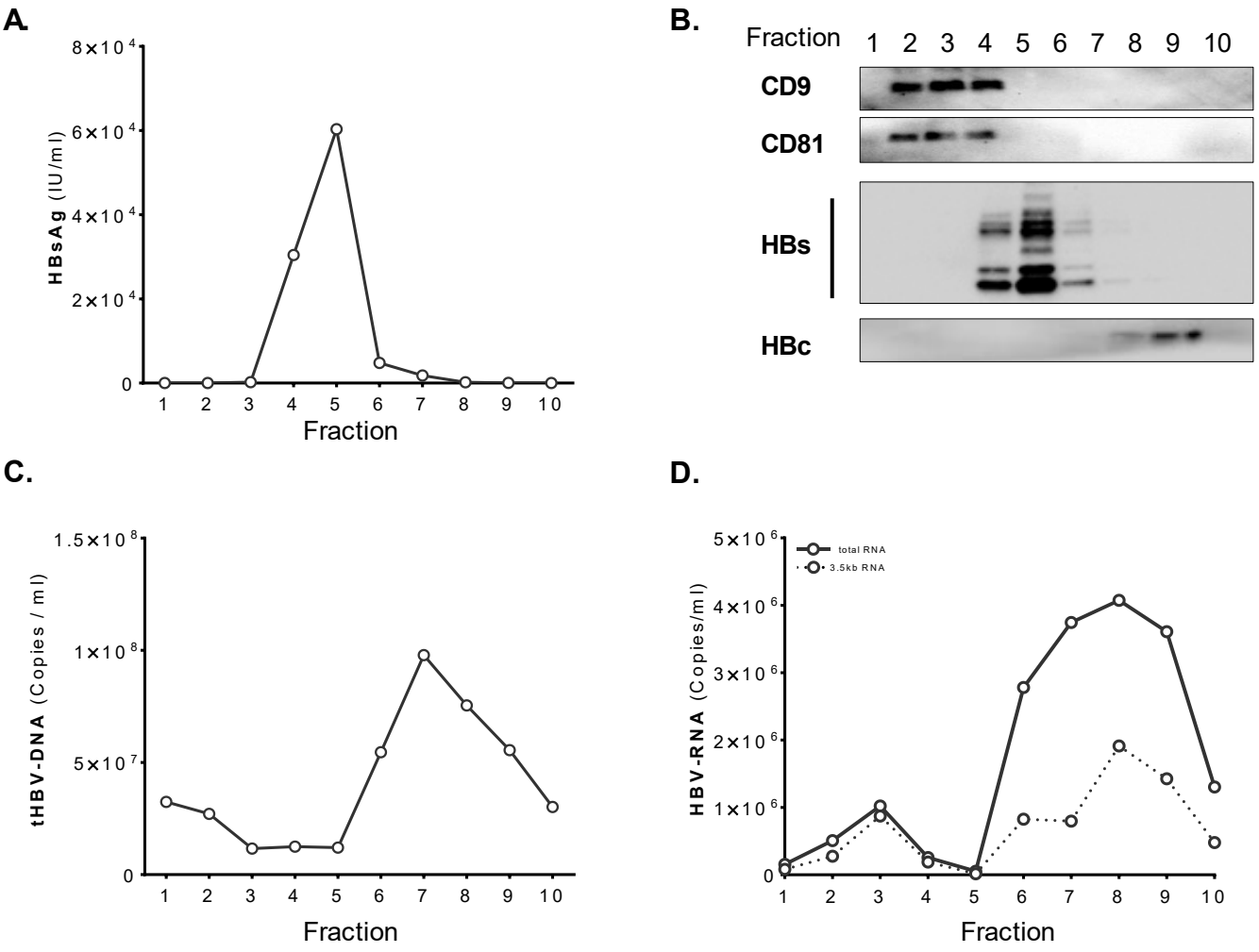

Fig. S5

P6 HBeAg(-) HBsAg(high), low viral load

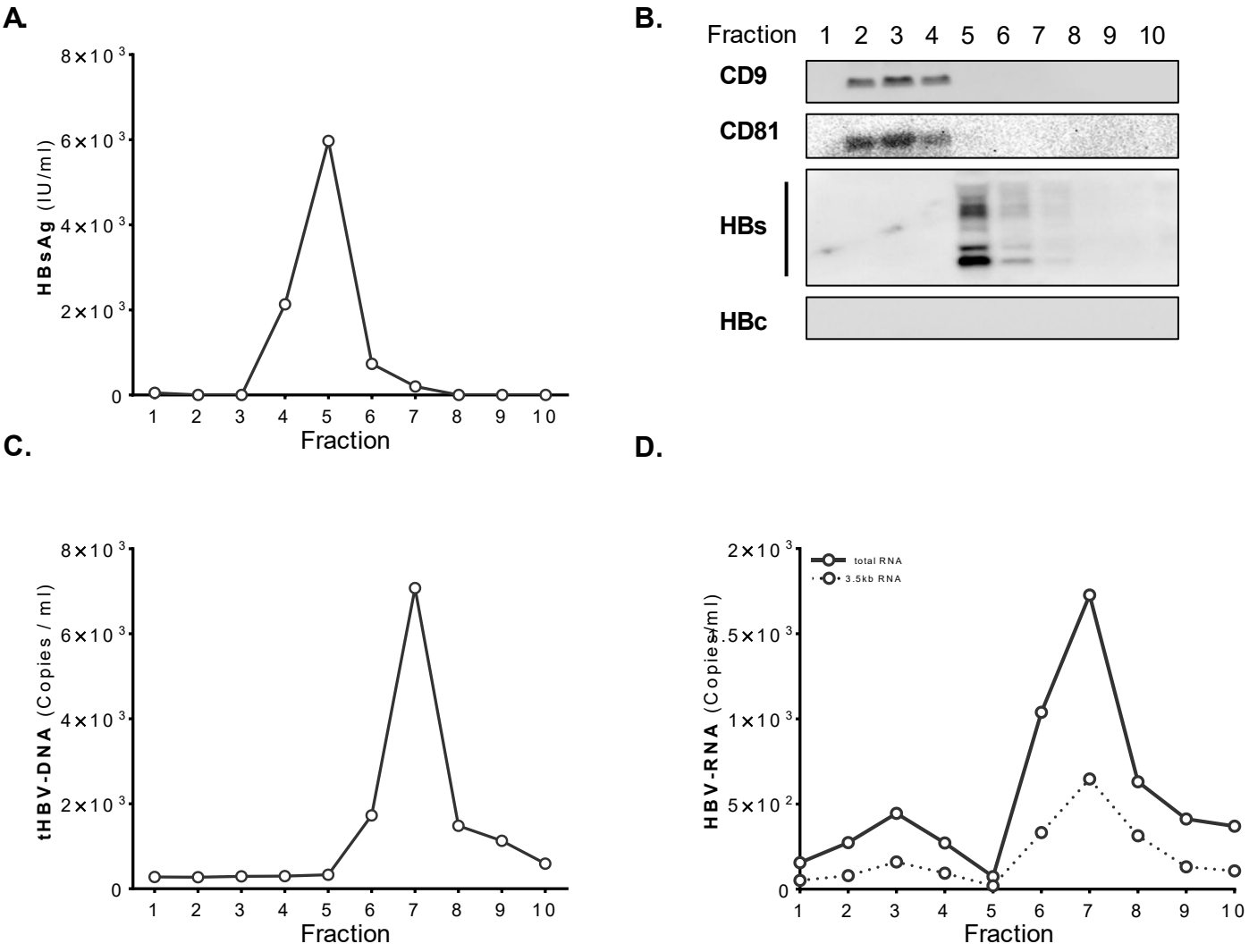

Fig. S6

P7 HBeAg(-) HBsAg(high), low viral load

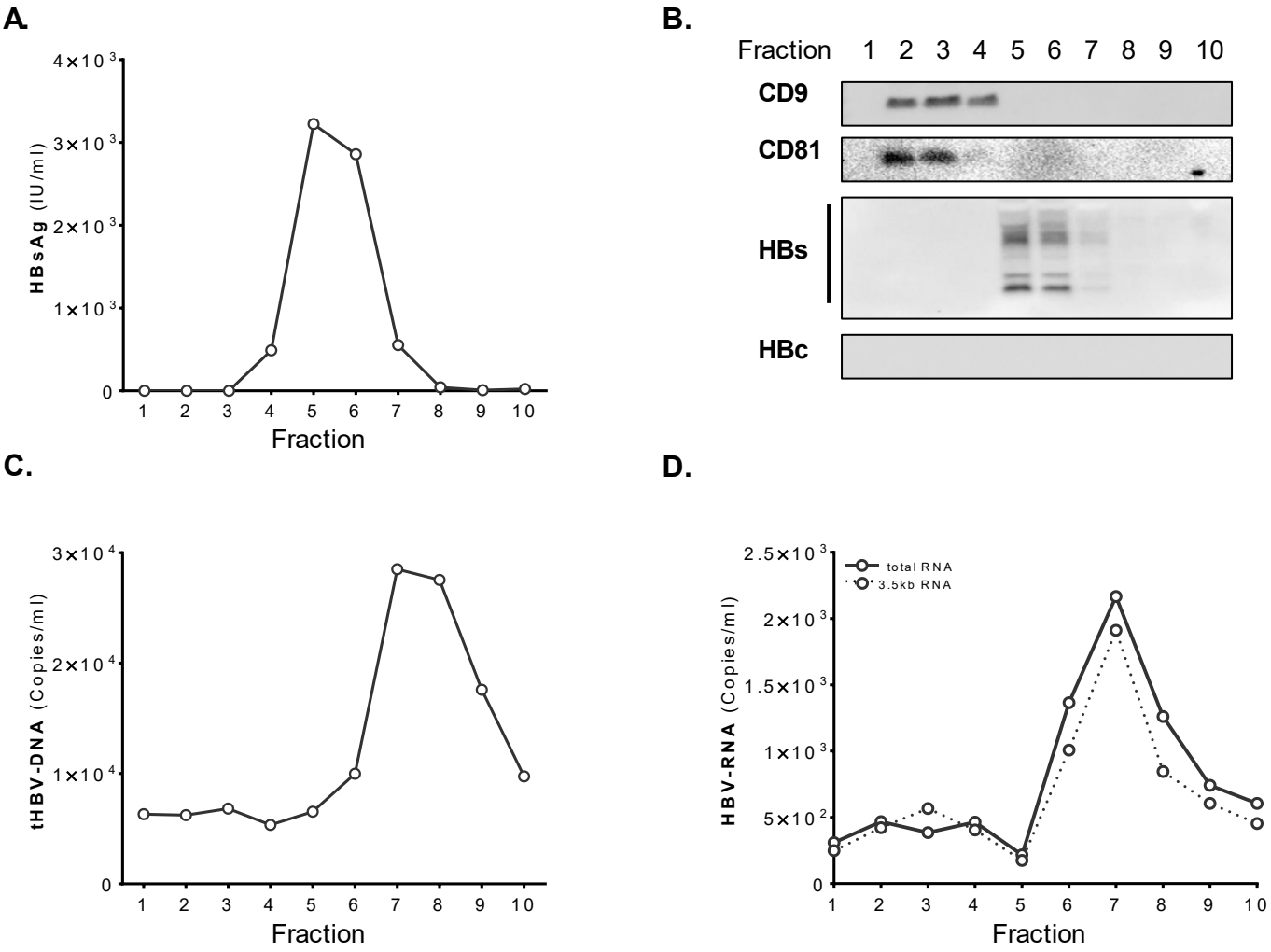

Fig. S7

P8 Inactive carrier case

A.

On-going

B.

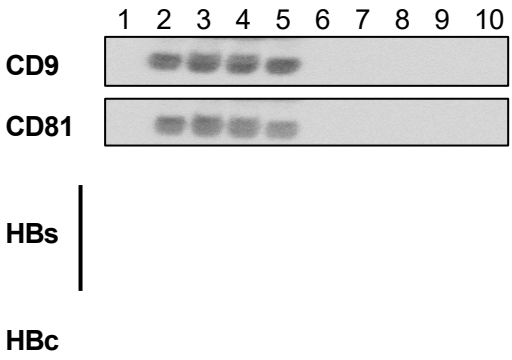

C.

D.

Fig. S8

P9 Inactive carrier case

A.

On-going

B.

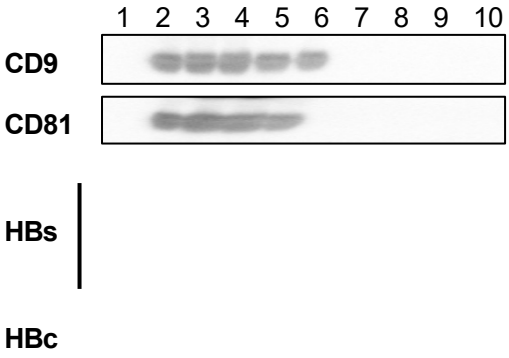

C.

D.

Fig. S9

H1 healthy control

A.

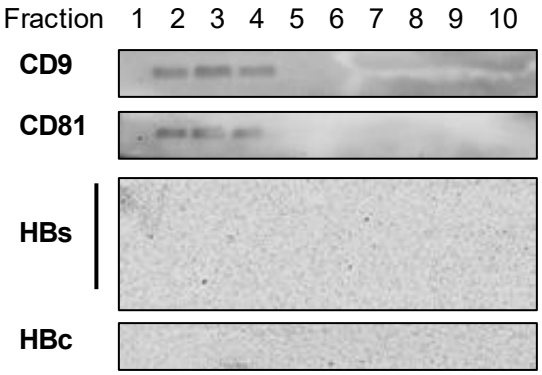

H2 healthy control

B.

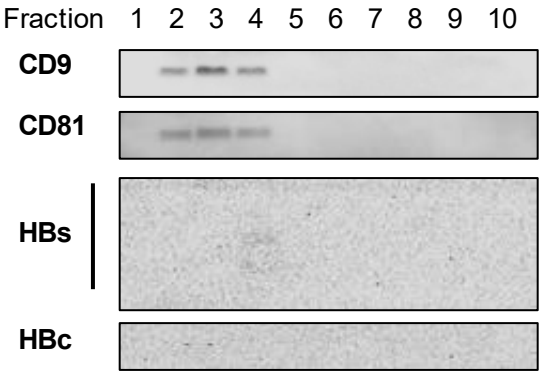

Fig. S10

P12 ETV longditudinal case

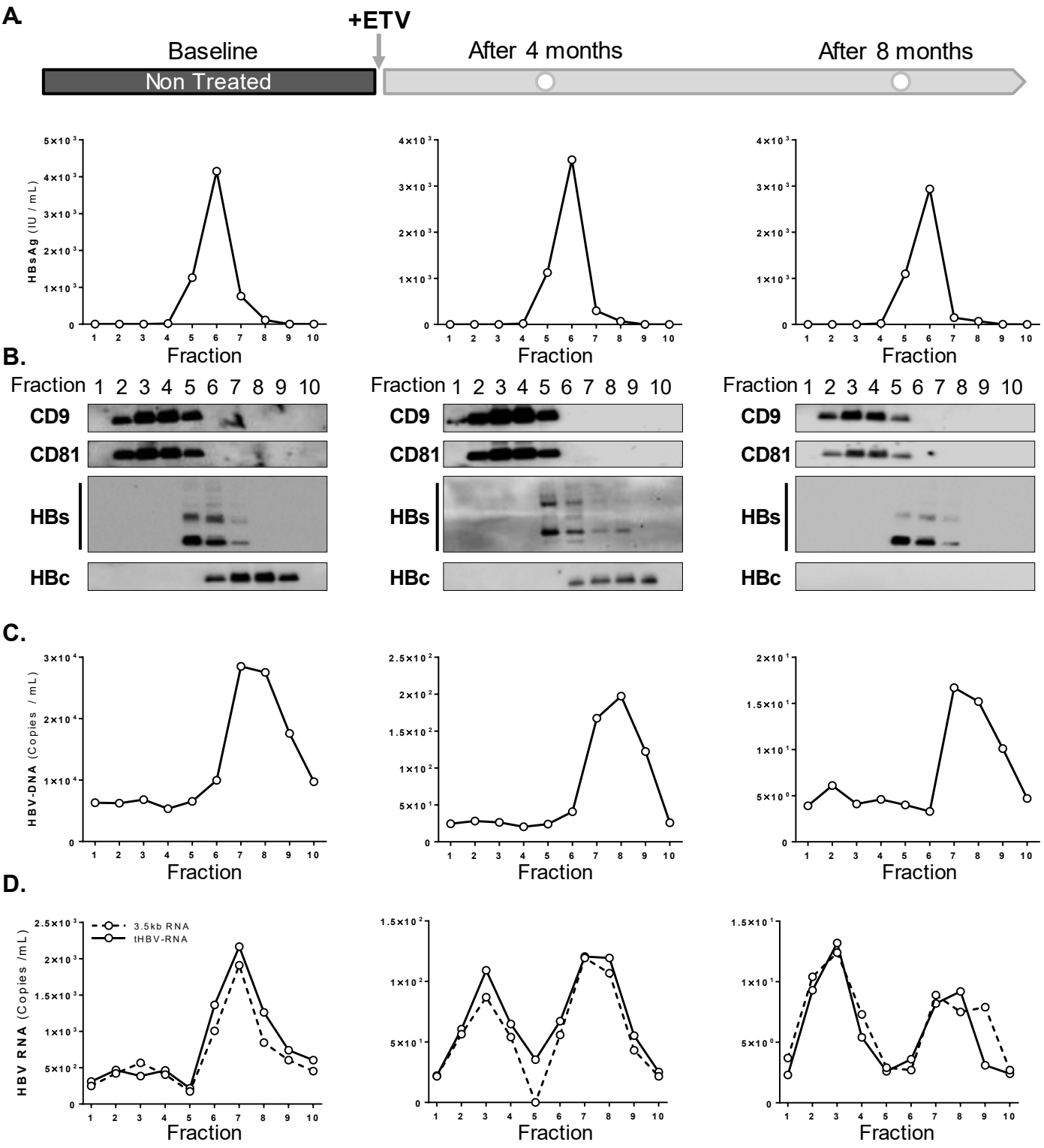

Fig. S11

P10 ETV case HBs, WB, DNA and RNA

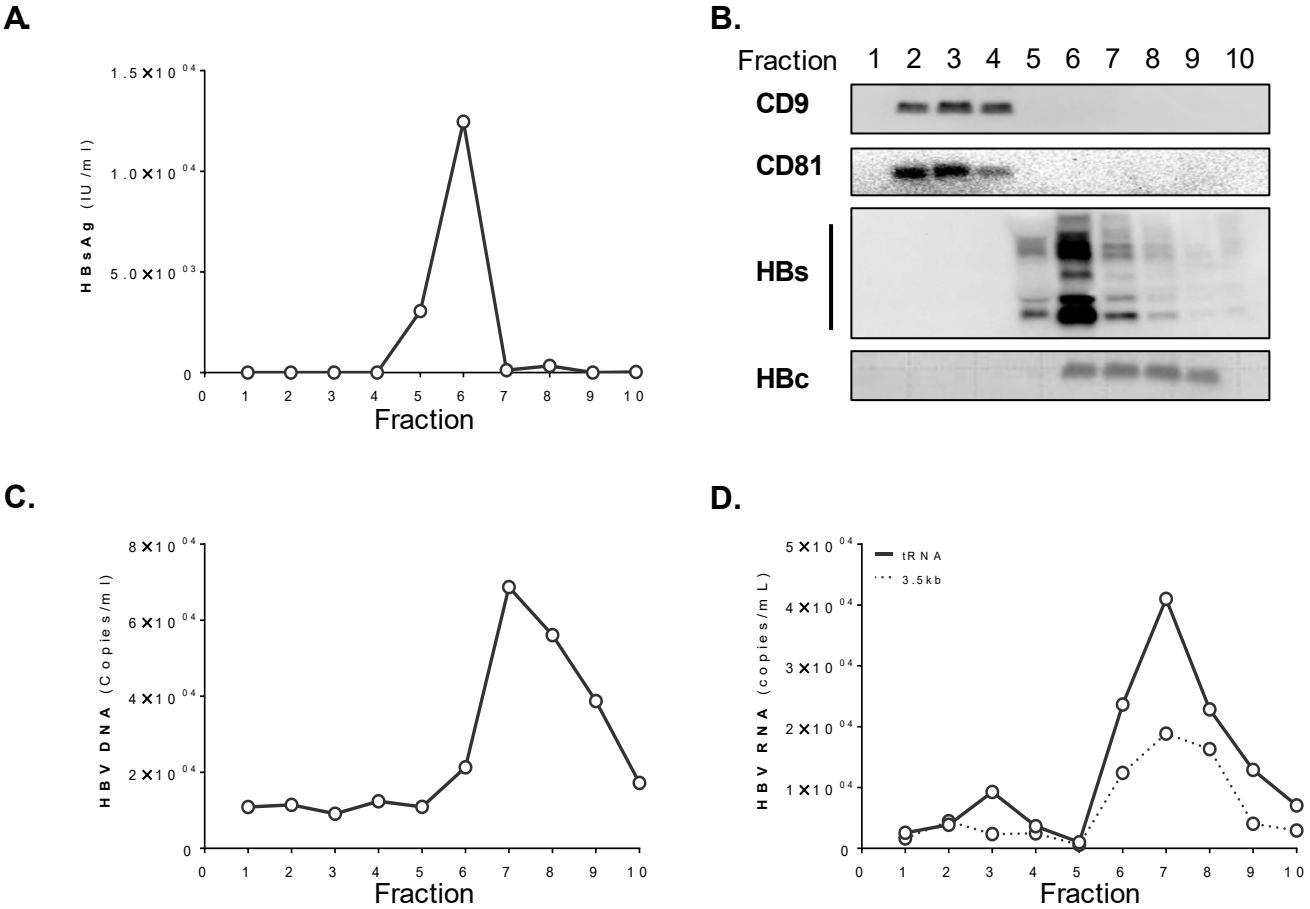

Fig. S12

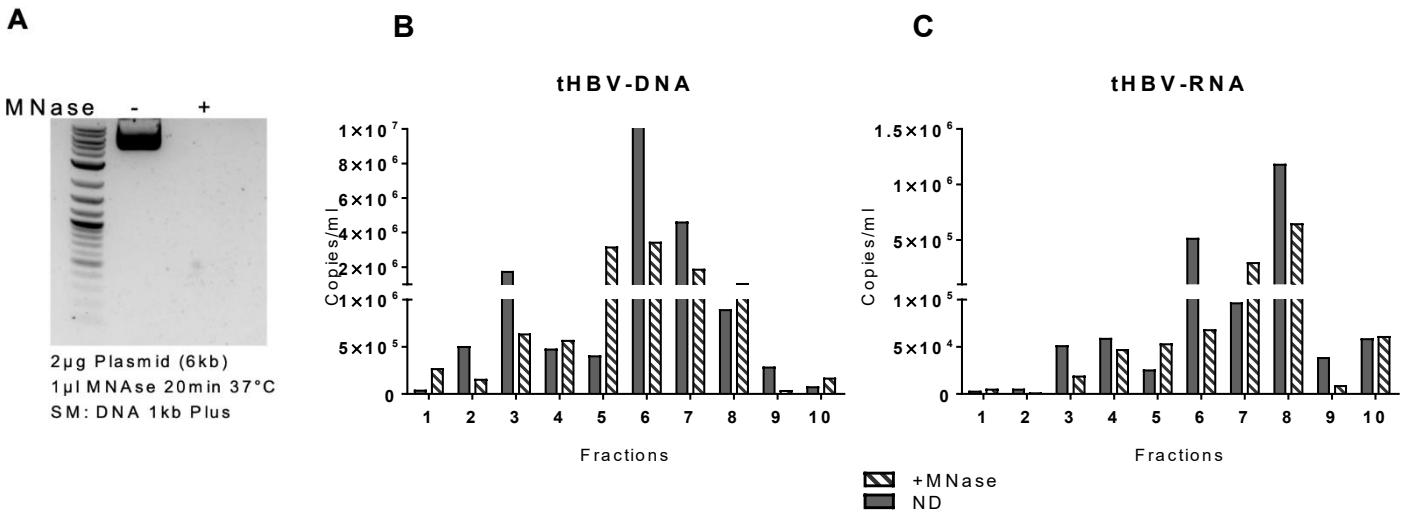

Supplementary Figures 12. MNase protection assay of sEVs fraction. Supernatant from HepAD38 was concentrated and separated through density gradient. MNase digestion step was added and reaction was stopped by trizol addition. (A) DNA Plasmid was added to monitor MNase digestion. (B) HBV DNA and (C) RNA were quantified by ddPCR.